Universidade de Aveiro Departamento de Biologia
2008

João Miguel da Silva Cordeiro

Efeito da translocação catiónica mediada por vesículas sinápticas na neurotransmissão

Universidade de Aveiro Departamento de Biologia
2008

João Miguel da Silva Cordeiro

Efeito da translocação catiónica mediada por vesículas sinápticas na neurotransmissão

Tese apresentada à Universidade de Aveiro para cumprimento dos requisitos necessários à obtenção do grau de Doutor em Biologia, realizada sob a orientação científica da Doutora Maria Paula Polónia Gonçalves, Professora associada do Departamento de Biologia da Universidade de Aveiro e do Doutor Yves Dunant Professor Honorário da Faculdade de Medicina da Universidade de Genebra (Suíça).

Apoio financeiro da FCT e do FSE no âmbito do III Quadro Comunitário de Apoio

o júri

presidente

Doutor José Pereira Costa Tavares, Professor Catedrático da Universidade de Aveiro.

Doutora Maria da Graça dos Santos Pratas do Vale, Professora Catedrática da Faculdade de Ciências e Tecnologia da Universidade de Coimbra.

Doutor Amadeu Mortágua Velho da Maia Soares, Professor Catedrático da Universidade de Aveiro.

Doutor Maria Ana Dias Monteiro dos Santos, Professora Catedrática da Universidade de Aveiro.

Doutor Robert Zorec, Professor Catedrático do Instituto de Patofisiologia da Universidade de Lubliana - Eslovénia.

Doutor Yves Dunant, Professor Honorário da Faculdade de Medicina da Universidade de Genebra - Suíça. (Co-Orientador)

Doutor Maria Paula Polónia Gonçalves, Professora Associada da Universidade de Aveiro. (Orientadora)

agradecimentos

At the end of this thesis I would like to express my deepest gratitude to all the people and institutions who helped me accomplish this work.

I deeply thank my supervisor, Professor Paula Gonçalves for her guidance through so many aspects of neurosecretion along these years of work together. They have been fundamental to see “the bigger picture” within the tiny microdomains where the players of this work operate. I am also grateful for the confidence deposited in me since the beginning of this work and for her patient perfection of the present manuscript.

I heartily thank my co-supervisor, Professor Yves Dunant who provided me with the unique opportunity of pursuing the objectives of this work in an extremely stimulating and friendly environment. I believe that the words welcoming, companionship or friendly fall short to describe the humane side of Yves. Thank you for teaching me what “l’ail des ours” is; that skiing in “carton” can lead you to fantastic places; along side with lessons on mediatophores and other partners playing sequential steps in a synapse; the importance of the dimension time, etc... I must also thank Yves for the many “manips” we did together with *Torpedo* and for all the helpful suggestions on the present manuscript.

I wish to thank my friend and colleague Victor Bancila for having me felt at home since my arrival in Geneva, and for his support in the lab.

I am also grateful to Alain Bloc for letting me learn from his scientific qualities, for the enlightening discussions and for his teachings on the patch-clamp technique.

And to Mircea Bancila for being such a good companion in the lab.

I am also indebted to Bernadett Boda for having done the gene constructs that enabled the FlAsh-FALI technique, and to Lorena Parisi for her assistance in that work.

I am thankfull to Professor Dominique Muller for facilitating the development of such experiments as well as for fruitful discussions.

And to Professor Lorenza Eder for many pleasant discussions and her cheerful way of helping me revive nearly abandoned ultracentrifuges and other material.

A big “merci” to Francoise Loctin for having the patience to correct my French when I arrived in Geneva as well as teaching me how to keep cells in culture and a great deal of help with *Torpedo* experiments.

Thank you Ago and Jean-Piere, for all the “bricolage” that provided me with the necessary tools for this work. Thank you also Ago for keeping my stock of cells alive.

My appreciation to Anna, Sylvianne, Nicole, Philippe, Fred and Domenica for being such pleasant company and for keeping things running so well.

My appreciation also to all my colleagues at the CMU for the exceptional ambience they provided.

To Virginie, Ignasi and my other Spanish friends in Geneva for their endless energy and joy.

I also have to thanking to Virgília, Paulo and Alexandra for welcoming me back in the Aveiro lab.; for their enthusiasm and their friendship.

I am most thankfull also to Cristina and Alex for being there for me whenever needed.

And all my other friends for their support.

My warmest thanks goes to my parents and my brother who supported me all along this work.

And my most affectionate gratitude to my wife, Ana, for her endless patience and support.

palavras-chave

Neurotransmissão, Neurosecreção, Cálcio, Trocador de Ca^{2+}/H^{+}, órgão eléctrico de *Torpedo marmorata*; Vesículas sinápticas; Células PC12, sinaptossomas de fibras musgosas de hipocampo de rato

resumo

O transporte de cálcio pelas vesículas sinápticas regula a duração da neurotransmissão: Como partir de uma actividade para chegar a uma função biológica e à identificação da proteína que a confere.

A neurotransmissão rápida ocorre na escala de tempo do milisegundo. Esta inclui
I) A entrada rápida de Ca^{2+} para dentro da célula através dos canais de cálcio sensíveis a voltagem.
II) A activação do mecanismo de libertação de neurotransmissor sensível a cálcio.
III) A difusão através da fenda sináptica
IV) A activação dos receptores pós-sinápticos
V) A terminação da sinalização
Um dos acontecimentos chave neste processo é que a elevação da concentração de Ca^{2+} no terminal sináptico tem de ser transitória, suficientemente elevada para garantir que a secreção ocorra num ápice e não perdure no tempo de modo a comprometer a "janela de tempo" da secreção (< 300 μs).
A necessidade de um mecanismo de sequestração rápida de Ca^{2+} de baixa afinidade foi postulado no passado como pressuposto teórico para garantir uma elevação da $[Ca^{2+}]i$ > 100 μM durante menos de 300 μs.
No nosso laboratório foi identificada uma tal actividade de transporte de Ca^{2+} energizada pelo gradiente de protões vesicular. Um trocador de Ca^{2+}/H^{+} em vesículas sinápticas de córtex cerebral de carneiro, activo para uma gama de concentrações de Ca^{2+} relativamente elevada, entre os 100 e os 800 μM (máxima actividade aos 500 μM).
A velocidade do transporte de Ca^{2+} por este antiporta depende do gradiente de H^{+} através da membrana vesicular que é mantido pela actividade da H^{+}-ATPase do tipo V e passível de ser inibida especificamente pela bafilomicina A1. Também o ião Sr^{2+} inibe o trocador de Ca^{2+}/H^{+} (sem afectar o gradiente de H^{+} vesicular). Estes dois inibidores foram utilizados para por em evidência a participação do trocador de Ca^{2+}/H^{+} vesicular na regulação da secreção da acetilcolina (ACh) nas sinapses do órgão eléctrico de *Torpedo marmorata*. Quer o Sr^{2+}, prevenindo a sequestração vesicular de iões, quer a bafilomicina, que dissipa o gradiente de H^{+}, induziram um aumento no tempo de resposta pós-sináptica de 2 ms para até ~10 ms, devido à persistência da libertação de ACh.
Os electrócitos do órgão eléctrico de *Torpedo* permitiram acompanhar esta libertação de ACh em tempo real através da medição da corrente eléctrica gerada pelo órgão eléctrico em resposta à ACh. Esta preparação permitiu simultaneamente a marcação da ACh libertada com ^{14}C, evidenciando assim a natureza pré-sináptica do aumento da libertação de ACh. Este aumento foi ainda confirmado em sinaptossomas isolados a partir do mesmo órgão, desta vez utilizando a quimioluminescência como técnica de visualização da libertação de ACh.

Ficou demonstrado que a principal função do antiporte de Ca^{2+}/H^{+} vesicular é a de restringir, no tempo, a libertação de neurotransmissor. Não se exclui, contudo, que essa mesma sequestração participe igualmente na homeostasia do Ca^{2+} "ajudando" a acção da Ca^{2+}-ATPase vesicular a manter os níveis basais de Ca^{2+}.

Agora que sabíamos o que o antiporte faz queríamos saber qual a proteína que o codificava. Para tal partimos da hipótese que a sinaptotagmina I codificava o nosso transportador. Usámos clones de células PC-12 em cultura que não exprimiam a sinaptotagmina (-/-) e comparámos a actividade de antiporte vesicular dessas células com a actividade nas células exprimindo a proteína (+/+). A perda de actividade nas células -/- foi de 100% relativamente às +/+. De modo a certificarmo-nos deste resultado usámos células -/- transfectadas com o gene da sinaptotagmina I ao qual foi fusionada uma sequência tetracisteínica (Cis-Cis-Arg-Glu-Cis-Cis) na proteína de fusão. Esta sequência é capaz de reconhecer uma sonda biarsénica, fluorescente quando ligada à proteína de fusão, e passível de criar radicais livres de alta reactividade (singletos de oxigénio) quando exposta a luz ultravioleta de alta intensidade. Técnica conhecida por "fluorescein-assisted light inactivation" ou FlAsh-FALI. Por este método pudemos verificar que a actividade de antiporte de Ca^{2+}/H^{+} vesicular requer uma sinaptotagmina I funcional, usando ensaios de transporte de $^{45}Ca^{2+}$ e uma sonda fluorescente sensível a protões.

keywords

Neurotransmission, Neurosecretion, Calcium, Ca^{2+}/H^{+} exchanger, *Torpedo marmorata* electric organ; Synaptic vesicles; PC12 cells, Rat hippocampus mossy fibre synaptosomes

abstract

Calcium transport by synaptic vesicles shapes neurotransmission timing:
From an activity to the biological function and the identification of it's encoding protein.

Rapid neurotransmission occurs in the millisecond timescale. This includes:
I) Fast Ca^{2+} entry into the cell through voltage operated calcium channels
II) Activation of the Ca^{2+}-sensitive neurotransmitter release mechanism
III) Diffusion through the synaptic cleft
IV) Post-synaptic receptor activation
V) Signalling termination
One of the key features in this process is that the Ca^{2+} concentration rise in the synaptic terminal must be transitory in nature. Rise above threshold level to guarantee flash-like secretion and don't endure in time as to compromise the time window for release (< 300 µs).
The need for a rapid Ca^{2+}-sequestering mechanism was postulated in the past as a theoretical pre-requisite to guarantee $[Ca^{2+}]i > 100$ µM in less than 300 µs.
We identified one such activity of Ca^{2+}-transport, energized by the vesicular proton gradient. A Ca^{2+}/H^{+} exchanger in synaptic vesicles of sheep brain cortex. Active for rather high Ca^{2+} concentrations ranging from 100 to 800 µM (maximum activity at 500 µM).
The speed of Ca^{2+} transport by this antiport depends on the H^{+} gradient existent across the vesicular membrane. This is maintained by the activity of a V-type-H^{+}-ATPase specifically inhibited by bafilomycin A1. Also, Sr^{2+} can inhibit the Ca^{2+}/H^{+} exchange (without affecting the vesicular H^{+} gradient). These two inhibitors were used to put in evidence the participation of this Ca^{2+}/H^{+} exchanger in the tight control of acetylcholine secretion (ACh) in *Torpedo marmorata* electric organ synaptic vesicles. Both Sr^{2+}, by preventing vesicular ion sequestration, and bafilomycin, able to annihilate the H^{+} gradient, induced an increase in time of the post-synaptic response from 2 ms up to ~10 ms, due to the persistence of ACh release.
Torpedo marmorata's electric organ electrocytes enabled us to follow ACh release in real time by registering the electric current generated by the electric organ in response to ACh. This preparation allowed the simultaneous marking of the ACh being released with ^{14}C, putting in evidence, in this way, the pre-synaptic nature of ACh release increase. This ACh rise was also confirmed in synaptosomes isolated from the same organ, this time using the technique of chemiluminescence to visualize ACh release.

It was demonstrated that the main function of the vesicular Ca^{2+}/H^{+} antiport is to restrain in time neurotransmitter release. However, we cannot exclude that such sequestration participates equally in Ca^{2+} homeostasis by "helping" the action of vesicular Ca^{2+}-ATPases to maintain basal Ca^{2+} low.

Now that we knew what the antiport does, we aimed at identifying the protein that codes for it. To do so, we started from the hypothesis that synaptotagmin I coded for our transporter. We cultured PC12 cell clones that did not expressed synaptotagmin I (-/-) and compared the vesicular antiport activity of those cells against that of positive control cells (+/+). To be certain of the result we used -/- cells to be transfected with the gene for protein synaptotagmin I fused with a tetracysteine sequence (Cis-Cis-Arg-Glu-Cis-Cis) in the resulting fusion protein. This sequence is responsible for the recognition of a biarsenical probe, able to fluoresce when bound to the fusion protein and liable to generate high reactivity free radicals (oxygen singlets) when exposed to intense UV light. That is, the fluorescein-assisted light inactivation or FlAsh-FALI. This method enabled us to conclude that the Ca^{2+}/H^{+} antiport activity requires a functional synaptotagmin I, as assessed by $^{45}Ca^{2+}$ transport assays and a fluorescence probe sensitive to protons.

Table of contents

List of tables

List of figures

Abbreviations used in the text

ACh – Acetylcholine

AChE – Acetylcholine esterase

A.O. – Acridine orange – bis [dimethylamino] acridine

ADP – Adenosine diphosphate

2-APB – 2-aminoethoxydiphenylborane

ATP – Adenosine triphosphate

ATPase – Adenosine triphosphatase

AU – Arbitrary units

BAPTA – 1,2-bis(2-aminophenoxy)ethane-N,N,N',N'-tetraacetic acid

BAPTA-AM – 1,2-bis-(o-Aminophenoxy)ethane-N,N,N',N'-tetraacetic acid tetra-(acetoxymethyl) ester

BHQ – 2,5-di-tert-butyl-hydroquinone

BHT – Butylated hydroxytoluene

cADPR – Cyclic ADP ribose

$[Ca^{2+}]_{Cytosol}$ – Calcium concentration in the bulk of the cytosol

$[Ca^{2+}]_{ext}$ – Calcium concentration in the extracellular medium

$[Ca^{2+}]_{int}$ – Calcium concentration in the intracellular medium

CCCP – Carbonyl cyanide n-chlorophehylhydrazone

CDI – Calcium dependent calcium channel inactivation

CRAC – Ca^{2+}-release activated channel

DBHQ (orTER) – 2,5-diterbutyl-1,4-benzohydroquinone

DCCD – N,N'-dicyclohexyl-carbodiimide

DHBP – 1,1'-Diheptyl-4,4'-bipyridinium dibromide

E_{Ca} – Equilibrium potential for Ca^{2+}

EDT_2 – 1,2-ethanedithiol

EEPP – Evoked excitatory post-synaptic potential

EGTA – Ethyleneglycol-bis(β-aminoethylether)-N,N,N',N'-tetraacetic acid

EGTA-AM – Ethyleneglycol-bis(β-aminoethylether)-N,N,N',N'-tetraacetic acid tetra -acetoxymethyl- ester

EPC – Excitatory post synaptic current

EPP – Excitatory post-synaptic potential (also found in literature as EPSP)

FALI – Fluorescence assisted light inactivation

FCCP – Carbonylcyanide p-trifluoromethoxyphenylhydrazone

FDNB – 1-fluoro-2,4-dinitrobenzene

FlAsH – 4',5'-bis(1,3,2-dithioarsolan-2-yl)fluorescein – or – Fluorescein-derivative arsenical hairpin binder probe

Glu – Glutamate

HEPES – N-2-Hydroxyethylpiperazine-N'-2-ethane-sulfonic acid

I_{Ca} – Calcium current

IP_3 –Inositol 1,4,5-trisphosphate

$K_{0.5}$ – Concentration of substrate at which 50% of maximal speed is reached

Kd – Dissociation constant

kDa – Kilodalton

MEPCs – Miniature excitatory post-synaptic currents

MEPP – Miniature excitatory post-synaptic potential

MES – 2[N-morpholino]-ethanesulfonic acid

MFS – Mossy fibre synaptosomes

NAADP – Nicotinic acid adenine dinucleotide phosphate

NMJ – Neuro muscular junction

PBS – Phosphate buffer saline

Pi – Inorganic phosphate

PPD – Paired pulse depression

PPF – Paired pulse facilitation

PPS – Paired pulse stimulation

PtdIns(3)P – Phosphatidylinositol 3-phosphate

PtdIns-4,5-P2 – Phosphatidylinositol-4,5-phosphate

QED – Quantum emission domains

RuR – Ruthenium red

SDS – Sodium dodecylphosphate

SV – Synaptic vesicles

Syn – Synaptosomes

Syt – Synaptotagmin

Tris – 22-amino-2-hydroxy-methylpropane-1,3-diol

VOCCs – Voltage operated calcium channels

ΔpH – Chemical component of the proton electrochemical gradient

1. Introduction

1.1. Calcium-dependent secretion: a historical sketch

The involvement of calcium ions in excitation-secretion (or contraction) coupling goes back to the time when brain cells were still believed by many to work as a syncytium (Reviewed by Shepherd, 1991), more than a century ago. It happens almost by chance in the course of the pioneer work of Sidney Ringer, while developing a formula for a physiological saline solution, subsequently named after him. He started describing the role of each component of the blood on the contraction of the frog heart ventricle in 1882 (Ringer, 1882). Soon after, he failed to reproduce his previous experiment and realized he had missed a key component in his "physiological" solution simply because he "*discovered that the saline solution which I had used had not been prepared with distilled water, but with pipe water supplied by the New River Water Company (in London)*", and after thorough analysis of that pipe water he revealed that it contained a significant amount of calcium, that was required for muscle contraction in the heart (Ringer, 1883).

A decade later, Locke stimulated frog sartorius muscle nerves with a platinum electrode and registered muscle contraction in normal Ringer (with calcium) while calcium removal resulted in no contractions (Locke, 1894). In the same work, Locke reported that excitation could be recuperated by substituting calcium with strontium, but not magnesium, or potassium.

The next landmark in the history of the role of calcium at the synapse came after a long Hiatus, into modern day's neuroscience. Harvey and MacIntosh (1940) established that calcium removal implicated failure of Acetylcholine (ACh) release from the pre-synaptic terminal rather than a failure of ACh to induce a post-synaptic effect. Later, Del Castillo and Stark (1952) showed that changing extracellular Ca^{2+} concentration varies the size of endplate potential at the neuro-muscular junction (NMJ), and if all Ca^{2+} was removed the potential disappeared. Similarly, Douglas & Rubin (1961) proposed that intracellular Ca^{2+} controls stimulus-secretion coupling in endocrine cells. This happened at the same time that Hodgkin, Huxley and Katz (1952) described the ionic basis of the action potential in the axon of the squid while, at this time, Del Castillo and Katz (1954) described the quantal nature of ACh release as well as miniature endplate potential at the neuro-muscular junction. Meanwhile, De Robertis and Bennett (1955) observed synaptic vesicles in the synaptic region for the first time.

At that time it was not known if Ca^{2+} participated in the spread of a depolarizing wave arriving at synaptic terminals or instead by activating the mechanisms leading to sudden increase in release probability of quantal transmitter release.

Katz and Miledi addressed this question in a pair of papers describing that nerve impulse was perfectly capable of invading the terminal in 0 Ca^{2+}, and if Ca^{2+} is applied iontophoretically it allowed to elicit ACh release locally, evoking a focal end plate potential (Katz and Miledi, 1965).

Later they demonstrated that local calcium concentration had to be raised extracellularly during the depolarization phase; "*if one delays the calcium pulse until the end of depolarization, no release occurs*" (Katz and Miledi, 1967a). At the same time, Dodge and Rahamimoff (1967) reported that the relation between $[Ca^{2+}]_{ext}$ and the excitatory postsynaptic potential (e.p.p.) is highly non-linear and establish that a co-operative action of about four calcium ions is necessary for the release of each quantal packet of transmitter by the nerve impulse in the frog NMJ.

These findings paved way to the formalization of the calcium hypothesis (Katz and Miledi, 1967b) saying that the: "*inward movement of a positively charged Ca compound, or of the calcium ion itself, constitutes one of the essential links in the "electro-secretory" coupling process of the axon terminal*" , in a paper where the pre-synaptic potential of the squid giant synapse was step raised up close to the Ca^{2+} equilibrium potential, with no postsynaptic response occurring until the end of that pulse.

This was the first demonstration of the theory proposed by Katz (1969) that "*depolarization opens a gate to calcium ions (or –what amounts to the same thing- that depolarization makes available specific carriers for calcium ions in the membrane)*" and that "*as a consequence of this increased "calcium conductance", Ca ions can move -down a very high concentration gradient- towards the inside of the axon membrane and thus reach the critical sites of release reaction*" and concluded "*we are suggesting that, at these sites, calcium is essential for the process which causes a transient fusion of axon and vesicular membranes and which leads to the release of a quantal packet of transmitter*".

The calcium theory was proposed by Katz as part of a wider view over "The release of neural transmitter substances", where he also hypothesized the so-called vesicular theory of transmitter release, which is part of the mainstream thinking in the field of secretion, nowadays.

Even though the calcium theory was proposed in 1967-1969, it would be somewhat unfair not to include in this section a reference to Miledi (1973), who contributed to the consolidation of the calcium theory by attributing an intracellular, near membrane, location to the Ca^{2+} site of action, by injecting $CaCl_2$ (0.1-0.5 mM) iontophoretically, directly into the cytosol of small squid giant synapses. This was his second report (first one was in 1966 with Slater, but somewhat failed) where he also proved that intracellular injection of strontium ions could substitute for calcium.

1.2. Calcium desensitization or "fatigue" of transmitter release

Katz and Miledi's studies had already given some indications that calcium activation of the secretory apparatus did not resume to some dicothomic "on signal" in the presence of calcium and "off signal" in the absence of the ion. It had to be brief also.

The intracellular calcium injection experiments of Miledi are a good example of this since he could not reproduce the very intense postsynaptic response obtained by calcium entry after depolarization of the terminal (in presence of extracellular calcium). Instead, he was able to induce a slower postsynaptic potential, with some faster components superimposed (especially with extra calcium) as calcium diffused away from delivery sites, promoting asynchronous release rather than synchronous in this way (Miledi 1973), and thereby explaining why he had missed that experiment the first time due to a weak calcium-dependent signal and Ca^{2+} buffering in the terminal.

Synaptic fatigue, or calcium induced desensitization of release is another important (even if not explored) Ca^{2+}-dependent effect that was first reported in 1969 by Katz and Miledi after the formulation of the calcium hypothesis.

They reported that if a squid pre-synaptic terminal sustains long-lasting depolarization, fatigue of synaptic transfer process will occur and this fatigue (or pre-synaptic inactivation) probably results from prolonged influx and accumulation of calcium on the inside of the membrane. Similarly, removing all NaCl from the extracellular medium resulted in the complete blockade of release process, possibly by blocking calcium extrusion and allowing calcium accumulation inside the terminals (Blaustein and Hodgkin, 1969; Katz and Miledi, 1969). Substituting extracellular NaCl (i.e., with LiCl) or using other calcium extrusion blockers, like cyanide (Baker et al., 1971), ruthenium red (RuR) (Alnaes and Rahamimoff,

1975), or FCCP (Adams et al., 1985) results in the progressive elevation of intra-terminal calcium above 1 micromolar.

This progressive intra-terminal calcium rise was dependent on both $[Ca^{2+}]_{ext}$ and synaptic terminal stimulation, resulting in the blockade of evoked transmission within 20-40 min (Adams et al., 1985).

More importantly, Adams et al. (1985) asserted a role for ionized calcium in this process of calcium-induced pre-synaptic desensitization by recuperating transmission with the injection of the calcium chelator EGTA directly into squid giant pre-synaptic terminals.

The molecular nature of the dual calcium effect on synaptic transmission was evidenced by Israël at al. (1987) by showing that calcium ions can both activate a calcium-sensor of transmitter release or desensitize it to further Ca^{2+}-dependent activation, depending on the Ca^{2+} concentration and time of exposure to elevated Ca^{2+}. They used both synaptosomes, and proteoliposomes endowed with the calcium-sensor of ACh release present in *Torpedo marmorata* neuro-electric synapse, the mediatophore.

Calcium binds to the mediatophore with an apparent affinity of ~25 μM which is in accordance with half maximal desensitization of ACh release attained at ~30 μM calcium for Ca^{2+} exposures lasting 3 to 5 min. Conversely, rapid Ca^{2+}-induced ACh release was half maximally activated at 500 μM Ca^{2+} leading to the conclusion that desensitization and release capacities co-inhabit within the same molecule and are functionally related.

Partial Ca^{2+}-induced desensitization of the release machinery has been functionally addressed in squid nerve terminals with repetitive Ca^{2+}-uncaging protocols. Consecutive 25 ms Ca^{2+}-uncaging pulses, separated by 100 ms between pulses, resulted in decreased postsynaptic response up to ~1/3 of the highest E.P.P. within 500 ms (Hsu et al., 1996). Even though named adaptation, it follows the same Ca^{2+}-dependent characteristics of "fatigue" or the desensitization of pre-synaptic release machinery.

Calcium-induced desensitization might also participate in a form of synaptic plasticity named paired pulse depression (PPD) obtained by stimulating Calyx of Held synapses at 150 ms intervals (Bellingham and Walmsley, 1999).

This form of depression is sensitive to pre-synaptic calcium and strontium levels and can be reversed by early application of cyclothiazide, a drug normally used to prevent post-synaptic AMPA receptor desensitization (Vyklicky et al., 1991; Yamada and Tang, 1993).

The frequency of MEPPs also increased during PPD, which is consistent with a sustained increase in intra-terminal calcium or strontium (Bellingham and Walmsley, 1999). In keeping with this strontium effect is the report that zinc substitutes for calcium both on *Torpedo* synaptic transmission and on desensitization, only this time with greater affinity (100-250 μM Zn^{2+}) than calcium (Dunant et al., 1996)

It seems then that, pre-synaptic Ca^{2+}-induced desensitization of the release mechanism occurs gradually within milliseconds up to minutes time scale and that it might be involved in the fine-tuning of synaptic function and/or in prevention of neurotransmitter exhaustion.

1.3. Calcium signal has to be transient

A corollary arises from the features presented above. The need for speed!
Calcium signals directed at activating the release machinery need to be very fast, sharply defined in space and in time to guarantee the necessary acuity for activating the calcium sensors of secretory apparatuses without incurring into undesirable desensitization. On the other hand, desensitization should be able to prevent the unsynchronized release of transmitter packets from release sites not coupled to the calcium source.

In line with this, transmitter release is a highly cooperative process with Hill coefficients varying from ~3 to ~5 (Dodge and Rahamimoff, 1967; Dunant et al., 1980a; Yazejian et al., 2000).

This means that calcium sensitivity for transmitter release is highly non-linear with both the amount and kinetics of transmitter release varying exponentially with the calcium concentration.

It means also that binding of a Ca^{2+} ion to its sensor is facilitated by previous allosteric binding of another Ca^{2+}, working cooperatively (up to 3-5 ions per sensor molecule) to activating the Ca^{2+}-dependent release apparatus.

If calcium activation does not occur as fast and intense as provided by calcium entry through calcium channels, cooperativity will be lost, even though the calcium affinity remains practically unaltered (Birman at al,. 1986; Cavalli, A et al., 1991; Bollmann and Sakmann, 2005). Similarly, Ca^{2+}-induced membrane accretion resulting from vesicular fusion can be activated by rising calcium to only a low intra-terminal micromolar concentration, but rather slowly and with low intensity.

Fusion rates increase exponentially when calcium rises suddenly into the hundreds of micromolar calcium (Heidelberger et al., 1994; Mennerick and Mathews, 1996; Beutner et al., 2001).

1.4. Ca-dependent secretion rides off the back of fast calcium current transients

Calcium signal does not occur uniformly throughout the terminal. There are precise spots of Ca^{2+} elevation near the membrane resulting from transient membrane barrier breach to calcium.

These spots correspond to the so-called pre-synaptic active zones where the release apparatus clusters at well defined spaces forming a "pre-synaptic web" (Couteaux and Pécot-Dechavassine, 1970; Zhai and Bellen, 2004; Girod et al, 1993).

Upon opening of voltage operated calcium channels (VOCC's) Ca^{2+} streams into the active zone, energized by the summation of a huge chemical Ca^{2+} gradient (15,000-100,000 fold) and an electric gradient mostly favouring Ca^{2+} entry.

In a couple of breakthrough papers Llinás et al. (1981a; 1981b) described pre-synaptic calcium currents (I_{Ca}) and their relationship with the post-synaptic response in the squid stellate ganglion synapse. There, calcium conductance change displays a rather late onset (~800 μs) after the beginning of depolarization and a sigmoidal time course. The I_{Ca} rate of rise and "bell"-shaped amplitude curve are voltage-dependent. Maximum rate of rise was reached at -8 mV and maximum amplitude at -10 mV (the resting potential was -70 mV). The current displayed no fast (i.e., <100ms) voltage-dependent deactivation.

Importantly, the time course of the calcium current is independent of $[Ca^{2+}]_{ext}$ while the amplitude of I_{Ca} is clearly dependent on $[Ca^{2+}]_{ext}$ (maximum at 10 mM), this means that the rate of I_{Ca} increase with voltage is also dependent on $[Ca^{2+}]_{ext}$. There is also a voltage shift of peak I_{Ca} to the right with increased $[Ca^{2+}]_{ext}$.

By applying a depolarizing pulse near Ca^{2+} equilibrium potential (E_{Ca}) Llinás et al. were able to demonstrate that I_{Ca} decreases exponentially with a time constant of ~630 μs after returning to the holding potential (-70mV). These, so-called "tail-currents" increase sharply with depolarization and are capable of generating brief and robust Ca^{2+} influx.

Similarly, the generation of excitatory post-synaptic potentials (EPP's) in the squid synapse (Llinás et al., 1981b) increased in amplitude and rate of rise, while synaptic delay

decreased to a minimum, by applying depolarization steps to -10 up to + 10 mV (from -70 mV), where I_{Ca} was maximal. Under these conditions the synaptic delay between the onset of the depolarizing stimulus varied from 633 μs up to 1.27 ms (averaging ~800 μs).

When release was elicited by a Ca^{2+} "tail-current" however, the delay varied from 133 and 233 μs (averaging 192 μs). This setted an upper limit of 200 μs for the activation of the release machinery, diffusion of transmitter into the synaptic cleft and binding and opening of post-synaptic receptors. These findings meant that most of the synaptic delay is due to the activation kinetics of calcium channels, while the delay between calcium entry and post-synaptic response is extremely brief.

This extraordinary finding was seconded by several reports confirming the tight onset of post-synaptic responses following calcium entry. Hence, similar activation kinetics for ACh release (<300 μs) were reported at *Torpedo marmorata* (Dunant and Muller, 1986) neuro-electrocyte synapse, recorded at 18-20 °C (like with the squid).

Xenopus nerve-muscle cultures took ~160 μs at 22-24 °C to activate an EPC (Yazejian et al., 2000). A similar value (150 μs) was reported by Sabatini and Regehr (1996) using rat cerebellar granule cell to stellate cell synapses at 18 °C.

Interestingly, the delay between the onset of the depolarizing stimulus and the beginning of EPC was ~2.5 ms (at 18 °C), but when the same experiment was repeated at 38 °C it took only 150 μs, and the lag between the calcium entry and beginning of EPC decreased to mere 60 μs. To achieve this, a significant amount of calcium has to enter during the upstroke of the action potential, reducing the delay between depolarization and calcium entry to 90 μs.

It seems then that factors controlling synaptic delays, like the activation of calcium currents (Sabatini and Regehr, 1996; Mennerick and Mathews, 1996) are of critical importance for secretory systems working at high speed.

While some neurons seem to require also rather short deactivation time constants of calcium currents to sharpen Ca^{2+}-signaling, like sensory neurons of chick (~160 μs) (Swandulla and Armstrong, 1988) or retinal bipolar cells (<120 μs) (Mennerick and Mathews, 1996), others, like squid giant synapse, manage to decrease the post-synaptic response after a depolarizing pulse in less than 200 μs (Simon and Llinás 1985) even if the I_{Ca} deactivation time constant there surpasses 600 μs.

This degree of synchronization is participated by an exquisite architectural arrangement of calcium channels in pre-synaptic active zones facing post-synaptic arrays of

receptors (Harlow et al.,2001; Zhai and Bellen, 2004), as demonstrated by an almost perfect match between pre-synaptic N-type calcium channels (labelled with fluorescent ω-conotoxin-GVIA) and post-synaptic cholinergic receptors (labelled with fluorescent α-bungarotoxin) (Robitaille et al., 1990; Cohen et al, 1991; Robitaille et al., 1993; Haydon et al., 1994).

Calcium channel labelling revealed a disposition of ca. 40 nm between neighbouring channels, irrespective of total channel density (Haydon et al., 1994). These authors correlated their findings with large transmembrane particles seen at release sites by freeze-fracture electron microscopy at a density of ca. 1500 μm^{-2}, corresponding to a channel every 10-30 nm (Heuser et al., 1974; Pumplin et al., 1981). A value that can accommodate other transmembrane channels known to be in close proximity to calcium channels like the Ca^{2+}-activated potassium channels (K_{Ca}), with a density of ~$\frac{1}{2}$ that of calcium channels (Roberts et al., 1990; Robitaille et al.,1993; Naoum and Hudspeth, 1994) and a set of large particles (10-15 nm) evoked by nerve impulse, that correspond to multimers of the Ca^{2+}-activated, ACh-release competent transmembrane channel - the mediatophore - present at least at 200 units μm^{-2} (Israël et al., 1986; Muller et al., 1987; Brochier et al., 1992; Dunant and Israël, 2000; Morel et al., 2003).

This regular distance between calcium channels is also consistent with the predicted separation determined by direct binding of calcium channels to synaptic vesicle protein synaptotagmin I (Sheng et al., 1998; Harlow et al., 2001; Evans and Zamponi; 2006), and plasma membrane proteins neurexin (Missler et al., 2003) syntaxin, as well as the synaptosome associated protein of 25 kDa (SNAP25) (Sheng et al., 1998; Harlow et al., 2001; Evans and Zamponi; 2006) and K_{Ca} channels (Müller et al., 2007).

The mediatophore ends up being physically linked to calcium channels through secondary binding to syntaxin (Shiff et al., 1996) and to the syntaxin binding partner synaptobrevin (VAMP), or other vesicular proteins like synaptophysin and its binding partner physophiline (Siebert et al., 1994; Galli et al., 1996).

Otoferlin is another protein arising as the putative calcium sensor involved in stimulus secretion coupling at mammalian auditory inner hair cell ribbon synapse, where no synaptotagmin I or II are expressed (Safieddine and Wenthold, 1999; Roux et al., 2006). It also binds syntaxin and SNAP25 in a Ca^{2+}-dependent manner, like synaptotagmin I does (Chapman, 2002; Roux et al., 2006).

Most of these proteins are not only physically linked, but in fact, functionally attached. For instance, syntaxin and SNAP25 down-modulate calcium channels. Synaptotagmin I removes this down-modulation after interacting with syntaxin (Sheng et al., 1998; Bezprozvanny et al., 2000; Harlow et al., 2001; Evans and Zamponi; 2006). On the contrary, neurexin seems to be fundamental for calcium channel function, as well as serving as a receptor for the Ca^{2+}/transmitter pore forming toxin a-latrotoxin (Missler et al., 2003). Soluble N-ethylmaleimide-sensitive factor (NSF) attachment protein (SNAP) receptor (SNARE) proteins like syntaxin, VAMP or SNAP25 cleavage with botulilnum and tetanus toxins seems to result in the disorganization of pre-synaptic active zone proteins (Dunant et al., 1995; Humeau et al., 2000). Toxin poisoning results in the uncoupling of calcium entry from transmitter release and vesicular fusion, blocking evoked secretion while maintaining spontaneous transmission (Dunant et al., 1995; Humeau et al., 2000).

Calcium channels seem to unify Ca^{2+}-secretion coupling machinery, interlinking the different preparatory, modulatory and executory partners involved in a response to a calcium transient streaming at the active zone.

1.5. Nanometre and micrometer domains of high calcium

The temporal profile of the onset and offset of rapid secretion seems to implicate a strategic location of the calcium sensor near calcium entry sites where local calcium concentrations could approach the millimolar range (Llinás et al., 1981b; Simon and Llinás 1985; Roberts et al., 1990; Llinás et al., 1992; Roberts, 1993; Roberts, 1994).

These very high concentrations were predicted to occur only in close proximity of calcium channel mouths. Ca^{2+} ions flowing into the cell though a channel are assumed to diffuse radially and thus, for a constant ion influx a steady state is reached (Parsegian, 1977), within microseconds (Pumplin and Reese, 1978). Llinás et al. (1981b) calculated that for a I_{Ca} of 200 nA the Ca^{2+} concentration reached near channel mouth after 200 μs was ~800 μM and decreased steeply to $\frac{1}{2}$ at ~39 nm, being almost unaltered (at the mM scale) at 150 nm from the source. The calcium concentration reached at channel mouths was predicted to climb to 1 mM or 1.5 mM if I_{Ca} climbed to 300 nA or 400 nA respectively.

These predictions were borne out by experimental demonstrations of such domains of calcium elevation near release sites, a decade later, by the hand of Llinás et al. (1992). They injected squid giant synapses with a low Ca^{2+}-affinity derivative of aequorin, a protein

extracted from *Aequorea forskolea* that emits light upon Ca^{2+} binding. By monitoring continuously the intensity and number of quantum emission domains (QEDs) within the terminals they were able to identify small domes of increased [Ca^{2+}] with 0.313 μm^2 arising near calcium entry sites up to ~200-300 μM and decaying sharply within 10-20 nm and participating synergistically in larger elevation of Ca^{2+} in the active zone. They were named microdomains and correlated with active zones determined by electron microscopy (Pumplin and Reese, 1978; Pumplin et al., 1981).

In this first experimental demonstration of localized calcium microdomains, represented in figure 1 (A and B), it is shown the sharp calcium rise within the calcium microdomain profiles arising as spirals erected above open calcium channels next to low resting calcium areas of bulk cytoplasm, buffered below 100 nM (Dipolo et al., 1976). They also showed the synergistic effect of having several nearby calcium channels contributing for broader calcium elevation at release sites.

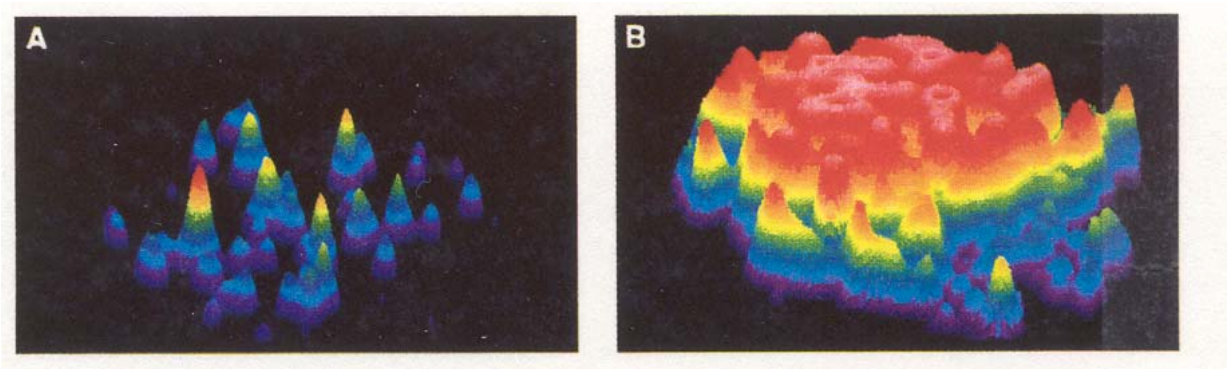

Figure 1. Calcium microdomains localized by QEDs produced in a terminal bulb of a pre-synaptic fibre. **Panel A**: before stimulation. **Panel B**: during stimulation. Light intensity levels range from white (maximum) to black (zero), with intermediate levels ranging from high (red) through intermediate (yellow and green) to low (blue) probabilities that a particular microdomain would be active. Adapted from Llinás et al. (1992).

Llinás et al. noticed that once a microdomain is activated, it displays a low probability of being reactivated, as compared to a resting active zone, due to calcium channel inactivation by high $[Ca^{2+}]_{int}$ (Young et al., 1984; Xu and Wu, 2005). This Ca^{2+}-induced channel desensitization was named "lateral inhibition" whereby a given channel would be temporarily depressed by calcium arising from the previous activity of a neighbouring channel. Yet to fully characterise the calcium transient that drives secretion within microseconds QEDs were not appropriate (they lasted ca. 200 ms due to the detection technique).

Roberts et al. (1990) developed a method for determining local $[Ca^{2+}]_{int}$ using K_{Ca} channels as reporters in frog hair cells. These cells depend on the interplay of K_{Ca} and calcium channel activities to produce fast calcium-dependent electrical resonance.

Resonance transduces very high frequency signals, typically above 1000-2000 Hz that phase-locks to the stimulus frequency (Roberts et al., 1990; Avissar et al., 2007). In order to keep the temporal precision required for the, some times extreme rate of transmission - i.e., in the cochlear nucleus of the barn owl phase locking was observed for frequencies up to 9000 Hz. (Sullivan and Konishi, 1984)- these synapses need to reduce their temporal jitter <80 μs (Avissar et al., 2007). Therefore, it is not surprising that some K_{Ca} channels locate next to calcium channels so that signalling is not limited by the time of Ca^{2+} diffusion from the channel mouth (Roberts et al., 1990; Roberts, 1993, 1994; Müller et al., 2007).

The intracellular calcium concentrations "sensed" by K_{Ca} in frog hair cells varied between 10 μM to 1 mM, over the physiological range of membrane potentials (Roberts et al., 1990), indicating that, at least some K_{Ca} channels had to be located within 10-20 nm from calcium channel mouths (Roberts et al.,1990, Roberts, 1993; Müller et.al., 2007). Moreover, K_{Ca} currents lag behind the rising phase of the calcium current by 39 μs, peaking within 50-100 μs and lagging behind the falling phase of I_{Ca} by 50-300 μs (Yazejian et al., 2000), making these channels the most accurate tools to follow quantitatively the time course of Ca^{2+}-buildup and decay during Ca^{2+}-transients that evoke neurotransmitter release (onset of release some 130 μs after K_{Ca}).

Such temporal acuity implies that K_{Ca} sensing high $[Ca^{2+}]_{int}$ are located within 20 nm of the calcium source. But it also implies the existence of fast calcium removal or buffering mechanisms to lower $[Ca^{2+}]_{int}$ immediately after calcium channel closure.

Roberts (1993) showed that native buffers reduced K_{Ca} activity in the frog saccular hair cells similarly to 1.6 mM concentration of the rapid calcium buffer, BAPTA, while EGTA was without effect, concluding that spatial buffering reduces the pre-synaptic free Ca^{2+} within the microdomain by up to 60% and restrict elevated $[Ca^{2+}]_{int}$ exceeding 1 μM under 250 nm of each synaptic site. Buffering can thus influence both electrical resonance and synaptic transmission by confining the large calcium transient to a very narrow zone of axoplasm in the immediate vicinity of the plasma membrane.

1.6. Buffering participates in local calcium transient definition: The nanodomain

The answer to how close are Ca^{2+}-sensors to the calcium source and how can a terminal evidence such temporally defined microdomains was demonstrated by the use of BAPTA. This calcium chelator was able to attenuate transmission whereas EGTA could not (Adams et al., 1985; Adler et al., 1991.; Roberts, 1993). These two calcium chelators have similar affinity for calcium (Kd~100 nM) and similar diffusional mobility (~20 μm^2 sec^{-1}). However, they markedly differ (~500 fold) in their activation kinetics (K_{on}) with BAPTA being faster (K_{on}= 6 x 10^8 M^{-1} s^{-1}) than EGTA (K_{on}= 1.5 x 10^6 M^{-1} s^{-1}) (Tsien, 1980). This results in a reduction by 60-95% in $[Ca^{2+}]_{int}$ from 1 mM within 100 nm with BAPTA (Roberts, 1993,1994; Müller et al., 2007), whereas an attenuation of only 10 % would occur without any buffer, or with EGTA at those distances (Roberts, 1993). This difference is enhanced by the fact that Ca^{2+} ions have a diffusion mobility of ca. 200-300 μm^2 sec^{-1} and need only ~30 μs to reach ~90% steady-state concentration at ~10-50 nm but take >1ms to reach equilibrium at 200-550 nm, where EGTA is an effective buffer (Roberts, 1993; 1994; Yazejian et al., 2000; Müller et al., 2007). This difference in the spatio-temporal definition of $[Ca^{2+}]_{int}$ profiles gave rise to the definition of the nanodomain (<20nm), corresponding to a calcium signal provided by a single channel and where BAPTA is somewhat an effective buffer (at high concentrations). While the microdomain represents a broader signal arising from several nearby channels in the same active zone (~200nm), where EGTA can effectively hinder Ca^{2+} action (reviewed in: Neher, 1998; Augustine et al., 2003).

Parvalbumin and calbindin-D_{28K} are common endogenous mobile buffers. While parvalbumin binds Ca^{2+} and diffuses more slowly than BAPTA or EGTA (Schmidt et al., 2003), calbindin binds Ca^{2+} ~2 times slower than BAPTA and have similar diffusion kinetics as EGTA or BAPTA (Nägerl et al.,2000; Burrone et al., 2002; Müller et al., 2007). Mobile buffers act by binding Ca^{2+} thereby inactivating it. Ca^{2+}-bound buffers diffuse away from calcium entry and in the reverse reaction will unbind calcium. This process is called buffered diffusion. Endogenous mobile buffer concentration ranges from ~50 μM in hippocampal neurons to 1 mM in low frequency turtle cochlear hair cells hair and 3 mM in high frequency cells.

Roberts (1994) modelled the action of fix and the mobile buffer, calbindin-D_{28K}. He considered an initial concentration of Ca-binding sites of 2 mM (~0.5 mM Calbindin), bearing a mean time capture for calcium of ~3.3 μs considering a Kd for Ca^{2+} ~1 μM.

Low calcium entry (I_{Ca}= 0.8 pA) can be substantially buffered (<10 μM from ~200 μM) within the first 50 μs of Ca^{2+} entry by fix or mobile buffers, without depletion. After calcium channel closure however, while the mobile buffer reduces calcium <1 μM in 10 μs, a fix buffer would actually maintain 10 μM Ca^{2+} by slow unbinding for as much as 10 ms.

High calcium entry (I_{Ca}= 8 pA) cannot be buffered by either fix or mobile buffer, depleting either one within 100 μs. After channel closure the mobile buffer maintains buffering capacity to <1 μM but only within 1 ms while the fix buffer also maintains the ability to keep $[Ca^{2+}]_{int}$ >10 μM for 100 ms.

In keeping with these predictions, Kreiner and Lee (2006) described some paradoxical effect of buffers in preventing or potentiating calcium-dependent Ca^{2+} channel inactivation (CDI). Low concentrations of EGTA (0.5 mM) induced CDI, while 10 mM BAPTA prevented it. But if 0.5 mM BAPTA was used inactivation was significantly greater. Similarly, HEK 293T cells transfected with either parvalbumin or calbindin were submitted to stimulation. At low frequency, both parvalbumin and calbindin prevented channel inactivation. But at higher frequency, parvalbumin induced more inactivation than without transfection. Slower kinetics and diffusional mobility seem to take part in this calcium induced inactivation (desensitization) of calcium channels.

These results argue to functional differences between active zones endowed with either parvalbumin or calbindin. For instance, while hair cells seem to prefer rather high concentrations of calbindin to keep ~19 active zones releasing at rates that often exceed 1000 Hz. The downstream calyx of Held synapse seems to prefer parvalbumin to reduce the time course of $[Ca^{2+}]_{int}$ and paired pulse facilitation (Müller et al., 2007). Interestingly, this synapse is strongly depressed after high frequency firing (Forsythe et al., 1998), while low to intermediate frequencies (2-30 Hz) were shown to induce calcium current inactivation and consequent short-term synaptic depression. Curiously, the calyx of Held holds hundreds of small active zones synapsing onto a single, large neuron (Moser et al., 2006), and needs particularly low $[Ca^{2+}]_{int}$ to activate secretion (Schneggenburger and Forsythe, 2006). Parvalbumin arises as an important participant in synaptic integration in cerebral cortex since its expression in the course of development in cerebellum synapses adds a slow phase that summates during bursts of action potentials (Collin et al., 2005).

Roberts (1994) modelled also different $[Ca^{2+}]$ landscapes according to intra-terminal conditions. Figure 2 shows steady state calcium concentrations at 5 nm distance from

individual channels $[Ca^{2+}]_{ss}$ in a microdomain. Figure 2 (A) shows all 85 calcium channels in an active zone (projected in the plane as closed symbols next to K_{Ca} channels with open symbols) where ~12 % of single channel current was assigned to each one ~0.094 pA. In figure 2 (B) the same total current (8 pA) was assigned to 10 channels only (0.8 pA each) in the presence of mobile buffer (figure 2, B). Notice that the K_{Ca} channels (open symbols) are subjected to much higher local $[Ca^{2+}]_{int}$.

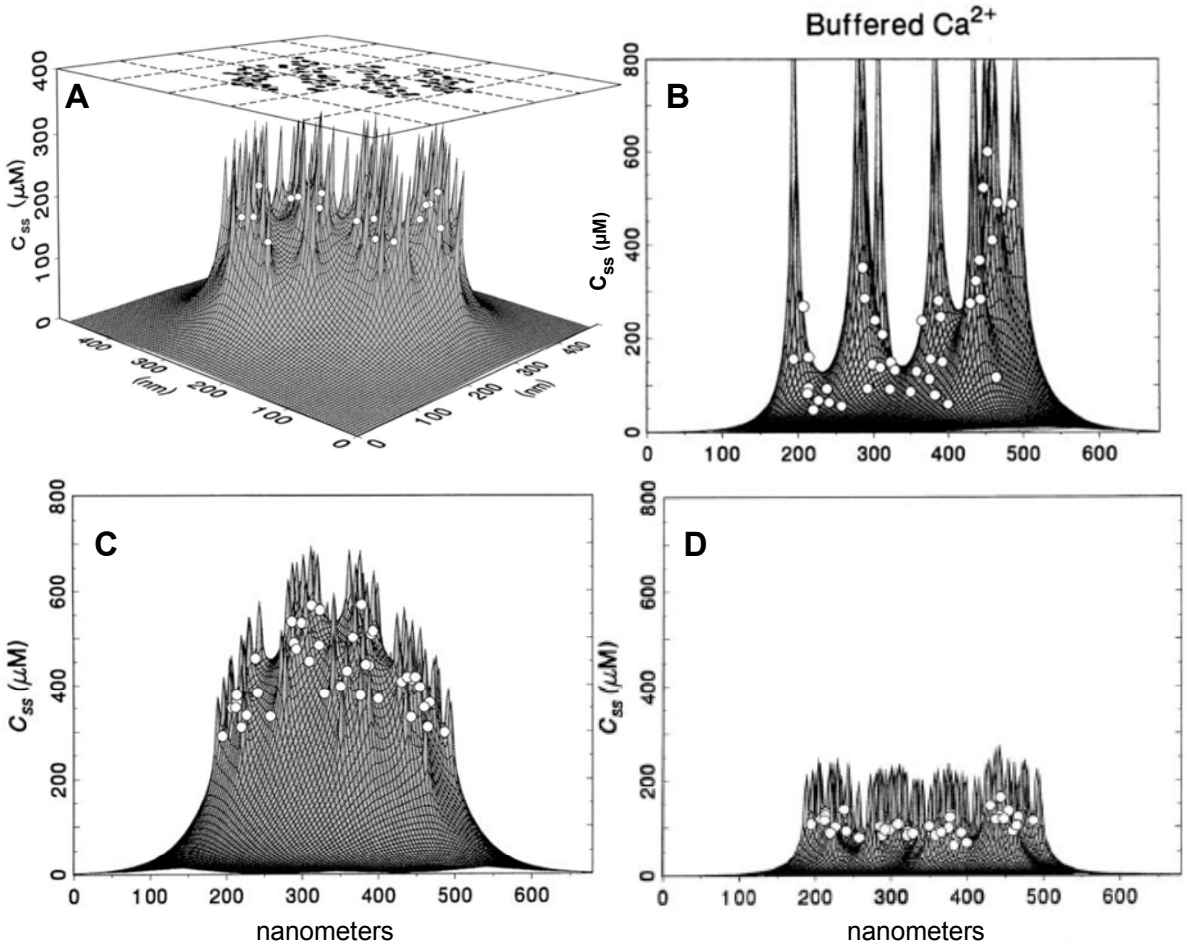

Figure 2. Steady state calcium concentration landscape within 5 nm of the membrane (97 x 97 array of 5 nm cubes) occurring within microdomains under different conditions. A total of 8 pA calcium current was divided by all 85 Calcium channels (black dots projected in the plane in (A) consisting of the "time-averaged" calcium topography (in A, C and D); alternatively, the 8 pA current was divided by 10 channels only and consisted of the "frozen" calcium topography in (B). Open circles represent the local $[Ca^{2+}]$ concentration sensed by K_{Ca} channels depending on their relative position to calcium channels within a microdomain (projected in the plane in (A). Simulations in (C) and (D) consider the existence of a barrier placed 40 nm away from plasma membrane behaving like a diffusion-limiting (to Ca^{2+} and buffer) barrier in (C) or like an unsaturable buffer in (D). Adapted from Roberts (1994).

Most interestingly still was the result of the model when the effect of having placed at 40 nm away from the membrane a diffusional barrier (figure 2, C) or an unsaturable sink (figure 2, D). This barrier or sink could represent the pre-synaptic body present in hair cells, like retinal photoreceptors, frog sacculus or some pineal neurons (Roberts, 1994). Alternatively, it could represent synaptic vesicle(s) found in close opposition to the calcium channel cluster(s) that could serve as a barriers as suggested by Shahrezaei and Delaney (2005).

In presence of a diffusional barrier (figure 2, C) for the buffer and for Ca^{2+} there was a generalised rise of $[Ca^{2+}]_{int}$ (~420 μM), and complete decrease in unbound mobile buffer concentration. On the contrary (figure 2, D), placing a sink permeable to Ca^{2+} and "transparent" to the buffer, so close to the cluster had major effects on the calcium concentration, even though calcium concentration 5 nm away from the membrane still reached 105 μM with an unsaturable sink 40 nm away. Such a sink could represent Ca^{2+} binding sites in the synaptic body (Roberts, 1994), or the action of putative high-speed calcium transport systems in synaptic vesicles. Interestingly, the actual calcium concentration reported by K_{Ca} channels for 8 pA I_{Ca} was 520 μM (Roberts, 1993), which goes in the direction of the effects of a barrier.

1.7. Synaptic vesicles in active zones

Despite some variability in active zone structures (Zhai et al., 2004) all synapses are characterised by having an array of synaptic vesicles in close proximity to the membrane. Even secretory neuroendocrine, chromaffin or neuropeptidergic secreting cells without specialized synaptic contacts, have vesicles and granules placed at larger intervals (300-600 nm) with calcium channels, as indicated by the sensitivity of secretion (Klingauf and Neher, 1997) or K_{Ca} activity to EGTA (Prakriya et al.,1996). Yet, there seems to be a population of ~10% of calcium sensors near calcium entry sites, responding with faster fusion of the ready releasable pool of vesicles (Voets et al., 1999) or ~10-20% K_{Ca} capable of reporting local $[Ca^{2+}]_{int}$ 6 times higher than that reported when all K_{Ca} channels are activated (Prakriya et al., 1996). This is in accordance with small near-synchronous transmitter release by a single action potential whereas a train of action potentials leads to large, desynchronized release (Fulop et al., 2005). These results are compliant with longer latency for most vesicles and

slow decay of Ca^{2+} transients in the order of the tens of milliseconds for calcium channels disposed 300-600 nm apart (Klingauf and Neher, 1997; Voets et al., 1999).

There is a clear distinction between fast synchronous neurotransmission and slow asynchronous secretion that points toward diversity in the geometric arrangement of calcium channels, vesicles, and Ca^{2+}-sensors, leading to the wide spectrum of Ca^{2+}-signals and kinetic components of release and exocytosis. For instance, in the calyx of Held the Ca^{2+}-sensor for transmitter release distances between 30 nm-300 nm (average is 100 nm) from the calcium source, with local $[Ca^{2+}]_{int}$ varying from 0.5 to 40 μM between those distances, and release probability ranging from <0.01 to 1, respectively (Klingauf and Neher, 1997; Voets et al., 1999).

On the other hand, other phasic synapses working at higher rates, like those of cochlear hair cells, or with low affinity Ca^{2+}-sensors for transmitter release, like the mediatophore at the neuro-electrocyte junction of the electric organ of *Torpedinae* seem to relate far more closely with calcium entry sites to produce synchronous responses.

Synapse geometry integrates with other factors affecting the space-time definition of transmitter release like the affinity of the Ca^{2+}-sensor, mobile buffer capacity, desensitization or inactivation of transmitter release or calcium entry apparatuses and calcium extrusion capability.

Calcium enters the cell through channels at a rate that is considered to be much higher than rates attainable by pumps and exchangers. Calcium extrusion at the plasma membrane is achieved through Na^+/Ca^{2+} antiporters in conjunction with Ca^{2+}-ATPases in plasma membrane or in the endoplasmic reticulum (maximum rate at 37 °C ~1 μM/s (Villalobos et al., 2002) which is close to the rates reported for endoplasmic reticulum Ca^{2+}-ATPase alone (Villalobos et al., 2002). Under low frequency stimulation, these are the main responsible for keeping low resting $[Ca^{2+}]_{int}$. Under stronger stimulus, mitochondria also participates in Ca^{2+} extrusion (Friel and Tsien, 1994; Herrington et al., 1996; Zenisek and Mathews, 2000; Villalobos et al., 2002; Kim et al., 2005), through the action of a high capacity Ca^{2+}-uniport, with exponential $[Ca^{2+}]$ dependencies and maximal Ca^{2+}-transport rates of 160 μM/s (for $[Ca^{2+}]$=100 μM). This uniport seems to work as an ion channel selective for $Ca^{2+}=Sr^{2+} >> Mn^{2+}= Ba^{2+}$ (Kirichok et al., 2004). Mitochondria have also a Na^+/Ca^{2+} exchanger capable of releasing Ca^{2+} from loaded mitochondria at ~20 μM/s (Villalobos et al., 2002). The rather high calcium concentrations reached near mitochondria seem to derive from "privileged" interplay between

mitochondria and the endoplasmic reticulum, rather than active zones (Rizzuto and Pozzan, 2006). The same happens with plasma membrane Na^+/Ca^{2+} antiport localised away from active zones near endoplasmic reticulum, while the plasma membrane Ca^{2+}-ATPase co-localizes with the vesicular marker synaptotagmin (Juhaszova et al., 2000).

Synaptic vesicles are the hallmark structures of synaptic active zones (Couteau and Pécot-Dechavassine, 1970, 1974) occupying a larger volume fraction than any other organelle (Oheim et al., 2006). Their volume was estimated by electron microscopy in tissue and in synaptosomes to be ~20% of total volume (Israël, 1972; Morel et al., 1980). Other secretory systems like neuroendocrine cells, chromaffin granules or peripheral neuropeptidergic terminals do not contain obvious morphological specializations but contain large amounts of vesicles, occupying ~20% of cell volume as well (Garcia et al., 2006). In most of these structures, small electronlucent (synaptic-like) vesicles are described in addition to the large, dense core granules or vesicles.

Synaptic vesicles are also spheric and rather small - mean diameter ~41.6 nm, according to Takamori et al. (2006) - therefore maximizing their surface to volume ratio and providing an immense membrane surface area in close proximity of Ca^{2+} ions entering an active zone that one would expect to find an intracellular store of large uptake, and release capacity.

Isolated *Torpedo* synaptic vesicles were reported to accumulate calcium through a Ca^{2+}-ATPase and accumulate up to 14 mM Ca^{2+} within the organelles (Israël et al., 1980; Michaelson et al., 1980; Rephaelis and Parsons, 1982).

Calcium transiently accumulates in synaptic vesicles of *Torpedo* electric organ submitted to brief stimulation (Párducz and Dunant, 1993; Párducz et al., 1994). Similarly, stimulation of chromaffin cells increases simultaneously cytoplasmic and vesicular calcium accumulation where total calcium reaches ~20-40 mM with >99% in "bound" state (Mahapatra et al., 2004). On the other hand, a robust Ca^{2+} release from pancreatic acinar cell granules can be elicited by nicotinic acid adenine dinucleotide phosphate (NAADP); cyclic ADPribose (cADPR) or inositol (1,4,5) triphosphate (IP_3) (Gerasimenko et al.,2006) that is capable of eliciting a combined Ca^{2+}/H^+ intracellular signal from mast cell granules (Quesada et al., 2003). Therefore vesicles can accumulate and secrete Ca^{2+}.

Besides participating in intracellular signalling, vesicular calcium seems to be of the up most importance in the process of rapid calcium turnover in excitable cells both at rest

(Babel-Guérin, 1974; Dunant et al., 1980b; Marsal et al., 1980) and specially upon stimulation (Babel-Guérin, 1974; Dunant et al., 1980b; Marsal et al., 1980; Borst and Sakmann, 1999) where it allows for the fast replenishment of the few Ca^{2+} ions accomodable in a synaptic cleft by Ca^{2+}-filled vesicle exocytosis (Párducz and Dunant, 1993; Párducz et al., 1994; Borst and Sakmann, 1999).

To accompany the Ca^{2+}-turnover rates expected to occur under heavy stimulus one should expect fast, high capacity calcium transport systems. Synaptic vesicle/secretory granule membranes have several channels with pore conductances ranging from 13 pS up to 350 pS (For a review see Woodbury, 1995; Meir et al., 1999) , including large, non-selective and Ca^{2+}-permeable voltage gated channels (Meir and Rahamimoff 1996), rapid (<1ms) Cl^- channels operating in bursts (Rahamimoff et al., 1988), channels activated by low SV-lumen [ATP] (Ahdut-Hacohen et al., 2006) and a Ca^{2+}-modulated channel that seems to be coded by synaptophysin under the control of other Ca^{2+}-binding proteins like synaptotagmin I (Lee et al., 1992; Yin et al., 2002).

The number of ions transported through these channels could approach that of Ca^{2+}-ions entering by VOCCs considering appropriate conditions of driving force and mean open time (Meir and Rahamimoff, 1996). Such large vesicular ion flux raised the proposition that the regulated activity of these channels could participate in pre and post-fusion regulation of transmitter release (Rahamimoff and Fernandez, 1997). The proposition is based on the observation that several secretory systems rely on a negatively charged intravesicular matrix to store large quantities of positively charged secretory molecules (Rahamimoff and Fernandez, 1997).

In general, matrices act as "smart" hydrogels (Tanaka 1981) and behave as cation exchange resins (Uvnäs and Åborg, 1983, 1989) that condensate when their internal electrostatic repulsion is reduced by trivalent and sometimes divalent cations and decondensate when mobile ions are exchanged for monovalent cations and the proteoglycan matrix expands as it gets hydrated by the increase in osmotic pressure (Verdugo, 1990; Curran and Brodwick, 1991; Fernandez et al., 1991; Parpura et al., 1996; Reigada et al., 2003).

Secretory molecules behave as divalent cations at acidic pH but could become monovalent cations at neutral pH (Uvnäs et al., 1970) thereby promoting the condensation of matrices (assisted by other divalents like Ca^{2+}) and behave as single particles at low pH. This

solves the problem raised by Katz (1969) of having prohibitive hyperosmotic concentrations of transmitters within the acidic vesicular space.

Pre and post-fusion control of release depends on the type of ion exchange, hydration and proteoglycan constitution. For example, the exocytotic release of histamine and serotonin from mast cell secretory granules; of catecholamines and ATP from chromaffin cell large dense core vesicles or the secretion of zymogen granule content in exocrine pancreas rely on K^+ ions in the pre-exocytotic phase and/or Na^+ ions in the exocytotic phase to displace molecules from their matrices by ion exchange as well as to promote vesicle swelling (Uvnäs and Åborg, 1987; 1989; Jena et al., 1997; Marszalek et al., 1997).

When secretion relies on fusion an explosive change of matrix molecular phase from condensated to the hydrated phase triggered by replacement of intravesicular Ca^{2+} with extracellular Na^+ would release secretory contents as in a "jack-in-the-box" and promote matrix swelling upon hydration (Verdugo, 1991). However, the diffusivity of a transmitter within a gel matrix (1.3×10^{-8} cm^2/s; Marzalek et al., 1996) is almost three orders of magnitude slower than in water ($\sim 10^{-5}$ cm^2/s; Almers et al, 1989) and would impose the emptying of a 50 nm wide vesicle in ~10 ms (Rahamimoff and Fernandez, 1997).

Rapid secretory systems work at sub-millisecond kinetics and rely on pores. The amount of transmitter releasable by a large conductance pore would be set by the availability of transmitter at the channel mouth and channel opening time (Almers et al., 1989; Dunant, 1994).

Oxidizable transmitter molecules were shown to be released by a transient form of fusion proposed initially by Ceccarelli et al. (1973) and later named kiss-and-run (Alvarez de Toledo et al., 1993; Valtorta et al., 2001). It was proposed that the pool of oxidizable transmitter that is readily releasable is dissolved in the liquid or halo fraction of PC12 (Sombers et al., 2004), adrenal chromaffin (Borges et al., 1997; Troyer and Wightman 2002) or beige mouse mast cell (Alvarez de Toledo et al., 1993; Troyer and Wightman, 2002) vesicles rather than associated with the dense core matrix and it could be determined by pre-fusion ion exchange with the matrix (Rahamimoff and Fernandez, 1997).

The amount and duration (in ms) of kiss-and-run release is directly related with vesicular volume and transmitter content while kiss-and-run frequency is inversely related to those parameters (Sombers et al., 2004). Kiss-and-run increases when cells are exposed to

high calcium (Alés et al., 1999) and depend also on synaptotagmin expression (Wang et al., 2003).

The fastest modes of secretion occur in the time scale of the few hundred microseconds (Dunant and Muller, 1986; Girod et al., 1993; Sabatini and Regehr, 1996; Yazejian et al., 2000) where the temporal jitter must be reduced to a minimum while maintaining a steady response even at high frequencies (Avissar et al., 2007).

In *Torpedo marmorata* electric organ synapses, the release of ACh from the cytoplasmic pool through mediatophores guarantees highly synchronised release with sub-millisecond precision (Israël et al., 1986; Muller et al., 1987; Brochier et al., 1992; Dunant and Israël, 2000). ACh molecules are released from a rather large cytoplasmic pool (ca. 27 mM; Dunant et al., 1974; Katz and Miledi, 1977) through plasma membrane mediatophores. The advantage is obvious: cytoplasmic ACh is free to diffuse at high speed (close to diffusion in water = ~10^{-5} cm^2/s; Almers et al., 1989) through the proteolipidic pore, fed by the enormous cytoplasmic pool. The terminal releases a precise amount of transmitter that is determined mainly by the mean opening time of mediatophores since free transmitter is considered to be available close to mediatophore channel mouths instead of having to be displaced from any molecular cage by ion exchange prior to secretion.

However, *Torpedo* electric organ nerve terminals are rich in synaptic vesicles that accommodate ~100,000-200,000 ACh molecules as well as ATP and varying number of calcium ions totalling ~800 mM ACh and ~120 mM ATP (Reviewed in Rahamimoff and Fernandez, 1997). The copious number of positive ACh charges are partially "neutralized" by interaction with the negative ATP and by complexation with a keratan sulfate proteoglycan matrix composed mainly of the highly glycosilated SV2 proteins (Stadler and Wittaker, 1978; Scranton et al., 1993; Reigada et al., 2003) as well as Svp-25, o-rab3 and VAT-1 proteins (Volknandt et al., 1990; Linial et al., 1995; Hausinger et al., 1996). Over 95 % of the vesicular ACh and ATP are tightly bound to the vesicular matrix with only a very thin layer of loosely bound transmitter molecules within each vesicle (Marchbanks and Israël, 1972; Reigada et al, 2003).

Calcium ions are able to displace ACh and ATP molecules from the vesicular matrix 10x more efficiently than Na^+ ions (300 Ca^{2+} ions needed against 3000 Na^+ to empty an SV; Reigada et al., 2003). Concordantly, calcium accumulation into synaptic vesicles of stimulated neuro-electric *Torpedo* synapses is accompanied by a decrease in vesicular ACh content

Marchbanks and Israël, 1972; Babel-Guérin, 1974; Dunant et al., 1980b; Diebler, 1982) that is particularly visible under very intense stimulation (Schmidt et al., 1980).

On the contrary to chromaffin cell granules and zymogen granules where calcium decreases the vesicular membrane elastic modulus, calcium accumulation within *Torpedo* vesicles increases the vesicular elastic modulus determined by hard vesicular central cores that correlate with decreased vesicular volume (Laney et al., 1997). Three distinct populations of synaptic vesicles were reported in the electric organ of Torpedo. VP0 are rather empty and actively accumulate ACh and ATP; VP1 represent the fully matured synaptic vesicle population, fully charged with transmitters displaying little ACh transport but active Ca^{2+}-uptake. Finally, the VP2 SV population, that occur mainly after stimulation, are smaller (less 25% in diameter), denser and regain active ACh and ATP accumulation capacities while loosing Ca^{2+}-transport activity (Kiene and Stadler, 1987; Stadler and Kiene 1987; Bonzelius and Zimmermann, 1990).

The transition from VP1 to VP2 vesicles was originally proposed to represent a pool of recently endocytosed vesicles devoid of ACh and filled with extracellular calcium (Kiene and Stadler, 1987). An alternative hypothesis combines (1) transient calcium rise within stimulated synaptic terminal (2) calcium entry into VP1 ACh-rich synaptic vesicles before vesicular fusion (Párducz and Dunant, 1993; Párducz et al., 1994) (3) dissociation of ACh from the internal matrix by Ca^{2+}-ACh exchange (Reigada et al., 2003) (4) shrinkage of vesicular matrix by glycosaminoglycan cross-linking facilitated by ACh/ATP unbinding and Ca^{2+} binding to the matrix under dehydrated conditions (Laney et al., 1997; Sombers et al., 2004) (5) ACh leakage into the cytoplasm by a yet unknown concentration-dependent mechanism (Williams, 1997) that could well be the choline transporter existing between 70-90% in synaptic vesicles (Ferguson et al., 2003, 2004; Nakata et al., 2004), is permeable to ACh at high concentrations (Marchbanks, 1969; Marchbanks and Wonnacott, 1979), is positioned to transport ACh out of the vesicles and is homologous to the Na^+-glucose transporter that can replace Na^+ with H^+ (Hirayama et al., 1994).

The mechanism of ion exchange would guarantee a stimulus-dependent supply of ACh out of the vesicular matrix into the cytoplasm near release sites (where synaptic vesicles are) thereby preventing transmitter rundown under intense stimulus (diminished flow of ACh due to decreased cytoplasmic concentration) at the same time that Ca^{2+} ions are extruded from the cytoplasm into vesicles and gets "packed" into the vesicular matrix until fusion delivers it back into the synaptic cleft. After exocytosis Ca^{2+}/Na^+ ion exchange from the matrix would

be promoted by the high Na^+ concentration at the same time that new choline transporters are placed in the membrane after a stimulus. Na^+ binds the proteoglycan matrix with ~10x less affinity than Ca^{2+} (EC_{50}=~0.27 mM for Ca^{2+} against ~2.6 mM for Na^+; Reigada et al., 2003) a fact that would favour refilling of recently endocytosed vesicles with transmitters (ACh and ATP) while regenerating the calcium retention capacity of those vesicles.

Two Ca^{2+} transport systems (figure 3) have been identified and characterized in synaptic vesicles isolated from brain cortex (Gonçalves et al., 1998, 1999a, 1999b, 2000a). An orthovanadate-inhibited P-type Ca^{2+}-ATPase with higher apparent affinity ($K_{0.5}$= 0.6 μM), and maximum velocity (1.9 nmol/min/mg protein) at 25 μM Ca^{2+} (pH 7.4), that declines to ~½ at 100 μM and is completely inhibited at [Ca^{2+}]>200 μM.

The other vesicular Ca^{2+} transport system is a Ca^{2+}/H^+ antiport, a low affinity system with a $K_{0.5}$= 217 μM and maximum velocity (1.9 nmol/min/mg protein) at 500 μM Ca^{2+}. In contrast to the Ca^{2+}-ATPase, the antiport shows only modest activity at 100 μM Ca^{2+} (~1/3 that of Ca^{2+} ATPase at same [Ca^{2+}]) , but increasing sharply for [Ca^{2+}]>200 μM up to 500 μM and slowly declining thereafter to ~½ at 1 mM Ca^{2+}. There are other cations capable of displacing H^+ from synaptic vesicles with decreasing affinity that seems to depend on their dehydrated ionic radius, with activities of Zn^{2+} > Cd^{2+} > Ca^{2+} while larger ions like Sr^{2+} Ba^{2+} or Cs^{2+} are excluded by the selectivity filter of the H^+ displacement mechanism (Gonçalves et al., 1999a). It is important to notice that vesicular Ca^{2+} uptake by the antiport is inhibited by Zn^{2+} and Cd^{2+} (transported by the antiport) but also by Sr^{2+} (500 μM), that apparently, is not transported.

Therefore, synaptic vesicles possess two calcium (figure 3) transportation systems: A Ca^{2+}-ATPase that relies on metabolical energy for Ca^{2+} pumping and a Ca^{2+}/H^+-antiport energised by the vesicular transmembrane gradient generated by the V-type H^+-ATPase which is inhibited by bafilomycin A1 (Tanaka et al., 1976; Stadler and Tsukita, 1984.; reviewed by Beyenbach and Wieczorek, 2006).

Together, the antiport and the ATPase endow vesicles with the possibility to pump Ca^{2+} out of the active zones and into the vesicles with unperturbed efficacy from the near millimolar [Ca^{2+}] up to low micromolar concentration, that gets further extruded by higher affinity ($K_{0.5}$= 0.017 μM) systems like the endoplasmic reticulum Ca^{2+}-ATPases (Gonçalves et al., 2000).

Having addressed the question of what are the functional implications of vesicular calcium transport, it is perhaps intuitive to address the question of: Who?

Recently, we were presented with the very first description of the so-called "molecular anatomy" of the trafficking organelle: synaptic vesicle. Far from trying to describe all the different aspects of particular vesicles and granules in individual systems it points to the establishment of the main proteins and lipids composing an "average" synaptic vesicle (Takamori et al., 2006).

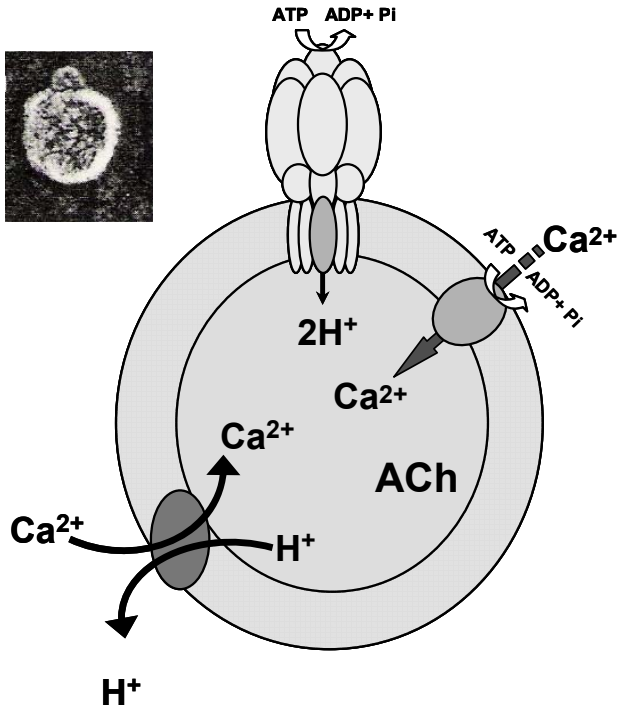

Figure 3. Schematic view of the complementary calcium transport systems existent in synaptic vesicles. Figure illustrates an ATP-dependent P-type ATPase (right) and the secondary active transporter Ca^{2+}/H^{+} antiport (left) that is energized by the transmembrane H^{+} gradient provided by the large macromolecular V-type H^{+}-ATPase at the centre. Inset shows an electron micrograph from the original study of Stadler and Tsukita (1984) showing a synaptic vesicle isolated from guinea pig brain with a "knob-like" protrusion corresponding to the H^{+}-ATPase. Functional details about vesicular Ca^{2+} transport are in the text.

The picture arising from that work (figure 4) is that of a round organelle, with 41.6 nm in diameter and packed with a dense array of transmembrane proteins covering at least 20% of the vesicular surface area and proposed to be organized in patches surrounded by lipidic rims instead of evenly distributed. One of the surprising findings is that despite the extensive list of ubiquitous and vesicle specific proteins, there is only a hand full of them that

dominate either in mass or in number. The "average" organelle has ~70 copies of synaptobrevin 2 (VAMP2); ~30 copies of synaptophysin; 15 copies of synaptotagmin I; similar number of copies of vesicular neurotransmitter transporters (14 copies) and few copies of other proteins, including SV2 (~2 copies) and 1 or 2 copies of V-type H^+-ATPase that, nevertheless, accounts for ~10-20% of vesicular protein (Takamori et al., 2006).

With the original hypothesis being that synaptic vesicle proteins have already been described previously (for detailed references see Takamori et al., 2006), the preliminary task sits on choosing the candidate fitting the characteristics of the transport systems described in synaptic vesicles. Among the proteins described in vesicles there is one that could become the next vesicular Ca^{2+}/H^+ antiport to be included on a "molecular anatomy" of an organelle. The question is then, which one?

VAMP is the vesicular counterpart of the SNARE complex (involving plasma membrane proteins syntaxin and SNAP25) that forms the minimal machinery for membrane fusion (Sollner, 1993; Rothman, 1994).

Synaptophysin was proposed to be a voltage-sensitive 150 picosiemens channel putatively implicated in the uptake or release of transmitters (Thomas et al., 1988; Woodbury, 1995) it interacts also with VAMP and the V0 sector of the V-type H^+ATPase (Galli et al., 1996), as well as the physophiline (Thomas and Betz, 1990; Siebert et al., 1994), that also interacts with the mediatophore and with the fusion pore (Peters et al., 2001; Bajjalieh, 2005; Hiesinger et al., 2005), therefore synaptophysin could be important for bringing about two hemichannels (one at the vesicle and another at the plasma membrane) in close apposition to form a proteinacious fusion pore.

SV2 is a highly glycosilated protein endowed with 12 transmembrane domains and has been proposed as a calcium transporter (Bajjalieh et al., 1992). Yet, despite the efforts, no substrate was been found for SV2 (Xu and Bajjalieh, 2001; Iezzi et al., 2005).

However, SV2 glycosilated intravesicular domains were proposed as neurotransmitter traps to diminish intravesicular osmotic pressure (Alvarez de Toledo et al., 1993) but also to bind calcium in exchange for transmitter within the vesicular matrix (Reigada et al., 2003).
The V-type H^+-ATPase comprehends a macrostructure with two subunits: V0 is the pore-forming subunit and V1 the catalytical sub-unit. The assembly/disassembly of V0/V1 regulates the pump and is itself regulated by Ca^{2+} (Kane, 2000; Crider and Xie, 2003). As stated above the V0 subunit comprises the elements of a proteinaceous fusion pore. However, the 15 kDa

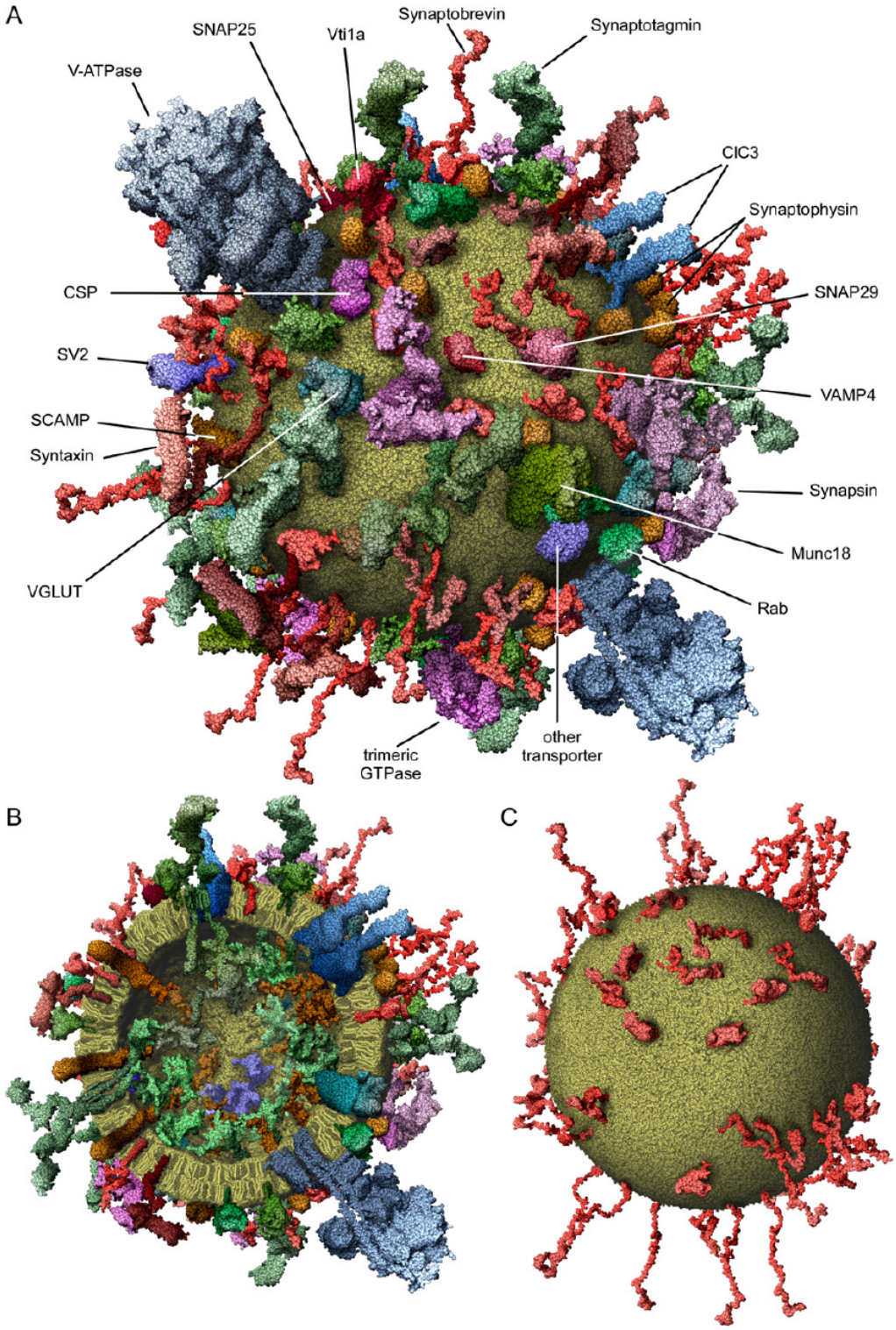

Figure 4. Molecular model of an average synaptic vesicle. Model is based on space-filling models of all macromolecules at near atomic resolution. ***A*** Outside view of an SV. **B** View of a vesicle sectioned in the middle (the dark-coloured membrane components represent cholesterol). ***C*** Model containing only synaptobrevin to show the surface density of the most abundant vesicle component. From Takamori et al. (2006).

monomeric units homologous to the c-subunit of the V0-sector of V-ATPase also compose the multimeric 220 kDa mediatophore (containing 15 monomers) (Israël et al., 1986; Muller et al., 1987; Brochier et al., 1992; Dunant and Israël, 2000). Both the mediatophore and V0 are oligomers composed of proteolipid subunits of 15-16 kDa, present both in the vesicular and plasma membranes. They can be extracted by chloroform-methanol, but not by the usual techniques used for membrane proteins (Israël et al., 1986; Muller et al., 1987; Brochier et al., 1992; Dunant and Israël, 2000) and for that reason are sometimes overlooked (Takamori et al., 2006).

Finally, synaptotagmin I (Syt I) is an integral vesicular protein with a short intraluminal N-terminal, a transmembrane segment and a cytoplasmic domain endowed with two Ca^{2+} binding modules, C2A and C2B (Reviewed by Chapman, 2002). Intrinsic affinity of C2 domains for Ca^{2+} is low. C2A binds three Ca^{2+} with Kd values of ~60 μM, 400 μM and >1mM, whereas C2B binds two Ca^{2+} ions with Kd ranging from 300-600 μM. Yet, some synaptotagmin I Ca^{2+}-dependent interactions occur at lower Ca^{2+} concentrations in situ in virtue of interactions with lipids and proteins involved in the process of exocytosis in active zones of secretion (Chapman, 2002). C2A domain plunges into lipid bilayers with fast kinetics in response to high calcium (<50 μs at 200 μM Ca^{2+}) whereas C2A-C2B forms ring-like heptameric oligomers in response to high calcium ($[Ca^{2+}]_{1/2}$ = 140 μM) with sub-millisecond kinetics, early after Ca^{2+} entry and prior to interactions with fusion proteins (Davis et al., 1999; Wu et al., 2003). The Ca^{2+}-dependent oligomerization via the C2B domain of Syt I occurs only if the several monomers are preassembled at the amino terminal at the interface between the transmembrane and spacer domains of Syt I by a Ca-independent oligomerization step (Fukuda, M. and Mikoshiba, K., 2000; Fukuda et al., 2001).

Syt I is the most abundant member of a family of membrane-trafficking proteins with putative Ca^{2+} sensing modules (Südhof, 2002). It is also one of the most abundant proteins in vesicular membranes (~15 copies per vesicle according to Takamori et al., 2006) where its low affinity Ca^{2+}-dependent reactions lead to its recognition as being the calcium sensor for synchronous transmitter release.

The molecular basis of synchronous release is still a mater of debate. On one hand there is the possibility that molecules like Syt I, Syt II and Syt IX code for the synchronous phase of release while other, yet unidentified molecules, code for the asynchronous phase of release (Xu et al., 2007). Alternatively, synchronous release would represent the activation of

sensors in close proximity of Ca^{2+} channels while asynchronous release represents the activation of sensors further away from the Ca^{2+} source. Either way, the local [Ca^{2+}] affecting the Ca^{2+}-sensor will determine the degree of synchrony of secretion. Higher calcium transients traduce into faster responses by low affinity calcium sensors with fast on rates (Dunant and Israël, 1995; Dunant and Bloc, 2003; Otsu et al., 2004; Shahrezaei and Delaney, 2005; Moser et al., 2006; Schneggenburger and Forsythe, 2006; Dunant, 2006; Wadel et al., 2007). Conversely, the same low affinity will guarantee that the time course of transmitter release will follow closely the Ca^{2+} transient within the Ca^{2+}-nanodomain. Failure to restrain the calcium into a localized nanodomain might result in activation of calcium sensors away from the Ca^{2+} source and promote asynchronous while reducing synchronous release.

The slower rise and lower Ca^{2+}concentrations reached in those domains could also result in decreased Ca^{2+}-cooperativity (Dunant and Israël, 1995; Dunant and Bloc, 2003; Otsu et al., 2004; Shahrezaei and Delaney, 2005; Moser et al., 2006; Schneggenburger and Forsythe, 2006; Wadel et al., 2007). Mutations in Syt I C2B region were reported to display either reduced cooperativity, increased asynchronous release, or both (for reviews see: Koh and Bellen, 2003; Tokuoka and Goda, 2003).

Furthermore, Syt I is one of the main proteins interacting with phosphatidylinositol (PtdIns) polyphosphates (Osborne et al., 2007). These lipids represent ~2-5% of lipid/phospholipid composition of the vesicular membrane (Takamori et al., 2006) and have long been implicated in the process of secretion (Larrabee et al., 1963; reviewed by Cremona and De Camilli, 2001). The C2B domain of synaptotagmin binds preferentially phosphatidylinositol-3,4,5-phosphate (PtdIns-3,4,5-P3) at resting Ca^{2+} but shifts to PtdIns-4,5-P2 in high calcium (Schiavo et al., 1996). In turn, PtdIns-4,5-P2 were reported to modulate the bovine heart Na^{+}/Ca^{2+} antiport activity that depended also on the local H^{+} microenvironment (Posada et al., 2007). Ca^{2+} and H^{+}-sensitivity of PtdIns-4,5-P2-synaptotagmin I interactions could play an important role in the temporal definition of rapid Ca^{2+}/H^{+}-antiport activities with sub-millisecond and nanometric resolutions.

The control of vesicular calcium influx via activity (rather than gene expression) represents a form of regulation far more suitable to be integrated in the control of events allowing sub-millisecond secretion of transmitter molecules.

1.8. Objectives

Having come to this point of knowledge about the molecular participants involved in vesicular calcium transport it seemed natural to ask myself the question that has crossed many other's minds for the last 30 years about calcium transport into synaptic vesicle: So What?

Far from depreciative, the question gains body if we aim at looking for specific effects on the characteristics governing stimulus-secretion coupling and calcium homeostasis.

What will be the effects of having (or not) a Ca^{2+}-ATPase and a Ca^{2+}/H^{+}-antiport activity in synaptic vesicles, during and after a stimulus?

Will they contribute to general homeostasis within synaptic terminals?

Will they be able to have an effect on the faster calcium transient occurring at active zones?

Will they be able to affect the time course for the onset and offset of release?

Will they participate in the modulation of vesicular transmitter content?

What will be their action on synchronization or the desensitization of transmitter release and inactivation of calcium channels?

What will be the relative contributions of these two complementary Ca^{2+} transport systems for the above mentioned questions?

In the course of the work presented at this thesis these questions were always at the base of specific hypothesis and experimental design for they constituted some of the objectives of this work.

In this work we focused on vesicular calcium transport partners with the prospect of having the capability to intervene in processes with very rapid kinetics involved in rapid neurosecretion.

Since vesicular proteins have been extensively studied, we looked for characteristics that would include or exclude possible candidates capable of executing rapid Ca^{2+}-transport.

After all the inconsistencies and hurdles to presenting synaptotagmin I as a possible candidate for the vesicular Ca^{2+}/H^{+}-antiport activity were removed by the literature we gained a candidate that became an objective to accomplish in the course of this thesis.

2. Material and methods

2.1. Reagents

All reagents were of analytical grade. Unless otherwise indicated the reagents were from Sigma Co (Sigma-Aldrich).

2.2. Fish supply

Male and female *Torpedo marmorata* fish specimens with 25–60 cm in length were supplied by the Station Biologique, 29682 Roscoff, France. They were kept alive in a sea-water aquarium at 10°C until usage.

2.3. Experiments using whole fish; stimulation and recording

All experiments with *Torpedo marmorata* were conducted at 20°C. In experiments using intact living animals the electric discharge from an entire electric organ was registered with an oscilloscope connected to two large electrodes placed in contact with the ventral and dorsal faces of an electric organ (averaging ~50 cm^2 in surface). Reflex electrical discharges (as in figure 6 A) were elicited by stimulating mechano receptors in fish tail or dorsal-front borderline. The discharge (~43 V in figure 6 A) was recorded with the fish placed for a short while outside of the water.

2.4. Experiments using dissected tissue; stimulation and recording

2.4.1. Dissection of prisms

The animals were anaesthetised with tricaine methanesulphonate (Fluka, Switzerland) dissolved in sea water at a concentration of 3 g/l. Such anaesthesia is rapidly reversible and does not affect the synaptic transmission of the electric organ (Dunant et al., 1980a).

The electric organ tissue was sliced into smaller portions maintaining both dorsal and ventral skin and kept in an elasmobranch saline medium of the following composition: 280 mM NaCl; 3 mM KCl; 3.4 mM $CaCl_2$; 1.3 mM $MgCl_2$; 5 mM $NaHCO_3$; 20 mM 4-(2-hydroxyethyl)-1-piperazine-ethanesulphonic acid (HEPES) buffer; 300 mM urea; 5.5 mM glucose. The medium was gazed with 95% 02 and 5% CO_2 before the experiment; its pH was adjusted between 7.1 and 7.3 with NaOH. Small fragments of tissue composed of one or two intact stacks of

electrocytes were dissected from slices excised from the electric organ. Each stack, also named prism, is composed of about 500 superposed electrocytes disposed in columns that are arranged side-by-side in the organ. When carefully excised, the prisms can survive in a good functional state for 2-3 days in elasmobranch saline solution at 20 °C, and still longer if they are kept at 4 °C.

2.4.2. Electric response of excised prisms

Pieces containing a single prism - or two prisms according to the size of the specimen -were placed under continuous superfusion with elasmobranch saline medium. Stimulation electrodes were placed parallel to the prism. The electrical stimulation consisted of "field" shocks of supra-maximal intensity (100 V; 0.5 ms) delivered by a pair of Ag-AgCl, electrodes applied to the fluid in close proximity to the prism. Such a procedure in the *Torpedo* electrogenic tissue excites only nerve branches at the surface of the prism, since the electrocytes themselves are not able to produce regenerative action potentials. Stimulated prisms generate a response (electroplaque potential, EPP) that was recorded by adjusting two platinum electrodes in contact with the extremities of the prisms. The electric signal was visualized in an oscilloscope and digitized through a Lab PC Plus card (National Instrument, USA) using a "home-made" device, and recorded in "Ophiuchus" computer program files. The characteristics of transmission were studied in response to a single stimulus, a pair of stimuli or repetitive stimulation (as seen in figure 6 and Table 1). Parameters of the registered data were further analysed using the WinWPC V.3.9 Strathclyde University software (courtesy of John Dempster).

2.4.3. Release of radiolabelled acetylcholine from excised prisms

Torpedo electric organ prisms were labelled with either [^{3}H]-acetate (2 μCi/ml; 8.5 μM) or [^{14}C]-acetate (6 μCi/ml; 8.5 μM) (both obtained from Amersham U.K.). The incubation with the radioactive precursors lasted for 4-6 h at room temperature in continuously stirred elasmobranch medium. In typical experiments, 20-40 prisms (weighing ~100 mg each) were incubated in 80 ml. After the incubation, the fragments were washed for three successive 20 min periods in 100 ml of the saline medium in the absence of the radioactive precursors. They

were then kept overnight in a large volume of saline (300 ml) at 4-7 °C to reduce the rate of ACh metabolism. The labelled fragments of Torpedo electric organ were gently placed on a small piece of nylon holder under continuous perfusion with elasmobranch saline medium at room temperature (20°C) for 1-2h. Prisms were submitted to paired pulse stimulation, with 20ms interval between stimuli. We collected the perfusate in fractions lasting 1 minute each, two minutes before stimulation, and another four fractions (1 minute each) after stimulation. Then the prisms were perfused another 30 minutes in elasmobranch saline medium before addition of drugs – or modification of the ionic composition of the medium- for another 1h30. This time was sufficient to allow complete exchange of the extracellular space by diffusion, even for rather thick prisms (0.4-0.7 cm in diameter) excised from large Torpedoes (Dunant et al., 1972). The stimulation protocol was then repeated again for assessing the effects of the new condition on synaptic transmission. Modifications of the above protocol modified in some experiments will be indicated in the text. Radiolabelled-ACh diffusing from excised tissue was measured by liquid scintillation spectroscopy.

2.4.4. ^{45}Ca accumulation and clearance in excised prisms

The procedures were as described by Babel-Guérin (1974). Excised prisms weighing 70–150 mg were incubated for 3h in elasmobranch medium (with 3.4 mM $CaCl_2$) in the presence of ^{45}Calcium (Amersham, U.K.) (2 μCi/ml), in the presence or absence of drugs such as 2 μM bafilomycin A or 10 μM orthovanadate at laboratory temperature (20°C). Then prisms were either stimulated at 100 Hz during 12 s or not stimulated. The stimulation-dependent calcium accumulation was determined as the surplus of ^{45}Ca measured in stimulated tissue as compared with unstimulated tissue. The clearance of the surplus ^{45}Ca to the perfusing medium (similar to incubation medium but without any ^{45}Ca) was evaluated 0, 5, 15 and 30 min after the tetanus. Calcium exchanges between tissue and solution were stopped at the desired time by incubating the prisms in ice-cold medium composed of 0.5 mM sucrose and 0.5 mM urea. After three 30 min periods of washing with this medium, the prisms were dissolved in 1 N NaOH overnight at 60°C. Then NaOH was neutralized by using HCl, and tissue ^{45}Ca was counted by scintillation spectrometry.

2.4.5. Assessment of ACh content in tissue

ACh content was determined as previously described by Dunant et al. (1972; 1980a). To assess the whole tissue content in ACh (total ACh), the prisms were plunged into ice-cold trichloracetic acid 5% (vol/vol) for about 1 h. Then the tissue was homogenised using a Potter device. After centrifugation, the acid was removed from the supernatant with water-saturated ether. Water soluble extracts were obtained by evaporating ether under N_2 flux. Total ACh in the extracts (10-50 µl aliquots) was measured by using the luminescence method of Israël and Lesbats (1981a; see below). For the measurement of vesicle-bound ACh, the prisms were first homogenised in the above-described elasmobranch medium. Any cytoplasmic or unstable ACh is hydrolysed in the procedure by the very active tissue cholinesterases while vesicular ACh remains protected by the vesicular membrane. Trichloracetic acid was added subsequently (~1min) to the homogenate and vesicular-bound ACh extracted and measured as described above for total ACh.

2.5. Determining ACh and glutamate by chemiluminescence

Acetylcholine was quantified using the chemiluminescent procedure of Israël and Lesbats (1981a; 1981b). The quantification is based on a series of reactions where ACh is hydrolyzed by acetylcholinesterase to acetate and choline. Choline is oxidized to betaine and H_2O_2 by choline oxidase; finally H_2O_2 triggers light emission from luminol in the presence of horseradish peroxidase. The amount of light can be detected by photomultiplier tubes built in luminometers that relay the amount of light into digital traces (in mV).

A typical ACh determination assay contained a chemiluminescence mixture (mix) of choline oxidase from *Alcaligenes sp*. (5U/ml), horseradish peroxidase (7U/ml) and luminol 60 µM dissolved in either 200 mM Na/Na_2 phosphate buffer at pH 8.6 (used for detecting ACh in extracts) or the appropriate saline medium (see below) for detection of continuous ACh release from synaptosomes. It is possible to evaluate the choline and ACh amounts in the same sample if acetylcholinesterase (9U/ml) from *Electrophorus electricus* is added after all choline content in the sample is oxidized to betaine. Evidently, this discrimination is not possible if an endogenous acetylcholinesterase activity is present (i.e., *Torpedo* synaptosomes), unless it is blocked by pre-incubating synaptosomes with ecothiopate iodide 50 µM (Wyeth-Ayerst; also named phospholine). The amount of light emitted by a given sample was calibrated by injecting acetylcholine perchlorate standards into the same reaction

tube. ACh content was computed by comparing the amplitudes of the responses to that of the nearest standards or by comparing the areas instead of the amplitudes in case of ACh release from synaptosomes.

Glutamate was quantified using the chemiluminescent procedure described by Israël and Lesbats (1982) and modified by Fosse et al. (1986). The quantification is based in three successive reactions where glutamate (in presence of NAD^+) is dehydrogenized into 2-oxoglutarate and $NADH_2$ by glutamate dehydrogenase. $NADH_2$ reacts with flavin mononucleotide (FMN) through the action of NADH-FMN oxydoreductase (Boehringer-Roche), regenerating NAD^+ and producing $FMNH_2$. Lastly, a long chain aldehyde (above 8 carbons) reacts with $FMNH_2$ and O_2 through the action of photobacterial luciferase to produce light and regenerate FMN.

For chemiluminescent detection of glutamate a mix of enzymes was prepared with: 250 µl of β-nicotinamide adenine dinucleotide (β-NAD) (16.6 mg in 2.5 ml Tris 0.2 M pH 8); 25 µl of flavin mononucleotide (1 mg in 8.3 ml H_2O); 100 µl of NADP(H) FMN oxydoreductase (2.4 mg in 1 ml H_2O); 80 µl of bacterial luciferase (de *Vibrio fisheri*, 25 mg in 1 ml H_2O) and 50 µl glutamate dehydrogenase (2.66 units/ µl) and kept at -20°C until usage.

Glutamate contained in a given sample was determined by adding 50 µl of the above described mix to 500 µl of 50 mM Na/Na_2 phosphate buffer at pH 7.1, and 5 µl of n-decyl aldehyde (from freshly prepared stock at 1/500 in phosphate buffer). A variable amount of light will be produced and stabilized at a baseline after a few minutes. After this the amount of light produced by glutamate contained in a sample (5-10 µl) is compared to that produced after the addition of known amounts of glutamate to the reaction tube.

2.6. Experiments using sub-cellular preparations from Torpedo

2.6.1. Isolation of *Torpedo* electric organ synaptosomes

Preparation of synaptosomes was carried out as described previously (Israël et al., 1976 ; Morel et al., 1977) with a slight modification ($CaCl_2$ was not present in the successive solutions used in the procedure).

Thirty grams of sliced electric organ tissue were washed out in ice-cold Ca^{2+}-free elasmobranch medium for 30 minutes and then the tissue was finely chopped (figure 5 A) with a razor blade, suspended in 280 mM NaCl, 300 mM urea, 3 mM KCl, 1.8 mM $MgCl_2$, 3 mM

$NaHCO_3$ and 50 mM Na/Na_2 phosphate buffer (pH 7.1) and left stirring for another 30 min at 4°C. The tissue was gradually comminuted by forced filtration through calibrated metallic grids with meshes decreasing square openings from 1000 to 500 and 200 µm side length (figure 5 B). The suspension was then filtered through a nylon gauze (50 µm side length mesh) under slight suction. The filtrate was then pelleted by centrifugation at 6000 x g for 20 min, then the pellet resuspended in 280 NaCl mM, 300 mM urea, 3 mM KCl, 1.8 mM $MgCl_2$, 3 mM $NaHCO_3$ and 50 mM Na/Na_2 phosphate buffer (pH 7.1) and centrifuged on a discontinuous sucrose gradient at 64000 x g for 40 min. After centrifugation, the wider band in the interface between sucrose 300–500 mM contains a very pure preparation of torpedo synaptosomes (figure 5 C) as determined by morphological criteria and biochemical analysis of the cytoplasmic marker lactate dehydrogenase, ATP and cholinergic markers (acetylcholine, choline acetyltransferase and acetylcholinesterases). This arises from the fact that unlike mammalian brain synaptosomal preparations *Torpedo* electric organ synaptosomes are free of any attached post synaptic elements (Israël et al., 1976; Morel et al., 1977, 1978, 1982).

The synaptosomes were kept at 4 °C for 3-24 h until the time of the experiment when they were re-warmed to 20°C.

2.6.2. ACh release from *Torpedo* electric organ synaptosomes

ACh release from *Torpedo* synaptosomes was determined in a continuous manner by the chemiluminescence method (Israël & Lesbats, 1981a and 1981b). 30 µl of synaptosome suspension were delivered into a tube containing 300 µl of saline elasmobranch saline medium composed of: 280 mM NaCl, 3 mM KCl, 1.8 mM $MgCl_2$, 300 mM sucrose, 5.5 mM glucose and 200 mM Tris-HCl, pH 8.5, containing the mix of enzymes for ACh detection (see above). The suspension was allowed to equilibrate for 10-15 min in presence or absence of drugs (details in figures). After that, ACh release was elicited by depolarizing synaptosomes with 100 µM veratridine followed by addition of 3.4 $CaCl_2$. Alternatively, calcium was already present in the pre-incubation medium and ACh release occurred right after veratridine addition. The amount of light produced by ACh released was compared to that produced by known amounts of ACh perchloride (standards). Total amount of ACh contained in a sample was determined by permeabilizing the synaptosomes with Triton X-100 (0.02% final concentration) and comparing the light emitted with that produced by another set of ACh standards.

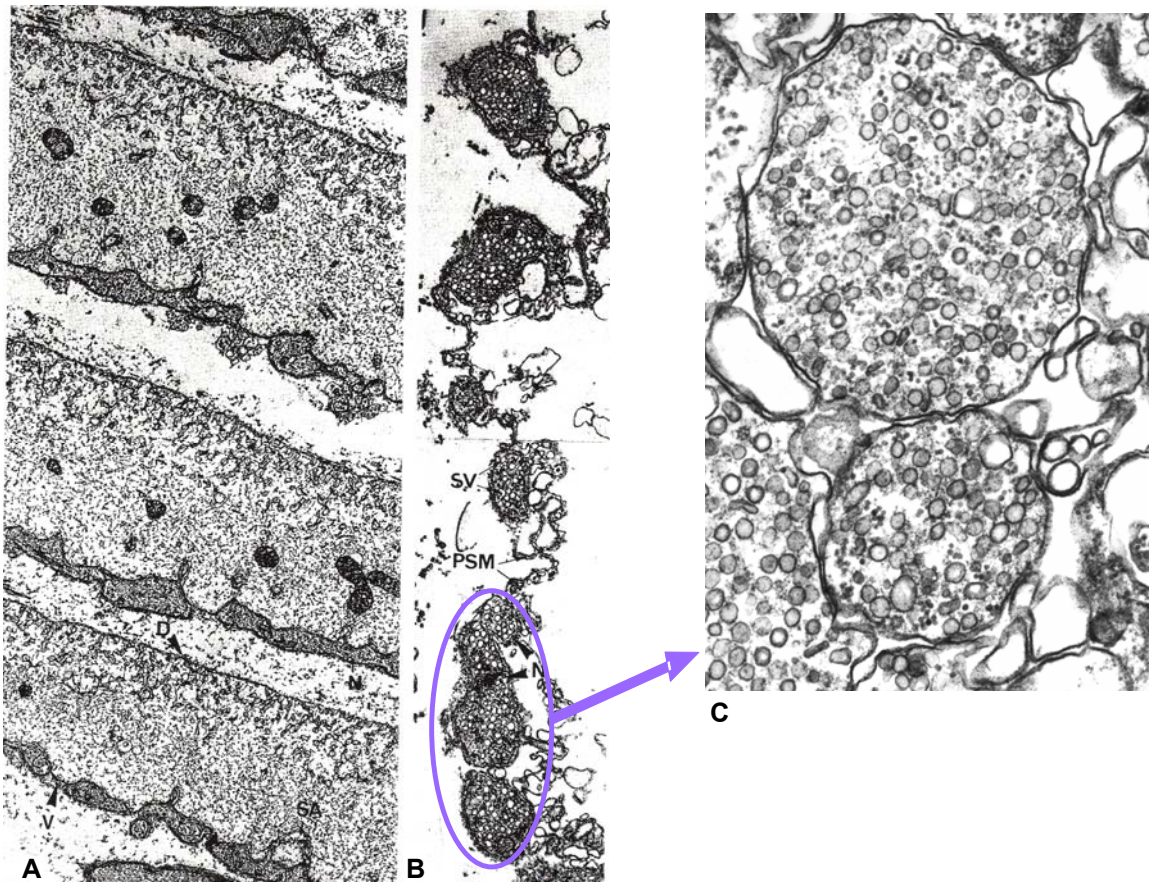

Figure 5. Isolation of *Torpedo marmorata* pinched off nerve terminals (synaptosomes). Picture **A**: electron micrograph showing four stacked electrocytes with numerous nerve endings covering their ventral surfaces (x 3,400). In **B** it is visible the "grapes" of nerve terminals detached from the electrocytes after comminuting the tissue (x 5,900). At this stage, the nerve terminals are still attached to segments of the post synaptic membrane (PSM). In **C**: an electron micrograph of fraction C (x 18,000) shows large synaptosomes copiously populated with synaptic vesicles. Adapted from Morel et al. (1977).

2.6.3. Isolation of *Torpedo* electric organ synaptic vesicles

Cholinergic synaptic vesicles were obtained from the electric organ of *Torpedo* by sucrose gradient centrifugation as described by Israël et al. (1980).

Thirty grams of sliced electric organ tissue were washed out in Ca^{2+}-free elasmobranch medium for 30 minutes at 20°C and then the tissue was grossly chopped with a razor blade. The mince was washed under gentle agitation for 2h30 in the same medium which was renewed every 30 min. A good washing was found to be essential to remove extracellular calcium thereby increasing the amount of bound (vesicular) ACh in the end.

All further steps were carried out at 4°C. 25 g of tissue were then homogenised in 100 ml of "KCl medium" composed of: 350 mM KCl; 100 mM sucrose, 10 mM Tris, pH 7.1. We used a glass-Teflon homogeneizer (Potter-Elvehejem) turning at 1000 rpm (9 strokes of the pestle). The homogenate was centrifuged at 5100 x g for 20 min. The pellet was resuspended in 45 ml of "KCl medium", frozen with liquid N_2 and powdered in a porcelaine mortar. The fine powder can be stored overnight immersed in liquid nitrogen.

The frozen powder was allowed to warm up in a Potter flask to melting sorbet consistence. The suspension was then smoothly homogenised (8 strokes of the pestle). The homogenate was centrifuged at 16,000 x g for 30 min. The supernatant collected and re-centrifuged 15 minutes further at the same speed. Six milliliters of supernatant per centrifuge tube were layered on top of a discontinuous sucrose gradient consisting of 4 layers (7 ml each) of sucrose-KCl mixtures buffered with 10 mM Tris, pH 7.1. The top layer was constituted by: 250 mM sucrose and 300 mM KCl; the second layer had: 380 mM sucrose and 250 mM KCl; the third layer had: 450 mM sucrose and 200 mM KCl and the bottom layer had: 550 mM sucrose and 150 mM KCl. 6 charged gradient tubes were centrifuged at 95,400 x g. After centrifugation, readily visible bands are found at the first and second interfaces and a pellet was also present. The second band at the interface of 250-380 mM sucrose and penetrating slightly in the 380 mM sucrose layer is the synaptic vesicle enriched fraction. Protein was determined with the BCA Protein Assay (Pierce, Rockford, IL, USA) as described by Lowry et al., 1951.

2.7. Experiments using mammalian sub-cellular preparations

2.7.1. Isolation of rat hippocampus mossy fibre synaptosomes

Hippocampal mossy fibre synaptosomes (MFS) were prepared from adult male Wistar rats as previously described (Israël and Whittaker, 1965; Helme-Guizon et al., 1998; Bancila et al., 2004; 2008). After animal decapitation, the brain was rapidly removed and placed in an oxygenated (95% O_2 and 5% CO_2) modified mammalian Krebs medium containing: 136 mM NaCl; 3 mM KCl; 1.2 mM $MgCl_2$; 2.2 mM $CaCl_2$; 16.2 mM $NaHCO_3$;5.5 mM glucose; 1.2 mM Na/Na_2 phosphate buffer; pH 7.4, on ice. The two hippocampi were rapidly dissected out, cut into small cubes of approximately 1 mm side, and placed into tubes containing 0.3 ml of the above medium. The preparation was then gently homogenised by repeated pipeting. The

homogenate was diluted to 2 ml and filtered through nylon gauze (mesh size 100 μm). The filtrate was left to sit during 30-45 min until a pellet was formed. The supernatant was discarded, the pellet resuspended into 1 ml Krebs solution and left to recover at room temperature (20 °C). This temperature was kept in all further steps of the experiments. Identification and characterisation of MFS in this fraction by using electron microscopy and other techniques have been presented elsewhere (Israël and Whittaker, 1965; Helme-Guizon et al., 1998; Bancila et al., 2004; 2008). The fraction revealed an abundance of large resealed nerve terminals of a complex shape. Synaptosomes larger than 1 μm represented 80% of all synaptosomes present in the fraction, which also contained nuclei, myelinated and other large membrane fragments. The mean MFS length was 2.05 ± 0.2 μm (SEM), some of them reaching 8 μm. Most MFS were full of synaptic vesicles and contained abundant mitochondria with a well-preserved ultrastructure. Small postsynaptic elements (dendritic CA3 spines) were regularly entrapped in MFS. Synapses could easily be identified at these places thanks to the characteristic local thickenings of the pre- and post-synaptic membranes. Although apparently crude, the MFS fraction had the advantage to exhibit exceptional functional capabilities when compared to more purified fractions of MFS (using sucrose gradient centrifugation) that had a lower membrane potential and were much less efficient in releasing glutamate.

2.7.2. Glutamate release from rat hippocampus mossy fibre synaptosomes

Glutamate release from MFS was monitored at room temperature (20 °C) by using the chemiluminescence method (Helme-Guizon et al., 1998; Israël et al., 1993; Fosse et al., 1986), as follows. MFS (3 mg protein/ml) were incubated during 20-30 min in a series of test tubes containing 250 µl of modified Krebs medium in presence or absence of drugs in test (see figure 41). Glutamate release was elicited by raising KCl to 30-40 mM. After 5 minutes, the tubes were briefly centrifuged. Glutamate was assayed in the supernatant by the above-described luminescence assay and the MFS pellet was collected for protein determination, using the BCA Protein Assay (Pierce, Rockford, IL, USA) as described by Lowry et al., 1951. All measurements were expressed as a function of the protein content of the sample.

2.7.3. Measurement of the vesicular proton gradient in rat hippocampus mossy fibre synaptosomes

The vesicular proton gradient established at mossy fibre synaptosomes was monitored at room temperature (20°C) using the fluorescent probe acridine orange (AO), as described by Zoccarato et al. (1999). Assays took place by addition of 100 µl of the MFS suspension (final protein concentration approximately 10 mg/ml) to 400 µl modified Krebs solution containing 3 µM A.O. (final concentration). Fluorescence was read in a Perkin-Elmer LS-50B fluorimeter at the rate of 2 Hz. Upon addition of MFS sample, the intense fluorescent signal, due to free AO, declined rapidly (see figure 10 B) since dimerisation occurs when the dye is exposed to the vesicular acidic medium, where it accumulates. Then KCl was added at the same concentrations as in the release experiments. Full dissipation of the proton gradient was eventually provoked by adding either the protonophore CCCP (10 µM) or bafilomycin A1, an inhibitor of V-ATPase (0.3 µM). This confirmed that virtually all the A.O. signal came from the H^+ gradient established in synaptic vesicles (see also Zoccarato et al., 1999).

2.7.4. Measurement of cytosolic [Ca^{2+}] in rat hippocampus mossy fibre synaptosomes

The cytosolic [Ca^{2+}] was monitored in MFS kept at room temperature (20 °C) using fura-2 (Molecular Probes, Invitrogen), as follows. MFS (0.3 mg protein) were incubated in 0.5 ml of saline medium composed of: 140 mM NaCl; 5 mM KCl; 5 mM $NaHCO_3$; 1.2 mM NaH_2PO_4; 1 mM $MgCl_2$; 1.33 mM $CaCl_2$; 10 mM glucose; 10 mM Hepes, pH 7.4. The saline medium was supplemented with 1 mg/ml of bovine serum albumin and MFS were allowed to equilibrate during 5 min under mild agitation. Then, Fura-2-acetoxymethyl ester was added (2 µM final concentration) and allowed to incubate for 30 minutes. After Fura-2 loading, synaptosomes were washed-out in two cycles of centrifugation for 1 min at 13,000 rpm and the pellet resuspended in 1.5 ml of saline medium. Then they were allowed to incubate in that medium for 1h30, before being centrifuged again and resuspended in saline medium devoid of calcium. The synaptosomal suspension was further incubated for 15 min in presence or absence of 0.5 µM bafilomycin under mild agitation in a quartz cuvette in a Perkin-Elmer LS-50B spectrofluorimeter. Fluorescence data were accumulated at 2 Hz with excitation wavelength

of 340 nm and emission wavelength of 510 nm. $CaCl_2$ was added to 1.33 mM final concentration 1 min after the beginning of the assay. MFS were depolarized with 40 µM veratridine (final concentration) 30 s after $CaCl_2$ addition. Cytosolic free Ca^{2+} concentration ($[Ca^{2+}]_{cytosol}$, nM) was calculated according to the method described by Grynkiewicz et al. (1985) following calibration procedures using 2.5 mM EGTA and 0.1% sodium dodecyl sulphate to obtain minimum fluorescence in the absence of any Fura-2/Ca^{2+} complex and maximal fluorescence with Fura-2 saturation with Ca^{2+} after addition of 5 mM $CaCl_2$.

2.7.5. Isolation of mammalian brain synaptic vesicles

The isolation of synaptic vesicle enriched fractions from either sheep brain cortex or rat brain was carried out according to the procedure described previously (Hell et al., 1988; 1990; Gonçalves et al., 2000b). Brains of young male rat (Wistar) or sheep (*Ovis aries*, breed merino) were removed immediately after death, cut in small pieces and frozen in liquid N_2, until further processing. They were subsequently transferred into N_2 cooled porcelain mortar and crushed with a pestle until a fine powder was obtained. The powder was homogenized in 6 volumes of homogenization buffer containing: 0.32 M sucrose, 10 mM HEPES–K, pH 7.3, 0.2 mM EGTA, 0.5 µg/ml pepstatin and 1 µg/ml leupeptin at 4°C by a motor driven Teflon-glass homogenizer at 900 rpm. All further steps were at 4°C. The homogenate was centrifuged at 47,000 x g for 10 min and the supernatant collected for new centrifugation at 120,000 x g during 40 min. The supernatant was layered onto 5 ml cushions of 0.65 mM sucrose and 10 mM HEPES–K, pH 7.3 and centrifuged for 2 h at 260,000 x g. The resulting pellets are resuspended in 0.32 M sucrose and 10 mM HEPES–K, pH 7.4 and centrifuged for 10 min at 27,000 x g. At this stage, the collected supernatant is essentially enriched in synaptic vesicles. Indeed, contamination with plasma membranes was not observed as judged by absence of ouabain-sensitive Na^+/K^+ ATPase activity, but a little contamination with microsomes; 15% was detected by measuring the activity of the marker enzyme glucose-6-phosphatase (Gonçalves et al., 2000b). Finally, the protein is determined by the method described by Gornall et al. (1949) using bovine serum albumin as a standard and the fraction is divided into various aliquots to store at -80°C. They were thawed at room temperature immediately before use in the experimental assays.

2.7.6. Measurement of the vesicular proton gradient in mammalian purified synaptic vesicles

ATP-dependent vesicular proton transport was measured by following the fluorescence quenching of acridine orange (Deamer et al., 1972; Gonçalves et al., 1998). To follow pump-mediated proton loading into vesicular lumen, synaptic vesicles (0.6 mg protein/ml) were incubated at 30°C in a medium containing 150 mM KCl, 2 mM $MgCl_2$, 60 mM sucrose, 10 mM Tris–HCl, pH 8.5, 50 μM EGTA, and 3 μM acridine orange. After addition of 0.5 mM ATP–Mg to the vesicle suspension, the ATP-dependent proton transport was visualized by following the fluorescence emission (λ at 525 nm) quenching of acridine orange using an excitation wavelength of 495 nm in a Perkin-Elmer spectrofluorimeter LS-50 B. The formation of the proton gradient (ΔpH) can be checked by inducing its dissipation with a protonophore like CCCP (2 μM final concentration). Partial dissipation of the proton gradient due to the activation of Ca^{2+}/H^{+}-antiport was elicited upon 500 μM free [Ca^{2+}] addition (as in figure 13).

2.7.7. Measurement of ATPase activity in mammalian purified synaptic vesicles

The ATPase activity of the synaptic vesicles was determined by measuring the liberation of inorganic phosphate (Pi) associated with the hydrolysis of ATP as reported by Gonçalves et al. (2000a). Membrane vesicles (600 mg protein/ml) were incubated in 1.1 ml of 60 mM sucrose, 2 mM $MgCl_2$, 150 mM KCl, 50 μM EGTA and 10 mM Tris, pH 8.5. The reaction was started by adding 504 μM ATP-Mg and, after 5 min at 30°C. It was stopped by adding 50 μl of ice-cold 20% (v/v) trichloroacetic acid. The precipitated protein was discarded by centrifugation and the supernatant was collected for Pi analysis by the method of Taussky and Shorr (1953). The assays were undertaken in the presence or absence of drugs indicated in the figures.

2.8. Acetylcholine release from synaptic vesicles

ACh release from synaptic vesicles isolated from *Torpedo* electric organ or sheep brain cortex was determined in a continuous manner by the chemiluminescence method (Israël

& Lesbats, 1981a and 1981b). 25 µl (~3 µg) of *Torpedo* synaptic vesicle suspension or 60 µg of sheep brain cortex synaptic vesicles were delivered into a tube containing the ACh detection enzyme mixture in 250 µl of: 380 mM KCl, 2 mM $MgCl_2$, 60 mM Hepes-KOH, pH 7.2 and 50 µM EGTA used with *Torpedo* SVs or: 150 mM KCl, 2 mM MgCl2, 60 mM sucrose, 60 mM Tris-HCl, pH 8.5 and 50 µM EGTA used with sheep brain cortex SVs. The suspension was allowed to equilibrate for a few minutes and ACh release from synaptic vesicles was tested in presence or in the absence of Ca^{2+} with or without permeabilization of vesicle membranes to calcium with ionomycin (in case of *Torpedo* vesicles) or by addition of 500 µM $CaCl_2$ to vesicle suspension energised with 1mM ATP (details in figures). The amount of light produced by ACh released was compared to that produced by known amounts of ACh perchloride (standards). Total amount of ACh contained in samples was determined by permeabilizing the synaptosomes with Triton X-100 (0.02% final concentration) and comparing the light emitted with that produced by another set of ACh standards.

2.9. Cell culture

PC12 cell clones (Shoji-Kasai et al., 1992) were kindly provided by Yoko Shoji-Kasai (Mitsubishi Kagaku Institute of Life Sciences, MITILS, 11 Minamiooya, Machida, Tokyo 194-8511, Japan). Cells were cultured in Dulbecco's modifed Eagle's medium (DMEM; Eurobio, France) supplemented with glutamine (0.2 mM), 5 % foetal calf serum (FCS; Amimed), 5% horse serum (HS; Amimed) and penicilin-streptomycin (5 units/l; Invitrogen). The cultures were carried out at 37°C in a 5% CO_2; 95% air mixture saturated with water in 175 cm^2 plastic bottles (Falcon). For morphological experiments, cultures were grown in monolayer until confluence on plastic coverslips (Thermanox, Nunc, USA).

2.10. Gene construct and transfection into PC12 Cells in culture

Two Synaptotagmin I genes were engineered for transfection of PC12 cell clones devoid of endogenous Syt I (F7). Constructs were similar to those described earlier by Marek and Davies (2002), but using the mouse sequence instead of Drosophila. For that, the pMH4-SYN-P65-I-EGFP plasmid (corresponding to mouse NM_009306 sequence) was used to amplify (F: AAA ATG GTG AGT GCC AGT CGT; R: TTA CTT CTT GAC AGC CAG CAT ; Rtag:

TTA AGC ACG AGC ACA TTC ACG ACA AGC TTC ACG AGC AGC TTC AGC CTT CTT GAC AGC CAG CAT) synaptotagmin I cDNA without (Syt) or with the FlAsH-binding tetracysteine motif (AEAAAREACCRECCARA) (Griffin et al., 1998) (Syt_tagg) and subcloned in pcDNA3.1. The constructs were sequenced. These mouse cDNA showed 96.32 % homology to rat synaptotagmin sequence and 99.76% homology was found between the two proteins. Cells were transfected with Lipofectamine™ 2000 (Invitrogen), according to the manufacturer's guidelines. After the formation of liposome/DNA complexes they were delivered into cell cultures during ~4h. After this period cells were cultured in normal growth medium for two more days before being assayed.

2.11. Preparation of post nuclear supernatants from PC12 cells

Crude post nuclear supernatants were prepared from PC12 cells according to Bloc et al. (1999). PC12 cells were detached from cultured flasks by washing in phosphate buffer saline (PBS) composed of: 137 mM NaCl, 2.7 mM KCl, 10 mM Na/Na_2 Phosphate, pH 7.4 at 37°C (no need for trypsin). Cells were centrifuged at 800 x g for 5 min and resuspended (~2.5 ml for every 10^6 cells) very gently in ice cold (4°C, temperature kept until the end of the procedure) homogenisation buffer (HB) composed of 250 mM sucrose, 3 mM imidazole, pH 7.4 and centrifuged again at 800 x g. Cells were resuspended again in HB and counted in an Neubauer haemocytometer. They were centrifuged at 1000 x g for 10 minutes. The cell pellet was diluted (~0.5 ml for every 10^6 cells) in HB containing protease inhibitors (10 µM leupeptin and 1 µM pepstatin A) and homogenized by 5-10 passages through a 22-gauge needle. The suspension was monitored by phase contrast microscopy. The homogenate was centrifuged at 2000 x g for 15 min and the post nuclear supernatant was collected and stored at -80°C until usage. A small aliquot was taken for protein quantification by the BCA protein assay (Pierce, USA)

2.12. Measurement of the vesicular proton gradient in PC12 post nuclear supernatants

ATP-dependent proton transport was measured on crude post nuclear supernatants by following the fluorescence quenching of acridine orange (Deamer et al., 1972; Bloc et al.,

1999) in a Perkin-Elmer spectrofluorimeter LS-50 B with excitation and emission wavelengths of 495 and 530 nm, respectively. The assay was carried out at 30°C in: 130 mM KCl, 2 mM $MgCl_2$, 20 mM MOPS/Tris, pH 7.4 and containing 50 µM EGTA and 3 µM acridine orange. Assays started by addition of PNS (300 µg/ml) from different cells. H^+ pumping into the acidic organelles started upon addition of 1 mM ATP-Mg. Partial dissipation of H^+ gradient was assayed in PNS from synaptotagmin I positive or negative cell clones by addition of 500 µM Ca^{2+}. In the end of each assay CCCP was added to allow full dissipation of the H^+ gradient.

2.13. Active Ca^{2+} uptake into acidic organelles of PC12 cell post nuclear supernatants

Ca^{2+} accumulation by acidic organelles in PNS was measured by rapid filtration and scintillation counting. A PNS sample (0.3 mg protein/ml) was incubated at 30°C in 850 µl of reaction medium containing 130 mM KCl, 2 mM $MgCl_2$, 20 mM MOPS/Tris, pH 8.5 and 50 µM EGTA. Radiolabelled calcium was from Amersham (U.K.).

In ATP dependent Ca^{2+} uptake assays PNS (0.3 mg protein/ml) suspensions were allowed to equilibrate for 6 minutes in reaction medium containing 10 µM Na-orthovanadate. Then, 1 mM ATP-Mg was added and a pH gradient was allowed to form for 2 minutes before $^{45}Ca^{2+}$ (550 µM free; 0.5 mCi/mmol calcium) addition. Rapid filtration took place 2 minutes after by placing the 800 µl aliquot in millipore filter HAWP (0.45 mm) under vacuum. The filtration cycle included pre-washing of filters with 1.5 ml ice-cold reaction medium without $MgCl_2$ followed by filtration of the sample and washing with 3 ml more of the same medium.

In another set of experiments Ca^{2+} uptake was driven by the pre-established pH gradient (pH-Jump) between the acidic vesicular lumen of the organelles in PNS (prepared at pH 7.4) and the reaction medium (pH 8.5). Ca^{2+} uptake assays started by adding PNS suspensions (0.3 mg protein/ml) to reaction medium already containing 10 µM Na-orthovanadate and $^{45}Ca^{2+}$ (550 µM free; 0.5 mCi/mmol calcium) and were stopped 2 min after by rapid filtration (as above).

The radioactivity of the filters was measured by liquid scintillation spectrometry and the amount of Ca^{2+} accumulated in the vesicular space was calculated. Radiolabelled $^{45}Ca^{2+}$ uptake assays were performed in the presence of orthovanadate (10 µM) to inhibit the

activity of Ca^{2+}-ATPases. In some conditions (indicated in figures) 0.6 µM bafilomycin A was present to inhibit the activity of the Ca^{2+}/H^{+} antiport.

Ionomycin-dependent Ca^{2+} retention in post nuclear supernatant (PNS) of PC-12 cells was also tested with PNS from tested cells. Conditions were as for pH-jump but in presence or absence of 2 µM ionomycin in the reaction medium.

2.14. Cellular and subcellular labelling of PC12 cell synaptotagmin I with FlAsH

Labelling of PC12 cells with the biarsenical derivative of fluorescein, FlAsH was done by combining the FlAsH cell loading protocol of Marek and Davies (2002) with PNS protocol by Bloc et al. (1999). FlAsH reagent was acquired from Invitrogen under the name of Lumio™ Green. It is not fluorescent until it binds the tetracysteine motif at which time it becomes highly fluorescent. The motif consists of Cys-Cys-Xaa-Xaa-Cys-Cys where Cys equals cysteine and Xaa equals any amino acid other than cysteine. This motif is rarely seen in naturally occurring proteins allowing specific fluorescence labelling of recombinant proteins fused to the tetracysteine motif (tag). Syt_tagg transfected cells are expected to bind FlAsH with high affinity (Gaietta et al., 2002) and guarantee nearly 100% labelling (Beck et al., 2002; Marek and Davies, 2002). FlAsH is supplied pre-complexed to (1,2-ethanedithiol) EDT_2 that solubilizes and stabilizes the molecule. It is membrane-permeable, and readily enters cells. Cells were labelled at room temperature (20°C) either in suspension (after harvesting with PBS as above) or attached to plastic coverslips. All further steps occurred under protection from light until the assays. FlAsH loading medium contained: 137 mM NaCl, 2.7 mM KCl, 2 mM $MgCl_2$, 0.5 mM $CaCl_2$, 1 mM Na-Pyruvate, 2.5 mM glucose, 10 mM Na/Na_2 Phosphate, pH 7.4 supplemented with 1 µM FlAsH- EDT_2 and 15 µM EDT_2 and lasted 20 min. Then cells were washed (in case of cells in suspension, they were centrifuged at 800 x g followed by resuspension) in loading medium supplemented with 250 µM EDT_2 to remove non-specific FlAsH binding and incubated under slight agitation for 10 minutes. After two additional washings in the loading medium alone, they were either visualized (figure 16) under a fluorescence microscope with a FITC (fluorescein) filter (excitation at 488 nm and emission at 528 nm) or proceeded to obtain PNS preparations as described earlier.

2.15. Fluorescence assisted light inactivation with FlAsH: FlAsH-FALI

FlAsH-FALI of synaptotagmin I was performed by adapting the method described by Marek and Davis (2002) to sub-cellular suspension. Briefly, PNS suspensions from cells transfected with Syt_tagg construct and labelled with FlAsH were kept at 4°C while being exposed for 1 minute to UV light from a 200W HBO lamp. After being "flashed" the samples were assayed within 5 minutes using the Ca^{2+} active uptake or the Ca^{2+}-induced H^{+} gradient dissipation protocols (details in figures).

2.16. Statistical analysis

Statistical analysis was performed using either a Two-way ANOVA test (Tukey post-test) or the Student's t-test (two-tailed distribution; unpaired) and P values are presented in the legends of the figures.

3. Results and discussion

3.1. Experimental models

3.1.1. Real-time measurement of neurotransmitter release and dynamic changes of calcium content in intact tissue

In this work we made a profuse use of a biological model that uses rapid ACh transmission to produce highly synchronized electrical discharges. The electric organ of *Torpedo* species has provided an invaluable tool for investigating the mechanisms of ultra-rapid synaptic transmission. Embryologically, the *Torpedo* electromotor system is homologous to the neuromuscular system, with which it shares most of its structural, functional and pharmacological characteristics.

The *Torpedo marmorata* (Figure 6 A) is an elasmobranch (cartilaginous) fish denizen from the north Atlantic Ocean and Mediterranean Sea. It possesses two kidney-shaped electric organs on either side of his body that together account for 1/5 of the animal's total weight. A single organ of a middle sized fish (approximately 40 cm length) is capable of delivering electrical discharges of ~40-60 V in open circuit (when the discharge is provoked in the air), or 15-30 V and 4-6 amperes in sea water. The discharge is composed of successive peaks arising at high rate (100 to 300 Hz); it lasts for less than 0.1 s for the defence reflex (figure 6 A), but up to 24 seconds when the fish is hunting a prey (Fessard, 1958).

Excitation of mechano receptors in the tail or in the dorsal-front borderline of the fish stimulates the generation of an electrical defensive discharge that is coordinated in the brain stem and transmitted to the electromotor system. The later consists of some 60,000 electro-motorneurons located in the electric lobe. The axons of those neurons project to the electric organ where they branch profusely, ending up in numerous nerve endings, innervating the ventral face of electrocytes. Electrocytes are actually modified muscle cells, very thin (10-15 µm) but large (2-8 mm diameter) cells. Upon excitation, the electro-motor terminals abruptly release the neurotransmitter acetylcholine (ACh), which binds and opens nicotinic ACh receptors in the electrocytes ventral membranes, provoking a sudden decrease in the electric resistance and the irruption of Na^+ ions into the cells. The resulting currents sum up to give the vigorous electrical discharge produced by the fish (Dunant and Israël, 1985). Indeed, the electric organ is composed of 400-470 stacks of electrocytes also called prisms that resemble honeycomb-like structures when the skin is removed (figure 6 B). Each prism spans the animal and is composed of ~514 superposed electrocytes that keep their innervation when they are excised from the electric organ. Excitation of an isolated prism by

a single field shock activates the nerves contacting the electrocytes, resulting in the generation of a highly synchronized electric response (figure 6 C-D). The discharge of a prism is the result of undistorted endplate potentials synchronously generated by the superposed electrocytes that, on the contrary to their muscular counterparts or to *Electrophorus* electrocytes, do not produce regenerative action potentials (figure 6 C-D).

Transmission is purely cholinergic in the electric organ and the release of the neurotransmitter is "quantal", i.e., the evoked electroplaque potentials (EPP) is composed of discrete units corresponding to simultaneous release of 7,000–10,000 acetylcholine (ACh) molecules (Dunant and Muller, 1986), a value close to that reported for vertebrate motor endplates (Kuffler and Yoshikami, 1975).

In the absence of stimulation, spontaneous miniature electroplaque potentials (MEPPs) can be recorded at electric organ synapses; they have the same size as evoked monoquantal potentials. In turn, like in nerve-muscle synapses (Kriebel and Gross, 1974), *Torpedo* MEPPs are composed of smaller discrete subunits, or subquanta, whose size is about a tenth of that of the mean quantal MEPPs or EPPs. Thus one subquantum is expected to arise from the release of a packet of 700-1000 ACh molecules (Muller and Dunant, 1987; Girod et al., 1993). In spite of these homologies, a few remarkable differences should be noticed between the two systems. In the *Torpedo* electric organ the synaptic vesicles are almost twice the size of those of the motor nerve terminals (80 nm *vs.* 45 nm). They were shown to contain 100,000 – 200,000 ACh molecules (Ohsawa et al., 1979), which would be enough for generating 10-25 quanta, or 100-250 subquanta (Dunant and Muller, 1986). Also the pre-synaptic specializations described as the active zone at the endplate (Couteaux and Pécot-Dechavassine, 1973) are not clearly observed at electric organ synapses. Importantly, the *Torpedo* nicotinic ACh receptors, although exhibiting a very high degree of homology with those of vertebrate neuromuscular junctions, are characterized by a much shorter mean open time (0.6 ms) and a linear current-voltage relation (Sakmann et al., 1985). This represents a favourable adaptation for a device designed to deliver brief electric discharges at a high frequency.

For investigating pre-synaptic mechanisms, the *Torpedo* electric organ offers several decisive advantages over neuromuscular preparations. First, the electroplaques do not contract. Also, they are devoid of voltage gated channels and thus unable to generate regenerative action potentials; their current-voltage relationship is linear both at rest and at the peak of the discharge (Fessard, 1958; Bennett et al., 1961). Therefore, the electrical

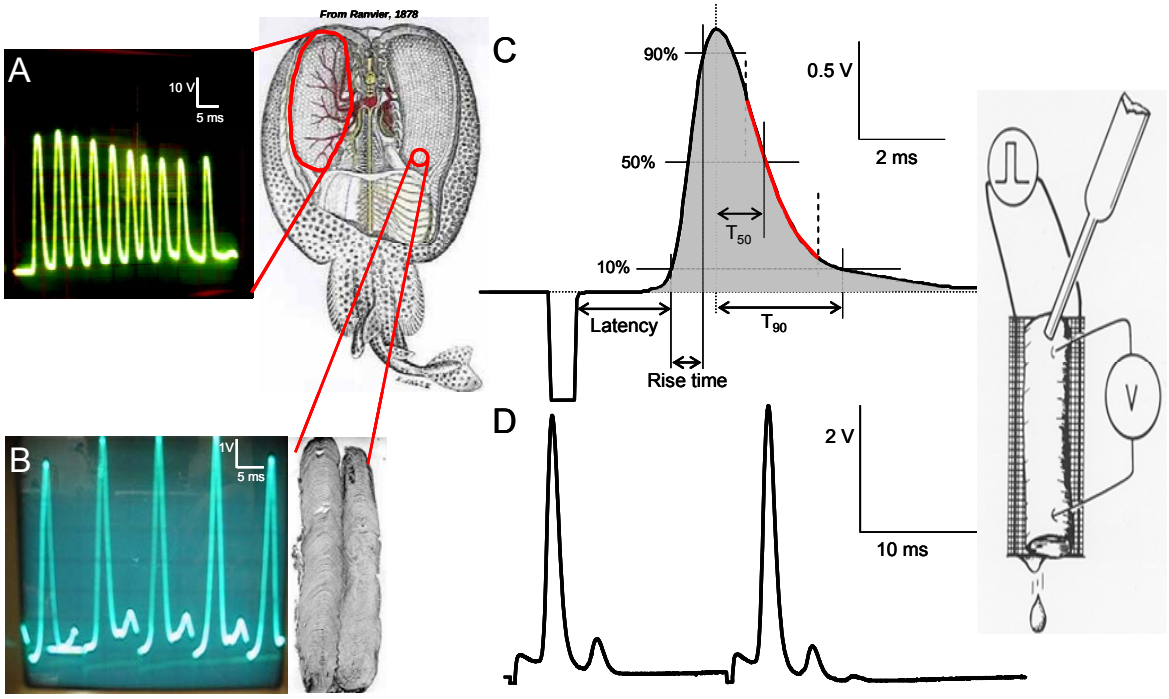

Figure 6. *Torpedo marmorata* electric organ as a model for the study of fast transmission. Panel ***A*** shows a train of 10 electric responses at high frequency (~200 Hz) produced by an electric organ. This, in vivo, experiment was registered out of the water after stimulation of mechanoreceptors in the animal's front (defence reflex discharge). Panel **B** shows the electric response generated by dissected stacks of electrocytes (prisms) under field stimulation at physiological frequency (100 Hz). Panel ***C*** analyses such an electrical response of a dissected prism to a 100 V-0.5 ms field shock (schematic view of the apparatus shown to the right). Trace show in succession the stimulation artefact, the synaptic delay (latency) and the electrical discharge produced by the prisms (area in grey). Indicated in the figure are 10, 50, and 90% of maximal amplitude (in volts) levels used to calculate several parameters like rise time, or T_{50} and T_{90} decay times lasting from peak response (dotted line) until the 50% and 90% decay values are reached, respectively. Broken lines define the segment of the decaying response where a single exponential curve (superimposed in red) can be fitted and used to calculate tau (decay time constant). Panel **D** illustrates a typical prism electric response resulting from paired pulse field stimulation (100 V; 0.5 ms) with 20 ms interval between stimuli. The facilitating (or depressing) effects of paired pulse responses were evaluated by analyzing parameters (as in panel ***C***) of the second response as compared to the first response. Traces are representative of >100 experiments.

discharge in the *Torpedo* is the summation of pure postsynaptic potentials, which are not distorted by all-or-none events.

Another remarkable property of the electrogenic tissue is its extremely low electrical resistance. This is explained by the cytology of electroplaques, which are large, but very thin and flat cells. Their dorsal membrane (a non innervated membrane) presents a huge area due to a dense network of micro-invaginations. To this large area corresponds a very low

Table 1. Electrophysiology of *Torpedo* electric organ

	In vivo This work and ref.[1]	Prisms This work N=59, 12 torpedoes	Unitary evoked Epp/Epc ref. [2,3]	Mepp or Mepc ref. [2,3]	Sub-Meps/ Mecs ref. [2,3]	Synaptosomes Mepc N=266 ref.[4]
Amplitude Immersed In air	15-30 V 4-6 A 40 mA.cm^2 52 V (40-60) V	2.2± 0.18 V	~1 mV 1,8± 0.4 nA	1.25±0.24 mV 2.25±0.72 nA	~0.1 mV ~0.2 nA	0.065±.0016 nA (noise to 0.2 nA)
Rise time 10-90% time to peak	0.61 ms	1.01± 0.037 ms	0.6 ms	0.43±0.02 ms	0.4 ms	0.9-3 ms mean (2.6 ± 0.4)
T_{50} (ms)	2.261	0.97± 0.026	0.5-0.7	0.4±0.025	0.3-0.4	0.5-5 (6.0± 1.1)
T_{90} (ms)	3.442	2.075±0.093				
Decay Tau (ms)	0.834	0.747±0.024	0.3-0.4	0.35± 0.01		6.2± 1.1
Latency (ms)	---	1.98± 0.048	1.4 ms true delay, (0.61±0.03 ms direct depol. of terminals)	--	--	--

Characteristics of adult Torpedo nicotinic ACh receptors : Mean open time : 0.6 ms, amplitude : 4.1 pA at -100 mV, 40 pS. (Reconstituted in oocyte, 17-21°C frog Ringer; Sackmann et al., 1985).

ACh release from Torpedo synaptosomes was recorded using embryonic Xenopus myocytes (Ref. [4]); Characteristics of Xenopus embryonic nicotinic ACh receptors*:* Mean open time : 3 ms, amplitude : ~1 pA (Brehm et al., 1982; Kikodoro and Rohrbough, 1990).

Under the experimental conditions presented above (either with prisms or local recordings using a loose patch clamp electrode) the time course of electroplaques currents is the same as that of electroplaques potentials. Rise time: 0.71 ± 0.15 and 0.71 ± 20 ms; T_{50}: 0.72 ± 12 and 0.84 ± 0.23 ms for MEPC and MEPP, respectively (SD; see Girod et al., 1993).

Table References: [1] (Fessard, 1958), [2] (Dunant and Muller, 1986), [3] (Girod et al., 1993), [4] (Girod et al., 1992).

electrical resistance. As a consequence the potentials recorded in this system (EPPs and MEPPs) and the corresponding currents (EPC and MEPCs) display an identical time course (Girod et al., 1993) (see table 1).

The post-synaptic response can therefore be taken as a measurement of the amount of transmitter release in each nerve impulse (Dunant and Israël, 2000). The electric potential generated by the prisms gives a wealth of information by comparative study of its composing parameters (figure 6 C and table 1).

For all the above reasons, the electrical responses of the *Torpedo* electrogenic tissue reflects in most circumstances quite faithfully the amplitude and time course of transmitter release in a given nerve impulse. As a matter of fact, an excellent correlation has been observed in the *Torpedo* electric organ between electrophysiological and biochemical assessments of release, even in response to a single or a few nerve impulses (Dunant et al., 1980a) (figure 7).

In the present work, we describe electrophysiological observations obtained using whole prisms, or stack of electroplaques, excised from the *Torpedo* electric organ. Pieces containing a single prism - or two prisms according to the size of the specimen - are carefully dissected and placed under continuous superfusion with an elasmobranch saline medium. In response to a field shock, such prisms generate a response (electroplaque potential, EPP) with the following characteristics (Figure 6 B and Table 1).

A latency of *Ca.* 2 ms always lags between the end of the stimulus artefact and the beginning of the EPP (measured at 10% the maximal amplitude). The excitation most probably fires off in the highly myelinated axons which extensively branch at the edge of the prisms, before penetrating in the space separating electroplaques (Wagner's bush; (Wagner 1847)). Axon excitation implies activation of voltage-operated Na^+ channels since no EPP could be recorded after stimulating in this way prisms perfused in presence of tetrodotoxin (Dunant, unpublished work). As measured here, the latency is expected to include a) axon excitation, b) conduction along nerve fibres from the Wagner bush into the terminal network, c) Ca^{2+} entry into terminals, d) ACh release, e) ACh diffusion in the synaptic cleft and f) activation of postsynaptic nicotinic receptor.

The rising phase of the EPP reflects the kinetics of activation of nicotinic receptors in all the synapses present in the prism. The rise time of a prism EPP (measured between 10% and 90% of the peak amplitude) is very short (*Ca.* 1 ms). The value is just twice the time-to-peak of unitary EPPs or MEPPs, as recorded locally at restricted innervated areas (Table 1) (Girod et al., 1993). Therefore, a single field stimulus elicits a highly synchronous activation of an enormous number of synapses, since there are approximately $3x10^6$ synapses per electroplaque and more than 500 electroplaques in a full length prism.

The peak amplitude of EPPs recorded in this way varies considerably among prisms, depending on recording conditions (size of the tissue piece, position of electrodes, degree of the short circuit due to the superfusing saline, etc.). Prisms take about two hours after

dissection to stabilize. During that period peak amplitude value usually rises slowly and then it remains at a steady level for 24 hours or more. The peak of prism EPP, like those of unitary EPPs or MEPPs, displays a somewhat "rounded" shape.

The EPP area is an integrated parameter, which in many circumstances gives a better correlation with biochemical measurements of transmitter release than the peak amplitude. A striking example is the effect of 4-amminopyridine which does not significantly increase EPP amplitude in the *Torpedo*, but enhances by two orders of magnitude both the EPP duration and the amount of transmitter released (Dunant et al., 1980a; Corthay et al., 1982). **The area to peak** ratio can prove an interesting parameter for comparing data from an experiment to another, since it depends less on the recording geometry and conditions than the amplitude or the area alone.

The falling phase of a prism EPP is characterised, between 75% and 15% of the peak amplitude, by a rapid decay which could be fitted with a single exponential. Measured in a large number of prism EPPs, the time constant of this exponential (**decay tau**) was 0.747 ± 0.024 ms. Surprisingly, this was only twice the value found in the elementary quantal EPCs, MEPPs or MEPCs (Table 1). It is interesting to note that the decay tau of a prism EPPs gives a value close to the mean open time (0.6 ms) reported for *Torpedo* nicotinic receptors reconstituted in *Xenopus* oocytes (Sakmann et al., 1985). This suggests that the speed of the EPP decay during the exponential phase is mainly governed by the rate of receptor closure, as will be discussed later. In addition to this parameter, we have also measured the falling times from the peak to 50%, and to 10% of its amplitude (**decay T_{50} and T_{90},** respectively). The latter parameters include the initial slowly-falling segment of the falling phase, which contributes to the more or less "rounded" aspect of the EPP summit.

The late section of the falling phase is quite variable from a preparation to another. Very often, small secondary responses are observed, most probably due to re-stimulation of nerve branches by the initial discharge (see Figure 6).

The striking observation is that the time course of an EPP elicited by stimulating a *Torpedo* electric organ prism with a single field shock is not greatly longer than that of elementary EPPs (or EPCs). The myriads of synapses in the prisms are activated and discharge with an impressive synchronisation. The remark also applies for the physiological discharge of the whole fish *in vivo*, elicited in response to a nociceptive stimulus (Figure 6 A and Table 1). The 300-400 prisms composing an electric organ fire with astonishing synchronisation.

It should be noted that while calcium ions have a very powerful influence on the secretory response of nerve endings submitted to a depolarizing stimulus, it has relatively little effect on the rate of spontaneous discharge, in the absence of a depolarizing agent (Fatt and Katz, 1952; Del Castillo and Katz, 1954; Boyd and Martin, 1956; Liley, 1956; Hubbard, 1961; Miledi and Thies 1967; Katz, 1969; Thesleff and Molgó, 198; Dunant, 1986; Lupa, 1987; Vautrin and Kriebel, 1991; Girod et al., 1993). One is left to thinking that the spontaneous occurrence of basic units of quantal transmitter release (MEPPs and sub-MEPPs), operating with low probability, are largely Ca^{2+} independent in nature, while the evoked responses are due to an extremely high probability of release during the very short period that Ca^{2+} invades the terminal at active zones, and are therefore absolutely Ca^{2+}-dependent (Katz, 1969; Girod et al., 1993). The neuro-electrocyte synapses of *Torpedo* electric organ seem to exacerbate this corollary by displaying rather low rates of spontaneous release, but explosively reaching maximal rates of release <150 μs after Ca^{2+}-entry due to a depolarizing stimulus (Dunant and Muller, 1986; Girod et al., 1993) that results in rapid activation of transmission (<1 ms) and decaying with a time constant (decay tau = 0.64 ms; table 2) that seems to follow closely the kinetics of nicotinic ACh receptors with mean open time <0.6 ms (Sakmann et al., 1985). This is due to an extremely rapid hydrolysis of the released ACh by acetylcholinesterase, which is highly concentrated in the synaptic cleft, like in neuromuscular junctions. Transmission in *Torpedo* electric organ is adapted to the phasic nature of a synapse capable of reaching high frequencies of stimulation.

The very high rates of transmitter release are coordinated by Ca^{2+} invading a terminal and activates ACh release channels (mediatophores) (Israël et al., 1981; Muller et al., 1987; Brochier et al., 1992; Dunant and Israël, 2000). Calcium ions act like gatekeepers of secretion that abruptly allow the passage of ACh in their presence. Yet, individual release events seem to occur almost instantaneously (under 150 μs according to Girod et al., 1993) and consequently it seems that the "guards" of those gates (calcium ions) must be themselves regulated. Who guards the guards? The nerve endings of the electric organ are endowed with a large number of synaptic vesicles that account for ~20% of its volume (Israël, 1972; Morel et al., 1980). This provides an enormous surface area of vesicular membrane in close vicinity of the plasma membrane where Ca^{2+} enters and ACh gets to be released from the terminal at <200 nm quantal release spots distant ~600-1000 nm from each other (Dunant and Muller, 1986; Girod et al., 1993).

Synapses of *Torpedo* electric organ do not have any specialized geometrical organization like the active zones of the endplate (Couteaux & Pécot-Dechavassine, 1973). Given that synaptic vesicles cover most of the terminal membrane they should be both in close proximity of <200 nm wide active zones as well as the ~800 nm plasma membrane space separating active zones. The first "layer" of *Torpedo* vesicles (~Ø 80 nm, each) provides the terminal with a membrane area that trebles that of the plasma membrane directly underneath it. Vesicles at more distant "layers" (>80 nm away) contribute with more vesicular membrane, but are relatively distant from the peak $[Ca^{2+}]_{int}$ at the time of a stimulus. Nevertheless, there is a wealth of vesicular membrane in close contact with high calcium concentration seemingly in perfect position to modulate the space-time profile of calcium microdomains.

The electric organ can also be used for biochemical assays that relate to synaptic function. Prisms can be loaded overnight with a radio-labelled ACh precursor (acetate or choline), that will enter the terminal and used to synthesise ACh. Removing the ACh precursor from the bathing medium and washing out copiously, reveals a rather "silent" tissue at rest; very low amounts of ACh leak out from the terminals in the absence of activation. This allows a signal to noise ratio that is good enough to detect ACh release from as little as a single nerve impulse. When a small number of stimuli are applied, ACh release can be assessed with an excellent proportionality (Dunant et al., 1980a). This technique allows therefore to correlate phasic ACh release measured by a biochemical method with post-synaptic recordings, being recorded at the same time on the same prisms (figures 6 and 7).

The *Torpedo* electric organ also provides an exceptional preparation for investigating dynamic changes of calcium metabolism in relation to synaptic transmission. Experiments where prisms were bathed in the presence of ^{45}Ca in addition to a physiological $^{40}Ca^{2+}$ concentration (3.4 mM) revealed that cellular and extracellular calcium fully exchange after 2-3 h incubation. Under such conditions, the relative changes in ^{45}Calcium give a faithful image of those of ^{40}Calcium. Brief nerve stimulation provokes a substantial calcium accumulation in the tissue, which in the electric organ takes place essentially in presynaptic nerve terminals at the active zones.

By washing the tissue in the standard solution (without ^{45}Calcium) right after the stimulation period, it is possible to assess calcium extrusion back into the extracellular medium, and to show the accumulation-induced surplus of cellular calcium return to control

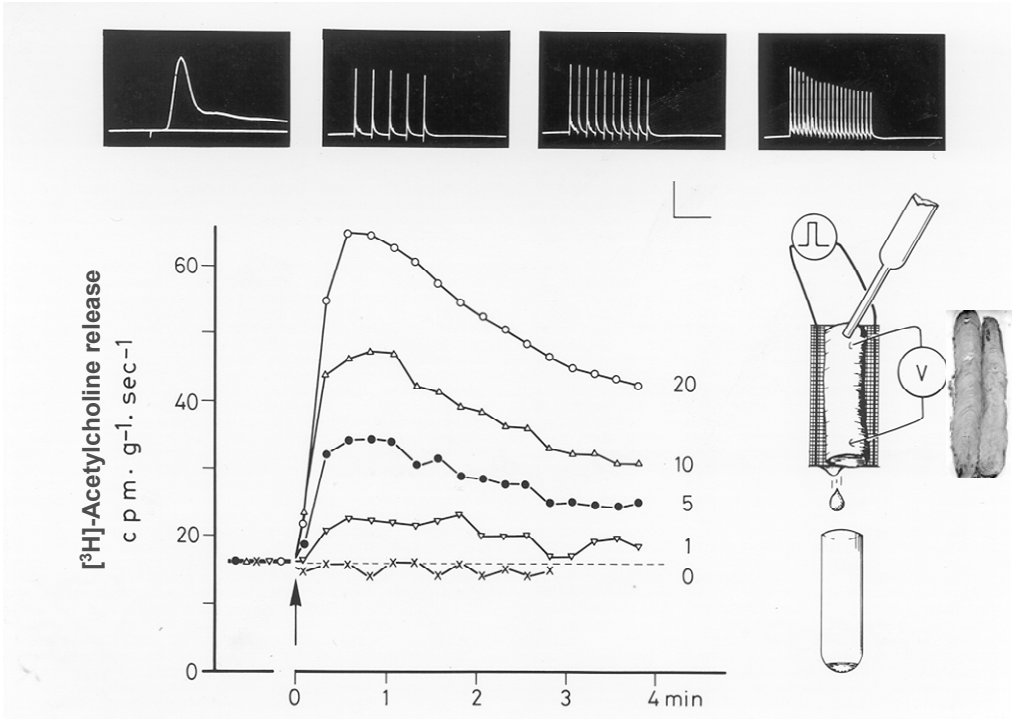

Figure 7. Measurement of radio-labelled [^{3}H]-Acetylcholine release from stimulated prisms. *Torpedo* electric organ prisms were labelled overnight with [^{3}H]-acetate. Prisms were placed on a holder under continuous perfusion with elasmobranch saline medium (right figure). [^{3}H]-ACh diffusing from excised prisms was collected in fractions lasting 15 seconds each, before and after field stimulation (↓) consisting of 0 (no stimulation) 1, 5, 10 or 20 shocks in 1 second. The electric responses from prisms were simultaneously registered (top traces) with calibration bars of 2V and 4 ms for the single response and 2V and 400 ms for the others (From Dunant et al., 1980a).

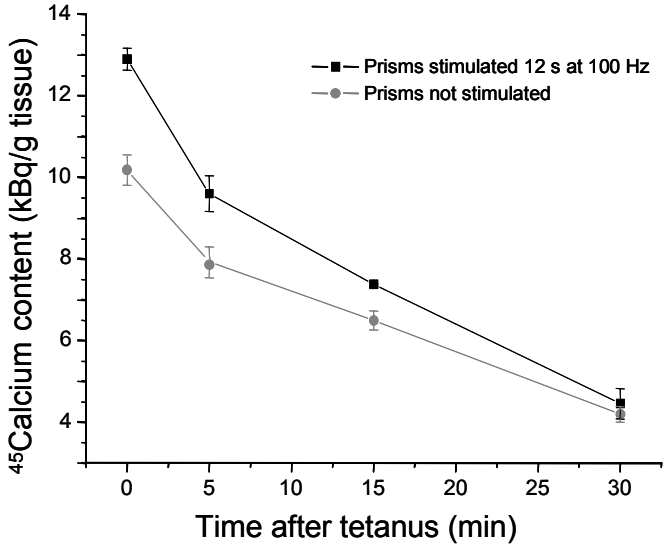

Figure 8. Extrusion of stimulus-dependent calcium accumulation from prisms following a 12 s tetanus at 100 Hz. Prisms were incubated with ^{45}Calcium containing elasmobranch saline medium for three hours. Then stimulated (black symbols) and not stimulated (grey symbols) prisms were washed in the standard medium without ^{45}Calcium and processed for quantification of tissue ^{45}Calcium 0, 5, 15 and 30 min after the tetanus. Values are mean ± SEM of 8 experiments.

value within approximately 30 min (figure 8) (Babel-Guérin, 1974; Dunant et al., 1980b; Párducz and Dunant., 1993; Párducz et al., 1994).

We took advantage of this approach to investigate alterations of calcium dynamics in nerve terminals by vesicular Ca^{2+}/H^{+} antiport and Ca^{2+}-ATPase inhibitors. This was possible because stimulation does not cause significant accumulation in post-synaptic electrocytes, contrarily to what happens in neuron-muscular preparations. In *Torpedo* electric organ virtually all calcium accumulates in the abundant nerve terminals where it was found to be particularly concentrated in close association with active zones after stimulation (Babel-Guérin, 1974; Dunant et al., 1980b; Párducz and Dunant., 1993; Párducz et al., 1994).

3.1.2. Neurotransmitter release in relation to proton and calcium transients in pinched off pre-synaptic nerve terminals (synaptosomes)

Nerve terminals can be detached from the post-synaptic cell as well as their own axons by homogenization, forming sealed synaptosomes (Whittaker., 1959; De Robertis et al., 1961; Israël at al., 1976). The synaptosomes are metabolically active, have active plasma membrane high affinity transport (i.e., choline), they synthesize and release transmitters and exhibit membrane potential (Israël et al., 1976, Morel et al., 1977; Meunier, 1984).

In this work we used two types of synaptosomes. The first ones were purely cholinergic nerve endings isolated from *Torpedo* electric organ as described previously (Israël et al., 19976; Morel et al., 1977). These synaptosomes are large (ca. 3.5 µm), very homogenous, and contain high concentration of cytosolic ACh (ca. 20 mM) in adition to vesicular ACh; they also contain ATP (ca. 3 mM) (Morel et al., 1978) This correlates very well with the estimated concentration of cytosolic ACh in *Torpedo* intact terminals (ca. 27 mM) (Dunant et al., 1974), and with the 27 mM and 34 mM ACh estimated respectively in the cytoplasm and whole tissue of the frog neuromuscular junction (Katz and Miledi, 1977).

Furthermore, *Torpedo* synaptosomes respond to a depolarizing stimulus only in the presence of Ca^{2+} by releasing ACh from their cytoplasmic compartment (Israël and Lesbats, 1981a), like it was demonstrated to occur in whole tissue (Dunant et al., 1972; 1974). ACh release can be followed continuously by a chemiluminescent method developed by Israël and Lesbats (1981a, 1981b). The amount of light emitted is proportional to the amount of ACh placed in contact with light-emitting enzymes, allowing for both measurement and calibration of transmitter release (figure 9).

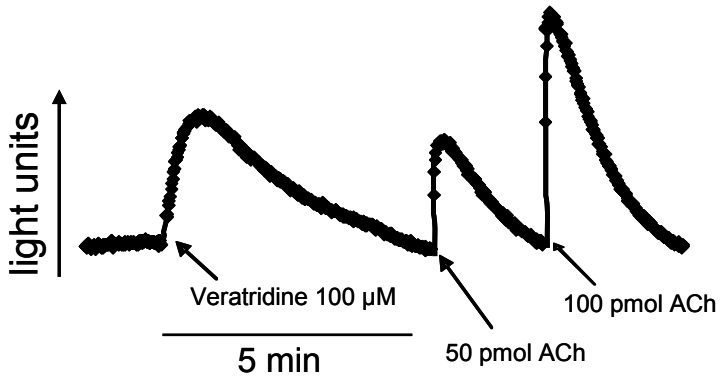

Figure 9. Acetylcholine release by 30 µl of electric organ synaptosome fraction using the chemiluminescent enzymatic method. Synaptosomes were kept in elasmobranch medium containing 3.4 mM $CaCl_2$ and depolarized with veratridine 100 µM to elicit ACh release. Standard amounts of ACh were added subsequently for calibration. Trace is representative of 10 experiments.

However useful for ACh release and other studies, we encountered some limitations to the use of several fluorescence techniques using *Torpedo marmorata* synaptosomes. We repetitively tried to use acridine orange and other fluorescent probes to assess pH changes within the acidic organelles of *Torpedo* synaptosomes, but our attempts were frustrated (figure 10 A and 13 A). It was only of little comfort to learn that previous attempts to use other fluorescence probes (including calcium probes) with fish preparations were without success in our and other laboratories. We hypothesize that *Torpedo* membrane and protein composition is not prone for the use of probes that were developed for mammalian preparations.

We overcame this unwieldy situation by using synaptosome and vesicle preparations isolated from mammalian tissue.

We prepared mossy fibre synaptosomes (MFS) from the rat brain hippocampus as previously described (Israël and Whittaker, 1965; Helme-Guizon et al., 1998). These synaptosomes are particularly large (1-8 µm)(Bancila et al., 2004). They come from the large mossy fibre of the CA3 region, which are the nerve endings of axons issued from granular cells of the dentate gyrus (Amaral and Witter, 1989). Furthermore, these giant synaptosomes maintain an astonishing vigour after isolation; as shown by a resting membrane potential of -85 mV (Bancila et al., 2004, 2008); capability of releasing glutamate as a function of Ca^{2+} concentration and membrane depolarization; and the presynaptic expression of pre-synaptic long-lasting potentiation (Helme-Guizon et al., 1998; Bancila et al., 2004, 2008).

Mossy fibre synaptosomes were used to measure glutamate release using a luminescence approach (figure 41) and changes of the vesicular proton gradient, using the fluorescent probe acridine orange (A.O.). The accumulation of A.O. in the acidic organelles of synaptosomes results in fluorescence quench due to dimerization of A.O. molecules. Therefore, any decrease in intravesicular H^+ concentration results in an increase in A.O. fluorescence, i.e., a transient dissipation of vesicular proton gradient (figure 10 B), as previously shown in experiments using rat brain cortex synaptosomes (Zoccarato et al., 1999). This phenomenon might be attributed either to the activation of vesicular Ca^{2+}/H^+ antiport, or by a cycle of vesicular fusion followed by endocytosis and re-acidification of vesicles.

We also used MFS to measure $[Ca^{2+}]_{int}$ rise in the bulk of the cytoplasm induced by a depolarization in the presence of calcium. For that we incubated MFS with the membrane permeable form of Fura-2 Ca^{2+} fluorescence probe, and determined the fluorescence changes due to Ca^{2+} entry induced by depolarizing the terminals with veratridine (figure 11).

In the set of experimental procedures described above we addressed the roles of vesicular Ca^{2+}-ATPase and that of the Ca^{2+}/H^+-antiport in the temporal-definition of fast post-synaptic responses (electrophysiology), as well as the amounts of ACh and glutamate released from synaptosomes under similar conditions (chemiluminescence). They were also used to relate the Ca^{2+}/H^+ antiport activity with the $[Ca^{2+}]_{int}$ and proton transients induced after applying a depolarizing stimulus to rat hippocampus MFS.

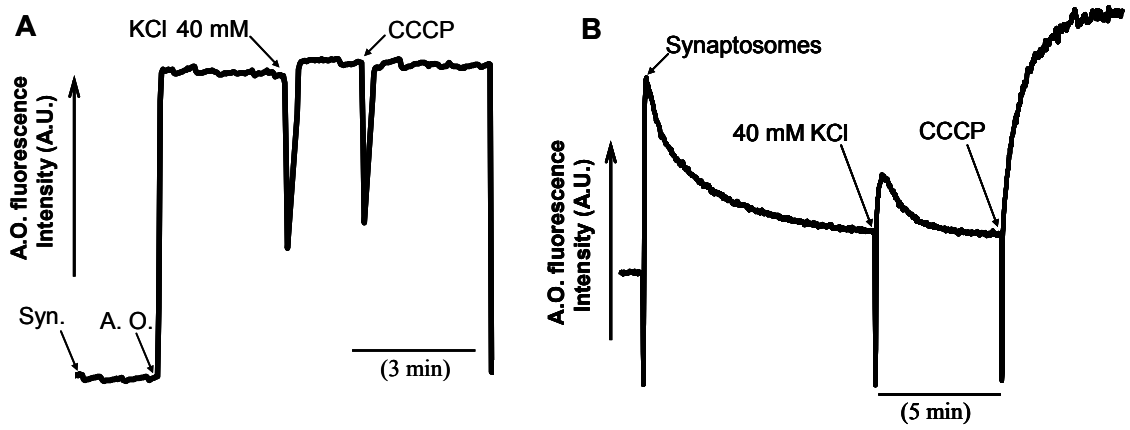

Figure 10. Monitoring proton gradient formation and dissipation with the acridine orange (A.O.) dye in synaptosomes. Panel **A**: Failure to record proton gradient using A.O. fluorescence in *Torpedo* electric organ synaptosomes (syn.).There was no quenching of A.O. fluorescence by synaptosomes (25 μl or ~50 μg protein), and consequently it has not been possible to measure any dissipation after adition of 40 mM KCl or of the protonophore CCCP. The downward deflections were due to the opening of the fluorimeter chamber for introducing the drugs Representative trace of (n=10). Panel **B**: Similar experiment using mossy fibre synaptosomes

isolated from rat brain hippocampus. Proton gradient was monitored by adding 10 mg/ml of the synaptosome suspension (arrow) to Krebs solution containing 3 μM acridine orange. Fluorescence quench occurred when the dye penetrated into and was exposed to acidic medium inside acidic compartments, where it dimerised and accumulated as the proton gradient was formed across acidic compartments. Addition of 40 mM KCl in the presence of 2.2 mM $[Ca^{2+}]_{out}$, induced a transient of the H^+ gradient, which was then fully dissipated by 10 μM CCCP. Representative A.O. fluorescence trace of (n=6).

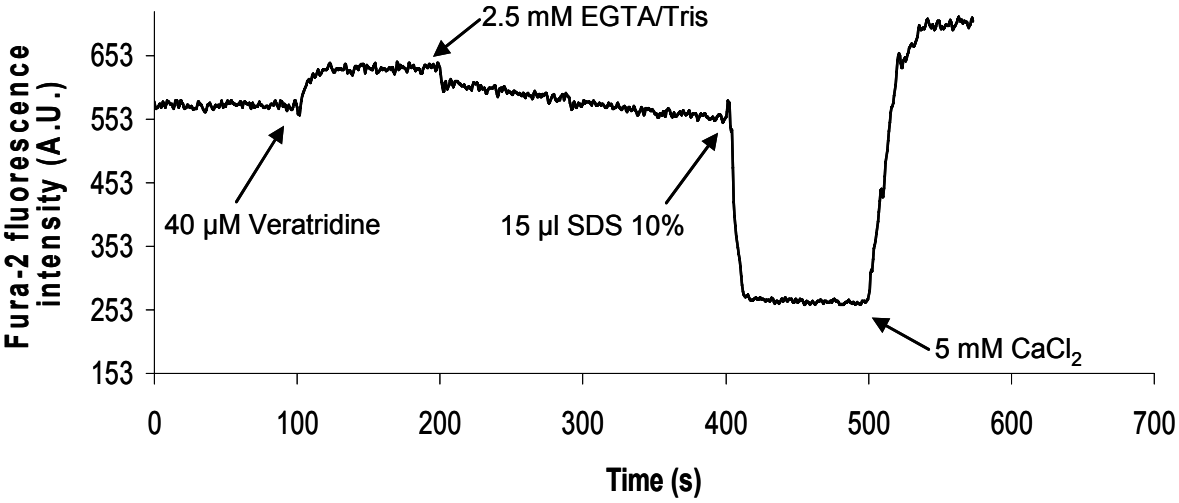

Figure 11. Calcium concentration within rat hippocampus mossy fibre synaptosomes monitored by Fura-2 fluorescence. Fluorescence trace of Fura-2-AM loaded synaptosomes kept in mammalian Krebs containing 1.33 mM $CaCl_2$. Fluorescence was measured before (basal) and after depolarization with 40 μM veratridine (arrow). Addition of EGTA caused a progressive decrease in fluorescence. Full decrease to a fluorescence minimum occurred after synaptosome permeabilization with SDS. An excess of calcium was added at the end of each assay for calibration (fluorescence maximum).

3.1.3. Neurotransmitter content and Ca^{2+} and H^+ transport by isolated synaptic vesicles

When synaptic vesicles were first isolated from mammalian brain by De Robertis et al. (1963) and Whittaker (1964), they were demonstrated to contain more ACh than other fractions. However, ACh is only a minor neurotransmitter in mammalian brain, where no more than 10-15% of synapses are cholinergic. In contrast, being purely cholinergic, the *Torpedo* electric organ allowed for isolation of a vesicle fraction of much higher yield and purity (Israël et al., 1968)

Torpedo synaptic vesicles have ~100,000-200,000 molecules of ACh per vesicle (Ohsawa et al., 1979). The amount of ACh and ATP existent in a given synaptic vesicle

suspension can be measured by chemiluminescence (Israël and Lesbats, 1981a, 1981b; Strehler 1974; Dunant et al., 1988). Figure 12 shows the comparative analysis of ACh content from two preparations of synaptic vesicles, one isolated from *Torpedo* electric organ and the other one from rat brain, according to the methods described by Israël et al. (1980) and Hell et al. (1988), respectively. ACh was quantified by the chemiluminescence method by permeabilization of vesicular content with Triton X-100 followed by ACh calibration. Inset shows the difference in ACh content between the two SV preparations.

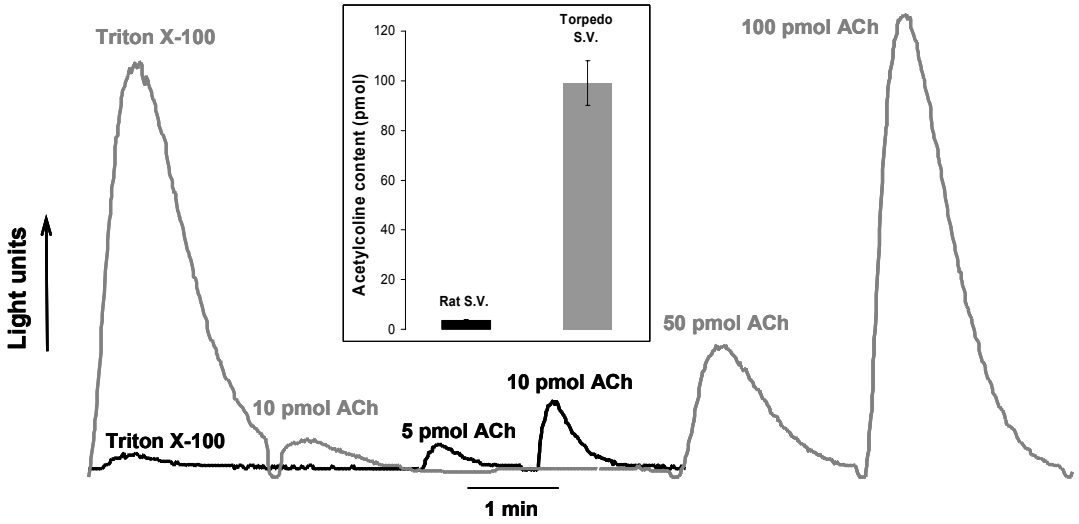

Figure 12. Comparison between the vesicular acetylcholine content in synaptic vesicles isolated from *Torpedo* marmorata electric organ and those from rat brain cortex. Traces show ACh-dependent light emission by chemiluminescence in elasmobranch or mammalian medium containing either 25 µl (~3 µg) of *Torpedo* s.v. fraction (grey) or 60 µg protein rat synaptic vesicles (black), respectively. Vesicular content was determined by adition of 5 µl Triton X-100 1% to the synaptic vesicle suspension followed by standard amounts of ACh. **Inset** Bars show the average ± SEM (n=6-11) ACh content within vesicles isolated from rat or *Torpedo*.

One of the methods that we can use to assess the activity of vesicular Ca^{2+}/H^{+} antiport is to follow acridine orange fluorescence response to changes in isolated S.V. internal acidic milieu (Gonçalves et al, 1998). Like with synaptosomes, we tried to use A.O. with synaptic vesicles isolated from *Torpedo* electric organ (figure 12 A) without any success (despite innumerous attempts). We moved for the isolation of synaptic vesicles from rat brain by the method described by Hell et al. (1988). Likewise to results obtained with synaptosomes, we were able to elicit dissipation of the vesicular proton gradient by addition of 500 µM Ca^{2+} to the vesicular suspension (figure 13).

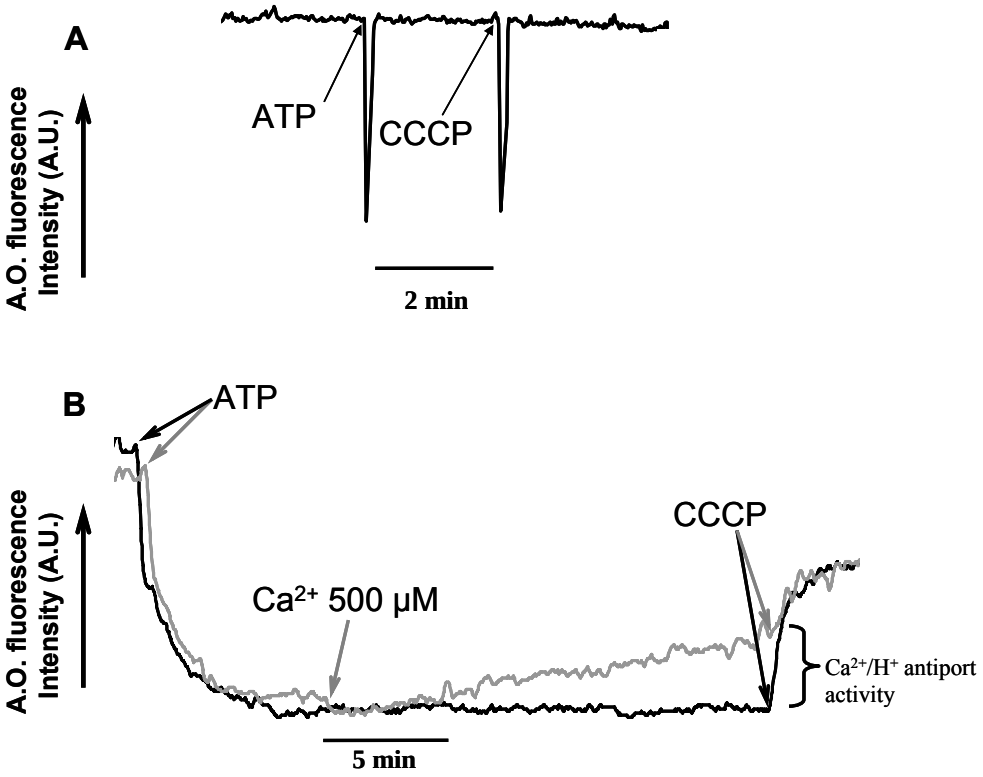

Figure 13. Following proton gradient formation and dissipation with the acridine orange (A.O.) dye in isolated synaptic vesicles. Panel **A**: With synaptic vesicles isolated from *Torpedo* (25 µl) in 200 mM KCl, 2 mM $MgCl_2$, 400 mM sucrose, 10 mM Tris-HCl, pH 8.5 and 50 µM EGTA. No fluorescence change could be detected using acridine orange dye (3 µM) after addition of 0.5 mM ATP or 10 µM CCCP. Representative A.O. trace (n= 10). Panel **B**: Representative A.O. fluorescence trace (n= 3) with synaptic vesicles isolated from rat brain (600 µg/ml) added to medium containing 60 mM sucrose, 2 mM $MgCl_2$, 150 mM KCl, 50 µM EGTA, 10 mM Tris–HCl, pH 8.5 and 3 µM A.O.. After a period of stabilization, 0.5 mM ATP was added to allow the formation of H^+ gradient. Quenching of the probe's fluorescence occurs when the dye is exposed to acidic medium within vesicles, where it dimerises and accumulates. After complete gradient formation H^+ gradient dissipation was assayed in the absence (black trace) or presence of 500 µM free [Ca^{2+}] (grey trace). Full dissipation of the proton gradient was eventually induced by addition of the protonophore CCCP (10 µM).

3.1.4. Genetically modified proteins to study vesicular Ca^{2+} transport in cultured cell clones

When we proposed ourselves to seek for the protein encoding the vesicular Ca^{2+}/H^+-antiport we did so by hypothesizing that synaptotagmin I was the most probable candidate for such activity (see also introduction).

Therefore we looked for a model where we could compare between synaptotagmin I expressing (+/+) versus non-expressing (-/-) cells. The model also had to be rich in synaptic vesicles so that we could clearly determine under similar conditions: 1) Ca^{2+}/H^{+} antiport-dependent vesicular $^{45}Ca^{2+}$ transport and 2) dissipation of the vesicular proton gradient induced by this vesicular Ca^{2+} transport.

The choice was for the use of PC-12 cells. These are originated from a rat benign tumour (pheochromocytoma) derived from chromaffin cells in the medulla of the adrenal glands. PC-12 cells can suffer spontaneous mutations with increasing number of passages. Shoji-Kasai et al. (1992) took advantage of this to selectively target synaptotagmin I expressing cells using specific antibodies and adding complement to kill them by cytolysis. This allowed for the selection of cell clones containing neither synaptotagmin I protein nor the corresponding mRNA. PC-12 cells are naturally devoid of synaptotagmin II, so we found ourselves on the one hand with a model without synaptotagmin I or II, called F7, and on the other hand, with a cell clone positively labelled for synaptotagmin I protein and mRNA named G11. Both of them were nevertheless capable of releasing dopamine and ATP upon stimulation (Shoji-Kasai et al., 1992). PC-12 cells are also cells endowed with a particularly large population of both large dense core granules as well as electronlucent synaptic-like vesicles. Post-nuclear fractions of PC12 cells are capable of generating particularly robust transvesicular membrane H^{+} gradients, as measured by acridine orange (Bloc et al., 1999). Furthermore, the post-nuclear suspensions (PNS) provide for an A.O. signal that is mostly due to bafilomycin-sensitive acidic organelles that are less H^{+}-leaky than synaptic vesicles isolated from sheep brain cortex (figure 14).

We cultured F7 and G11 clones of PC-12 cells (kindly provided by Dr. Shoji-Kasai) (figure 15) and prepared post nuclear supernatants that contained the acidic organelles where we tested for Ca^{2+}/H^{+}-antiport activity (figures 51-57). Similar results were obtained with these cells differentiated with nerve growth factor (figure 15 B) to induce differentiation into neurons (data not shown).

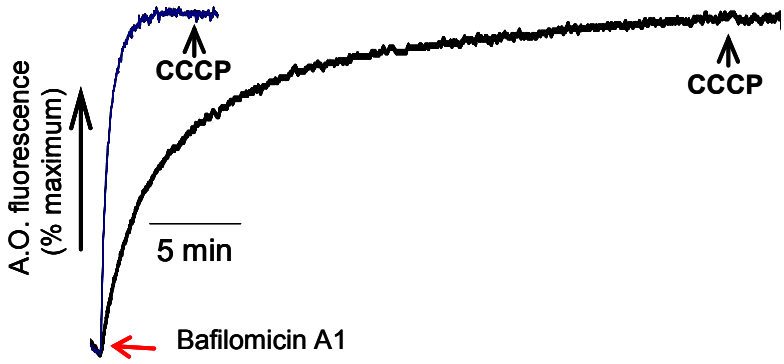

Figure 14. Slow proton gradient dissipation from PNS suspensions of PC12 cells. Traces illustrate proton gradient dissipation induced by 0.6 μM bafilomycin A1 in PNS suspension (0.3 mg protein/ml; black trace) or synaptic vesicles isolated from sheep brain cortex (0.6 mg protein/ml; blue trace). Proton gradient was monitored using A.O. fluorescence and bafilomycin A1 was added after complete H^+ gradient formation (red arrow). CCCP (10μM) was added in the end of assays to check for complete H^+-gradient dissipation. Fluorescence traces were scaled to their full dissipation for comparison.

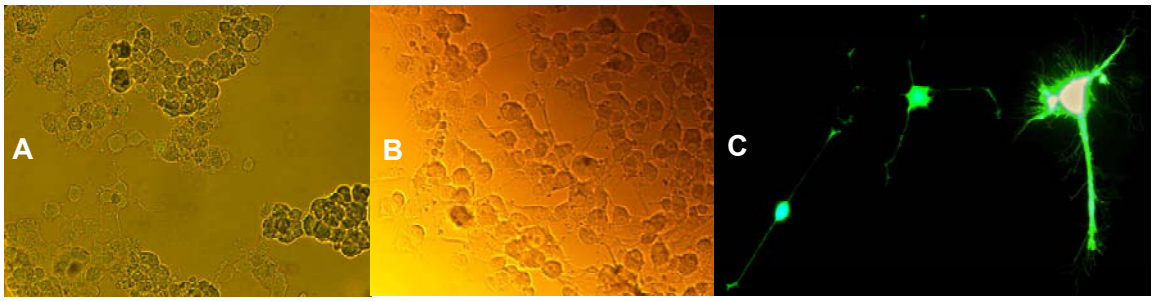

Figure 15. PC12 F7 cell culture. Panel ***A***: undifferentiated cells observed by phase contrast microscopy. Panel **B**: Cells differentiated with mNGF 7S for 4 days by phase contrast microscopy. Panel ***C***: Cells transfected with the gfp gene and differentiated with mNGF 7S for 4 days, observed in fluorescence microscopy (excitation at 488 nm and emission at 528 nm).

It was also possible to transfect these cells with a gene of interest i.e., egfp gene transfection in figure 15 C or Syt_tagg labelled with FlAsH (figure 16). However, when one uses a model that is genetically impaired, there is always the possibility of having had developmental compensation (Madhani and Fink, 1998; Plum et al., 2002) by closely related proteins (for example, Syt IX seems to be up-regulated in F7 cells (Fukuda et al., 2002)) that could lead to false interpretation of results. To avoid this one could use rather common techniques like those interfering with normal RNA processing or the use of the pharmacological approach (inhibitors). However, interfering with RNA processing takes

prolonged periods of time (since it relies on the gradual turnover of endogenous RNA) and would not prevent rapid compensatory mechanisms. On the other hand we do not know any inhibitory substance that is specific for the Ca^{2+}/H^{+}-antiport.

Therefore we used a recent technique that allows to studying the function of a protein in vivo by acutely, non-invasively and specifically inactivate our protein of interest and proceed immediately with our assays.

We transfected a transgene encoding synaptotagmin I fused with a tetracysteine sequence (Cys-Cys-Pro-Gli-Cys-Cys) in the resulting fusion protein. This sequence is responsible for the recognition of a biarsenical probe, able to fluoresce when bound to the fusion protein (notice in figure 16 the punctuate labelling of vesicles) and liable to generate highly reactive free radicals (oxygen singlets) when exposed to intense UV light, in a process called fluorophore assisted light inactivation (FlAsH-FALI). FlAsH is a fluorescein derivative of fluorescein which has been shown to be 50 x more efficient than malachite green or GFP for FALI (Surrey et al., 1998).

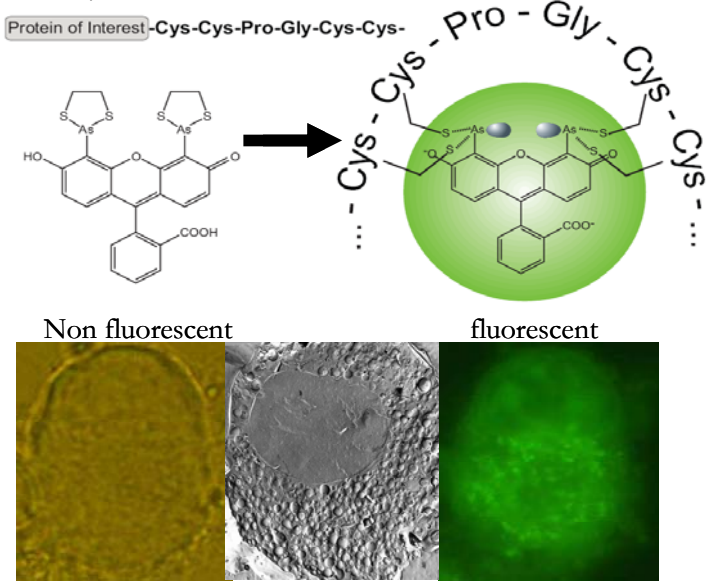

Figure 16. FlAsH punctuate labelling of a tetracysteine motif inserted within synaptotagmin I in cell granules of PC12 cells. Top: Schematic view showing the molecular formula of fluorescein-based arsenical hairpin binder (FlAsH) dye, before (non fluorescent) and after (fluorescent) binding to a tetracysteine motif inserted into the protein of interest. Bottom: PC 12 cells were transfected with a construct coding for synaptotagmin I with a tetracysteine motif fused to its C-terminal. Cells were labelled with FlAsH-EDT_2 and phase contrast image (left) or fluorescence image (right) was taken with a FITC (fluorescein: excitation at 488 nm and emission at 528 nm) filter. The electron micrograph (center) shows a chromaffin cell (from witch PC12 cells derive) vastly populated with vesicles and granules. Micrograph by Schmidt et al. (1982).

FlAsH binds the tetracysteine motif with a dissociation constant of 10^{-11} M (Gaietta et al., 2002), guaranteeing nearly 100% labelling and very efficient inactivation (Beck et al., 2002; Marek and Davies, 2002). Furthermore, FALI is very specific because the tetracysteine motif is hardly found in endogenous proteins and because the estimated half maximal inactivation distance is approximately 30-40 Å (Surrey et al., 1998; Beck et al., 2002), making it possible that not all functional domains of a protein are accessible to the destructive effects of FALI, but certainly enough to destroy the C2B domain of synaptotagmin I, that is, a site very close to the C-terminus where the tetracysteine tag was fused to (Wang et al., 1996; Marek and Davis, 2002).

3.2. Experimental findings

3.2.1. Ca^{2+}/H^{+} antiport shapes the time-course of fast neurotransmitter release

3.2.1.1. Bafilomycin shapes secretion timing and interferes with calcium clearance in nerve terminals

We addressed the participation of synaptic vesicle Ca^{2+} sequestration through a Ca^{2+}/H^{+} antiport in rapid neurotransmission. To achieve the high temporal definition needed to follow "real-time" synaptic transmission we registered the electric response of prisms excised from *Torpedo* electric organ (described in section 3.1.1.), and submitted to field stimulation (figure 6 and 17). The response of prisms is a compound electroplaque potential (EPP) resulting from the summation of an enormous number of quantal EPP generated with an astounding synchronization. The compound EPPs display a very similar time course as the elementary EPPs, as well as the spontaneous MEPP or even the miniature eletroplaque current (MEPC) (Girod et al., 1993) (Table 1).

We tested for a role of vesicular Ca^{2+} sequestration in the temporal definition of ACh release in *Torpedo* prisms. To do so, we compromised vesicular Ca^{2+}/H^{+} antiport activity by inhibiting the V-type H^{+}-ATPase (Gonçalves 1999a) with the specific blocker, bafilomycin A1 (Dröse and Altendorf, 1997). The use of bafilomycin A1 has the advantage of targeting only the organelles relying on a proton pump and leaving other organelles like mitochondria intact. In this way we were able to restrict our analysis to the effect of collapsing vesicular proton gradient on synaptic transmission.

Bafilomycin significantly affected the evoked electroplaque potential of prisms (Figure 17, table 2 and 3). It affected chiefly the time course of secretion, prolonged from <3 ms up to 10 ms in some cases, like at the example in figure 17 A. It was fully reversible by washing out during one hour (figure 17, B). The prolonging effect resulted from bafilomycin incubation, since control prisms (figure 17 C, without bafilomycin) stimulated after 1h or 2h in saline medium kept the same time course. It should be noticed that some prisms produce small secondary responses to the field stimulation due to re-stimulation of nerve fibres. In that case, the enlargement profile of transmission due to bafilomycin resulted in the loss of resolution of primary and secondary spikes that merged in a single response with particularly long time course as compared with single spike responses. For this reason we

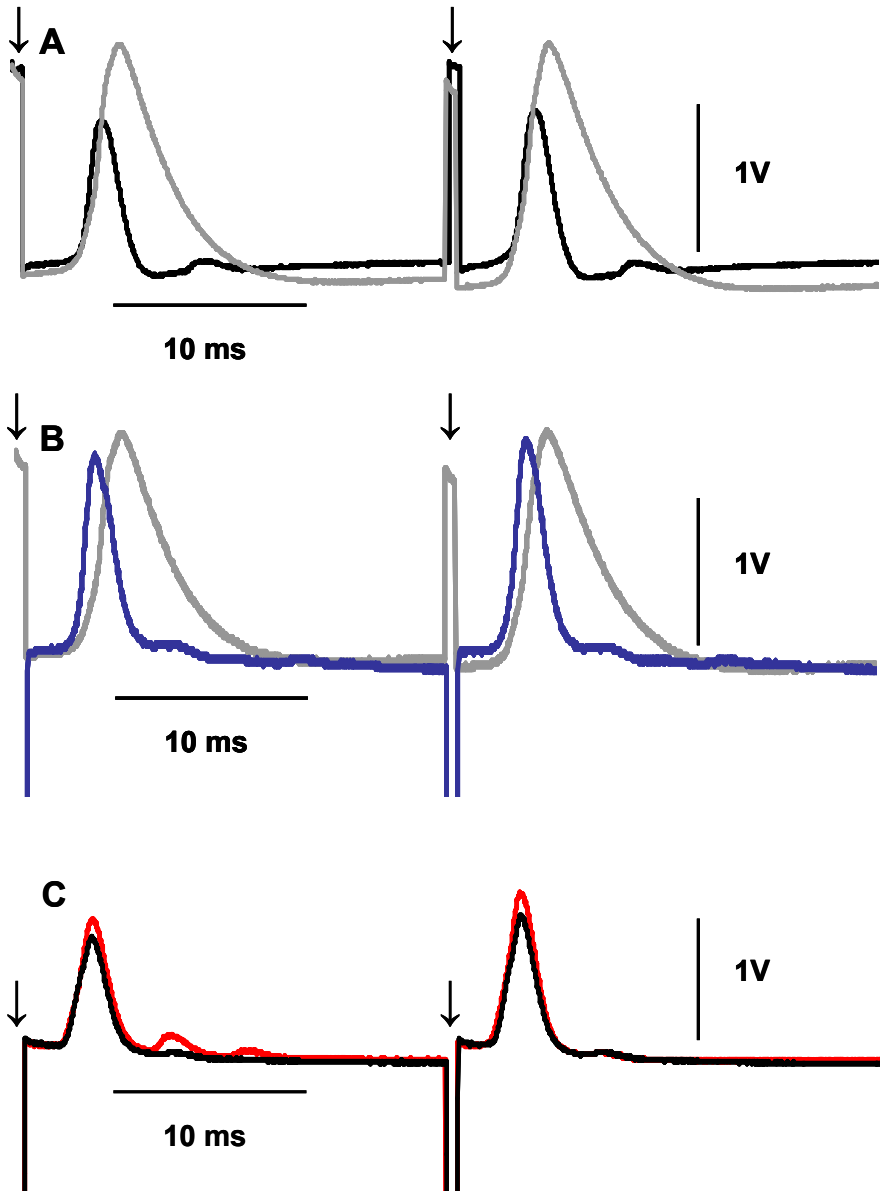

Figure 17. Effect of bafilomycin A1 on neurotransmission in the electric organ of *Torpedo*. Representative experiment from n=18. Prisms of electroplaques were excised from the electric organ and submitted to paired pulse field stimulation (20 ms interval between stimuli). Traces show in succession the stimulation artefact (↓), the synaptic delay, and the electrical discharge (postsynaptic potential or electroplaque potential, EPP). The elasmobranch saline medium contained 3.4 mM $CaCl_2$, in the absence (control) or presence of 2 μM bafilomycin A1. Panel **A**: Control EPP recorded after 1h incubation in elasmobranch saline medium (——), and EPP produced by the same prism perfused in presence of bafilomycin A1 during 1h (——). Panel **B**: Reversion of bafilomycin A1 effect (——) after washing out during 1h (——). Panel **C**: EPP recorded from another prism after 1h (——) and 2h (——) under control conditions.

measured parameters (described in section 3.1, figure 6) that best describe and separate each phase of evoked secretion and analysed the influence of bafilomycin on them (tables 2 and 3). Table 2 reflects the analysis made on 18 independent experiments where the electric response of bafilomycin-incubated prisms was compared to the same prisms prior to drug exposure. Bafilomycin exerted a marked effect on the time course of transmission without changing significantly its amplitude or onset. This is reflected by ~92% increase in prism EPP area, a parameter that integrates the amount of transmitter release over the time course of transmission. It is interesting to notice that there was only a slight, non-significant, increase in peak amplitude. This probably arose from the fact that even under control conditions the maximum rate of transmission is already reached at the peak of the response.

This is not surprising if we take into consideration that the action of a given release site on neighbouring receptor field (~800 nm away) is strongly limited by the activity of acetylcholinesterase that degrades ACh very fast (Rosenberry, 1975; Wathey et al., 1979) and is capable of limiting the number of ACh molecules capable of activating receptors a few hundred nm away (Girod et al., 1993). In *Torpedo* synapses however, evoked quantal release under normal physiological conditions occurs at release sites that are capable of synchronous ACh release in a super-additive manner that already uses most of the partial activation of neighbouring receptor field's capacity (Girod et al., 1993). Therefore, the slight bafilomycin-induced increase in prism amplitude might also be attributed to an increase in the amount of ACh being released but whose post-synaptic action on neighbouring receptor fields was strongly limited by an abundant (Salpeter et al., 1978) and extremely efficient ACh esterase activity (Rosenberry, 1975 and Wathey et al., 1979).

Since the response of dissected prisms differs slightly from each other, it is useful for the sake of comparison to calculate the prism EPP area/peak ratio. Bafilomycin increased area/peak ratio by 71% indicating that the main influence is on increasing ACh release duration, rather than influencing peak amplitude.

From the above parameters we learned that bafilomycin can increase prism EPP timing, probably by increasing the time course of ACh release. However, they do not tell us if those effects are due to an early onset of ACh release or rather a late effect, or even a combination of both early and late effects.

The time a prism EPP takes to reach its maximal value (peak) can give some information on the kinetics and wave form of activation of ACh receptors by ACh released.

Table 2. Amplitude and time characteristics of bafilomycin A1 effects on neurotransmission in *Torpedo* electric organ

Parameter	Control	Bafilomycin A1	
Area (V.ms)	4.99 ± 0.85	9.08 ± 1.28 *	(192 ± 21 *)
Peak (V)	2.99 ± 0.47	3.11 ± 0.50	(108 ± 8)
Area/peak (ms)	1.70 ± 0.09	2.79 ± 0.24 ***	(171 ± 21 ***)
Rise Time (ms)	1.01 ± 0.08	1.26 ± 0.06 *	(128 ± 9 *)
Rate of Rise (V/ms)	3.37 ± 0.48	3.32 ± 0.37	(99 ± 7)
Latency (ms)	2.23 ± 0.06	2.94 ± 0.39	(102.6 ± 3)
T.50% (ms)	0.90 ± 0.03	1.56 ± 0.23 **	(178 ± 29 **)
T.90% (ms)	1.70 ± 0.09	3.37 ± 0.50 **	(206 ± 35 **)
Decay tau (ms)	0.64 ± 0.03	1.25 ± 0.20 **	(205 ± 37 **)

Prisms were submitted to field stimulation in elasmobranch saline medium containing 3.4 mM $CaCl_2$ in the absence (control) or presence of 2 µM bafilomycin A1. Values are mean ± SEM of 18 experiments. Values between parenthesis show bafilomycin data expressed in percentage of control. Statistical significance was computed for bafilomycin data with respect to control values using Student unpaired T-test (*$p<0.05$; **$p< 0.01$; ***$p<0.001$).

The parameter used to measure such kinetics is called rise time and measures the time between 10% and 90% of peak response to avoid ill defined onset points and the somewhat rounded shape of EPPs. It is interesting to recall that prism EPPs are the summation of unitary EPPs (MEPPs) released with such a synchrony that makes it possible that prim rise time is only twice that of MEPPs or MEPC (see table 1).

Bafilomycin-incubated prisms showed 28% increase in time to peak as compared to control prisms (table 2). The effect was fairly visible during the experiments with the upper portion of the EPPs accentuating the round form. The idea that the bafilomycin effect happens with more extent in the upper portion of the rising EPP is corroborated by the fact that the rate of rise was unchanged by bafilomycin.

The 28% effect on rise time might indicate a slight de-synchronizing effect (with some release sites being activated slightly later in presence of bafilomycin) or alternatively, the possibility that the increased number of ACh molecules shifts the peak response to the right as a result of delayed activation of receptors due to some super-additive activation of

neighbouring receptor fields coming to action slightly later (they would be at few hundred nm away and activated by the few ACh molecules having escaped AChE hydrolysis) but just in time to contribute to the peak response occurring slightly later.

This rather late effect of bafilomycin is in line with minor, non-significant, change in the latency between the stimulus and the beginning of prism EPP wave response. It also implies that bafilomycin has (as expected) minor or no effect on the generation or conduction of action potentials, on calcium entry into the terminal, or on the kinetics of activation of the calcium sensor that is responsible for ACh secretion and has no effect on the activation of post-synaptic nicotinic ACh receptors, either. Ruling out these participants accentuates the idea that bafilomycin acts at a stage downstream of secretion activation and puts the tonic in the possible modulators of secretion time-course, like calcium transient timing and intensity (but we'll come back on this afterwards).

In spite of affecting rise time already by 28%, bafilomycin exercises its full power over the later phase of transmission. This can be appreciated by looking at the parameters measuring the rapid decay of prism EPP, that normally correlate closely with the mean open time of *Torpedo* nicotinic ACh receptors (0.6 ms; Sakmann et al., 1985). In fact bafilomycin increased the time required to decrease EPP to $\frac{1}{2}$ of its amplitude (or T_{50}) by almost 80% and more than doubled the time required to decrease EPP by 90% (or T_{90}). Both of these parameters are fairly sensitive to the "rounded" profile of the EPP wave form (possibly affected by the interference of, out of phase, secondary stimulation of prisms superposed to the later part of enlarged EPP waves). Yet, the decay phase mean time constant (or decay tau), that in normal circumstances, reflects the kinetics of channel closure also suffered a markedly increase, more than doubling in presence of bafilomycin. This "prolonging" effect could be either related to some post-synaptic action, like increasing the mean time opening of nicotinic receptors or interfering with acetylcholinesterase activity. We found evidence, however, that the effect arose from a prolongation of ACh release.

The fact that we used an antibiotic that is specific for the V-type-H^+ ATPase leads to ruling out a post-synaptic effect and to follow the lead that ACh release is augmented by bafilomycin (see below). Additionally, the fact that the decay tau more than doubled its value argues for a prolonged time-course of ACh secretion instead of just increased amount of ACh being released over the usual time and what is more, it sets a minimum time limit to surplus ACh secretion in ~0.61 ms (1.25-0.64) that relate only to the decaying phase of the EPP and

to which should be added some time (probably less) related to the 28% effect on rise time (some 0.25 ms). In all, ACh release endures at least 860 μs over normal release time. That should be below the calculated rise time (ca. 1 ms). If we take into consideration that rise time of normal excised prisms only doubles (up to 2.5 x the rise time of sub-MEPPs) that of quantal and sub-quantal events and that those events (minis) are believed to result from synchronous release of ACh from a given active zone (<200-300 nm wide) in less than ~150 μs (Girod et al., 1993) we can assume that ACh released by the billions of active zones in a single prism release their cargo in <400 μs and come to the conclusion that roughly, bafilomycin-treated prisms extend the ACh release period at least to 1260 μs ("normal" 400 μs + "extra" 860 μs) and the resulting EPP over three ms.

The fact that bafilomycin appears to induce a protracted time course of ACh secretion from excised prisms seems to bear out the original hypothesis proposed in the introductory chapter of this thesis that Ca^{2+} sequestration by a vesicular Ca^{2+}/H^{+} antiport might be involved in restricting the microdomain of high [Ca^{2+}] both in time (to a few microseconds) and in space (to a few nanometres away from the calcium sources that coordinates ACh release).

(Katz and Miledi, 1968; Miledi and Thies, 1971; Rahamimoff, 1968; Rahamimoff and Yaari, 1973; Zucker and Lara-Estrella, 1983; Van Der Kloot and Molgó, 1993; Kamiya and Zucker, 1994; Xu-Friedman and Regehr, 2000). Paired pulse facilitation (PPF) is a form of synaptic plasticity in which a pre-synaptic terminal stimulated twice in a short interval (Ca. 20 ms interval, as in figures 6 and 17) yields an increase in the second response (EPSP) with a time course that is similar to the time course of delayed release (Zucker and Lara-Estrella, 1983; Van Der Kloot and Molgó, 1993; Xu-friedman and Regehr, 2000).

The calcium theory for transmitter release (first section of introduction) contemplated the formulation of the residual calcium hypothesis for facilitation. Katz and Miledi (Katz and Miledi, 1968; Miledi and Thies, 1971) proposed that facilitation is the natural consequence of nonlinear calcium dependency of transmitter release, with a power dependency of 3-5 (Dodge and Rahamimoff, 1967; Hubbard et al, 1968; Katz and Miledi 1970; Dunant et al., 1980a; Yazejian et al., 2000) and that after an action potential, some subthreshold residual calcium persists in transmitter release sites (Miledi and Parker 1981; Charlton et al., 1982; Xu-friedman and Regehr, 2000).

It is interesting to notice that facilitation depends on the initial (first EPP) probability of transmitter release. Low release probability of release (i.e., in low Calcium) enhances paired pulse facilitation (Rahamimoff, 1968; Creager et al., 1980; McNaughton, 1982; Dobrunz and Stevens, 1997; Xu-friedman and Regehr, 2000; but see figure 27). Yet, calcium entry during the first spike causes facilitation whether or not transmitter is released by the first spike –i.e., release failure, or the "release of zero quanta"- as reported by Del Castillo & Katz (1954) and Dudel & Kuffler (1961). Low release probabilities are achieved in low calcium, where the percentual increase of the second EPP is much greater than in high calcium (figure 27). This is in line with the prediction that facilitation resulted from the building-up of a second Ca^{2+} microdomain "on top" of the Ca^{2+} mould resultant from the remaining ions after the collapse of the previous microdomain enabling to reach the necessary [Ca^{2+}] needed for Ca^{2+} binding up to saturation of a greater number of calcium sensors. When all sensors in release sites are fully activated no facilitation of peak amplitude can occur simply because it is already at its maximum (figure 27).

We considered the possibility that residual calcium responsible for paired pulse facilitation should be sensitive to the action of a vesicular Ca^{2+} transport system capable of restricting calcium microdomain that seems to be capable of preventing lingering ACh secretion.

Excised prisms were submitted to 20 ms interval paired pulse stimulation in elasmobranch saline medium containing 3.4 mM $CaCl_2$ (control) or after supplementation with 2 μM bafilomycin A1 during 2h before stimulating. Paired pulse facilitation was compared for the two groups (with or without bafilomycin) and the second EPP was expressed as a percentage relatively to the first EPP (table 3). The experiments were done with 3.4 mM $CaCl_2$ in the extracellular medium, a concentration that yields only mild facilitation presumably because synapses are close to maximal activation, already during the first impulse.

Nevertheless, it is interesting to notice that facilitation of the second peak in normal calcium saline medium (control in table 3 but see also above mentioned references) is marked by an increase of the peak response when compared to the first stimulus.

The increase in EPP area is the result of increased peak response yet, it declines as fast as the first EPP, which is reflected in unaltered area/peak ratio. The rise time was

Table 3. Effect of bafilomycin A1 on the facilitation obtained with paired-pulse stimulation

	Facilitation (2^{nd} response in % of 1^{st} response)	
Parameter	**Control**	**Bafilomycin A1**
Area (V.ms)	**115 ± 6**	**105 ± 3**
Peak (V)	**110 ± 5**	**102 ± 2**
Area/peak (ms)	**104 ± 2**	**103 ± 2**
Rise Time (ms)	**131 ± 15**	**112 ± 5**
Rate of Rise (V/ms)	**95 ± 4**	**99 ± 6**
Latency (ms)	**82 ± 5**	**83 ± 4**
T.50% (ms)	**101 ± 2**	**105 ± 5**
T.90% (ms)	**96 ± 3**	**100 ± 4**
Decay tau (ms)	**103 ± 5**	**102 ± 8**

Prisms were submitted to paired-pulse field stimulation (20 ms interval between stimuli) in the absence (control) or presence of 2 μM bafilomycin A1. Parameters of the second EPP are expressed in percentage of those measured in the first EPP. Values are mean ± SEM of 11 experiments.

increased and was accompanied by small decrease in EPP rate of rise, which could be motivated by small desynchronization of ACh release in the second EPP. The parameters sensitive to the decay phase (T_{50}; T_{90}; tau) were unaltered if not decreased; corroborating the idea that facilitation affects mainly the amount of transmitter being released but not its time course. However, it should be noticed that the latency between the stimulus and the onset of prism EPP was decreased.

Most of the latency measured here is due to the generation and conduction of action potentials (Llinás et al., 1981b; Dunant and Muller, 1986) whereas the time needed to activate the release machinery after calcium entry is less than 300 μs (Dunant and Muller, 1986) or even somewhere around 150 and 300 μs if we take into account the time for ACh release per release site (Girod et al., 1993). Shortening the latency of the second EPP seems to be also calcium independent (figure 26). Therefore, it seems likely that the >15% reduction in latency is perhaps due to a facilitation effect of the previous action potential on the generation and/or conduction of a second action potential rather than related to the activation of the

release machinery.

The EPPs of bafilomycin-incubated prism showed virtually no facilitatory effects (table 3). The second EPP was very similar to the first one. The only parameter affected was a decrease in the latency. As discussed above, this is more likely to be related with action potential generation and conduction. There was also no statistical distinction between facilitation with bafilomycin and facilitation without bafilomycin (control). Yet, bafilomycin incubated prisms had a minor increase in EPP area and virtually no increase in peak amplitude, possibly because amplitude in the first peak was already slightly larger than in the absence of the drug (table 2). More importantly, the temporal profile reflecting protracted ACh secretion was kept or only slightly increased as reflected by T_{90}, T_{50} and decay tau.

Paired pulse facilitation and delayed release are distinct Ca^{2+}-dependent processes. While the amplitude increase obtained with PPF is mainly due to increased peak calcium whose time course within the terminal continues to be strongly restricted by rapid and slow extrusion mechanisms the enhancement in ACh secretion due to Ca^{2+}/H^{+} antiport inhibition should result from compromising the early phase of calcium extrusion leading to a calcium transient that endures.

Even if the above assumptions -i.e., that the described effects arose from changes in the amount and time course of ACh release- seem logic, they should be confirmed by biochemical methods which provide more direct assessment of the amount of ACh release under these conditions.

We incubated excised prisms overnight with [^{14}C]-acetate to allow the synthesis of radiolabelled [^{14}C]-ACh within prism nerve terminals. The labelled precursor was then washed so that [^{14}C]-ACh could be measured both at rest and upon stimulation (figure 18, see also figures 6 and 7). The rate of basal ACh release from *Torpedo* terminals is low enough to provide a signal to noise ratio that allows to register ACh release elicited by a single or a few stimuli (Dunant et al., 1980a).

Figure 18 shows the amount of [^{14}C]-ACh being released from prisms perfused with normal elasmobranch saline medium (control prisms) or supplemented with 2 μM bafilomycin. The tissue was kept under continuous perfusion for 1h prior to stimulation to allow for drug incubation and washout of any [^{14}C]-ACh leaking from the tissue. Two samples of the perfusate were collected in 1 min aliquots just before application of a paired-pulse stimulus

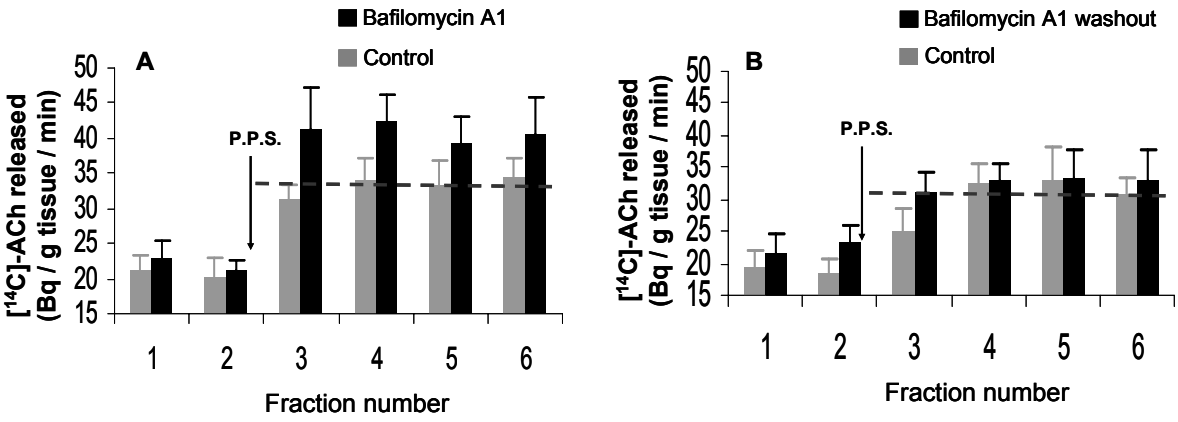

Figure 18. Bafilomycin A1 increases ACh release evoked by pair-pulse stimulation (P.P.S. 20 ms interval between stimuli). Prisms from Torpedo electric organ were labelled with [^{14}C]-acetate. Radioactivity was then washed out overnight, and the prisms perfused with elasmobranch saline medium containing 2 μM bafilomycin A1 (black bars) or without drug (control in grey), for 1h prior to stimulation. Panel **A**: The amount of [^{14}C]-ACh diffusing in the fluid was measured in fractions lasting 1 minute each, before and after P.P.S. stimulation (↓). Panel **B**: The same protocol was applied to the same prisms after 1h of drug washout (Values are mean ± SEM; n=8). The average value of ACh released in the last 3 fractions under control conditions is shown as reference (— —). The amount of [^{14}C]-ACh released after stimulus (fractions 3 to 6) was significantly higher in the presence of bafilomycin A1 than in control (Two-way ANOVA: $p<0.01$).

(equivalent to the one applied in figures 6, 17 and tables 2 and 3); four additional 1 min aliquots were taken right after the stimulus and during the consecutive four minutes. The amount of [^{14}C]-ACh measured in the fluid increased right after the stimulus (demonstrating that the method is sensitive to the stimulation and recollection protocol) and was kept high for a few minutes (presumably the time for [^{14}C]-ACh release from deep tissue synapses to diffuse out into the perfusate). Bafilomycin-incubated prisms had a similar [^{14}C]-ACh amount leaking out of unstimulated prisms, but showed a significant (~70%) increase in [^{14}C]-ACh release following paired-pulse stimulation as compared to control prisms (figure 18 A). The effect was fully reversible after 1h washout (figure 18 B) with the amounts of [^{14}C]-ACh collected in perfusates of control and bafilomycin-incubated prisms being virtually the same.

These experiments were undertaken in parallel with electric recording of prisms used in figure 17 and tables 2 and 3, demonstrating by another way that the protruded transmission we registered electrophysiologically was most likely the result of an increase in the amount of ACh release.

Considering that we are at hands with an effect that nearly doubles ACh secretion per pulse in response to compromised Ca^{2+} sequestration into synaptic vesicles within nerve

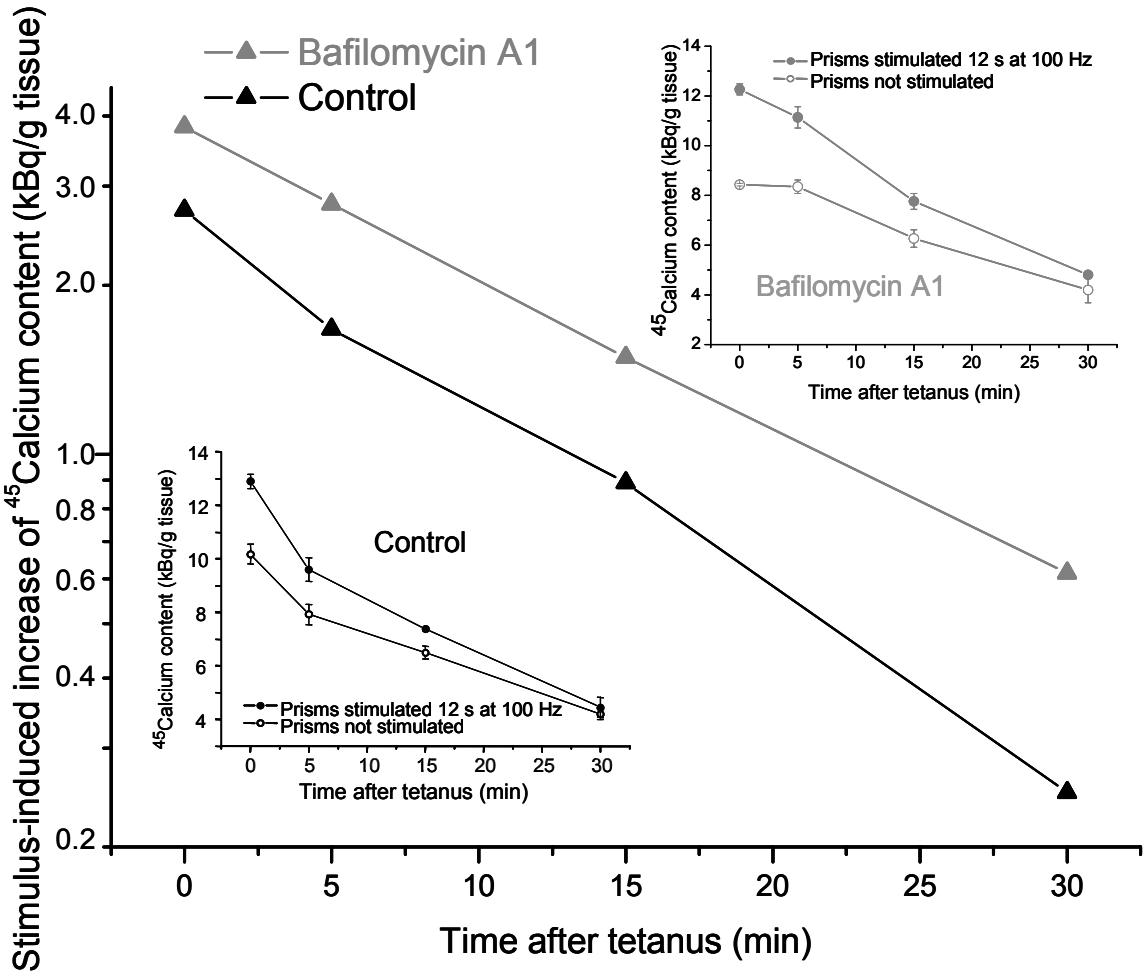

Figure 19. Bafilomycin A1 effect on the accumulation and extrusion of calcium in prisms submitted to a 12 second tetanus at 100 Hz. Prisms were incubated with ^{45}Calcium containing elasmobranch saline medium with 2 µM bafilomycin A1 or without the drug (control). Then the prisms were washed in the standard medium without ^{45}Calcium but still in the presence of the drug if any. Prisms were processed for quantification of cellular ^{45}Calcium at 0, 5, 15 and 30 min after the tetanus. In **inset**, closed circles show the amount of tissue ^{45}Calcium found in stimulated prisms, and open circles the amount found in non-stimulated prisms. Triangles in the main graph show difference between stimulated and non-stimulated prisms for bafilomycin-treated prisms (grey) and controls (black) calculated from the data shown in insets (mean ± SEM of 4 to 8 experiments). Bafilomycin A1 significantly increases ^{45}calcium accumulation in – and slows down ^{45}calcium extrusion from - stimulated prisms (Two-way ANOVA: $p<0.05$).

terminals, it is perhaps pertinent to ask: What happens to calcium accumulation and extrusion from Torpedo prisms when they are stimulated after being incubated with bafilomycin?

The accumulation of ^{45}calcium within excised prisms was shown to be stimulus-dependent and maximal with a 12 s tetanus at 100 Hz; and to decrease over time (less than

1h) back to unstimulated levels (Babel-Guérin, 1974; Dunant et al., 1980b; Párducz and Dunant., 1993; Párducz et al., 1994).

Figure 19 shows stimulus-dependent $^{45}Ca^{2+}$ accumulation within small (70-150 mg) excised prisms incubated in the absence (control) or in the presence of 2 µM bafilomycin. ^{45}Calcium retained within the tissue is obtained from the subtraction of ^{45}Calcium found within stimulated prisms versus unstimulated ones (Figures inserted in figure 19). ^{45}calcium accumulation after a 12 s tetanus at 100 Hz was significantly larger in bafilomycin-incubated prisms that in controls.

We could also follow ^{45}calcium extrusion rates from prisms by washing them out with standard elasmobranch medium (+/- Bafilomycin), without ^{45}calcium, during 5, 10, 15 or 30 minutes before placing the tissue in ice-cold medium and proceed with radioassay counting.

It is interesting to notice that most of the bafilomycin effect appears soon after the stimulus (time 0) and to much lower extent after 5 min of extrusion of calcium after the stimulus by comparing the slopes of control prisms (inset to the left in figure 19) and bafilomycin incubated prisms (inset to the right in figure 19). However, there seems to be no later effect of bafilomycin in calcium extrusion from prisms. This seems to indicate that, normally, the vesicular Ca^{2+}/H^{+}-antiport is capable of decreasing calcium accumulation into the prisms by accumulating them into nearby vesicles and most probably by further rapid extrusion early after the stimulus.

The results seem to implicate synaptic vesicles in calcium retention or extrusion capacity in tissue. They also point-out to the very rapid (a few seconds) nature of bafilomycin-sensitive calcium accumulation within the prisms, since the protocol relies in placing the tissue immediately after the stimulus in ice cold medium that stops any further calcium exchange with the extracellular medium. These assumptions are borne out by previous experiments reporting that the $^{45}Ca^{2+}$ accumulated in the tissue was proposed to be preferentially accumulated in synaptic vesicles (and under such strong stimulus also in the few mitochondria that exist in *Torpedo* terminals) where calcium precipitates into electron-dense granules with oxalate-pyroantimonate fixation viewed in electron microscopy. (Dunant et al., 1980b; Párducz and Dunant., 1993; Párducz et al., 1994). Furthermore, the tissue was submitted to rapid freezing (ms resolution) and cryofractured for analysis of the number of membrane depressions or pits (~20-40 nm wide) that are thought to result from vesicular openings (Párducz et al., 1994). Exocytotic pits were counted using freeze-fracture replicas

of the P-face of the pre-synaptic membrane. There was no increase in the number of pits during the 12 s stimulus (~20/100 μm^2). Conversely, there was an increase in the number of pits right after the end of the stimulus (~27/100 μm^2) that reached its maximal value one minute after the stimulus (~33/100 μm^2) and fell back to control density (~21/100 μm^2) after 5 minutes. Maximal occurrence of pits correlated also with a decrease in the number of vesicles with a calcium spot seen by electron microscopy. However there were still a significantly high number of vesicles containing a calcium dense spot after 10 minutes, indicating that not all Ca^{2+}-containing vesicles fuse with the membrane in the exocytotic burst right after the end of the stimulus (one minute after), but will decrease over one hour presumably by the basal fusion rate reflected by the number of pits (~21/100 μm^2) that is not much lower than maximum number of pits registered.

If we bear in mind that torpedo synapses rely on a calcium-activated ACh channel in the plasma membrane (mediatophores) instead of vesicular fusion (Reviewed in Dunant and Israël, 2000 and Dunant and Bloc, 2003), it is perhaps easier to consider that vesicles within *Torpedo* cholinergic terminals specialized into doing somewhat different tasks, like accumulation and extrusion of calcium ions entering in nearby active zones. However, the fact that there is also considerable Ca^{2+} accumulation in synaptic vesicles in other systems like the neuro-muscular junction, brain synapses, or chromaffin granules upon stimulation (Von Grafenstein and Powis, 1989; Buchs and Muller 1996; Mizuhira and Hasegawa, 1997; Pezzati and Grohovaz, 1999; Mahapatra et al., 2004), indicates that the task could be far more common -perhaps ubiquitous- after all.

Torpedo vesicles are themselves almost twice as big as light dense-core synaptic vesicles found in mammals (and in *Torpedo* brain and NMJ as well) (see Girod et al., 1993 and Takamori, 2006). A two-fold increase in SV diameter implies an 8-fold increase in SV volume that is capable of accommodating an impressive number (100,000-200,000) of ACh molecules per SV (a quantity that would be enough to generate 10-20 quanta) and a presumably greater number of calcium ions as well (Girod et al., 1993; Párducz et al., 1994). The increase in SV volume per active zone can however be somewhat mitigated (only 2x increase in volume) by the fact that a greater number of smaller vesicles is capable of occupying the planar area directly above the active zones where calcium channels and mediatophores presumably cluster (Girod et al., 1993). If an active zone occupies a 240 nm/240 nm (in accordance with Girod et al., 1993) there will be maximumly 9 *Torpedo* SVs covering each release site and a maximum

of 82 vesicles between active zones distant on average 800 nm (Girod et al., 1993).

When the terminal is invaded by a stimulus, there is a considerable calcium entry close to release sites. Ca^{2+} ions reach high concentrations near mediatophores but also near the Ca^{2+}/H^{+} antiport in SVs directly above the active zone. Both have particularly low affinity for calcium (Israël et al., 1987; Gonçalves et al., 1998, 2000a; Dunant and Bloc, 2003 Dunant, 2006) and should be operative for the short period of time required for phasic ACh release.

The antiport should be able to restrict both in time and in space the $[Ca^{2+}]_{int}$ within the terminal as a backup system that decreases Ca^{2+} concentrations very fast, within a particular cluster limiting an active zone, dealing with short-term Ca^{2+} homeodynamics.

Right after, there seems to be a need to rapidly extrude the accumulated calcium ions out of nerve terminals and back into the synaptic cleft. The results in figure 19 point-out for a role of vesicular Ca^{2+}/H^{+} antiport in keeping Ca^{2+} homeostasis by limiting the calcium load within the terminal. Notice that late decrease in ^{45}Calcium retained within tissue exposed to bafilomycin seems to follow similar kinetics of release as control prisms arguing in favour of a prevention of excessive calcium load in the terminal by the antiport (see section 3.2.2. below).

That later calcium extrusion should depend on plasma membrane transporters like Na^{+}/Ca^{2+} exchangers (minorly expressed in *Torpedo*) and Ca^{2+}-ATPases both in plasma membrane, but also in the remaining synaptic vesicles within the terminal and apparently fusing after the initial exocytotic burst (Párducz et al., 1994).

There is another reason for rapid Ca^{2+} exocytosis by nerve terminals. The space occupied by the synaptic cleft is rather small. The height (ca. 50 nm in NMJ and central synapses; ca. 75 nm in *Torpedo*) is similar to the diameter of synaptic vesicles, such a tiny space that diffusion of a given molecule (i.e., of ACh) takes no more than a few microseconds (Bartol et al., 1991). On the contrary, active zone surface in *Torpedo* and at NMJ synapses are larger (ca. 1 μm^2). Girod et al. (1993) considered a 750 nm radius disk in their model of an active zone, rather than an infinite space, where the time needed for the diffusion of a given molecule at the edge of the synapse needs to be taken into consideration (Egelman and Montague, 1999).

The active zone volume is also very small (1 μm^2 x 0.075 μm = 0.075 μm^3) even when we consider the reserve of volume that has been developed at *Torpedo* and NMJ in the form of arcs (2 per active zone) in *Torpedo* and folds in the NMJ that increase the total volume per active zone to 0.467 μm^3, that creates additional reserve space for ions, choline, acetate and

pH buffering in synapses capable of rapid repetitive firing (Girod et al., 1993).

As a consequence of space limitations, calcium concentration in the synaptic cleft may decrease sharply, dependent on the size of consumption zone, local diffusion of calcium and the geometrical arrangement of the synapse (Egelman and Montague, 1999). Calcium depletion in the synaptic cleft has been reported in: (1) heavily stimulated synapses of cat cerebellum showing up to 20-90% $[Ca^{2+}]_{ext}$ decrease (Heinemann et al 1977), (2) in Aplysia ganglion showing a decrease of up to ~1 mM $[Ca^{2+}]_{ext}$ (Keicher et al., 1990), (3) in calyx of Held implicating 35% reduction of EPSC amplitude (Borst and Sakmann, 1999; Stanley, 2000), (4) in cortical neurons where $[Ca^{2+}]_{ext}$ depletion serves to regulate "silent" periods of activity during sleep (Massimin and Amzica, 2001), (5) in rod photoreceptors (Rabi and Thoreson, 2002) and (6) in hippocampus CA1 area where the $[Ca^{2+}]_{ext}$ depletion measured with a calcium probe was also extensive (Rusakov and Fine, 2003).

What is more, there is an >28-fold discrepancy between the amount of Ca^{2+} ion charge accomodable in the calyx synapse (7 pC) and the charge measured in a 100 ms stimulus (200 pC) that reflects the existence of fast Ca^{2+} replenishment system (Borst and Sakmann, 1999). There is a slow component of replenishment attributable to diffusion from extra-synaptic spaces and replenishment from Ca^{2+} pumping out of the terminal seems to be far slower than the observed time-course of replenishment and even more delayed when submitted to larger Ca^{2+} loads (Borst and Sakmann, 1999). Those authors proposed that there could be a third line of synaptic Ca^{2+} replenishment due to synaptic vesicle exocytosis, whereby a single 50 nm synaptic vesicle filled with close to 100 mM calcium (Grohovaz et al., 1996) would be able to resupply the synaptic cleft with ~1/3 of the calcium that had entered the terminal. The additional observation that the Ca^{2+}-depletion effects were somewhat larger with Ba^{2+} as the charge carrier than with Ca^{2+} argue in favour of the participation of rapid vesicular Ca^{2+} transport through a Ca^{2+}/H^{+} antiport capable of filling-up nearby SV before exocytosis since Ba^{2+} is unable to dissipate the vesicular proton gradient nor interfere with Ca^{2+} transport through the vesicular antiport (Gonçalves et al., 1999a).

In summary, annihilation of the proton gradient of synaptic vesicles by bafilomycin in acute experiments does not impair rapid neurotransmission, but on the contrary enhances transmission by prolonging the duration of phasic transmitter release. This effect most probably arises from inactivation of the vesicular Ca^{2+}/H^{+} exchange, as will be demonstrated below.

3.2.1.2. Strontium mimics bafilomycin effect on cholinergic secretion

Strontium cation (Sr^{2+}) is unable to induce measurable H^+ displacement from sheep brain cortex synaptic vesicles while being capable of preventing Ca^{2+} accumulation into isolated SVs via the antiport (Gonçalves et al., 1999a). It is also known since the days of Locke (1894) that Sr^{2+} ions can substitute Ca^{2+} to activate transmission. Dodge et al. (1969) demonstrated that strontium elicited quantal transmitter release in frog NMJ but far less effectively than Ca^{2+} does at equimolar concentrations and if the concentration of strontium used surpassed 10 mM there was a blockade of transmission presumably resulting from failure in the propagation of nerve impulses. The lower potency of Sr^{2+} than Ca^{2+} to support transmitter release was confirmed in other synapses and related with a lower affinity of strontium for the calcium sensor (Mellow et al., 1982; Bain And Quastel, 1992; Goda and Stevens, 1994; Abdul-Ghani et al., 1996; Xu-friedman and Regehr, 2000; Kishimoto et al., 2001). Some of those reports also suggested that strontium induces an increase in asynchronous and late transmitter quanta (Mellow et al., 1982; Goda and Stevens, 1994; Abdul-Ghani et al., 1996 Xu-friedman and Regehr, 2000; Kishimoto et al., 2001), due to persistence of the ion within the terminal (Xu-friedman and Regehr, 2000).

Substitution of strontium with calcium as the trigger for evoked transmitter release seemed perfect to confirm the assumptions made with bafilomycin. In this way we could confront the results obtained with an inhibitor of the V-type H^+-ATPase (that blocks the driving force of the Ca^{2+}/H^+ antiport-mediated transport) with the activation of transmission by Sr^{2+} that is not submitted to removal into SVs by the Ca^{2+}/H^+ antiport, but does not tamper with the vesicular proton gradient.

Figure 20 shows the response of excised prisms where all $CaCl_2$ in the elasmobranch medium was substituted with increasing $SrCl_2$ concentrations. EPPs generated by excised prisms bathed in control (+ 3.4 mM $CaCl_2$) elasmobranch medium are shown for comparison. It is clear that Sr^{2+} has very limited capacity to evoke a response from prisms at concentrations that would generate near maximal response with calcium. However, as the concentration of Sr^{2+} rose in the perfusion medium there was a progressive increase in the EPP size until a response equivalent to –or even larger than- the control was obtained for 34 mM Sr^{2+} and kept at that level for 50 mM Sr^{2+}.

It is noteworthy that as long as the EPP amplitude was kept low (low [Sr^{2+}]), the time

course of transmission followed closely that of control, However, when $SrCl_2$ was such that ACh released produced an EPP of similar amplitude as control there was a significant enlargement of the post-synaptic response that was very similar or even greater than with bafilomycin.

The evoked response followed a steep dependency on extracellular strontium concentration, but the apparent affinity for the sensor of ACh release was ~10 fold lower than that of Ca^{2+}, a value that is in accordance with the apparent affinity determined intracellularly by rapid Sr^{2+} uncaging (Kishimoto et al., 2001).

It is worth mentioning that we were probably rather lucky in being able to reach such high $SrCl_2$ concentrations to elicit similar responses to control since, as stated above, it had been reported that 10 mM $SrCl_2$ was enough to "silence" frog NMJ synapses (Dodge et al. (1969). This was probably achieved because intact prisms maintain the rather idle nature of *Torpedo* discharge pattern until evoked responses develop synchronously in a typically phasic way without the interference of asynchronous release events reported to occur with strontium (Mellow et al., 1982; Goda and Stevens, 1994; Abdul-Ghani et al., 1996 Xu-friedman and Regehr, 2000; Kishimoto et al., 2001). Also, the elasmobranch medium used in these experiments has a very high ionic strength, equivalent to that of sea-water, and addition of 35 or 50 mM $SrCl_2$ could be applied since they do not cause serious osmotic or other changes.

Figure 20 also evidences the facilitation observed under all $SrCl_2$ concentrations tested. Both facilitation and EPP enlargement can be explained by the persistence of Sr^{2+} within the terminal after the action potential, due to deficient Sr^{2+} extrusion. On one hand the Sr^{2+} ions, entering the terminal in the first pulse, are not enough to activate maximal ACh secretion but remain in the terminal where they are summed-up to Sr^{2+} ions entering the second pulse. Facilitation of EPP amplitude is the result of higher $[Sr^{2+}]$ attained under those conditions that prolongs time-course of Sr^{2+} transient (Xu-Friedman and Regehr, 2000) and consequently the time of ACh secretion also.

We assessed the $[SrCl_2]$-dependency of radiolabelled $[^{14}C]$-ACh release (figure 21) submitted to paired pulse stimulation as described for bafilomycin-incubated prisms. There was a concentration-dependent exponential increase in $[^{14}C]$-ACh released by excised prisms until maximum release occurred with 34 mM $SrCl_2$ that followed closely the amplitude and area of the EPP response.

The calcium and strontium dependencies of the cholinergic response of excised prisms

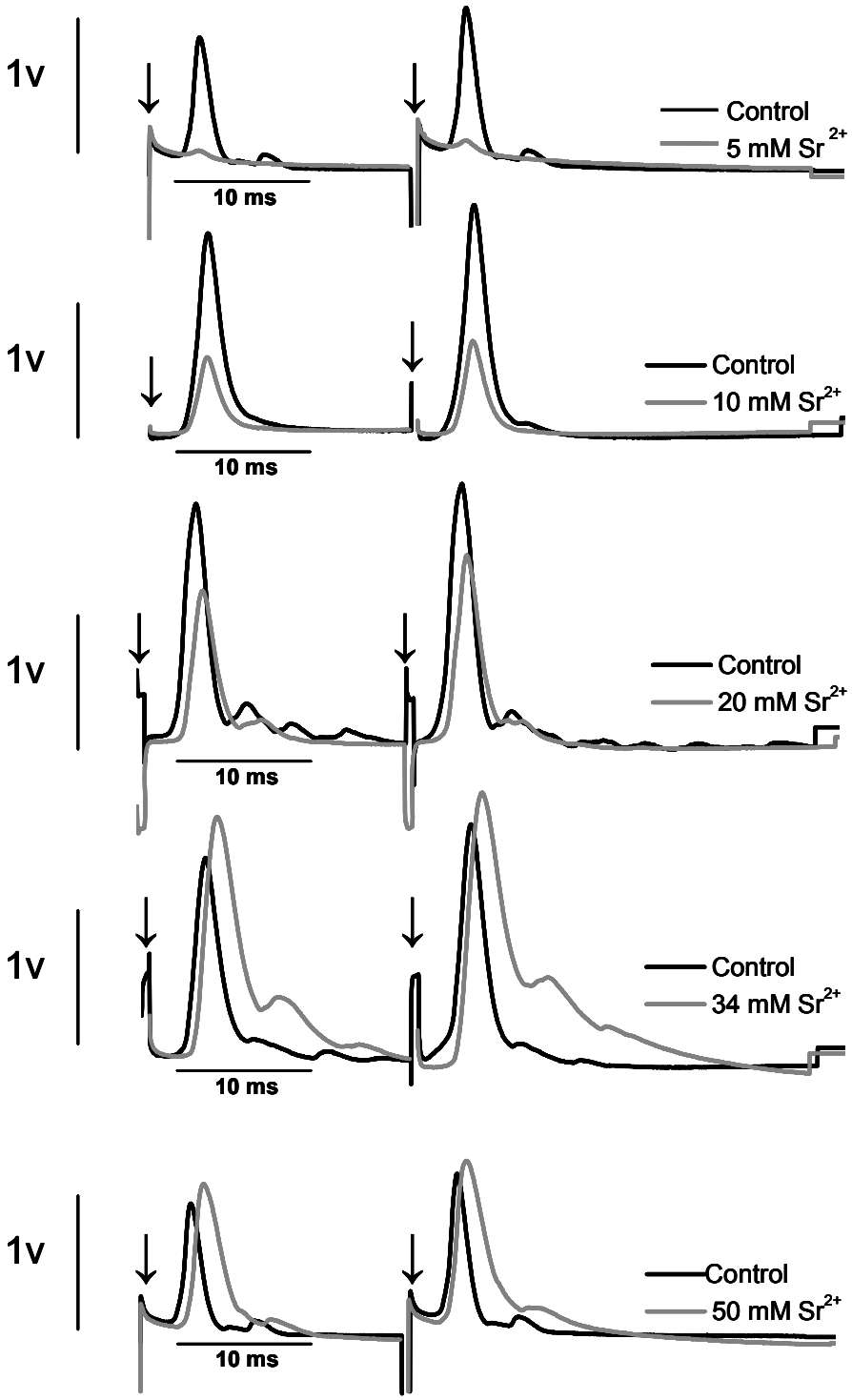

Figure 20. Effect of strontium on synaptic transmission in the *Torpedo* electric organ. Conditions were like in Figure 17. Prisms were perfused for 1h in the elasmobranch saline medium (3.4 mM $CaCl_2$; controls traces in black) and then in the same medium where $CaCl_2$ was replaced with increasing $SrCl_2$ concentrations (traces in grey). Representative traces from 12 experiments.

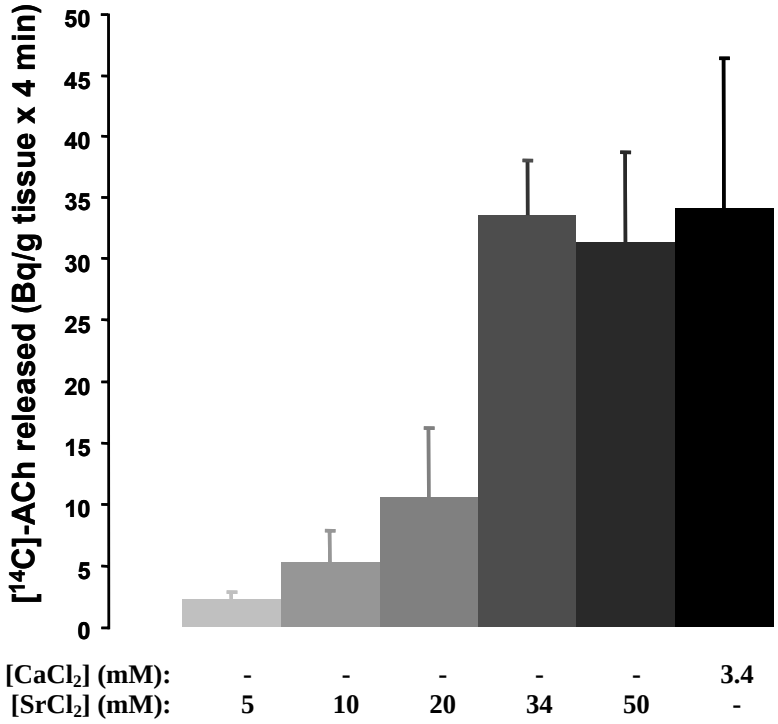

Figure 21. Strontium supports neurally-evoked ACh release. Conditions were like in figure 18. The amount of transmitter release in response to a pair of electrical impulses was measured in elasmobranch saline medium (3.4 mM $CaCl_2$ black bar) or in a medium containing increasing $SrCl_2$ concentrations instead of $CaCl_2$ (grey bars). Histograms show mean ± SEM (n=4) of the stimulus-dependent [^{14}C]-ACh release. The mean basal release was subtracted.

were represented on a semi-logarithmic plot (figure 22) where the EPP amplitude and the area under the EPP wave were resented together with [^{14}C]-ACh release.

The plot shows that all methods used to assess ACh (either electrophysiological or biochemical) were equally sensitive to changes in cation concentration. We also calculated the Hill coefficient or cooperativity index given by the slope of the sigmoid fit adapted to the data set. Calcium ions display a cooperativity index of 3.4 while strontium has 2.8 (*not significant*). The cooperativity index reflects the non-linear binding of each cation to the Ca^{2+} (Sr^{2+})-sensor where the binding of the previous ion favours the allosteric binding of the next ion to the sensor. It has been argued that this measure yields a value that is somewhat underestimated (Zucker, 1989). Therefore, it seems ACh release in *Torpedo* electric organ is determined by the 4th power of calcium concentration and the 3rd to 4th power strontium concentration at release sites, in line with MEPP frequency rise with the 4th power [Sr^{2+}] registered in rat diaphragm nerves (Bain and Quastel, 1992).

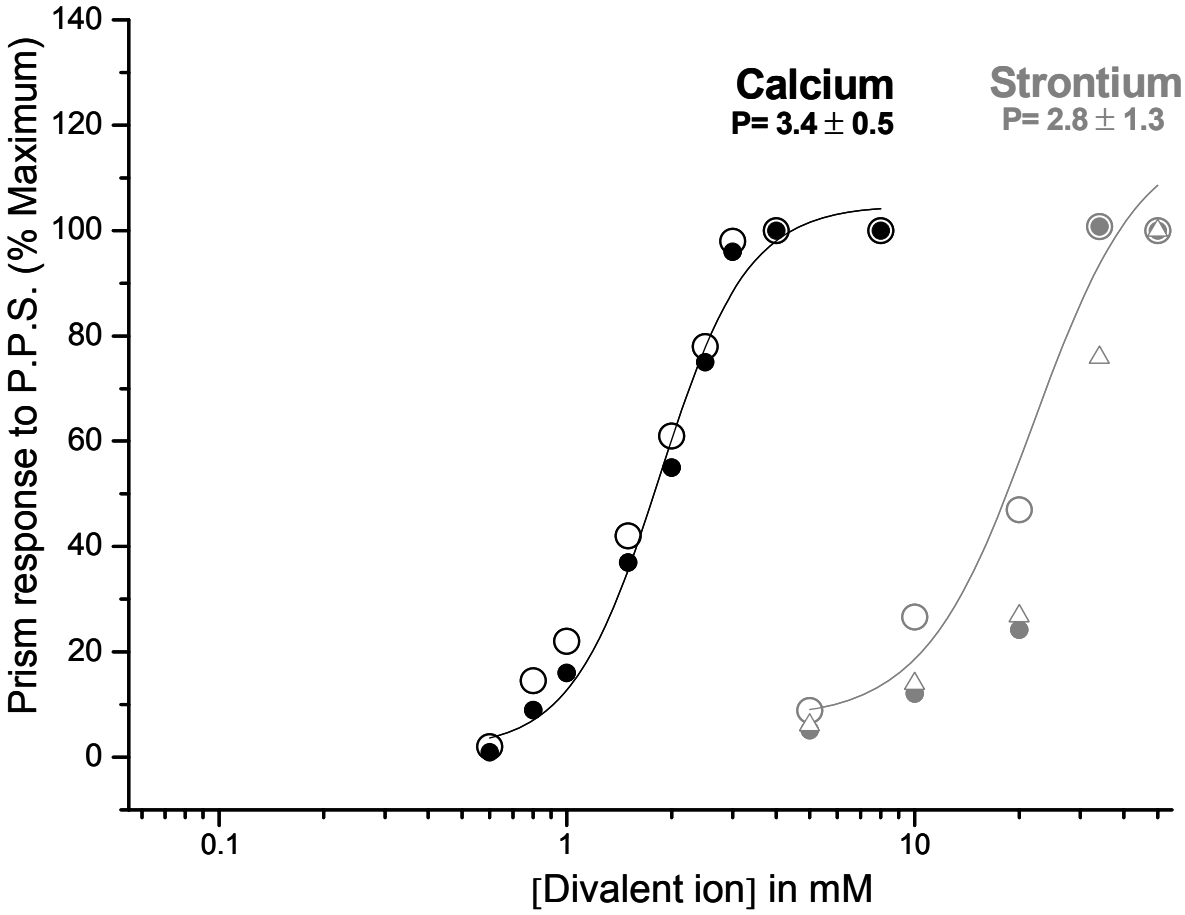

Figure 22. Concentration-release relationship of Ca^{2+} and Sr^{2+} in electric organ. Prisms were kept in elasmobranch saline medium with increasing concentrations of either $CaCl_2$ (in black) or $SrCl_2$ (in grey). Open circles represent the EPP amplitude (V) of the first response to paired stimuli; open triangles show area (V*ms) in the same EPPs; filled circles stand for the amount of radiolabelled [^{14}C]-ACh released from pair-pulse stimulated prisms. The sigmoid curves were fitted to each set of data, expressed in percentage of maximal effect. The cooperativity index is indicated ± SD.

3.2.1.3. Calcium and strontium-dependency of EPP parameters

Synaptic transmission and more precisely ACh release have long been known to be dependent on the presence of Ca^{2+} in the extracellular medium (Locke 1894; Harvey and MacIntosh 1940; Katz 1969). We shall pay here special attention to the changes affecting the different EPP parameters when transmission was tested in various Ca^{2+} concentrations in response to paired-pulse stimuli applied at 20 ms intervals (Figure 23 through 25).

Latency remained constant at physiological $[Ca^{2+}]_{ext}$ but increased significantly at 10 mM Ca^{2+}. The same happened with $[Sr^{2+}]_{ext}$, only that latency was consistently higher than with calcium. Coincidently, when bafilomycin was present in the incubation medium, there was

also some increase. The effect seems dependent on the accumulation of Ca^{2+}/Sr^{2+} ions within the terminal, whether as the result of an excessive extracellular calcium/strontium load promoting basal ion entry into the terminal or as the combined result of having Ca^{2+}/Sr^{2+} entry added to inefficient Sr^{2+} extrusion through plasma membrane Ca^{2+}-ATPase (Graf et al., 1982; Xu-friedman and Regehr, 2000) and no Ca^{2+}/H^{+} antiport-mediated Ca^{2+}/Sr^{2+} vesicular transport. How can slow Ca^{2+}/Sr^{2+} accumulation affect latency?

Latency in this preparation comprehends the time for axonal conductance and the synaptic delay which is very short (Dunant and Muller, 1986) and usually not taken as modifiable. Yet, there seems to be a slight increase in latency in conditions that might favour subthreshold Ca^{2+} or Sr^{2+} accumulation that could have a down-regulatory effect on Ca^{2+}-channels (Birman and Meunier, 1985; Catterall, 2000; Forsythe et al., 1998) or the mediatophore (Israël et al., 1987) (with partial instead of full desensitization). This could determine either a reduced I_{Ca} or an increase in $[Ca^{2+}]$-threshold for mediatophore activation (Israël et al., 1987). Under those circumstances, there could still be activation of the release machinery but after a time-lapse whereby enough Ca^{2+} accumulated in the microdomain and overcome the limitations of the down-regulation.

Fedchyshyn and Wang (2007) have recently reported that an increase in latency develops in calyx of Held synapses submitted to high frequency (20-200 Hz) stimuli (it happens in *Torpedo* too). The effect was prevented by lowering the $[Ca^{2+}]_{ext}$ or diminishing I_{Ca} by inhibiting VOCCs with baclofen or still by increasing the temperature (also increasing Ca^{2+} extrusion capacity) or by pre-incubating the terminals with the membrane permeable form of EGTA (EGTA-AM). The natural conclusion for that report and for the effects reported here is that residual Ca^{2+} (and Sr^{2+}) accumulation in pre-synaptic nerve terminals induces the observed increase in latency.

As for the **rise time**, it showed a regular prolongation both with $[Ca^{2+}]_{ext}$, and specially with strontium, which is in line with the bafilomycin effect. Like with bafilomycin where Ca^{2+} ions are expected to remain and activate ACh more time there seems to be a super-additive effect on receptor fields resultant from late ACh release and shifting the peak response to the right.

The EPP **area** was related to the concentration of calcium or strontium ions in the external medium. The relation could be described by a steep sigmoid with a potency factor of 3.4 for Ca^{2+} or 2.8 for Sr^{2+}, in good accordance with the data measured by biochemical

assessment of transmitter release in this and other synaptic preparations (Muller et al., 1987; Dunant et al., 1980a; Dodge and Rahamimoff 1967; among others). Sr^{2+} was 10 x less potent in activating ACh release but induced a significant enlargement in EPP area at concentrations above 20 mM.

As for the peak **amplitude**, whereas it increased from 0.85 to 3.4 mM Ca^{2+}, it did not so significantly with higher concentrations. The observation was confirmed in other experiments where Ca^{2+} concentrations higher than 10 mM were used (not shown). Strontium followed a similar profile but at concentrations 10 x higher. Therefore, it is mainly the duration of the EPP which was enlarged at "supranormal" Ca^{2+} or Sr^{2+} concentrations. A fact that is well patent in **area/peak** ratio.

The increase in **decay T_{50} ,T_{90}**, and **decay time constant** (**tau**) with increasing $[Ca^{2+}]_{ext}$ was hardly significant from 0.85 to 3.4 mM, but frankly prolonged at 10 mM. Similarly with $[Sr^{2+}]_{ext}$ there was a rather small increasing effect at lower concentrations that reached enormous proportions with 20 mM $SrCl_2$ and above. At these concentrations, the decay was greatly prolonged and a secondary exponential could be adjusted with time constant ranging from 3 to 10 ms.

In conclusion, not only the amplitude of *Torpedo* prism EEPs but also their time course of the response exhibited Ca^{2+}-dependency. The decay phase was particularly prolonged at 10 mM Ca^{2+}, a concentration about 3 times the physiological value. This result is in close relationship with both the effects of bafilomycin and Sr^{2+} and seems to reflect an effect of endured Ca^{2+} (Sr^{2+}) transient within active zone microdomains that will determine the enhancement of ACh secretion, reflected more in the EPP duration than in its amplitude.

As for **facilitation and depression** in experiments with calcium and strontium (figures 26 through 28) we should recall that facilitation depends on the initial (first EPP) probability of transmitter release. Low release probability (in low Calcium) enhances paired pulse facilitation of ACh release (Rahamimoff, 1968; Creager et al., 1980; McNaughton, 1982; Dobrunz and Stevens, 1997; Xu-friedman and Regehr, 2000).

In low Ca^{2+} concentration, the area of the second EPP was larger than the area of the first, elicited 20 ms before (facilitation). In contrast, at high Ca^{2+} concentrations, the area of the second EPP was smaller than that of the first one (depression). Such a Ca^{2+}-dependency of the facilitation-depression phenomenon has long been described in various preparations (Zucker, 1989). Under the present experimental conditions, facilitation only

occurred at low Ca^{2+}, and Figure 27 shows that the process affected more the EPP amplitude than its area. Previous work using direct measurement of transmitter release (Dunant et al., 1980a) clearly showed that, at least in case of depression, the phenomenon can be chiefly attributed to a pre-synaptic change. In other words, the bigger amount of transmitter is delivered in the first impulse, the smaller amount is delivered in the second impulse.

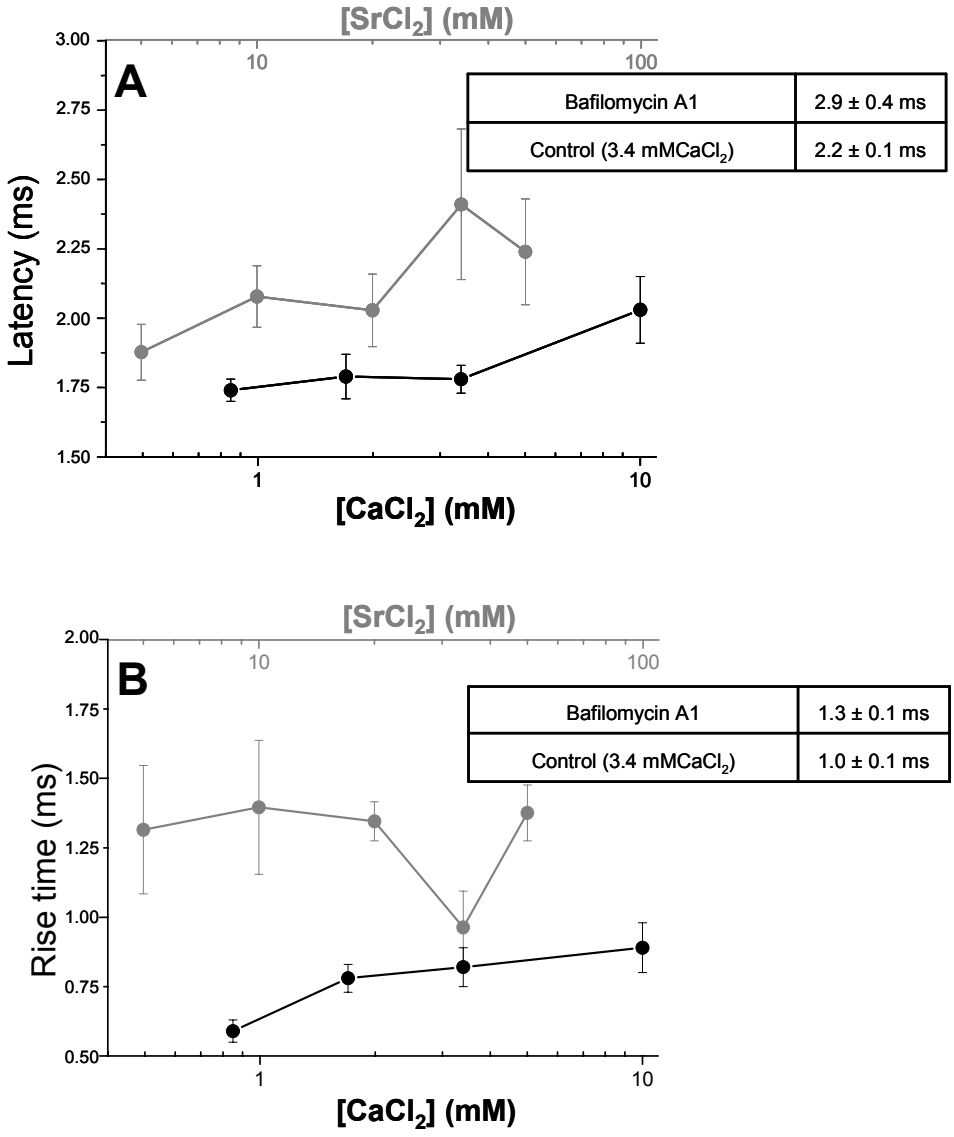

Figure 23. Synaptic delay (latency; graph **A**) and rise time (graph **B**) of EPPs generated in the presence of increasing concentrations of either Ca^{2+} (black scales and symbols) and Sr^{2+} (grey scales and symbols) in response to a single stimulus. Values are means ± SEM of 3-15 experiments. Values of the corresponding parameters obtained with prisms treated with 2 µM bafilomycin A1 for 1h in the presence of 3.4 mM $CaCl_2$ are given in inset. With Sr^{2+} both the latency and the rise-time last longer than with Ca^{2+}.

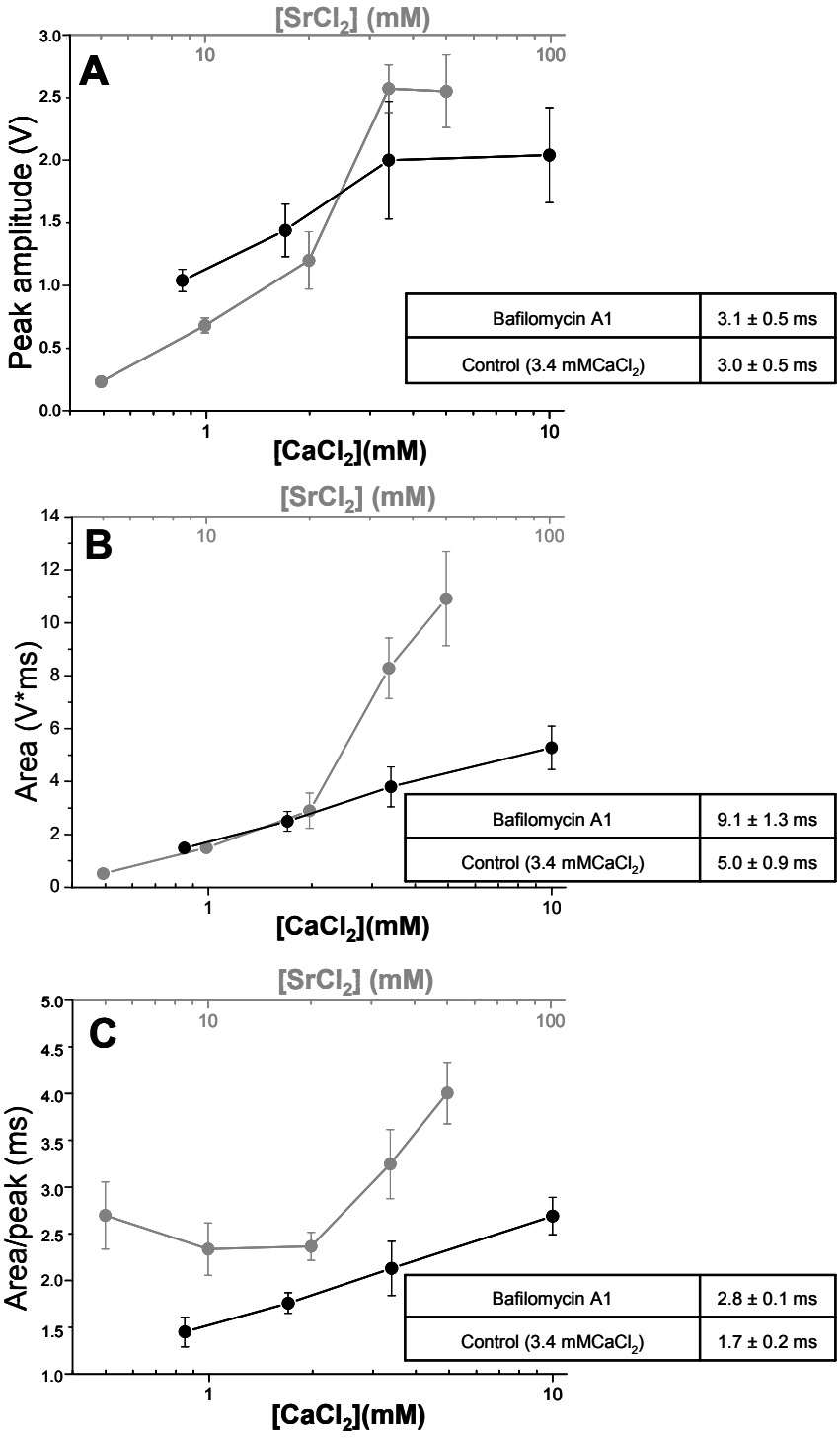

Figure 24. Peak amplitude (panel **A**); area (panel **B**) and area/peak ratio (panel **C**) of EPPs generated in the presence of increasing concentrations of either Ca^{2+} (black scales and symbols) and Sr^{2+} (grey scales and symbols) in response to a single stimulus. Values are means ± SEM of 3-15 experiments. Values of the corresponding parameters obtained with prisms treated with 2 μM bafilomycin A1 for 1h in the presence of 3.4 mM $CaCl_2$ are given in inset. When compared to Ca^{2+}, Sr^{2+} affects more the time course than the amplitude of the EPP.

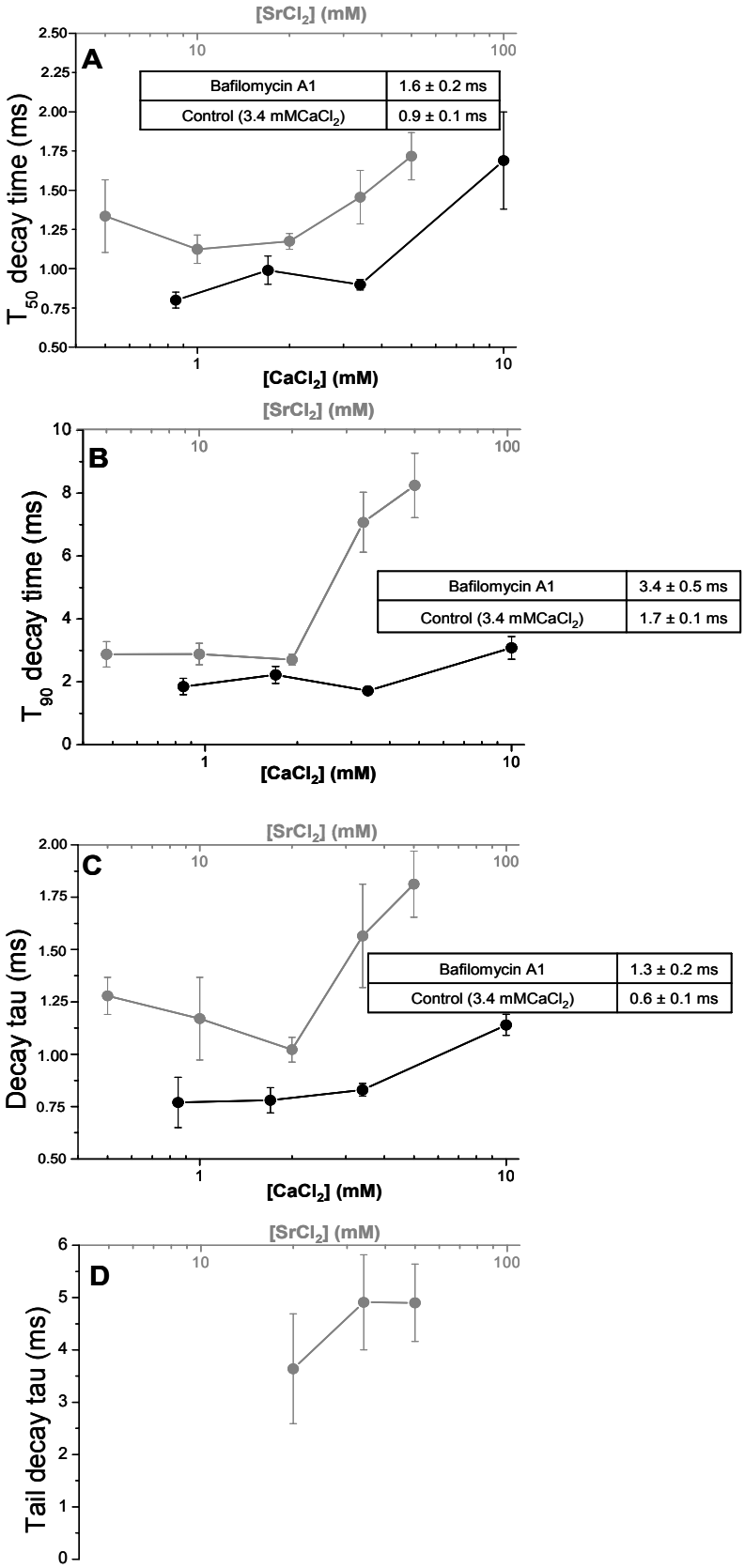

Figure 25. Parameters of the decaying phase of EPPs generated in the presence of increasing concentrations of either Ca^{2+} (black scales and symbols) and Sr^{2+} (grey scales and symbols) in

response to a single stimulus. Parameters were the T_{50} decay time (panel **A**); T_{90} decay time (panel **B**) and the decay time constant (tau; panel **C**). In the presence of high Sr^{2+} concentrations, the EPP was greatly prolonged in time; in some cases the final decay could be described by a secondary exponential of slower time course (see Figure 20 and panel **D**). Values are means ± SEM of 3-15 experiments. Values of the corresponding parameters obtained with prisms treated with 2 µM bafilomycin A1 for 1h in the presence of 3.4 mM $CaCl_2$ are given in inset. All the decay parameters are prolonged by Sr^{2+}.

As for **strontium, facilitation** of the peak amplitude –and that of the area– was enormously increased when compared to calcium. This may reflect the rather low probability of release with low Sr^{2+} when compared with Ca^{2+}, due to the ~10 x lower affinity of Sr^{2+} to the Ca^{2+} (Sr^{2+})-sensor.

The effect of $[Sr^{2+}]_{ext}$ on EPP peak facilitation is very high at low concentrations and decreases steeply at 34 and 50 mM $SrCl_2$. This might be attributed to the approximation of higher release probability with a consequent decrease in the second EPP. On the contrary, the area and area/peak of the second EPP were significantly prolonged with increasing $[Sr^{2+}]_{ext}$, which reflects the fact that Sr^{2+} load is particularly important above 20 mM, a value above which the decay parameters are all potentiated, while with calcium they are depressed. This rather odd discrepancy could arise from the fact that Sr^{2+} has a much lower affinity for the mediatophore than Ca^{2+} does and an increased Sr^{2+} transient will stand a better chance of activating such low affinity release channel at higher concentrations reached in the second pulse (greater amplitude). Mediatophore activation will also endure longer with higher $[Sr^{2+}]_{ext}$ because there is no fast component of Sr^{2+} extrusion and the persistence of suprathreshold Sr^{2+} within the terminal will exceed that of Ca^{2+}.

The time parameters, particularly latency and decay tau, are shorter at all $[Ca^{2+}]_{ext}$ in the second EPP, as compared to the first. The second EPP occurred earlier and its time course was shorter. This finding was somewhat unexpected but we can assume that contrary to the effects of long-term exposure to slightly raised $[Ca^{2+}]_{int}$ that enhances the synaptic delay downstream of calcium channel activation, paired pulse stimulation decreases the onset of the second EPP. The effect seems quite Ca^{2+} independent and it is also bafilomycin independent and no effect with increasing $[Sr^{2+}]$ was obtained either. This leads to thinking we're looking at an effect related to the generation and conduction of the action potential rather than on the synaptic delay.

As for the shortened rise and decay times, they could arise from rapid onset of

transmitter release (the calcium transient piles upon Ca^{2+} remaining from previous stimulus) combined with an early activation of rapid vesicular Ca^{2+} extrusion provided by the Ca^{2+}/H^+ antiport (presuming that in the first EPP the antiport displays slower activation kinetics). As for strontium, it confirms the notion that the vesicular Ca^{2+}/H^+ antiport is involved since both the onset and decay parameters were prolonged (instead of decreased) with increasing strontium.

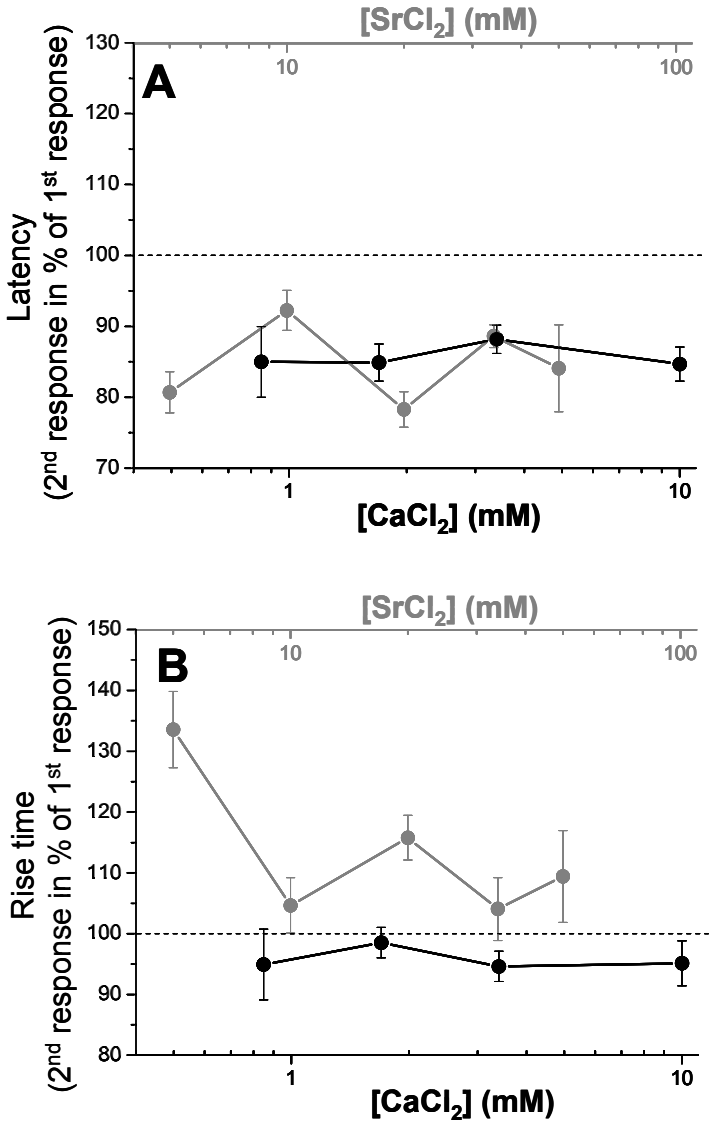

Figure 26. In this and the two following figures, the effect of either Ca^{2+} or Sr^{2+} on facilitation (or depression) will be presented. In the pair-pulse configuration, the parameters of the second EPP will be presented in percentage of the corresponding parameter of the first EPP (interval: 20 ms). Values are means ± SEM of 3-15 experiments. The latency of the 2nd EPP is shorter with both Ca^{2+} and Sr^{2+} independently of concentrations.

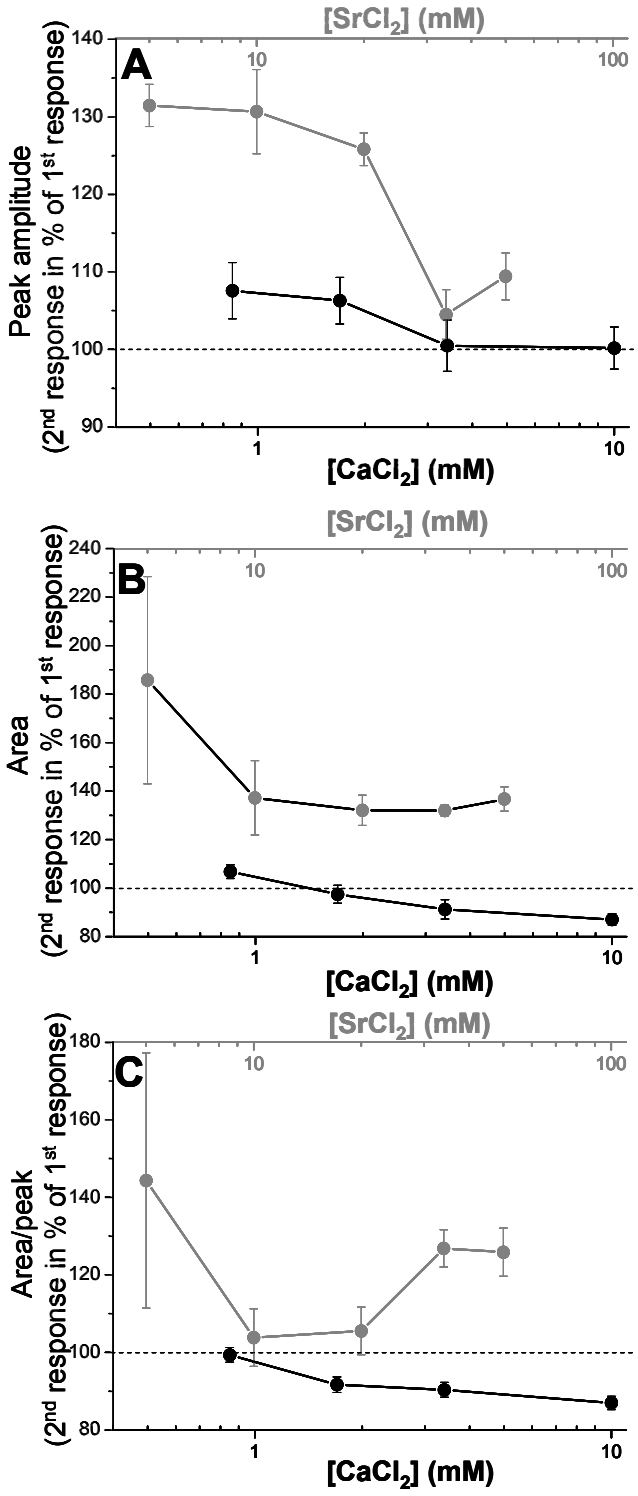

Figure 27. Same conditions and same mode of expression like in figure 26. Considering the amplitude and the area of the EPP, Ca^{2+} causes a modest facilitation only at low concentrations. In contrast, facilitation is much stronger with Sr^{2+} in the whole range of concentration.

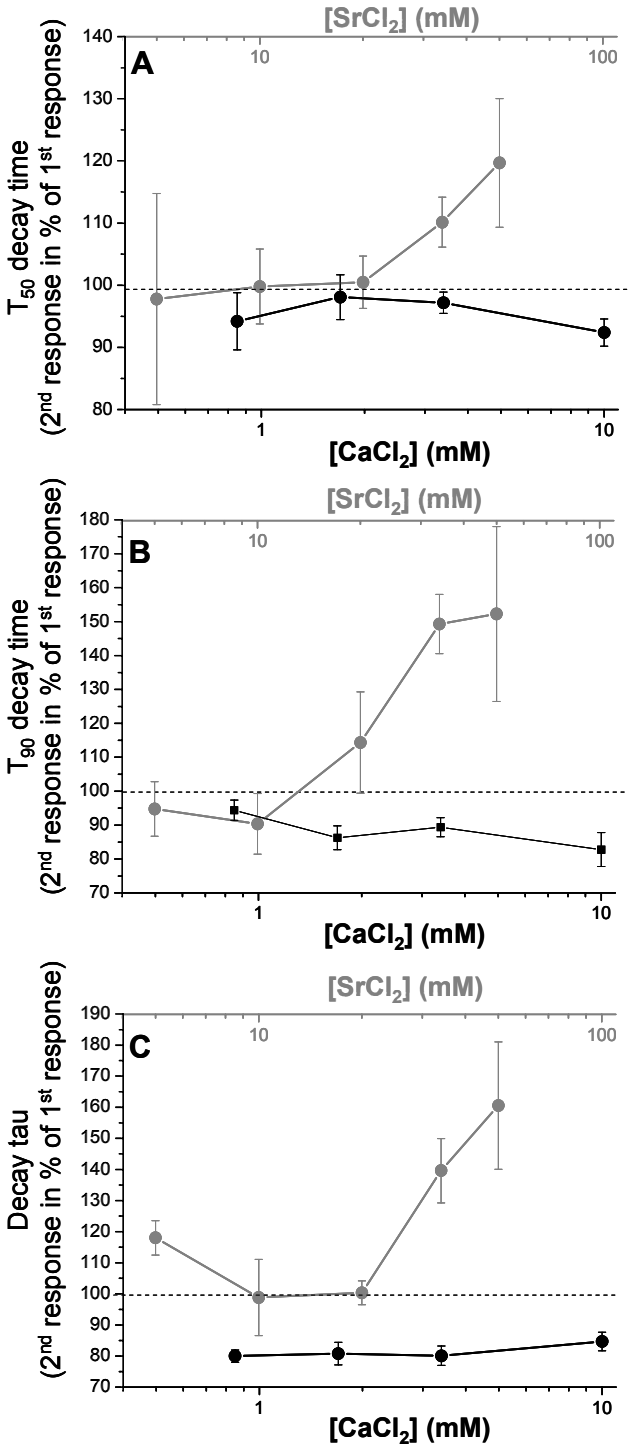

Figure 28. Same conditions and same mode of expression like in figure 26. With Ca^{2+}, the parameters of the decaying phase are shorter in the 2nd EPP than in the first, independently of concentration. In contrast with high Sr^{2+} concentrations, the decay phase of the second EPP is still prolonged, with comparison to the first EPP.

3.2.1.4. Other compounds affecting vesicular Ca^{2+} transport: CCCP, DCCD and DBHQ

Changes in [Ca^{2+}] profile have been measured in a number of reports using proton ionophores like carbonylcyanide p-trifluoromethoxyphenylhydrazone (FCCP) or Carbonyl cyanide n-chlorophehylhydrazone (CCCP) (Herrington et al., 1996; Park et al., 1996; Xu et al., 1997; Billups and Forsythe, 2002 and Bennett et al., 2007, to name but a few). In those studies the protonophores were intended to target mitochondrial inner membrane and dissipate its transmembrane H^+ gradient that drives Ca^{2+}-uptake by a Ca^{2+}-uniport (Villalobos et al., 2002; Kirichok et al., 2004; Kim et al., 2005). However, protonophores like CCCP also dissipate the vesicular proton gradient of isolated synaptic vesicles (Gonçalves et al., 1998 and figure 14) as well as all the acidic organelles endowed with a V-type H^+-ATPase within a synaptosome (Zocarato et al., 1999 and figure 36) or a PC12 secretory cell (figure 14), far more rapidly than bafilomycin does and extinguish Ca^{2+}/H^+ antiport vesicular calcium transport (Gonçalves et al., 2000a).

Normal $[Ca^{2+}]_{int}$ profile after a stimulus includes an almost instantaneous rise followed by slightly less rapid, but still very fast exponential decay phase of Ca^{2+} concentration (Sabatini and Regehr, 1996; Yazejian et al., 2000) that continues into a second much slower exponential decay phase (Herrington et al., 1996; Park et al., 1996; Xu et al., 1997; Castonguay and Robitaille, 2001; Billups and Forsythe,2002). That profile is markedly affected by CCCP. The rapid decline phase is enlarged or even annihilated and substituted by a slower $[Ca^{2+}]_{int}$ decay (Herrington et al., 1996; Park et al., 1996; Xu et al., 1997; Billups and Forsythe, 2002). This effect was attributed to compromised calcium transport by mitochondria; however, the possibility that the vesicular Ca^{2+}/H^+ antiport might be involved in CCCP action is borne out by the presented data, since CCCP alone is capable of blocking almost completely the rapid phase of the calcium transient while oligomycin adds little to the CCCP effect (Park et al., 1996).

On the other hand, the initial rapid decay in [Ca^{2+}] was not targeted by inhibitors of Ca^{2+}-pumps like thapsigargin (Castonguay and Robitaille, 2001) cyclopiazonic acid (David and Barret, 2003) or vanadate (Lajas et al., 2001) nor by inactivation of Na^+/Ca^{2+} exchange (Park et al., 1996). CCCP-dependent calcium clearance was markedly more rapid than Ca^{2+}-pumps or the Na^+/Ca^{2+} exchanger (Herrington et al., 1996).

This fast calcium clearance rates along with early extrusion capability are in favour of a localization of the target organelle near calcium entry sites where synaptic vesicles are

preferably clustered (Couteaux and Pécot-Dechavassine, 1970, 1974), rather than mitochondria, more distant and involved in the sequestration of calcium arising from stronger stimulus (Friel and Tsien, 1994; Herrington et al., 1996; Zenisek and Mathews, 2000; Villalobos et al., 2002; Kim et al., 2005).

CCCP can also increase secretion up to five fold in chromaffin cells (Montero et al., 2000; Haynes et al., 2006; Lim et al., 2006) and neurohypophysial terminals (Sasaki et al., 2005). It has been used to increase MEPP frequency in frog neuromuscular junction (Molgó and Pécot-Dechavassine, 1988; Van Der Kloot et al., 2000) where H^+-gradient sensitive vesicular calcium uptake or release occurs (Von Grafenstein and Powis, 1989; David et al., 1998; Christensen et al., 2002; Churchill et al., 2002; Mahapatra et al., 2004; Haynes et al., 2006; Michelangeli et al., 2005; McGuinness et al., 2007). CCCP is responsible for the period of massive MEPP frequency followed by either very low or no MEPPs whatsoever (Molgó and Pécot-Dechavassine, 1988) as a consequence of ATP synthase reversal followed by ATP depletion within the terminal that stops ATP driven pumps (Budd and Nichols, 1996).

In a couple of independent recent papers (Guo et al., 2005 and Verstreken et al., 2005) two different Drosophila mutants lacking pre-synaptic mitochondria were studied. They showed normal acute Ca^{2+} buffering and normal basal neurotransmission that was impaired only if submitted to intense stimulation that could be rescued with exogenous ATP. The authors concluded that pre-synaptic calcium dynamics are marginally participated by mitochondria that seem to be recruited for calcium extrusion only under prolonged stimulation. We also recall that mitochondria are very scarce in the *Torpedo* electric organ; they are present only in a small proportion of nerve terminals. Mobilisation of energy is very fast during the electrical discharge at the expense of ion gradients, ATP and creatine phosphate, but recovery of energy stores afterwards is very slow, mainly provided by glycolysis (Abbott et al., 1958; Aubert et al., 1961; Chmouliovsky-Moghissi and Dunant, 1979).

We incubated excised prisms with CCCP in an attempt to mimic bafilomycin effect with a proton uncoupler. Yet, evoked electrical response after 1h incubation with CCCP was completely abolished (data not shown). A straight forward explanation for this result seems to be related to the long incubation period needed to allow diffusion throughout the entire prism (>30 min) for the drugs tested. When CCCP reaches the tissue proton dissipation is very fast as compared to bafilomycin or DCCD (Christensen et al., 2002; figure 36) and contrary to bafilomycin induces ATP depletion and inhibition of secretion after as little as 1h

incubation in tissue (Molgó and Pécot-Dechavassine, 1988; Van Der Kloot et al., 2000) or ~8 minutes in guinea-pig cerebro-cortical synaptosomes (Sanchez-Prieto et al., 1987). In *Torpedo* prisms energy depletion (ATP and creatine phosphate) induced by metabolic poisons and through a less known effect of botulinum toxin results in marked reduction in ATP and creatine phosphate levels or availability, inducing an increase in spontaneous events (including giant MEPPs and sub-MEPPs) at the same time that evoked responses decrease and cease (Dunant et al., 1988) and could explain failed transmission obtained with CCCP.

We also incubated excised prisms with N,N'-dicyclohexyl-carbodiimide (DCCD) that was shown to bind covalently both the proteolipid of the V-type H^+-ATPase, blocking ATP-dependent proton translocation (Sutton and Apps, 1981; Arai et al., 1987 and Sun et al., 1987). DCCD binds also the proteolipid mediatophore, but has little effect on ACh translocation (Sbia et al., 1992). DCCD also inhibited $^{45}Ca^{2+}$ accumulation into sheep brain cortex synaptic vesicles by compromising the H^+ gradient energising the vesicular Ca^{2+}/H^+ antiport (Gonçalves et al., 1999b). We registered a concentration dependent effect of DCCD, capable of prolonging the time-course of secretion similarly to bafilomycin with 20 μM DCCD inducing a ~30-50% increased time–course that reached ~2 fold increase (like bafilomycin) with 100 μM DCCD (data not shown). However, we also noticed that while the Area/peak; T_{50}; T_{90} or decay tau increased with increasing DCCD concentrations, EPP area and peak response decayed (~20 % with 20 μM DCCD; up to ~60% with 100 μM DCCD). We did not investigate any further this inhibiting effect of high DCCD concentrations on transmission, but preferred to concentrate our efforts with bafilomycin that is a more potent (Gonçalves et al., 1999b) and specific (Dröse and Altendorf, 1997) inhibitor of the V-type H^+-ATPase.

We also assessed the effect of 2,5-diterbutyl-1,4-benzohydroquinone (DBHQ; also named TER) on the electric response of prisms. DBHQ is said to be a specific blocker of Ca^{2+}-ATPase pumps (Kass et al., 1989; Fossier et al., 1998) and reported to induce increased ACh secretion in synaptosomes from *Torpedo* electric organ and mouse caudate nucleus, as well as to increased cholinergic transmission in *Aplysia*. An effect correlated with ~50% decrease in $^{45}Ca^{2+}$ uptake capacity of isolated synaptic vesicles (Fossier et al., 1998). Later work confirmed DBHQ concentration-dependent ACh release increase in mouse caudate nucleus and ACh and glutamate (Glu) release increase in *Torpedo* synaptosomes while being ineffective to potentiate Glu release from cerebellum mossy fibre synaptosomes (Israël and Dunant, 2004). Interestingly, DBHQ was proposed to inhibit preferentially the sarco-

endoplasmic reticulum Ca^{2+}-ATPase or SERCA 3 pump reported to occur in bafilomycin sensitive acidic organelles in human platelets, where [Ca^{2+}] transients were significantly prolonged by 20 μM DBHQ (López et al., 2005, 2006). The effects are of particular interest since the proposed targets are vesicular Ca^{2+}-ATPases capable of a similar shaping of transmitter release we have found with bafilomycin.

DBHQ decreased the formation of vesicular H^+ gradient (measured by A.O.fluorescence) in a concentration-dependent manner (figure 29). The decrease in fluorescence is most probably the result of inhibition of the V-type H^+-ATPase by DBHQ , that is responsible for all the fluorescence signal (complete dissipation with bafilomycin) in sheep brain cortex synaptic vesicle preparations (figure 14). In addition, DBHQ seems to reduce the bafilomycin-sensitive Pi production resultant from ATP consumption by the V-type H^+-ATPase working either at maximum speed (presence of CCCP) or in normal conditions (without the H^+-uncoupler; figure 30). These results point out to a double effect of DBHQ in synaptic vesicle calcium transport systems, blocking both the vesicular Ca^{2+}-ATPase and partially compromising normal vesicular H^+-gradient that is the driving force of the Ca^{2+}/H^+ antiport.

In the course of this work we were interested in finding a blocker for the Ca^{2+}/H^+ antiport activity. Several compounds reported to interfere with Ca^{2+} sequestration were tested in preliminary assays with acridine orange used to report Ca^{2+}-induced H^+ gradient dissipation in sheep brain cortex synaptic vesicles (data not shown). They were the Plasma membrane Na^+/Ca^{2+} antiport blocker KB-R7943 (20 μM); the mitochondrial Na^+/Ca^{2+} antiport blocker, CGP37157 (50 μM); the ryanodine receptor inhibitors, 1,1'-diheptyl-4,4'-bipyridinium dibromide or DHBP (100 μM) and heparin (2mg/ml); the Ca^{2+}-release activated channel or CRAC inhibitor 2-aminoethoxydiphenylborane (2-APB at 100 μM); the unspecific Ca^{2+}-ATPase inhibitor butylated hydroxytoluene (BHT at 100 μM) and the above mentioned SERCA and Ca^{2+}-ATPase inhibitors 2,5-di-tert-butyl-hydroquinone (BHQ at 100 μM) and the benzylated homologue DBHQ (100-300 μM) also named TER.

We were surprised to find that while none of them specifically inhibited the antiport, most (all but heparin) induced a significant decrease in proton pump activity, measured by the decrease in fluorescence amplitude (shown only for DBHQ in figure 29). We concentrated further clarification of these unexpected (those drugs are supposed to be specific) results in DBHQ, which was reported to interfere with vesicular calcium transport and modulate

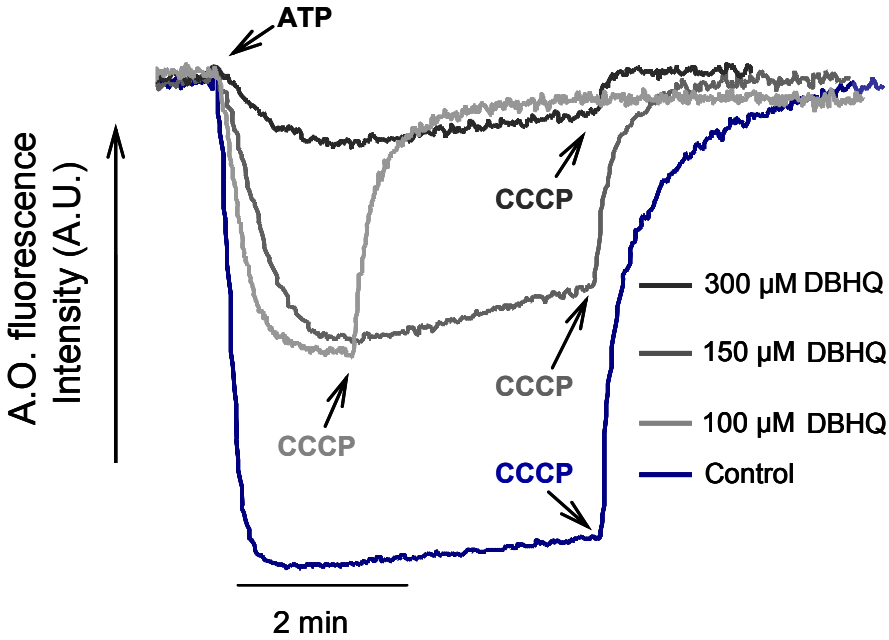

Figure 29. Concentration-dependent effect of DBHQ on proton transport across synaptic vesicles isolated from sheep brain cortex. Synaptic vesicles (0.6 mg protein/ml) and 3 µM A.O. were added (not shown) to medium containing 150 mM KCl, 60 mM sucrose, 2 mM $MgCl_2$, 10 mM Tris at pH 8.5 and 50 µM EGTA, with (grey traces) or without (blue trace) increasing DBHQ concentrations. H^+ pumping by the V-type H^+-ATPase started by addition of 500 µM ATP (arrow) and was accompanied by acridine orange fluorescence quench as described in the text. CCCP 2µM was added at indicated times (arrows) for calibration.

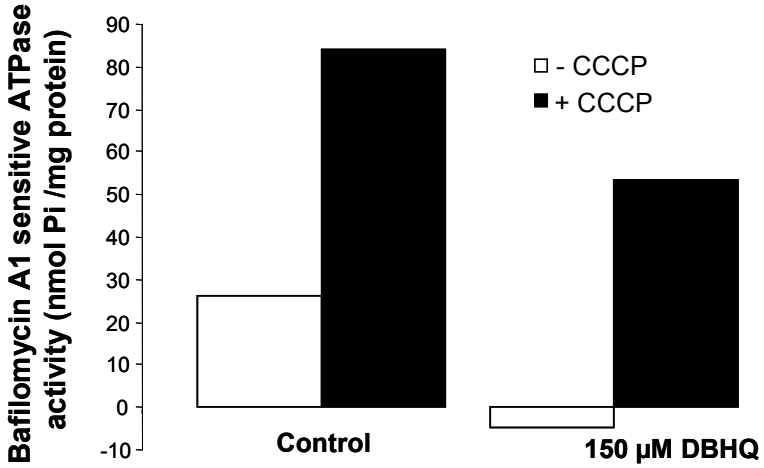

Figure 30. Effect of DBHQ effect on the H^+-ATPase activity of synaptic vesicles isolated from sheep brain cortex. H^+-ATPase activity in vesicles (0.6 mg protein/ml) was assayed as the amount of Pi produced per minute in the same medium as in figure 31. Values show Pi quantified after 2 min in presence of 504 µM ATP after subtraction of Pi produced in presence of 504 µM ATP and 300 nM bafilomycin A1. Assays occurred in the absence (white bars) or in the presence of the proton uncoupler CCCP (2µM) (black bars). Reaction were carried out in the absence (control) or presence of 150 µM DBHQ.

transmitter release (see discussion and references above).

We then tested the effects of DBHQ on excised prisms electric response (figure 31 and 32). There is a concentration-dependent effect of EPP waveform enlargement that partially mimics the bafilomycin effect (figure 17 and table 2), with the time-dependent parameters (area/peak, rise time, decay T_{50},T_{90} and tau) all being increased by ~20% (figure 32). The ~20% effect is also in line with partial H^+ gradient dissipation when compared with the ~100% increase in ACh release timing by bafilomycin (that completely inhibits the proton pump). However, at higher concentrations (100 μM), we registered an additional time-dependent decrease in EPP amplitude, that was never present with bafilomycin even for prolonged incubations (>24h). This decreased EPP response was accompanied by a slow (hours) concentration-dependent increase in the levels of $^{45}Ca^{2+}$ accumulation in non-stimulated tissue while maintaining unaltered the total $^{45}Ca^{2+}$ that accumulates in the tissue right after a 12 second stimulation at 100 Hz. Thus, the more Ca^{2+} accumulated at rest in the tissue, the less could be added as a surplus upon stimulation (figure 33).

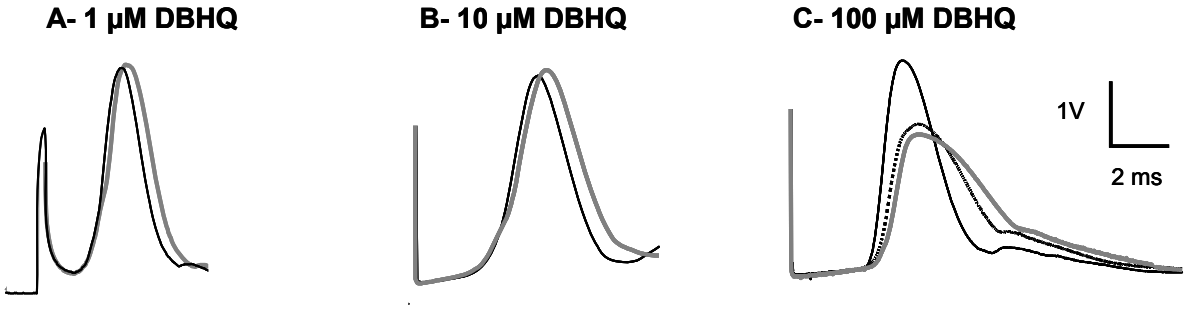

Figure 31. Concentration-dependent effect of DBHQ on synaptic transmission in the *Torpedo* electric organ. Traces show in succession the stimulation artefact, the synaptic delay and the electrical discharge produced by excised prisms in response to field stimulus. Prisms were incubated in 3.4 mM $CaCl_2$ containing elasmobranch saline medium (Control traces in black) and then 1h later after addition of 1; 10 or 100 μM DBHQ (grey traces) in **A** and **B**, respectively. Traces in **C** show a control EPP (black trace), and the response generated by the same prism after 1h (doted line) and 2h (grey line) incubation in the presence of 100 μM DBHQ . Representative experiment of n= 5-6.

These results highlight the possibility that DBHQ compromising the vesicular Ca^{2+}-ATPases combined with a decrease in vesicular Ca^{2+}/H^+ antiport Ca^{2+} extrusion alters both the temporal definition of the calcium microdomain responsible for ACh release activation at the same time that it compromises normal calcium extrusion into synaptic vesicles (and

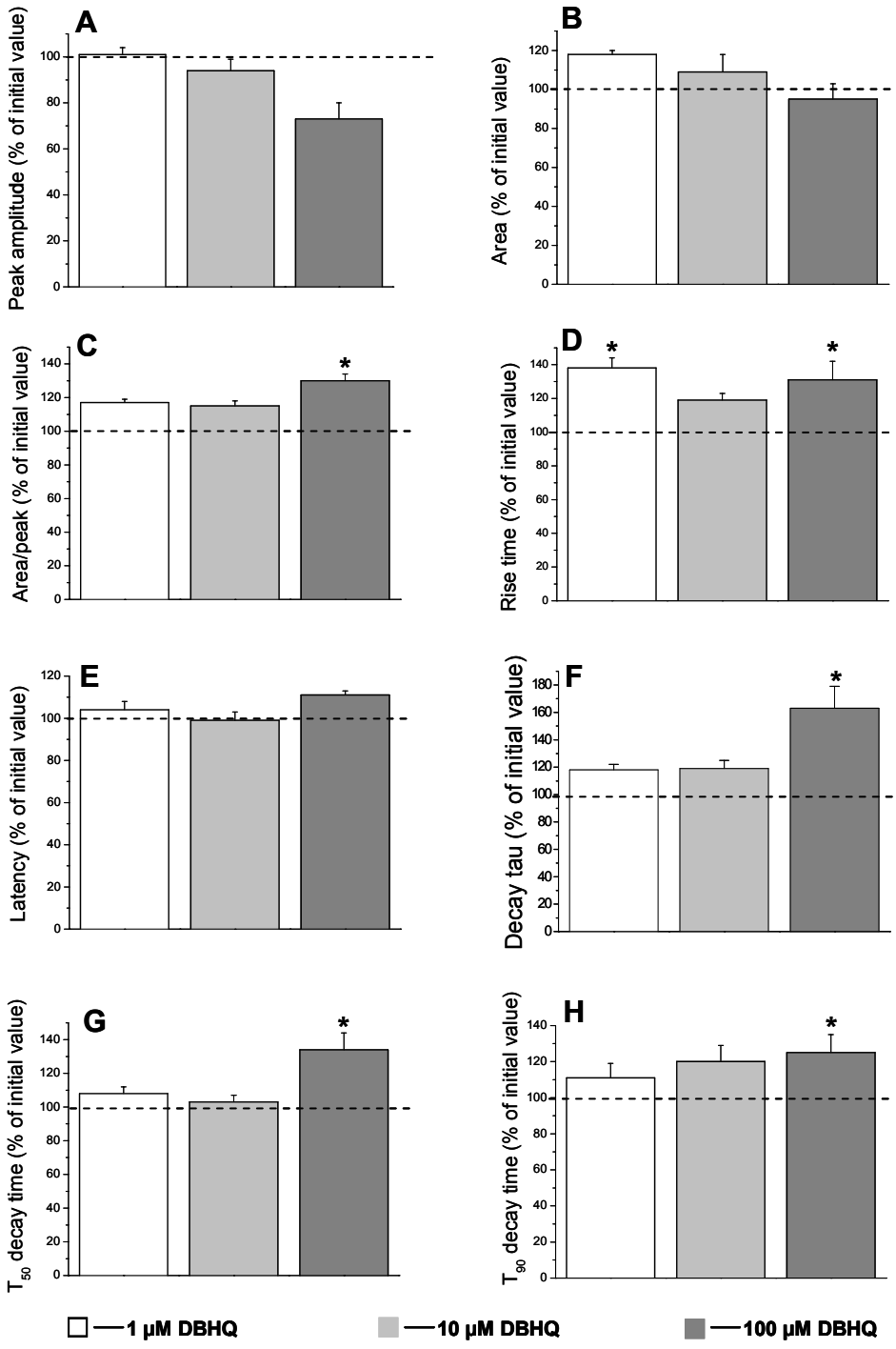

Figure 32. Characterization of the concentration-dependent effects of DBHQ on prisms EPPs in response to a single stimulus. Prisms were submitted to field stimulation in 3.4 mM $CaCl_2$ containing elasmobranch saline medium supplemented with 1 (□); 10 (■) or 100 (■) µM DBHQ for 1h. Values show mean ± SEM (n=6) expressed in percentage of the control EPP generated by the same prisms before drug incubation. DBHQ prolonged significantly the time course of the electrical discharge (Unpaired T-test: * $p<0.05$). At high concentrations the EPP amplitude was reduced.

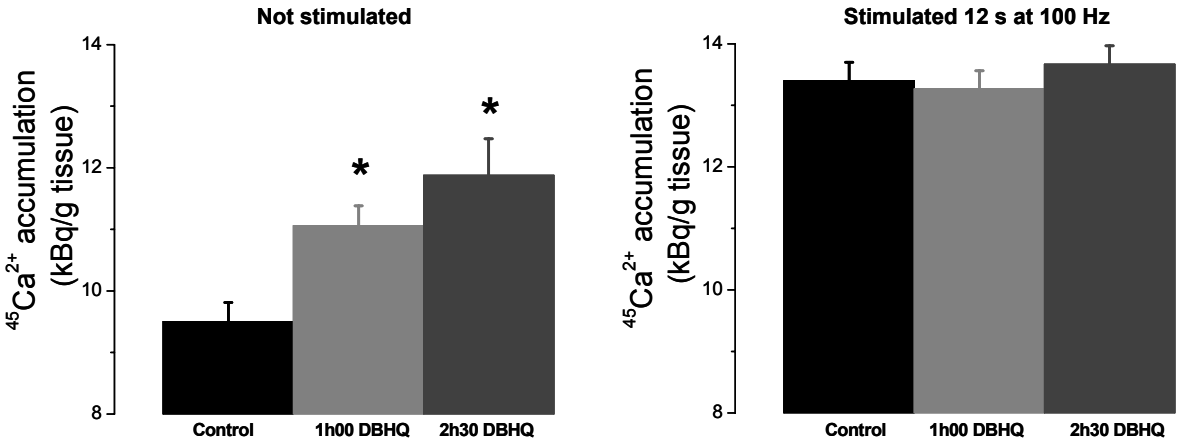

Figure 33. Effect of DBHQ on calcium retention within resting prisms (left panel) or in prisms submitted to a 12 s tetanus at 100 Hz (right panel). Prisms were incubated in $^{45}CaCl_2$ containing medium for 3h without DBHQ (control) or supplemented with 100 µM DBHQ during either 2h30 or 1h before quantification of cellular ^{45}Calcium. Stimulated prisms had ^{45}calcium quantified soon after the tetanus. Bars show average ± SEM (n= 5 to 9) of prisms bathed in elasmobranch saline medium (controls in black) or supplemented with 100 µM DBHQ (grey bars). DBHQ significantly increased ^{45}Calcium accumulation of "resting" prisms, in the absence of stimulation (Unpaired T-test: *p<0.01). At the end of the stimulation ^{45}Calcium reaches the same level in the presence or absence of DBHQ.

possibly also by non vesicular Ca^{2+}-ATPases), that seem to participate in the "housekeeping" task of cytosolic calcium removal that allows to maintaining resting calcium levels within cells <100 nM. It is also likely that the slow Ca^{2+} accumulation induced by DBHQ leads into the Ca^{2+}-induced desensitisation of the mediatophore (there is a time/concentration-dependant transmission decrease; figure 31 and 32) or of VOCCs (time-dependant decrease in the surplus of Ca^{2+} accumulation in stimulated prisms; figure 33).

In conclusion, we have learned that besides bafilomycin, a number of drugs (CCCP; DCCD; DBHQ, among others) capable of annihilating the vesicular proton gradient end up interfering with calcium homeostasis and compromise normal secretory activity. When we look at these results under the light of the mechanisms unveiled by the experiments done with bafilomycin and strontium (see chapters above for acute effects and below for long-term effects), it becomes evident that at least some of the reported effects in the presence of those drugs should be attributed to compromising proton-gradient-dependent Ca^{2+} transport into acidic organelles.

3.2.1.5. The pre-synaptic effect of bafilomycin reported in synaptosomes

Having established a pre-synaptic effect of vesicular Ca^{2+}/H^{+}-antiport blockers on phasic ACh release in the *Torpedo* electric organ, we aimed at confirming that effect on isolated nerve terminals. For that we prepared synaptosomes from ***Torpedo*** electric organ tissue according to Morel et al. (1977) and proceeded with the quantification of ACh released from synaptosomes in response to a depolarizing stimulation (100 μM Veratridine). The incubation medium contained enzymes that responded continuously to ACh released by emitting light in proportion to the number of ACh molecules (Israël and Lesbats, 1981a, 1981b), which could be quantified by subsequent addition of known amounts of ACh (figure 34 A).

We compared the amounts of ACh released in response to a Ca^{2+}-veratridine challenge following a 10 min incubation in calcium-free saline medium either in the absence (control) or in the presence of 2 μM bafilomycin A1 (figure 34). Under these conditions, bafilomycin-incubated synaptosomes released over twice as more ACh than control synaptosomes (figure 34 B). After the release run, the synaptosomes were ruptured using Triton X-100, which allowed for the measurement of their final ACh content. Those treated with bafilomycin, which had released more ACh in response to veratridine, were found to contain less transmitter at the end of the run, which was another way to demonstrate that bafilomycin considerably enhanced transmitter release from *Torpedo* isolated nerve terminals.

This result mimics the ca. 2 fold increase in transmitter release at *Torpedo* electric organ synapses in response to electrical stimulus when the vesicular Ca^{2+}/H^{+}-antiport is inoperative (previous sections). It also confirms that such effects are mostly pre-synaptic.

We extended the study of vesicular Ca^{2+}/H^{+}-antiport blockade to another synaptosome preparation. **Rat mossy fibre synaptosomes** (Israël and Whittaker, 1965; Helme-Guizon et al., 1998) are also large (Bancila et al., 2004) robust (-85 mV resting potential versus -50 mV in Torpedo synaptosomes; Meunier, 1984; Bancila et al., 2004, 2008) and glutamate release competent (Bancila et al., 2004, 2008). These synaptosomes are also prone to the usage of fluorescence probes while it was not possible to use those in *Torpedo* despite the efforts in ours and other laboratories.

We proceeded with the measurement of $[Ca^{2+}]$ within the bulk of the cytosol ($[Ca^{2+}]_{cytosol}$) of rat hippocampus mossy fibre synaptosomes incubated with Fura-2-AM.

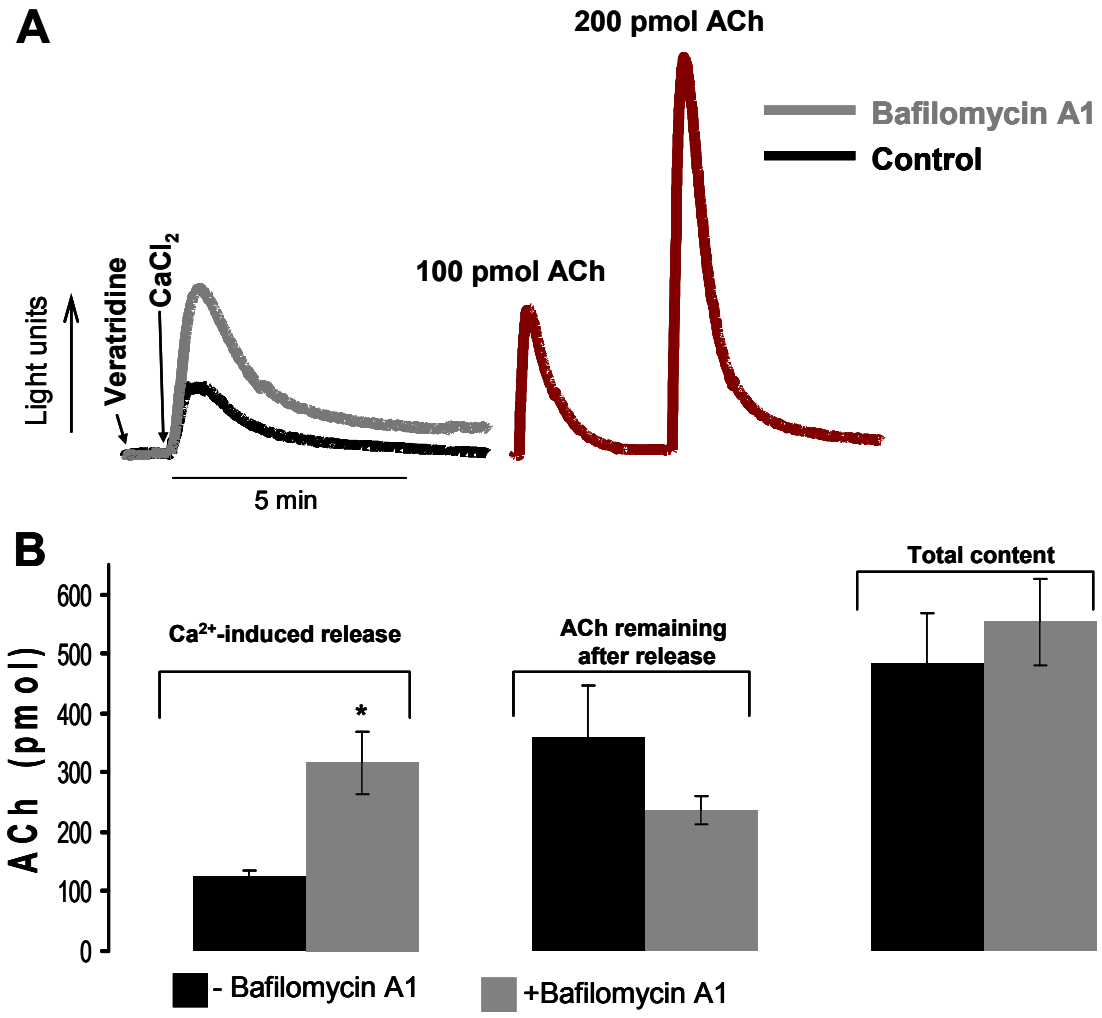

Figure 34. Effect of bafilomycin A1 on acetylcholine release from *Torpedo* electric organ synaptosomes. Samples were pre-incubated 10 min in Ca^{2+}-free elasmobranch saline medium in the absence (black) or presence of 2 μM bafilomycin A1 (grey). Panel **A**: Synaptosomes were depolarized with 100 μM veratridine followed by addition of $[Ca^{2+}]_{final}$= 3.4 mM (arrows) to elicited ACh release. The figure shows representative traces of ACh release from 30 μl of the synaptosome fraction (~60 μg protein), using the chemiluminescent enzymatic method. Then, the remaining ACh content within synaptosomes was quantified after permeabilization with 5 μl Triton X-100 1%. Standards with known amounts of ACh were finally used for calibration (brown trace). **B**: Values show average ± SEM of at least 3 experiments of conditions shown in panel **A**. Ca^{2+}-dependent ACh release was measured for 5 min. Total ACh was obtained by the summation of the amount of ACh released by Ca^{2+}-depolarization and that measured upon Triton X-100 permeabilization. The amount of Ca^{2+}-dependent ACh released from bafilomycin A1-treated synaptosomes (grey bars) was significantly higher than from control synaptosomes (Unpaired T-test: *$p<0.05$) (black bars).

Synaptosomes were then kept for 15 minutes in Ca^{2+}-free mammalian Krebs (control) or supplemented with 0.5 μM bafilomycin A1 prior to the addition of 1.33 mM $CaCl_2$ to the cuvette where Fura-2 fluorescence was measured (figure 35). Synaptosomes were then depolarized with 40 μM veratridine ~30 s after calcium addition. Bafilomycin induced a small but significant increase of "basal" $[Ca^{2+}]_{cytosol}$ measured 60 s before calcium addition. This effect might have arisen from Ca^{2+} release from acidic stores (Christensen et al., 2002; Churchill et al., 2002; López et al., 2005; Kachoei et al., 2006) after full H^+-gradient dissipation induced by bafilomycin (which takes <10 min; figure 36). What is more, bafilomycin caused an over two-fold increase in $[Ca^{2+}]_{cytosol}$ when the synaptosomes were depolarized with veratridine in the presence of 1.33 mM $CaCl_2$ (inset in figure 35), arguing in favour of the fact that Ca^{2+} accumulation increase within stimulated synaptosomes as a result of compromised vesicular Ca^{2+}/H^+-antiport transport.

Like in *Torpedo* excised prisms (figure 19), calcium accumulation was enhanced in rat synaptosomes devoid of rapid vesicular calcium transport provided by the antiport. Therefore, besides acting on secretion timing, rapid Ca^{2+}-sequestration within synaptic vesicles seems to contribute also to increasing the Ca^{2+}-load within nerve terminals (figures 19 and 35). This loss of rapid Ca^{2+}-sequestration while maintaining slower Ca^{2+}-transport systems with first order kinetics has been put in evidence in the past with protonophores (CCCP/FCCP; Herrington et al., 1996; Park et al., 1996; Xu et al., 1997; Billups and Forsythe, 2002) and with strontium (Xu-friemann and Regehr 2000), that embody working conditions without the participation of a functional vesicular Ca^{2+}/H^+-antiport.

The H^+ gradient across the membrane of acidic organelles (essentially synaptic vesicles in synaptosomes), can be followed using acridine orange (A.O.) fluorescence as a reporter (Zoccarato et al., 1999). We incubated rat hippocampus mossy fibre synaptosomes with A.O.. It is expected that A.O. penetrates cell membranes and accumulates in acidic compartments where its fluorescence is quenched. Thus any dissipation of the intracellular proton gradient should result in an increase in fluorescence.

Figure 36 illustrates a typical experiment where A.O. (3 μM) was added to the synaptosome suspension, causing an increase in fluorescence followed by a slow quenching which reflects the incorporation of the dye in acidic compartments. When a plateau is reached, addition of 40 mM KCl (final concentration) in the presence of extracellular Ca^{2+}

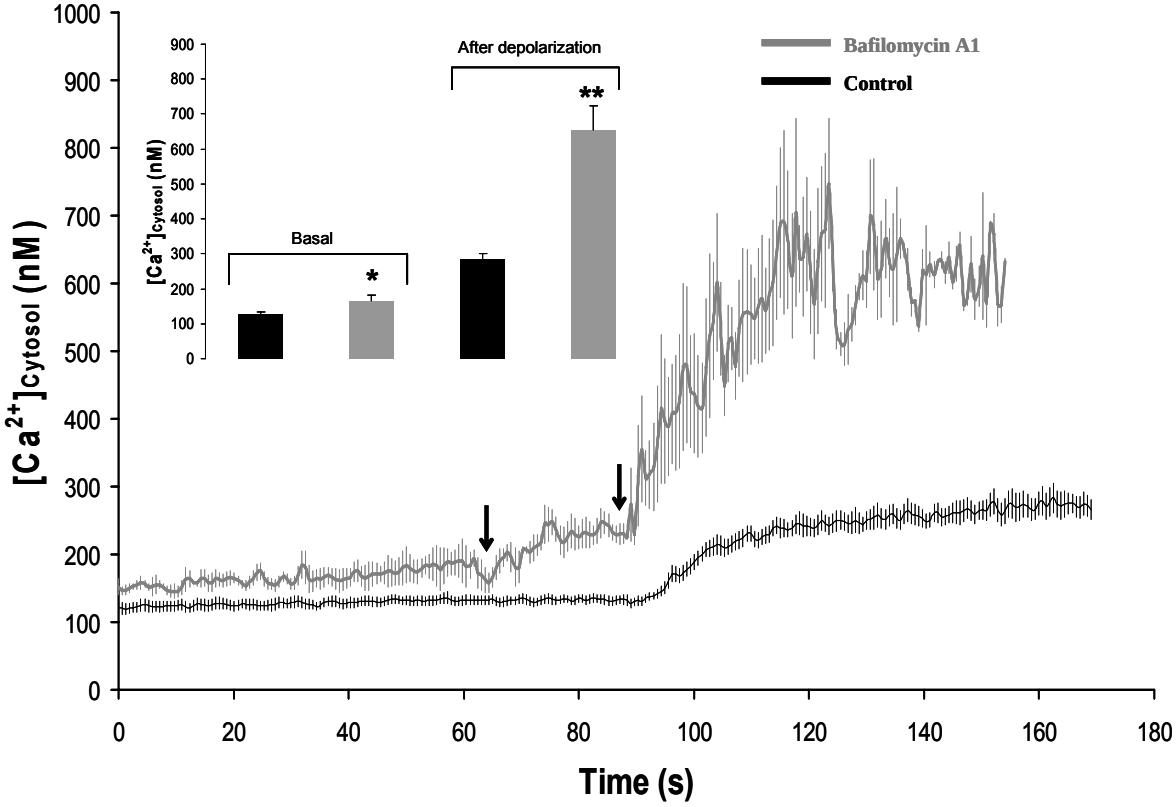

Figure 35. Bafilomycin A1 effect on the $[Ca^{2+}]_{Cytosol}$ rise occurring after depolarization of rat hippocampus mossy fibre synaptosomes. Traces show average fluorescence. Synaptosomes were loaded with Fura-2-AM and kept in Ca^{2+}-free mammalian Krebs, during 15 min in the absence (black) or presence (grey) of 0.5 μM bafilomycin A1. Then, 1.33 mM $CaCl_2$ was added (first arrow) followed by depolarization with 40 μM veratridine (second arrow). Values show averages ± SEM of 4 to 9 experiments. Inset shows the basal $[Ca^{2+}]_{Cytosol}$ as the average ± SEM of the first 60 seconds (basal) and $[Ca^{2+}]_{Cytosol}$ after depolarization as the average ± SEM of the last 40 seconds. Bafilomycin A1 (grey) increased significantly both basal $[Ca^{2+}]_{Cytosol}$ (*$p<0.05$) and $[Ca^{2+}]_{Cytosol}$ of depolarized synaptosomes (Two-way ANOVA: **$p<0.0001$) as compared to control (black).

caused a transient dissipation of H^+ gradients (Figure 36 A). Afterwards the proton ionophore CCCP was added to induce a full dissipation of the gradient.

The H^+ gradient measured this way is completely generated by V-type H^+-ATPases (Figure 36 B-E; Zoccarato et al., 1999). Indeed, when 1 μM bafilomycin A1 was added at any moment of the experiment, it caused a dissipation of the proton gradient that was slower than with CCCP; the gradient was nevertheless completely dissipated in less than 10 minutes. When the synaptosomes were pre-incubated with bafilomycin A1, the gradient was not established (Figure 36 B) and DCCD (100 μM) mimicked bafilomycin H^+-gradient dissipation (figure 36 D and E).

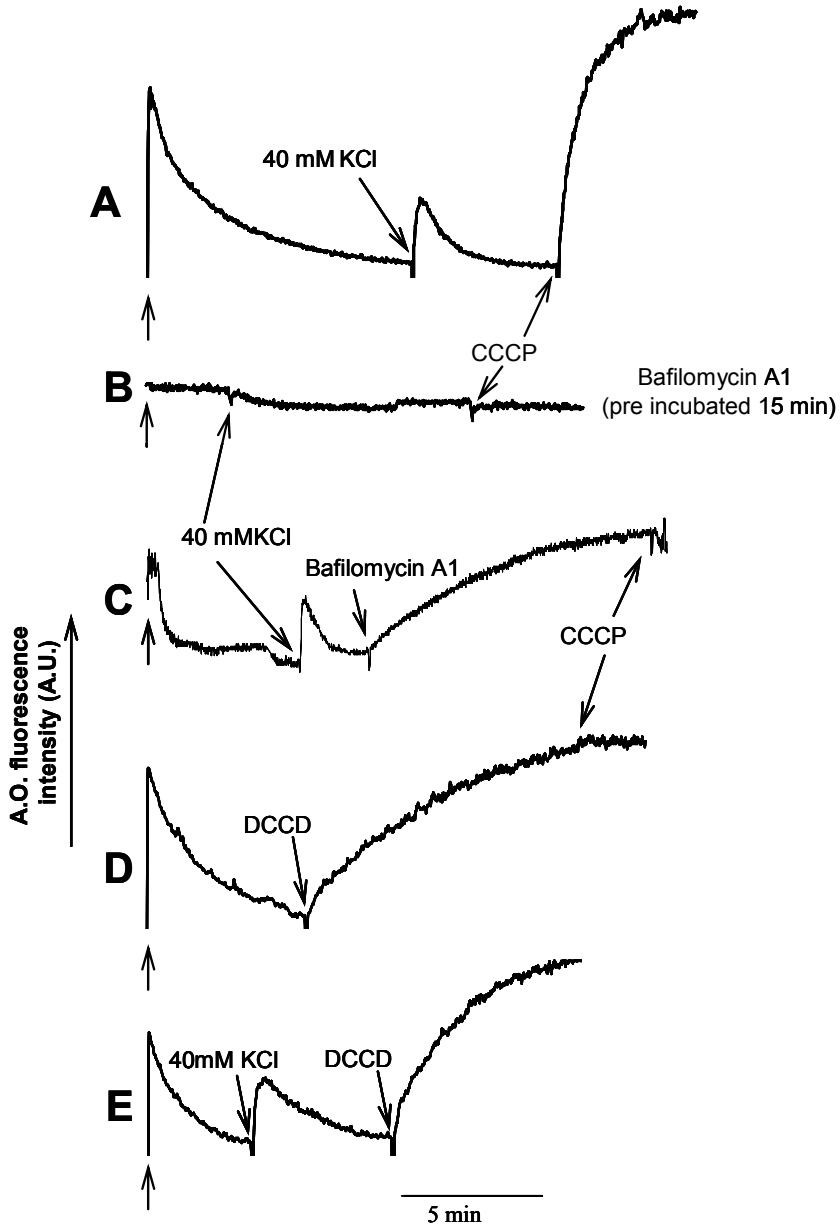

Figure 36. Effect of vesicular H^+-ATPase inhibitors on the formation and proton gradient dissipation across acidic compartments within mossy fibber synaptosomes isolated from rat hippocampus. Proton gradient was monitored by adding 10 mg protein/ml synaptosome suspension (arrows) to Krebs solution containing 3 μM acridine orange. Fluorescence quench occurs when the dye is exposed to acidic medium within acidic compartments, where it dimerises and accumulates. Panel ***A*** shows H^+ gradient formation and transient dissipation by 40 mM KCl in the presence of 2.2 mM $[Ca^{2+}]_{out}$, and then fully dissipated by addition of 10 μM CCCP. Pre-incubation of synaptosomes for 15 minutes with 1 μM bafilomycin A1 prevented any gradient formation, hampering also the typical KCl or CCCP responses (panel **B**). Addition of 1μM Bafilomycin A1 after KCl depolarisation resulted in total proton gradient dissipation, as shown by CCCP not increasing fluorescence any further (panel ***C***). Similar dissipations were observed with DCCD, in resting (Panel **D**) or depolarized (panel **E**) synaptosomes. Traces are representative of 3-6 experiments.

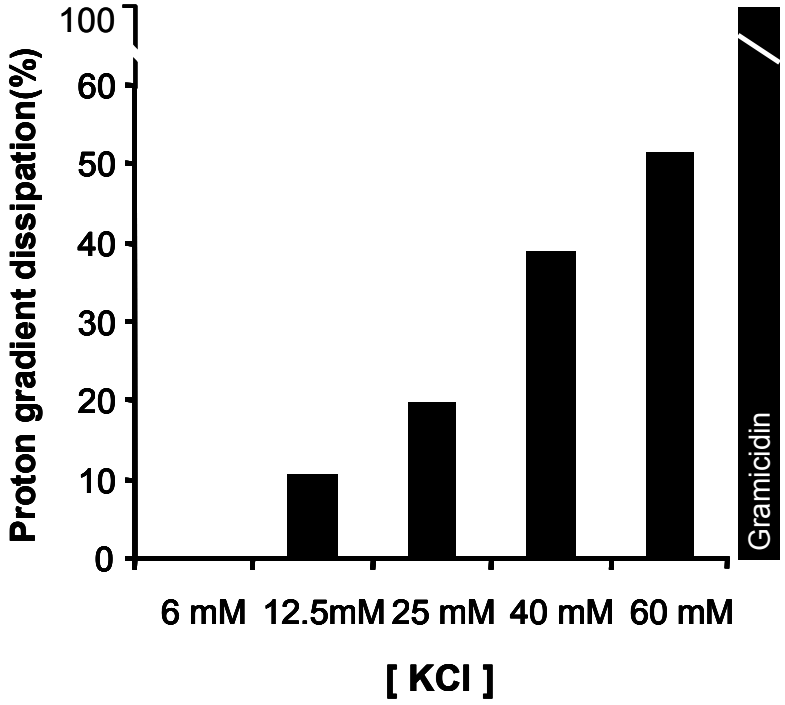

Figure 37. Depolarization-dependent proton gradient dissipation across acidic compartments within mossy fibber synaptosomes isolated from rat hippocampus. Proton gradient across acidic compartments was monitored with acridine orange (as in figure 36). Bars show the dissipation induced by application of increasing KCl concentrations in the presence of 2.2 mM $CaCl_2$. Gramicidin (2 μg) dissipated completely the proton gradient. Values were plotted as the percentage of total gradient as determined after application of CCCP.

The partial transient dissipation of the proton gradient elicited by KCl challenge lasted 20-40 seconds and was followed by re-acidification of acidic organelles lasting 5 more minutes (figures 36 A; 38 B). The phenomenon may be explained in two ways. First, the H^+-gradient transient could be interpreted as the result of exocytosis shuttling H^+-filled synaptic vesicles directly into contact with the extra-synaptosomal medium, followed by re-acidification of endocytosed vesicles lasting 5 minutes on average (Zoccarato et al., 1999). Alternatively, rapid Ca^{2+}/H^+ exchange mediated by the vesicular antiport originates the transient dissipation of the H^+-gradient in synaptic vesicles remaining *in situ*. The gradient would then be re-established by the H^+-pump within the same or newly formed vesicles (by endocytosis). Either way, the phenomenon was strictly calcium dependent (figures 37-40).

At a constant calcium concentration (2.2 mM), the amplitude of the peak dissipation was found to be a function of the KCl concentration added (Figure 37) and thus, to the size of the depolarisation step (maximal with gramicidin). The dependency seemed to arise from

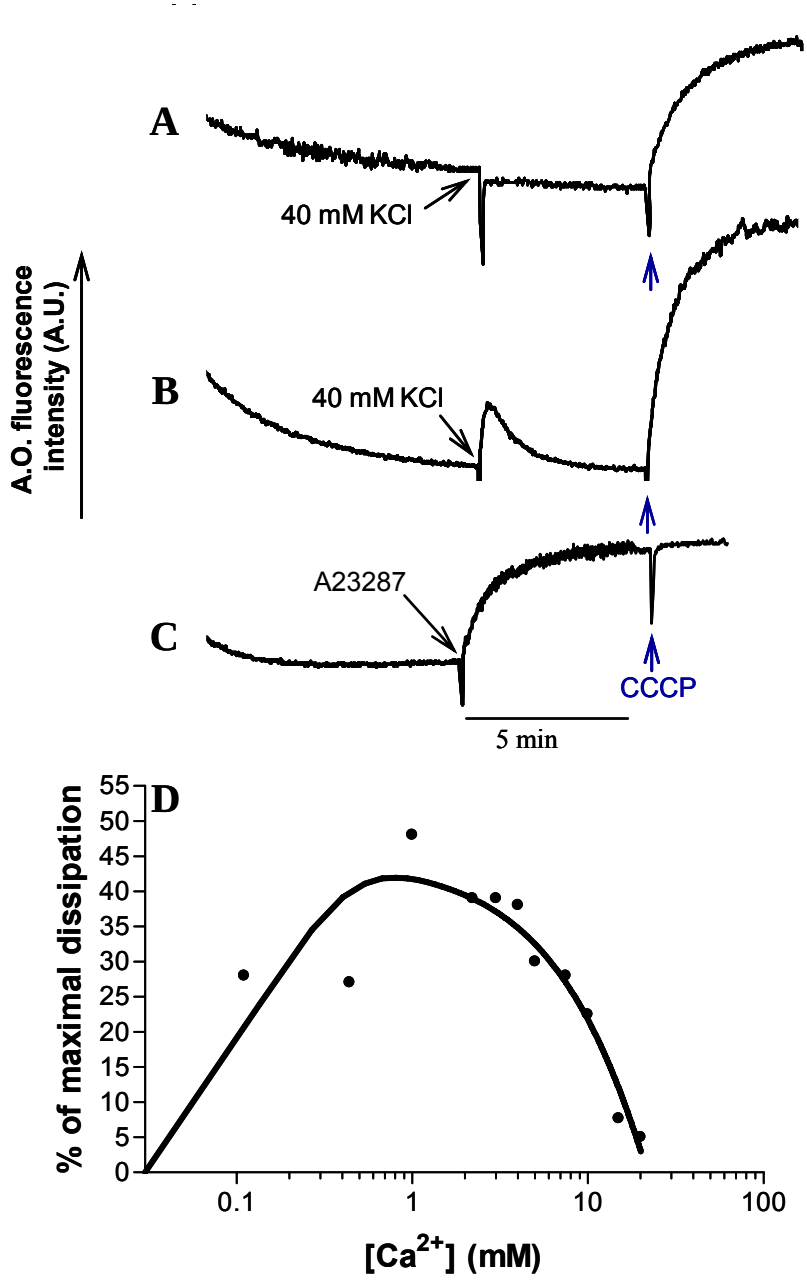

Figure 38. Calcium dependence of depolarization-induced proton gradient dissipation from acidic compartments within mossy fibber synaptosomes isolated from rat hippocampus. Proton gradient across acidic compartments was monitored with acridine orange (as in figure 36). Panel ***A*** shows that there is no transient dissipation of the gradient induced by 40 mM KCl in mammalian Krebs containing 0.5 mM EGTA (no free Ca^{2+}). Panel **B** shows proton gradient transient dissipation after synaptosome depolarization with 40 mM KCl in presence of 2.2 mM $[Ca^{2+}]_{out}$. Panel ***C*** evidences rapid, full dissipation of the pre-established H^+ gradient induced by selective permeation of synaptosomes to calcium by application of the calcium ionophore A23187 (50 μM) in presence of 2.2 mM $CaCl_2$. Panel **D** shows the extent of the dissipation induced by 40 mM KCl in the presence of increasing calcium concentrations (0.11; 0.44; 1; 2.2; 3; 4; 5; 7.5; 10; 15 or 20 mM $CaCl_2$). The bell-shaped curve results from a two phase exponential fit to the dataset. Values were plotted as the percentage of total gradient as calibrated after application of CCCP (blue arrows in A-C).

increased calcium entry into the synaptosomes for when a depolarizing stimulus was applied in the absence of calcium (0.5 mM EGTA; figure 38 A) the signal was absent. Conversely, the more calcium entered the pre-synaptic terminal, between 0 and 1 mM, the more dissipation of the H^+ gradient occurred. Stable dissipation occurred between 1-4 mM $CaCl_2$ while higher Ca^{2+} concentrations resulted in a decrease in the acridine signal (Figure 38 D). Moreover, the calcium ionophore A23187 caused a rapid and maximal dissipation of the gradient (Figure 38 C). Therefore, the results evidence that the transient dissipation of the proton gradient by high KCl is clearly Ca^{2+}-dependent.

3.2.1.6. The pre-synaptic effect of strontium reported in synaptosomes

Despite the fact that calcium is directly involved in depolarization-induced transient H^+-gradient dissipation there was still some doubt as to which molecular determinant(s) participate in that event. Therefore, we addressed this question by substituting calcium with increasing strontium concentrations (figure 39). We found that equimolar $SrCl_2$ was capable of eliciting sub-maximal H^+-gradient dissipation in response to a depolarising stimulus. This was overcomed by increasing $SrCl_2$ to 10 mM that rendered a response with a similar amplitude to the one obtained with 2.2 mM $CaCl_2$. Yet, the time course of that transient was markedly different from the one obtained with calcium. The H^+-gradient dissipation endured much longer than with calcium and there was almost no recuperation of A.O. fluorescence signal with high strontium (figure 39 A). Moreover, there was a marked increase in the rise time (from 10%-90%) with strontium which was also concentration-dependent (figure 39 B).

The experiments with strontium were quite revealing since strontium was found to tamper with vesicular Ca^{2+} accumulation through the antiport and to be unable to induce measurable H^+ displacement from sheep brain cortex synaptic vesicles (Gonçalves et al., 1999). These arguments favour the hypothesis that Sr^{2+} is not transported through the vesicular Ca^{2+}/H^+-antiport while it is capable of entering the terminal upon depolarization (Xu-friedmann and Regehr, 2000) and interact with Ca^{2+}-binding partners like the mediatophore (as reported above with *Torpedo*) as well as to elicit vesicular fusion (Kishimoto et al., 2001; Neves et al., 2001; Shin et al., 2003) and support endocytosis (Guatimosim et al., 1998; Neves et al., 2001; Kilic et al., 2001). Despite doing so with decreased efficiency in all these

functions due to reduced affinity to Ca^{2+}-binding partners when compared to calcium (see section 3.2.1.2).

In figure 39, strontium also displayed a lower potency but was capable of substituting calcium and elicit transient H^+-gradient dissipation in depolarised synaptosomes with a similar efficiency at high [Sr^{2+}]. Strontium-induced dissipation was probably due to vesicular fusion only, since rapid efflux of H^+ from vesicles was not expected to occur with strontium. Yet, the time required to develop a H^+-gradient dissipation similar in amplitude to the one obtained

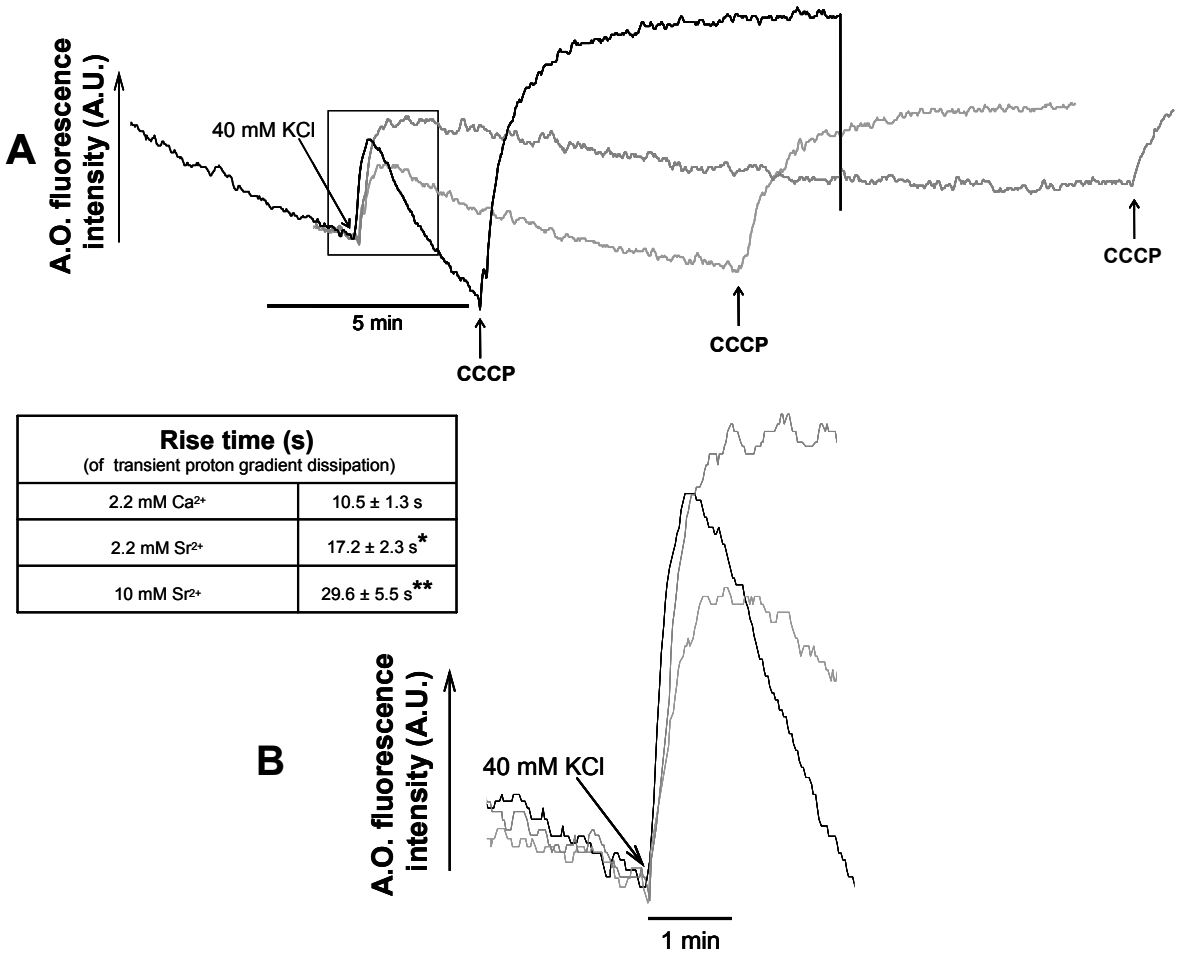

Rise time (s) (of transient proton gradient dissipation)	
2.2 mM Ca^{2+}	10.5 ± 1.3 s
2.2 mM Sr^{2+}	17.2 ± 2.3 s*
10 mM Sr^{2+}	29.6 ± 5.5 s**

Figure 39. Strontium is a slower substitute of calcium for depolarization-induced dissipation of the proton gradient from acidic compartments within mossy fibber synaptosomes isolated from rat hippocampus. Panel **A**. Proton gradient across acidic compartments was monitored with acridine orange (as in figure 36). Traces show transient H^+ gradient dissipation by 40 mM KCl, in the presence of either 2.2 mM $CaCl_2$ (black trace) or alternatively 2.2 mM (light grey) or 10 mM $SrCl_2$ (dark grey) and then fully dissipated by addition of 10 µM CCCP. Traces are representative of 6 experiments. Panel **B** shows KCl-induced transient from panel **A** in detail. **Inset** table shows mean ± SEM of the rise time (from 10% to 90%) of the transient proton gradient dissipation following depolarization with KCl of the same set of experiments (n=6). Strontium dissipates the proton gradient significantly slower than calcium (Unpaired T-test: *p<0.05; **p<0.01).

with calcium was considerably extended (from ~10.5 s to ~29.6 s) reflecting the loss of rapid response with strontium but present with calcium. The difference in H^+-dissipation rates observed between the two cations probably reflects an early action of the Ca^{2+}/H^+- antiport present with calcium, followed closely by exocytosis that is present with calcium and strontium. The exocytosis of recently calcium-filled vesicles is also concordant with the participation of vesicular fusion in intra-terminal (Dunant et al., 1980b; Párducz and Dunant., 1993; Párducz et al., 1994) and extracellular (Heinemann et al 1977, Borst and Sakmann, 1999; Stanley, 2000; Massimini and Amzica, 2001; Rabi and Thoreson, 2002; Rusakov and Fine, 2003) calcium homeostasis.

Strontium was also revealing to intra-terminal ionic homeostasis mechanisms, since the H^+-gradient dissipation was significantly prolonged. This could have arisen from the persistence of exocytosis due to sustained $[Sr^{2+}]_{int}$ elevation or by decreased vesicular re-filling of endocytosed vesicles. This later hypothesis seems unlikely because increasing $[Sr^{2+}]$ should result in an increase in the endocytotic rates (Guatimosim et al., 1998) and not the opposite. Concordantly, lingering H^+-gradient dissipation is consistent with the persistence of Sr^{2+} ions within the synaptosomes reported by Xu-friedman and Regehr, (2000) originating consecutive rounds of fusion that maintain H^+-gradient dissipation until Sr^{2+} clearance from the cytosol falls $[Sr^{2+}]_{int}$ under the threshold of vesicular fusion activation. In a sense, A.O. reported the persistence of $[Sr^{2+}]_{int}$ within depolarised rat hippocampus mossy fibre synaptosomes.

3.2.1.7. The pre-synaptic effect of nicotine reported in synaptosomes

As shown above, when a KCl challenge is applied in the presence of Ca^{2+} or Sr^{2+} , transmitter release is accompanied by a significant dissipation of the vesicular H^+-gradient. We expected therefore that this phenomenon will take place in any circumstance where transmitter release would be elicited efficiently. To our surprise, it is not the case. We applied 25 μM nicotine to mossy fibre synaptosomes, a dose which was sufficient to induce Ca^{2+}-dependent glutamate release in an amount equivalent to that released by 30-40 mM KCl (Bancila et al., 2004, 2008). However, this was not accompanied by any change in A.O. fluorescence (figure 40), nor by any detectable modification of the synaptosomes membrane

potential (Bancila et al., 2008). The fundamental difference between the two secretagogues may be that while KCl opens VOCCs through a depolarization step, conveying abrupt Ca^{2+} entry at active zones that are packed with vesicles, nicotine binds Ca^{2+}-permeable ACh receptors that allow for a slower calcium entry elsewhere, probably triggering the liberation of intracellular stores of calcium (Bancila et al., 2008). In that case, it seems that there must be a robust calcium transient occurring close to synaptic vesicles to elicit measurable H^+-gradient dissipation with A.O. (figure 40).

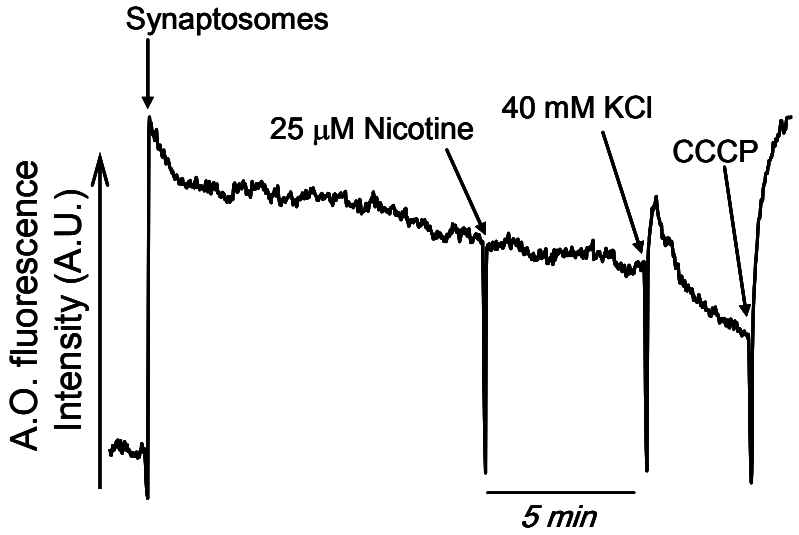

Figure 40. Although able to efficiently trigger glutamate release, nicotine is unable to elicit any transient dissipation of the vesicular proton gradient, in mossy fibber synaptosomes from rat hippocampus. Proton gradient was monitored by adding 10 mg protein/ml synaptosome suspension to Krebs solution containing 3 μM acridine orange. Trace shows that vesicular transmembrane H^+ gradient was not dissipated by nicotine (25 μM) but was transiently dissipated by 40 mM KCl in the presence of 2.2 mM Ca^{2+}, and then fully dissipated by addition of CCCP (10μM). Representative experiment of n= 10.

3.2.1.8. Can antiports and carriers work at the speed of ion channels?

It is known that Ca^{2+}-pumps that transport Ca^{2+} at expense of metabolical energy are far more slower to completely dissipate Ca^{2+} than the explosive Ca^{2+} entry through VOCC's occurring <1ms. Ca^{2+}-ATPase provide slow calcium decay time constants that are typically in the time scale of ca. 100 ms in neurons (Helmchen et al., 1996) up to 10 s in chromaffin cells (Neher and Augustine, 1992). Particularly high rates of extrusion obtained with Ca^{2+}-ATPAses have been demonstrated in the stereo-cilia of bullfrog hair cells where the plasma membrane

Ca^{2+}-ATPase isoform 2a clusters at high density (2000/μm^2; Yamoah et al., 1998) producing a ~1.3 pA current and, nevertheless, extrudes Ca^{2+} with a time constant of ~75ms (Lumpkin and Hudspeth, 1998; Dumont et al., 2001).

On the other hand, secondary active transport provided by carriers that rely on pre-existent ionic gradients has been viewed until recently as no match for the flow that is obtainable with ion channels (Usually ~1000-fold lower; Kirichok et al., 2004; Accardi and Miller, 2004).

Recently, the borderline between carriers and channels has dimmed considerably. The mitochondrial calcium uniport was thought to be a carrier, driven by the inner mitochondrial electrochemical gradient, with a maximum turnover rate of ~2 x 10^4 $Ca^{2+}s^{-1}$ as measured in suspension (where apparently transport was saturable). It turned out to be a high affinity ion channel with multiple conductance states (2.6 pS up to 5.6 pS) and capable of impressive turnover rates of 5 x 10^6 $Ca^{2+}s^{-1}$ at very high [Ca^{2+}] (Kirichok et al., 2004).

Similarly, some members of the CLC gene family that encode for anion (mainly Cl^-) channels at plasma, endosomal/lysosomal or vesicular membranes turned out to behave as antiports with turnover rates of ~10^5 s^{-1}, which is rather low for an ion channel but high for an antiport (Accardi and Miller, 2004; Piccolo and Pusch, 2005; Scheel et al., 2005; De Angeli et al., 2006). These antiports rely on the pre-established gradient of either ion that drives the active transport of its exchange partner (Accardi and Miller, 2004). This mechanism has revealed itself far advantageous for the accumulation of nitrate into plant vacuoles with an accumulation factor of 50 instead of 3 through a nitrate-selective channel (Angeli et al., 2006).

Within a nerve terminal microdomain, $[Ca^{2+}]_{int}$ rises rapidly and, especially in the case where vesicles constitute an obstacle for free diffusion of Ca^{2+} and buffers (Roberts, 1994; Shahrezaei and Delaney 2005) it might reach very high concentrations. High $[Ca^{2+}]_{int}$ provides favourable conditions for the observed very rapid uptake of Ca^{2+} into synaptic vesicles that benefits from both the H^+ and the Ca^{2+} gradients, since most of the vesicular calcium within SVs is bound to the vesicular matrix (Mahapatra et al., 2004).

These observations conjugated with our results point to the conclusion that antiports might work fast enough to control sub-millisecond Ca^{2+}-dependent reactions, like rapid neurosecretion.

3.2.2. Vesicular Ca^{2+} transport shapes long-lasting intracellular [Ca^{2+}] and neurotransmitter release

3.2.2.1. Inhibition of vesicular Ca^{2+}/H^{+}-antiport raises [Ca^{2+}] to desensitization levels

Mossy fibre synaptosomes were used to assess the effect of vesicular proton pump inhibitors in glutamate secretion (figure 41). MFS were pre-incubated for 20-30 minutes in the absence (control) or in presence of V-type H^{+}-ATPase inhibitors (bafilomycin or DCCD). It is recalled that after such a treatment, the H^{+} gradient is fully dissipated (figure 36). MFS were then depolarised with 40 mM KCl during 5 min after which the synaptosomal suspension was centrifuged and the amount of glutamate in the supernatant was measured by chemiluminescence (Fosse et al., 1986; Israël et al., 1993; Helme-Guizon et al., 1998; Bancila et al., 2008).

MFS submitted to bafilomycin or DCCD pre-incubation released approximately the same amount of glutamate as control synaptosomes (figure 41). This was a rather unexpected result since it had been reported previously a time-dependent inhibition of either glutamate release from guinea-pig cerebral cortex synaptosomes with CCCP (Sanchez-Prieto et al., 1987); aspartate release inhibition from cultured cerebellar granule cells with bafilomycin (Cousin and Nichols, 1997) as well as glutamate release inhibition with bafilomycin in rat hippocampal synaptosomes (Bradford and Nadler, 2004). However, the later study also revealed that aspartate release was slightly increased with bafilomycin instead of decreased like glutamate release; the divergent effect was proposed to arise from the putative release of aspartate from the cytoplasm by a yet-undescribed Ca^{2+}-dependent mechanism.

In the MFS preparation one such mechanism might have been involved in Ca^{2+}-dependent glutamate release, as proposed recently (Israël and Dunant, 2004).

However, the differences in bafilomycin (and DCCD or CCCP) effects on transmitter release might have a simpler explanation related to the calcium load supported by the different preparations. Bafilomycin induced a small but steady increase in MFS basal $[Ca^{2+}]_{cytosol}$ (figure 42) during 15-20 min that did not compromise further $[Ca^{2+}]_{cytosol}$ increase upon depolarization (which was approximately twice that of controls; figure 43) and did not

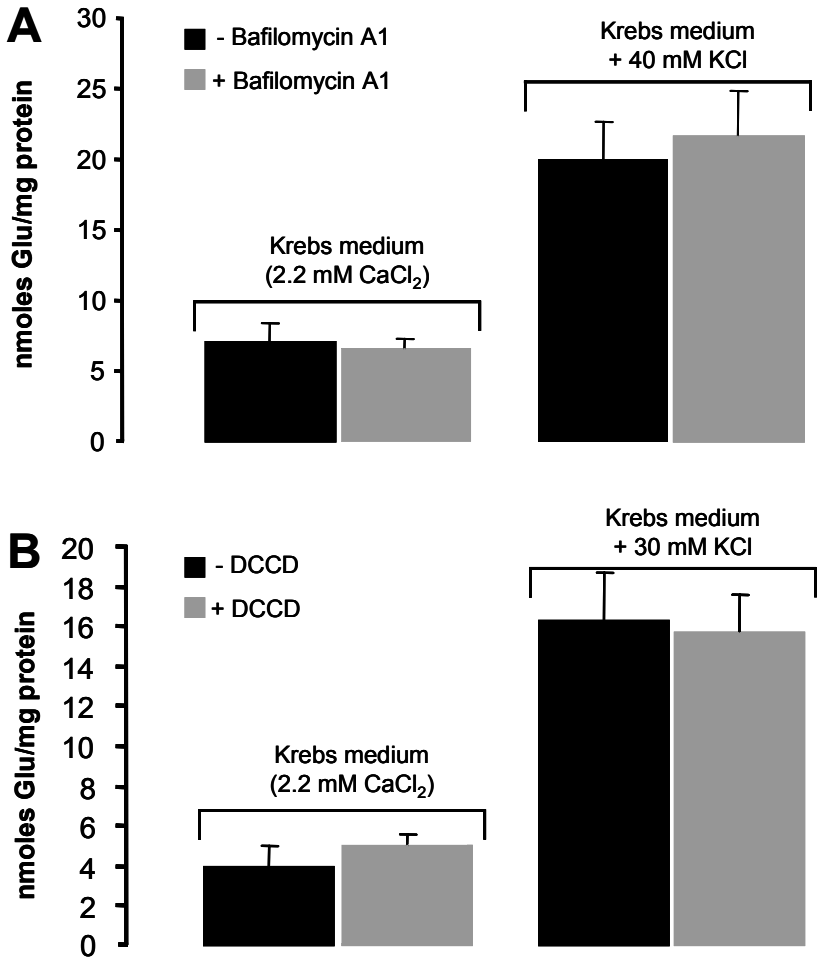

Figure 41. Effect of vesicular H^+-ATPase inhibitors on glutamate release by rat hippocampus mossy fibre synaptosomes. Glutamate was released from synaptosome suspension (3 mg protein/ml) kept in Krebs medium containing 2.2 mM $CaCl_2$ during 5 minutes. Then, synaptosomal suspension was centrifuged and the amount of glutamate released into the supernatant was monitored by chemiluminescence. Reactions were carried out in the absence of stimulation (Krebs) or after depolarization with KCl. Panel **A**. Glutamate release from synaptosomes pre-incubated for 30 min in the absence (control), or in the presence of 1 μM bafilomycin A1. Panel **B**. Glutamate release from synaptosomes pre-incubated for 20 min in the absence (control), or in the presence of 50 μM DCCD. Values show mean ± SEM of 5-6 experiments.

compromise glutamate release (figure 41). Conversely, pre-incubating *Torpedo* electric organ synaptosomes with bafilomycin for 15 minutes in the presence of 3.4 mM $CaCl_2$ was enough to block ACh secretion (figure 44 B and D). A major difference between the two preparations is their resting membrane potential: -85 mV in rat MFS (Bancila et al., 2004, 2008) versus -50 mV in *Torpedo* (Meunier, 1984). This means that, under resting conditions, rat MFS are exposed to minor Ca^{2+} entry through VOCCs (Catterall, 2000) than synaptosomes of the electric organ.

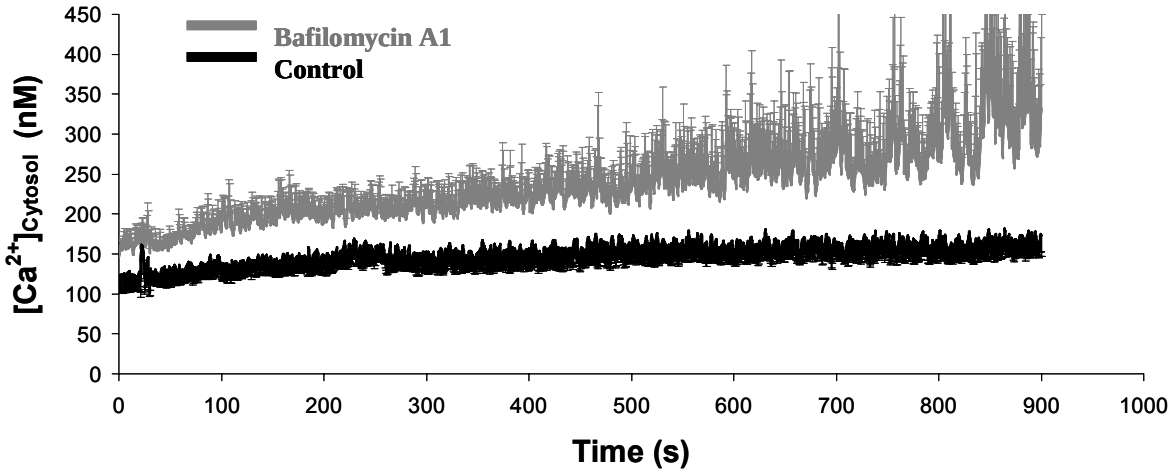

Figure 42. Bafilomycin A1 effect on basal $[Ca^{2+}]_{Cytosol}$ increase in rat brain hippocampus, mossy fibre synaptosomes. Traces show average fluorescence with Fura-2-AM loaded synaptosomes after 15 minutes incubation in Ca^{2+}-free mammalian Krebs in the presence (grey trace) or absence (black trace) of bafilomycin A1 (0.5 μM). 1.33 mM $CaCl_2$ was added at 20 s. Values show averages ± SEM of 4-5 experiments. Bafilomycin A1 (grey) increased significantly basal $[Ca^{2+}]_{Cytosol}$ (Two-way ANOVA: *p<0.05) as compared to control (black).

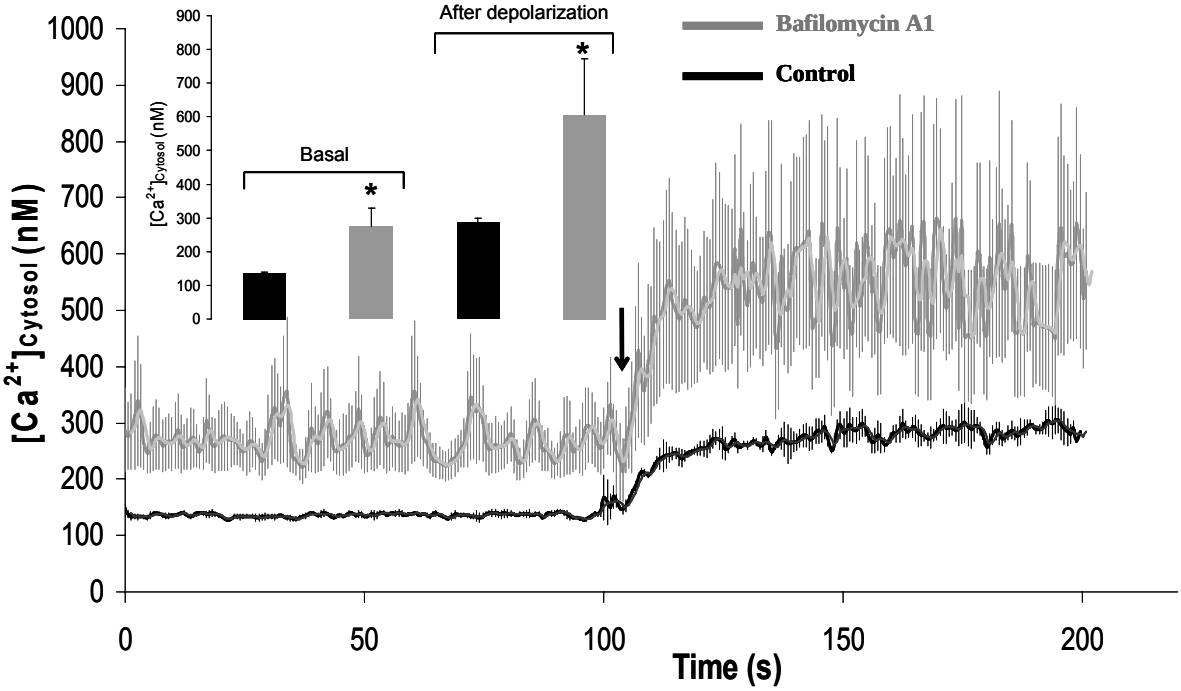

Figure 43. Effect of bafilomycin A1 incubation during 20 minutes in presence of calcium on $[Ca^{2+}]_{Cytosol}$ rise after depolarization of rat brain hippocampus, mossy fibre synaptosomes. Traces show average fluorescence with Fura-2-AM loaded synaptosomes after incubation for 20 minutes in 1.33 mM $CaCl_2$ containing mammalian Krebs in presence (grey trace) or absence (black trace) of bafilomycin A1 (0.5 μM). Fluorescence was measured for 100 s before (basal) depolarization with 40 μM veratridine (arrow). Values show averages + SEM of 3-4 experiments. **Inset** shows the basal $[Ca^{2+}]_{Cytosol}$ as the average ± SEM of first 60 seconds (basal) and $[Ca^{2+}]_{Cytosol}$ after depolarization as the average ± SEM of last 60 seconds. Bafilomycin A1 (grey) increased significantly the $[Ca^{2+}]_{Cytosol}$ before (basal) and after a depolarizing stimulus (Two-way ANOVA: *p<0.0001) as compared to control (black).

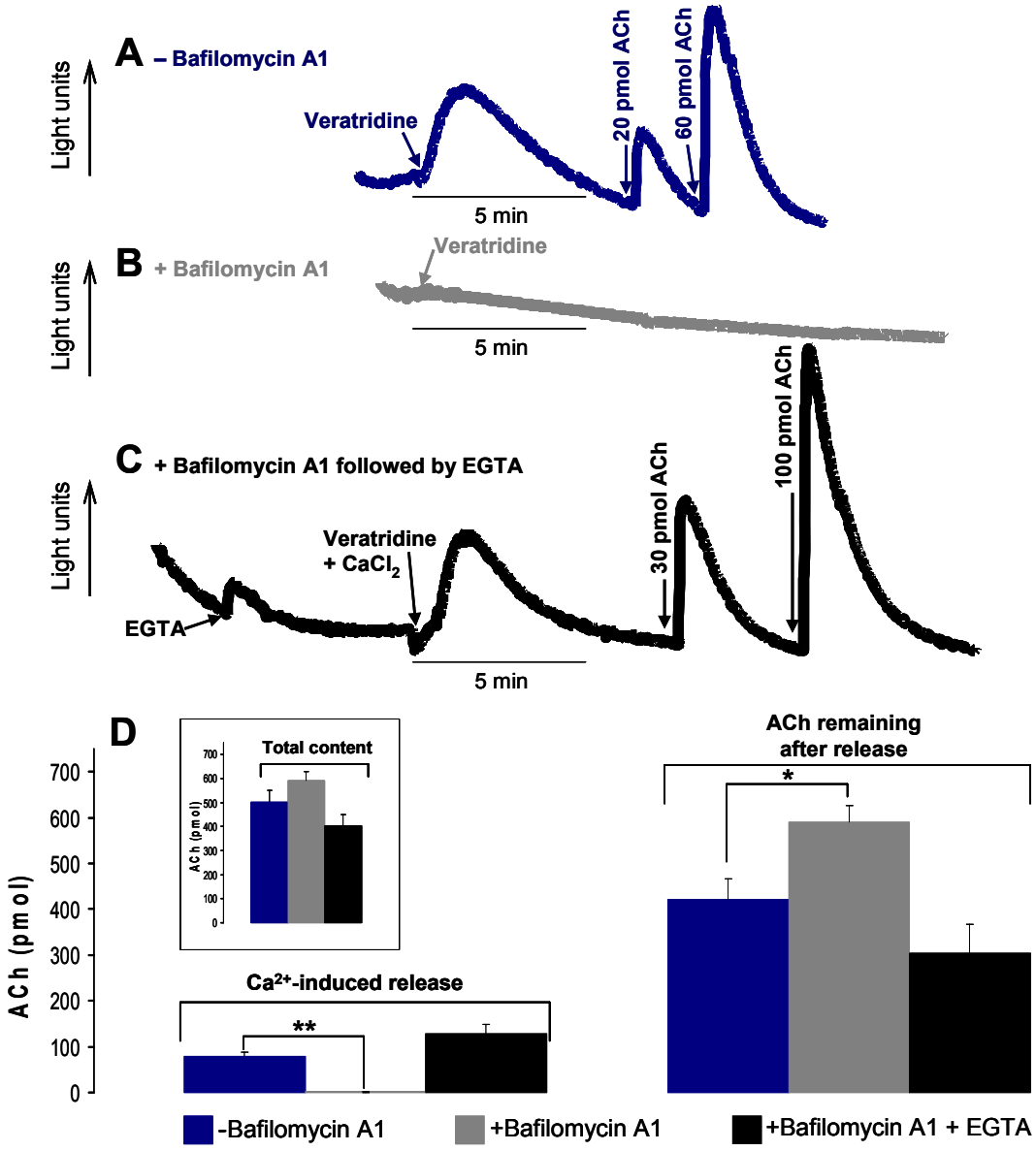

Figure 44. Bafilomycin A1-induced desensitization of ACh release from *Torpedo* electric organ synaptosomes. Panel ***A-C***: Representative traces of ACh release from the synaptosomal fraction (30 µl; with ~60 µg protein), using the chemiluminescent enzymatic method. Panel **D**: Values show mean ± SEM (n=4) of conditions shown in panel ***A-C***. Samples were pre-incubated 15 min in elasmobranch saline medium containing 3.4 mM $CaCl_2$, with (+, grey and black traces and bars) or without (-, blue trace and bars) 2 µM bafilomycin A1. After this pre-incubation, samples were either promptly depolarized with 100 µM veratridine to elicit ACh release (blue and grey traces) or were allowed to rest in low Ca^{2+} for 5 min (by adding 3.5 mM EGTA) before 100 µM veratridine followed by more 3.4 mM $CaCl_2$ additions to elicit ACh release (black trace and bars). Remaining ACh content within synaptosomes was quantified after permeabilization with 5 µl Triton X-100 1%. Standards with known amounts of ACh were used to calibrate transmitter release and remaining content of synaptosomes. **Inset** shows total ACh obtained by addition of Ca^{2+}-induced ACh release and the remaining ACh revealed using Triton X-100. Pre-incubation of synaptosomes with bafilomycin A1 in the presence of calcium completely suppressed Ca^{2+}-dependent ACh release (Unpaired T-test: **p<0.0001) and was

accompanied by preservation of ACh content remaining within synaptosomes after stimulus (Unpaired T-test: *p<0.05).

On the contrary, calcium entry through VOCCs in slightly depolarised *Torpedo* synaptosomes whose calcium clearance is impaired is expected to results in Ca^{2+}-induced desensitization of transmitter release (Adams et al., 1985), due to a desensitization of the mediatophore (Israël et al., 1987). The experiment illustrated in the figure 44 B and D clearly support this explanation. Desensitised terminals could regain ACh release capacity provided that intracellular Ca^{2+} concentration was reduced, during 5 minutes, with EGTA. After that period, simultaneous addition of veratridine and normal $[Ca^{2+}]_{out}$ fully recuperated ACh release (figure 44 C and D). This later result pinpoints $[Ca^{2+}]_{int}$ rise as responsible for bafilomycin action on ACh release, in detriment of any another effect bafilomycin might do.

Interestingly, there was no desensitization of ACh release in *Torpedo* synaptosomes without bafilomycin (figure 44 A and D), revealing that vesicular Ca^{2+}/H^{+}- antiport activity is important in keeping basal calcium under desensitization levels.

3.2.2.2. Inhibition of Ca^{2+}-pumps and desensitization of transmitter release

Calcium homeostasis and the keeping of very low $[Ca^{2+}]_{int}$ under resting conditions has been attributed to the action of Ca^{2+}-pumps (P-type Ca^{2+}-ATPases) at the plasma membrane, endoplasmic reticulum and synaptic vesicles (Israël et al., 1980; Michaelson et al., 1980; Rephaelis and Parsons, 1982; Fossier et al., 1998; Gonçalves et al., 2000a; Villalobos et al., 2002; Rizzuto and Pozzan, 2006).

We addressed the participation of P-type Ca^{2+}-ATPases in the regulation of synaptic transmission in *Torpedo* electric organ prisms. Figure 45 shows representative experiments of prisms kept under continuous perfusion with elasmobranch saline medium (control; figure 45 A) or supplemented with 10 μM orthovanadate (figures 45 B and C). Electric responses were elicited (by paired pulse field stimulation) at indicated times over a ~10h period. Control prisms (figure 45 A) constantly held robust electrical responses of approximately constant amplitude during the entire experiment. On the contrary, prisms perfused in 10 μM orthovanadate-containing saline medium developed a time-dependent decrease of the evoked response until full inhibition occurred after 5h55. After that, prisms exposed to orthovanadate were either washed out by replacement with normal elasmobranch saline

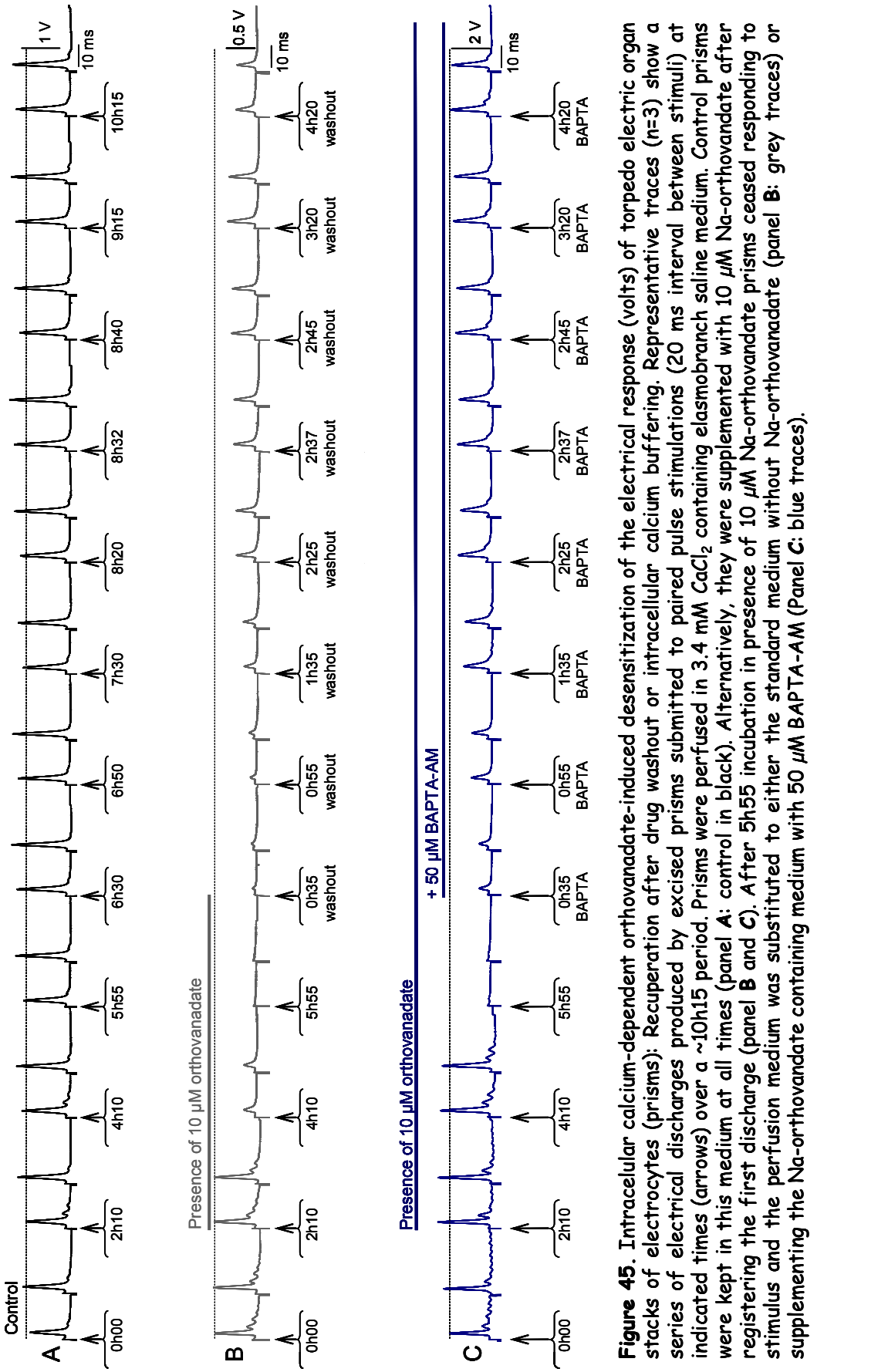

Figure 45. Intracelular calcium-dependent orthovanadate-induced desensitization of the electrical response (volts) of torpedo electric organ stacks of electrocytes (prisms): Recuperation after drug washout or intracellular calcium buffering. Representative traces (n=3) show a series of electrical discharges produced by excised prisms submitted to paired pulse stimulations (20 ms interval between stimuli) at indicated times (arrows) over a ~10h15 period. Prisms were perfused in 3.4 mM $CaCl_2$ containing elasmobranch saline medium. Control prisms were kept in this medium at all times (panel **A**: control in black). Alternatively, they were supplemented with 10 µM Na-orthovandate after registering the first discharge (panel **B** and **C**). After 5h55 incubation in presence of 10 µM Na-orthovandate prisms ceased responding to stimulus and the perfusion medium was substituted to either the standard medium without Na-orthovanadate (panel **B**: grey traces) or supplementing the Na-orthovandate containing medium with 50 µM BAPTA-AM (Panel **C**: blue traces).

medium (figure 45 B) or supplemented with 50 μM BAPTA-AM to the orthovanadate containing medium (figure 45 C). There was a very slow recuperation of transmission resultant from orthovanadate washout, with little recuperation after 1h drug washout that evolved to a maximum of ~75% of initial amplitude after 3h20 (figure 45 B). Strikingly, BAPTA-AM addition to the perfusion medium resulted in ~50% recuperation of original amplitude in less than 1h and full recuperation (100%) after 4h20, in spite of the remaining presence of orthovanadate (figure 45 C). The fact that the fast calcium chelator (BAPTA) was more effective than the simple washout of the Ca^{2+}-pump inhibitor (orthovanadate) supports for an intracellular Ca^{2+}-dependent inhibition of transmission that is normally prevented by the rather slow pumping activity of Ca^{2+}-ATPases. These are normally responsible for bringing Ca^{2+}-levels within the terminals under the threshold of ACh-release machinery desensitization.

The rather slow nature of the effects of Ca^{2+}-ATPase pumping inhibition are also patent in the time-course of ^{45}calcium accumulation and extrusion within stimulated or unstimulated prisms with normal Ca^{2+}-ATPase activity (control) or prisms whose Ca^{2+}-pumping activity was compromised with 10 μM orthovanadate pre-incubation (figure 46). The rate of ^{45}Calcium extrusion from prisms was measured by washing them out with standard elasmobranch medium (+/- orthovanadate), without ^{45}calcium, during 0, 5, 10, 15 or 30 min before placing the tissue in ice-cold medium and proceed with measurement of cellular ^{45}calcium using a radioassay counting (see figure 19 as well).

Orthovanadate did not affect the initial content of ^{45}calcium within unstimulated prisms or within prisms soon after a 12 s tetanus at 100 Hz. This result is in striking contrast to the effect reported with bafilomycin (figure 19) and highlights the little, if any, participation of Ca^{2+}-ATPases in the immediate (up to a few seconds) extrusion of Ca^{2+} that entered the terminal during the 12 s train. In contrast to bafilomycin, there was a slowly developed retention (or decreased extrusion) of ^{45}calcium within stimulated as well as unstimulated prisms that became significant between 15 and 30 min (figure 46).

It is interesting to notice that there was no greater effect with stimulated prisms as compared to non-stimulated ones, highlighting the rather slow nature of Ca^{2+}-ATPases in keeping low resting calcium concentrations within nerve endings and contributing to the notion that other Ca^{2+}-transporting partners (like the Ca^{2+}/H^{+}-antiport) are responsible for the early phases of Ca^{2+}- extrusion (compare figures 19 and 46).

3.2.2.2. Ca^{2+}/H^{+}-antiport and Ca^{2+}-ATPase play complementary roles in Ca^{2+} homeostasis

These results highlight the complementary nature of the different vesicular calcium transport systems. On the one hand, a Ca^{2+}/H^{+}- antiport which is operative from the near mM $[Ca^{2+}]_{int}$ reached within few microseconds of VOCC opening (LLinás et al., 1992; Roberts, 1993) until $[Ca^{2+}]_{int}$ drops <100 μM (Gonçalves et al., 2000a) within calcium microdomains at active zones, and is capable of modulating the timing of phasic transmitter secretion (see section 3.2.1). On the other hand, a vesicular Ca^{2+}-ATPase which participates in later (from few ms up to several minutes) Ca^{2+} extrusion when $[Ca^{2+}]_{int}$ drops under 100 μM (Israël et al., 1980; Michaelson et al., 1980; Rephaelis and Parsons, 1982; Fossier et al., 1998; Gonçalves et al., 2000a), helping to bring $[Ca^{2+}]_{int}$ at <1 μM level, where other Ca^{2+}-ATPases working at higher

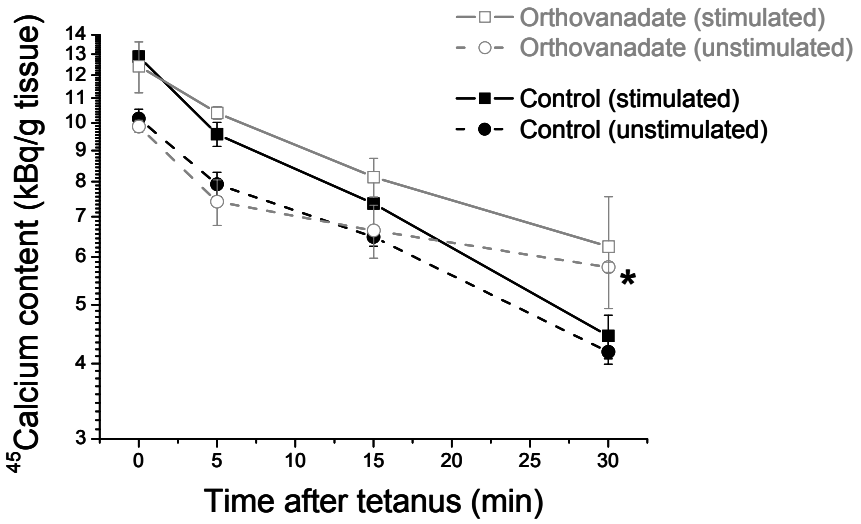

Figure 46. Ortovanadate effect on the accumulation into and extrusion of calcium from prisms. Excised prisms were incubated in elasmobranch saline medium with 3.4 mM $CaCl_2$ supplemented with ^{45}Calcium (2 μCi/ml) in the absence (control in black) or presence of 10 µM Na-orthovanadate (grey). Then, unstimulated (circles) or stimulated (squares) prisms were prepared for quantification 0, 5, 15 and 30 min after the tetanus, by washing in standard medium without ^{45}Calcium in absence (control) or presence of 10 µM Na-orthovanadate. Traces show mean ± SEM (n=4) ^{45}Calcium accumulated within prisms. Orthovanadate increased basal ^{45}Calcium levels above control after 30 min (Unpaired T-test: *p<0.001).

Ca^{2+}-affinity (Gonçalves et al., 2000a; Villalobos et al.,2002; Rizzuto and Pozzan, 2006) at the plasma membrane and the endoplasmic reticulum help to bring down $[Ca^{2+}]_{int}$ to the 10^{-7} M

range (Rizzuto and Pozzan, 2006).

These two, complementary, vesicular Ca^{2+}-transport systems seem to be intimately related with the vesicular exo-endocytic cycling rates (estimated by the number of pits at any given time) since there is an exocytotic burst of vesicle fusion activity occurring right after (but not during) a train of stimuli (Párducz and Dunant, 1993; Párducz et al., 1994) that conveys the recently accumulated Ca^{2+} by the vesicular Ca^{2+}/H^{+}-antiport (see figure 19) out of *Torpedo* terminals. The exocytotic burst is likely to continue at even higher rates for at least one minute more (maximum of ca. 33 pits/100 μm^2) and falling back to resting rates after 30 min. Within this time-frame it is more likely that the Ca^{2+} transported by the vesicular Ca^{2+}-ATPase will get to be preferably discharged out of the terminal since bafilomycin has little effect on later ^{45}calcium extrusion (figure 19), while orthovanadate significantly affected extrusion rates within that period (figure 46).

Orthovanadate is not a selective inhibitor of vesicular Ca^{2+}-ATPases alone and the extrusion of Ca^{2+} by Ca^{2+}-ATPases in other locations is probably affected by this drug as well. Yet, there seems to be a striking coincidence for the need of fusion events following periods of neuronal activity that support the need for Ca^{2+}-extrusion through vesicular fusion convergent with periods of vesicular Ca^{2+}-ATPase activity. Moreover, basal fusion rates occurring within *Torpedo* terminals are also rather high (ca. 22 pits/100 μm^2) and argue in favour of a participation in Ca^{2+} extrusion even in resting conditions (and to accomplish other functions like molecular trafficking at the membrane, etc…).

This is also consistent with the high calcium levels registered within synaptic vesicles in unstimulated (Goffinet, 1978; Mizuhira and Hasegawa, 1997; Pezzati and Grohovaz, 1999) as well as stimulated neurons (Párducz et al., 1987; Párducz and Dunant, 1993; Párducz et al., 1994) and adrenal medulla cells where calcium is first accumulated into vesicles and granules and released by exocytosis in later stimulations (Von Grafenstein and Powis, 1989; Mahapatra et al., 2004).

The immense membranous surface area provided by synaptic vesicles seems to contribute to dealing with some Ca^{2+} leaking into cells (Rizzuto and Pozzan, 2006) under resting conditions and with any uncoordinated Ca^{2+} entry occurring through clusters of VOCCs at active zones that may participate in resting calcium entry. These notions arise also from the data presented on this and the previous sections highlighting a joint action of vesicular

Ca^{2+}-ATPases, as well as the vesicular Ca^{2+}/H^{+}-antiport participating in the maintenance of resting calcium homeostasis that adds to the participation in calcium dynamics upon activity.

Indeed, when the antiport is not tampered with (no inhibitor), nerve terminals seem quite capable of keeping low basal $[Ca^{2+}]_{cytosol}$ levels (figures 35, 42 and 43) and to sustain transmitter release (figures 41 and 44), but fail to sustain ACh release in slightly depolarised nerve terminals and show a slight basal increase in $[Ca^{2+}]_{cytosol}$ (figures 42 and 43) if the antiport is inoperative. Since bafilomycin has been shown not to affect exocytosis or endocytosis (Cousin and Nichols, 1997; Sankaranarayanan and Ryan, 2001; Zhou et al., 2000), it seems that nerve terminals rely on the H^{+}-gradient to energise rapid vesicular Ca^{2+} transport followed by Ca^{2+}-rich vesicle fusion that "unload" calcium into the extracellular medium. When rapid vesicular calcium transport is compromised vesicles keep fusing with the membrane but can no longer occupy themselves of Ca^{2+}-extrusion and probably no longer carry their normal calcium load into the extracellular space. On the other side of the membrane there is also an additional Ca^{2+}-load within the terminal that seems not to be balanced by slower calcium extrusion (figure 19).

An additional suggestion that the lack of vesicular Ca^{2+} (or Sr^{2+}) transport can implicate a slow accumulation of the divalent within the terminal was obtained under long incubations of *Torpedo* excised prisms with high $SrCl_2$ concentrations in substitution for $CaCl_2$. Figure 47 show a concentration-dependent effect of strontium on paired pulse stimulated prisms over a 20h period. At 20 mM $SrCl_2$ prisms responded with unperturbed amplitude, even after 20h of incubation (figure 47 A). However, with 34 mM $SrCl_2$ there was a decrease in the amplitude that was especially evident after 17h30 (figure 47 B). The amplitude of the response was strikingly affected with 50 mM $SrCl_2$ with substantial amplitude decrease after 4h in $SrCl_2$ and full inhibition after 18h (figure 47 C).

This result might also explain why there was also a small (non significant) reduction both in the amount of $[^{14}C]$-ACh release and a small reduction in the evoked EPP with 50 mM $SrCl_2$ (figures 21 and 22) that could be attributed to an exhaustion of release capacity (or partial desensitization) since it was possible to maintain normal responses with high calcium concentrations but not with strontium.

There was also a prolongation of the EPP time-course especially evident in the second pulse and with longer incubation times (figure 47). As discussed previously (sections 3.2.1.2/3), EPP prolongation is the result of the absence of vesicular Sr^{2+}/H^{+}-antiport activity

leading to increased levels of residual Sr^{2+} within the active zones (Xu-friedman and Regehr, 2000) and prolongation of the second EPP even more than the first stimulus. Desensitization was both concentration and time-dependent arguing in favour of an imbalance between slow Sr^{2+} entry and Sr^{2+}-extrusion capacity resulting from the lack of a vesicular Sr^{2+}/H^{+}-antiport as well as a decreased efficiency of Ca^{2+}-ATPases for Sr^{2+} transport (Graf et al., 1982). There is some resemblance between the results obtained with strontium and those obtained with 100 μM DBHQ (figure 31 *C*) where both vesicular calcium transport systems were either inhibited or overwhelmed with the end result being the desensitization of release over time.

Lacking or reduced Sr^{2+} (also valid for calcium) exocytosis could also have contributed to the long-term desensitization effect. Indeed, drosophila temperature-sensitive dynamin

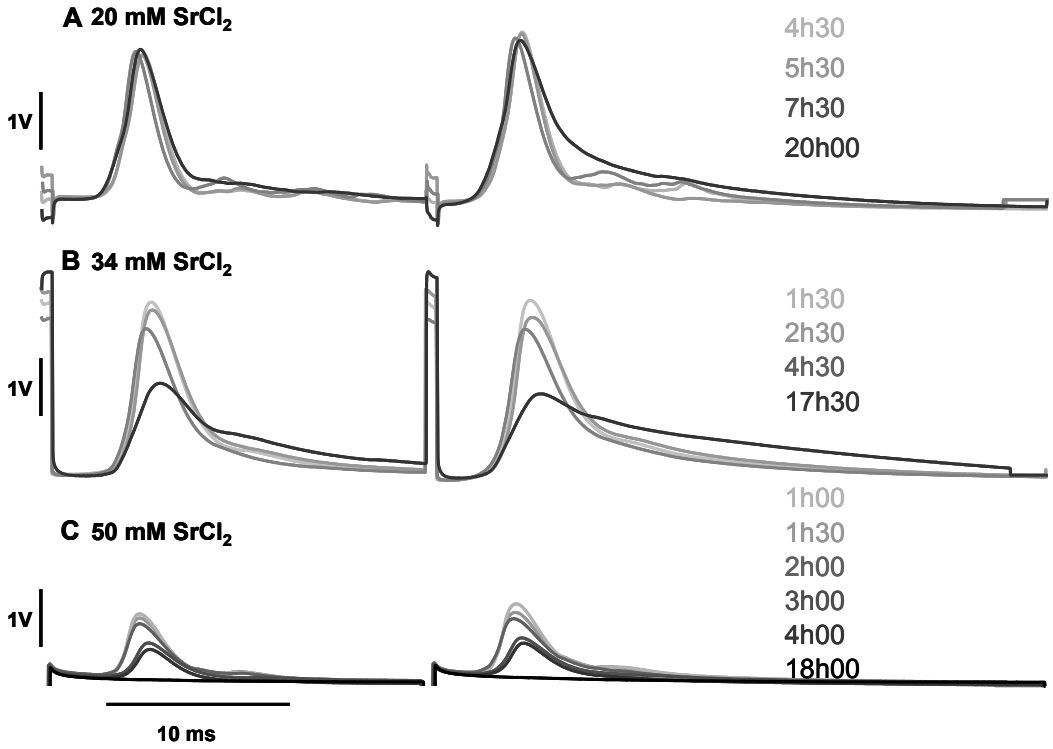

Figure 47. Concentration and time dependence of Sr^{2+}-induced desensitization of evoked electric response of *Torpedo* electric organ stacks of electrocytes (prisms). Traces show in succession the stimulation artefact, the synaptic delay and the electrical discharge produced by excised prisms submitted to paired-pulse field stimulation (20 ms interval between stimuli). Prisms were perfused with elasmobranch saline medium where $CaCl_2$ was replaced by 20; 34 or 50 mM $SrCl_2$ in **A**; **B** and **C**, respectively. Electrocyte responses were registered after indicated times in $SrCl_2$. Representative experiments of n= 4.

mutant (shibire) that fails to endocytose above 29°C show activity-dependent depletion of synaptic vesicles in nerve endings (Kosaka and Ikeda, 1983). Shibire mutants show decreased

Ca^{2+} entry even before vesicle depletion (Macleod et al., 2004) that gets accentuated (Macleod et al., 2004) or even suppressed (Umbach et al., 1998) after intense stimulation leading also to vesicle depletion occurring after complete inhibition of transmission at the fly NMJ (Delgado et al., 2000; Macleod et al., 2004). Decreased calcium entry in temperature sensitive mutants also seems to derive from VOCCs inhibition (Umbach et al., 1998; Macleod et al., 2004, 2006) but could also derive from Ca^{2+}-dependent VOCCs desensitization after $[Ca^{2+}]_{int}$ rise (Birman and Meunier, 1985; Forsythe et al., 1998; Lee et al., 1999; Catterall, 2000; Findlay, 2004; Guo and Duff, 2006; Kreiner and Lee, 2006). Similarly, transmitter release blockade could be a direct result of compromised exo-endocytosis or resulting from subthreshold $[Ca^{2+}]_{int}$ rise capable of inducing Ca^{2+}-dependent inhibition of transmitter release. If so, the original intent of Macleod et al. (2004) to test for a role of vesicular calcium transport in pre-synaptic calcium regulation might not have been completely frustrated. Their results (as well as Umbach et al., 1998) point-out for an essential participation of normal vesicle cycling in the maintenance of calcium homeostasis. To get to a conclusion about Ca^{2+}-induced desensitization of calcium entry and transmitter release it would have been quite clarifying to reverse the putative desensitization effect (i.e., with EGTA for 5 min.; see also figure 44) while maintaining vesicle depletion conditions (>29ºC) and assay for calcium entry and transmitter release, which was unfortunately, not done. If the drosophila NMJ synapses also rely on cytosolic ACh release through a mediatophore (like demonstrated with *Torpedo*), transmission would have been recuperated also.

Besides, to visualize the effects of Ca^{2+}/H^{+}-antiport on rapid (ms) calcium homeodynamics rapid detectors like K_{Ca} channels or fast post-synaptic detectors of ACh release like EPP's would be the choice of election. Alternatively, one could measure the effects of not having synaptic vesicles in the amplitude of bulk $[Ca^{2+}]_{cytosol}$ under conditions where rapid calcium transport into synaptic vesicles could contribute to the calcium load, instead of rather low $CaCl_2$ (0.5 mM) and 30 times more $MgCl_2$ (15 mM) used by Macleod et al. (2004) that, along side with diminished Ca^{2+}-entry, typify conditions where hardly any rapid vesicular Ca^{2+} transport will be elicited.

From the results presented above we have learned that reduced or compromised vesicular calcium transport has both short-term effects on calcium dynamics that affect transmitter release time-course and long-term effects dealing with calcium homeostasis that affect Ca^{2+}-dependent inactivation processes like transmitter release desensitization (or

fatigue) or calcium-dependent VOCCs inactivation (CDI) (Birman And Meunier, 1984; Israël at al., 1987; Forsythe et al., 1998; Lee et al., 1999; Findlay, 2004; Guo and Duff, 2006; Kreiner and Lee, 2006).

Both the short and long-term effects must be well present when trying to address the role of vesicular calcium in a given system. If for instance, we incubate bafilomycin in a system that is not fundamentally idle (like with *Torpedo* synaptosomes) one could get partial or total inhibition of transmission instead of increased secretion. Similarly, the use of strontium was quite revealing of the short-term effect but with a 10-fold decreased affinity and a slowly-developed desensitization effect at higher concentrations. Another important issue is the choice of an appropriate reporter of local Ca^{2+} microenvironment within active zones. We measured post-synaptic currents that result from very rapid highly synchronised Ca^{2+}-dependent ACh release, with submillisecond precision. We were also able to register the effects of increased Ca^{2+} entry in the bulk $[Ca^{2+}]_{cytosol}$ by using particularly fit synaptosome preparation (rat MFS: resting membrane potential of – 85 mV) and sufficiently strong Ca^{2+} entry to visualise the bafilomycin effects (high Ca^{2+}/Mg^{2+} ratio).

3.2.3. Ca^{2+}-induced ACh depletion from synaptic vesicles

Besides influencing the calcium concentration transients within synaptic terminals in the time scale of the millisecond up to minutes, vesicular calcium transport deeply affects the biochemical environment within that organelle.

In fact, it has long been established a direct relationship between calcium entry into stimulated *Torpedo* nerve terminals and vesicular ACh depletion that is accompanied by Ca^{2+} accumulation within synaptic vesicles (Marchbanks and Israël, 1972; Babel-Guérin, 1974; Dunant et al., 1980b; Schmidt et al., 1980; Diebler, 1982). Vesicular calcium slowly increases ACh leakage out of vesicles and feeds the cytoplasmic pool of ACh from where the ACh is released through plasma membrane mediatophores (Dunant et al., 1972; Dunant et al., 1980b).

Already in the early studies with *Torpedo* vesicles it was shown that they contained a core of tightly bound ACh and a small compartment of loosely bound ACh (Marchbanks and Israël, 1972).

More recently, it was demonstrated that no more than ~5% of ATP and ACh exists in "free" unbound form within the vesicles. The remaining ACh and ATP are found in association with a proteoglycan vesicular matrix that is composed mainly by the glycan chains of the SV2

protein (Stadler and Wittaker, 1978; Scranton et al., 1993; Reigada et al., 2003). Most interesting was last author's findings that both Na^+ and Ca^{2+} can completely devoid vesicles of ACh and ATP with Ca^{2+} (EC_{50}=~0.27 mM) being 10 x more potent than Na^{2+} (EC_{50}=~2.6 mM) in a cooperative way ($Hill_{Ca}$=2; $Hill_{Na}$=4). The effect was exerted by binding of the ions to sulphate residues and sialic acid-Ca^{2+}-galactose complexes to which ACh and ATP were bound, respectively.

Vesicular ACh/ATP depletion was reversible by lowering ionic strength (this was prevented by EGTA) and re-filled vesicles were again competent for ACh/ATP unbinding upon addition of Ca^{2+} or Na^+ (Reigada et al., 2003). They used lysed or Triton X-100 permeabilised vesicles where both ions and transmitters were in contact with the assay medium. Ca^{2+}-binding to the matrix resulted in a substantial hydration, causing a 2-fold increase in matrix dimensions (Reigada et al., 2003).

We wanted to determine whether synaptic vesicles are capable of releasing their ACh content in response to calcium challenges with different intensities. For that we isolated *Torpedo* electric organ synaptic vesicles and continuously followed the ACh released from the vesicular compartment (Figure 48). *Torpedo* synaptic vesicles are quite rich in ACh that remains stably within the organelles, even in the presence of calcium (first two columns). When vesicles were selectively permeabilised to calcium with 3 μM ionomycin free acid, there was no significant decrease in ACh content of vesicles provided that Ca^{2+} was not present. However, when as little as 6 μM up to 2.5 mM $CaCl_2$ was also added there was an ~70% decrease in the vesicular ACh content that increased to 100 % depletion when the calcium salt of ionomycin was used (last two columns to the right). The calcium salt form of ionomycin was also capable of eliciting calcium-induced ACh release from *Torpedo* vesicles much faster than the free acid form (inset in figure 48).

In figure 49 we used synaptic vesicles isolated from sheep brain cortex where ACh release from synaptic vesicles was elicited by adding 500 μM $CaCl_2$ even in the absence of permeabilisation. It seems therefore that Ca^{2+}/H^+-exchange is capable of releasing ~2/3 of ACh from this vesicle suspension under the present experimental conditions.

The results in figures 48 and 49 highlight the existence of an adapted response of synaptic vesicles to slow or rapid calcium entry that is capable of partial or total depletion of vesicular ACh that diffuses away from the vesicular compartment.

Torpedo vesicles are particularly rich in ACh (figure 48). However, when Ca^{2+} ions gained access to the intravesicular compartment by using ionomycin, there was a considerable decrease in the total vesicular ACh content that was more pronounced with the calcium salt than the free acid form of ionomycin (figure 48). The calcium salt form of ionomycin was also faster in depleting *Torpedo* vesicles from their ACh molecules (inset in figure 48). Similarly, sheep brain cortex synaptic vesicles released most of their ACh content when Ca^{2+} was allowed inside the vesicular compartment by the Ca^{2+}/H^{+}-antiport (figure 49).

The actual mechanism of ACh leakage is still a matter of debate. The vesicular ACh transporter (VAChT) working in reverse mode may convey "free" ACh out of SVs. However, this hypothesis has been discarded on the account that the over expression of VAChT actually increases the quantal size (Song et al., 1997). Another plausible candidate is the

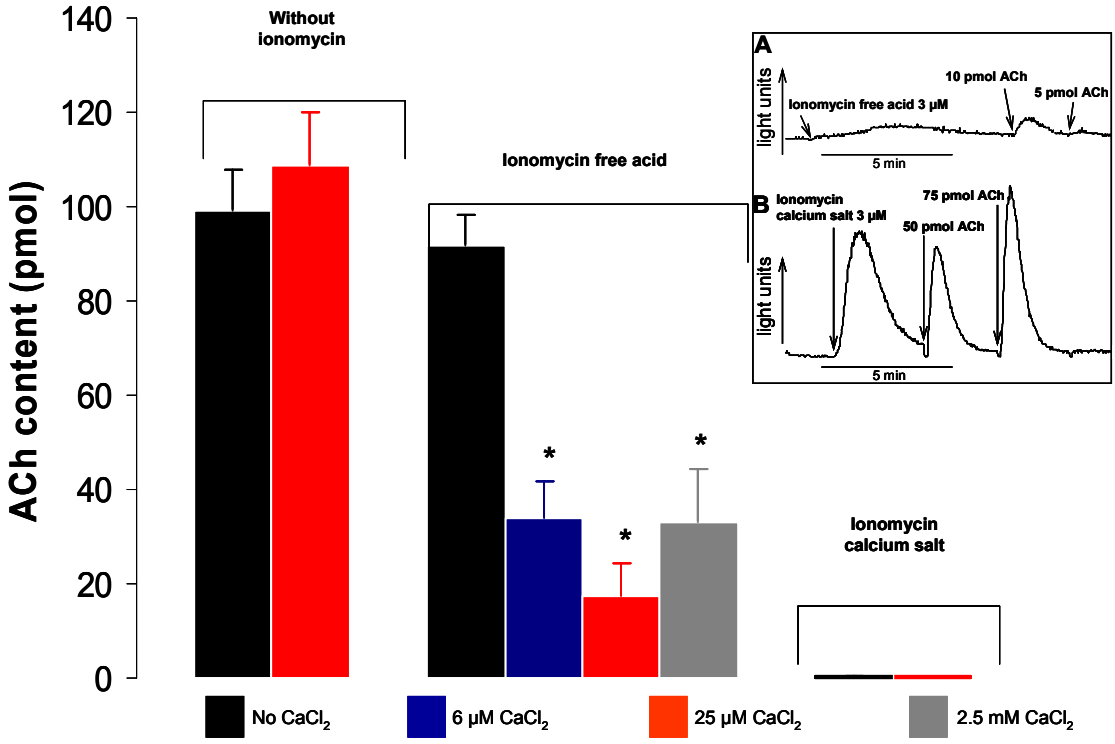

Figure 48. Modulation of vesicular acetylcholine content by calcium-acetylcholine exchange in synaptic vesicles isolated from *Torpedo* marmorata electric organ. Vesicles (25 µl of *Torpedo* s.v. fraction) were allowed to release ACh for 20 min in increasing calcium concentrations (0 to 2.5 mM) in presence or absence of ionomycin (free acid or Ca^{2+}-salt). After that, vesicular content was determined by chemiluminescence by addition of 5 µl Triton X-100 1% to the synaptic vesicle suspension followed by standard amounts of ACh. Bars show the average ± SEM (n=3-11) of remaining ACh within vesicles after 20 minutes. **Inset** graph shows ACh release from *Torpedo* synaptic vesicles upon addition of 3 µM ionomycin free acid (panel **A)** or 3 µM ionomycin calcium salt (panel **B**) to medium containing 25 µM $CaCl_2$. Whenever calcium was allowed inside vesicles there was a significant reduction in vesicular ACh content (Unpaired T-test: *p<0.001).

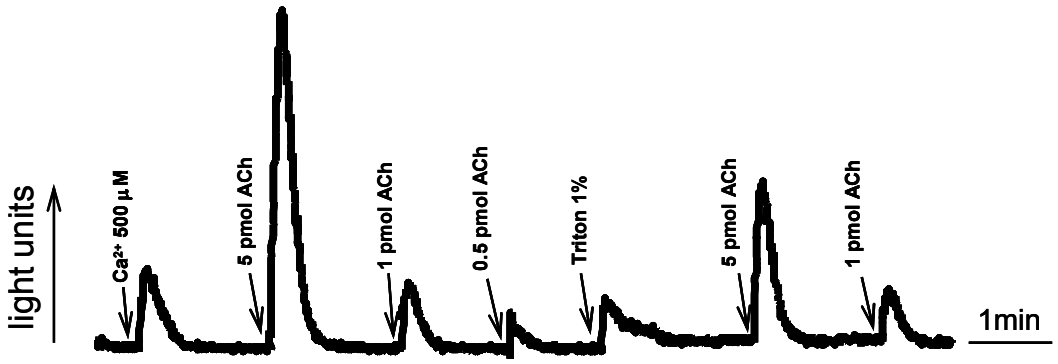

Figure 49. Ca^{2+} transport through vesicular Ca^{2+}/H^{+}-antiport induces ACh release from sheep brain cortex synaptic vesicles. Vesicle suspension (0.6 mg protein/ml) was added to medium containing 1 mM ATP and enzymes for chemiluminescent ACh detection. Trace shows ACh release from vesicles after 500 µM Ca^{2+} addition, followed by addition of known amounts of ACh. After that, the remaining ACh within vesicles was determined by addition of 5 µl triton x-100 1% followed by standard amounts of ACh.

plasma membrane choline transporter that is permeable to ACh at high concentrations (Marchbanks and Wonnacott, 1979) and is positioned to transport ACh out of synaptic vesicles where it is largely concentrated (70-90%) in cholinergic nerve terminals (Ferguson et al., 2003; Nakata et al., 2004). Although the choline transporter is a Na^{+}-coupled transport system, it is homologous to the Na^{+}-glucose transporter (SGLT1) which is capable of driving transport by using the pH gradient (Hirayama et al, 1994).

Irrespective of which is the ACh-leakage mechanism out of synaptic vesicles we found functional evidences that support for a modulatory role for Ca^{2+}/H^{+}-antiport and Ca^{2+}-ATPase vesicular calcium transport in the displacement of ACh out of synaptic vesicles (figure 50). *Torpedo* prisms were incubated in the absence (control) or in the presence of 2 µM bafilomycin plus 10 µM orthovanadate and submitted to 12 s tetanus at 100 Hz. Prisms were allowed to recuperate and the amount of "bound" or vesicular ACh and total ACh content in tissue was determined. Under such conditions, there was a strong reduction of the vesicular ACh content, but in the tissue stimulated in the presence of vesicular Ca^{2+}-transport inhibitors, vesicular ACh was greatly preserved in the stimulated terminals, as compared to untreated controls.

This result evidences the fact that *Torpedo* synaptic vesicle ACh content is modulated by the action of vesicular calcium transport systems. It was obtained after a rather intense stimulation but finds an echo in previous reports where calcium turnover between the extracellular medium and tissue calcium happened already in non-stimulated

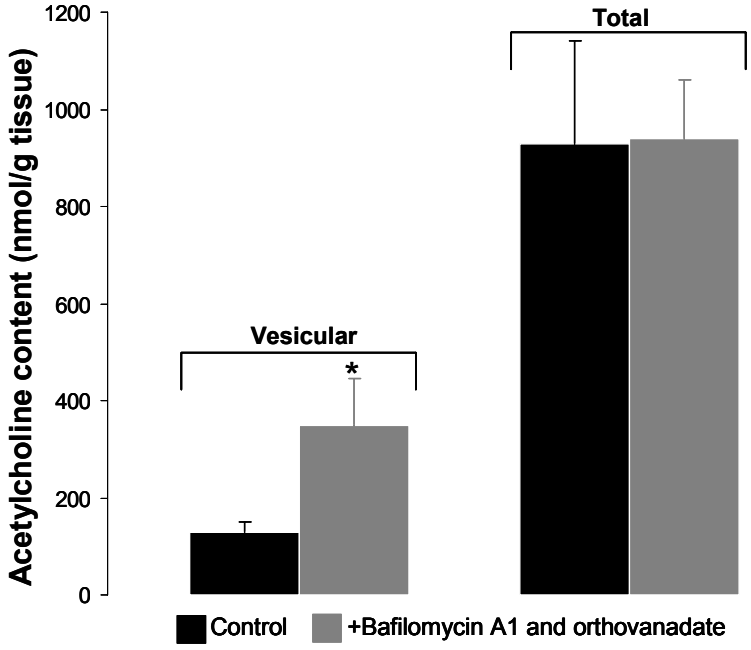

Figure 50. Effect of bafilomycin A1 and orthovanadate on the acetylcholine content of prisms after stimulation. Prisms were incubated for 2h in elasmobranch saline medium with 2 μM bafilomycin A1 and 10 μM Na-orthovanadate; they were stimulated at 100 Hz for 12 seconds and allowed to rest for 2h30 before extraction of ACh from prisms. Total ACh was obtained by homogenizing the tissue in presence of T.C.A. while in the vesicular pool homogenization took place in the iso-osmotic medium, with T.C.A. being added 1 min later. Bars show average of 4 experiments ± SEM. Vesicular ACh content was significantly higher in tissue bathed and stimulated in presence of both bafilomycin A1 and Na-orthovanadate than in untreated controls (Unpaired T-test: $p < 0.05$).

tissue (but not in 0 $[Ca^{2+}]_{out}$) and fastened with stimulation when vesicular ACh was also decreased (Babel-Guérin, 1974; Dunant et al., 1980b).

Synaptic vesicles at *Torpedo* terminals seem to have many faces. They begin as recently arrived organelles, emptied of ATP, ACh and calcium. This population was named VP0 and is capable of accumulating ACh and ATP but not Ca^{2+}. In resting terminals, they mature into a new population (named VP1) of fully charged (with ACh and ATP) vesicles displaying little ACh uptake activity but a high capacity of Ca^{2+} accumulation. Finally there is a third population of vesicles (VP2) that are seen preferably after prolonged stimulation, these are denser and no longer accumulate Ca^{2+} but accumulate ACh and ATP again (Kiene and Stadler, 1987; Stadler and Kiene, 1987; Bonzelius and Zimmermann, 1990). There is good evidence that the latter population is composed of vesicles which were emptied either by stimulation or by other causes and which are in the process of refilling by newly synthesised ACh from the

cytosol. Vesicular filling with either transmitter or metal ions, therefore, seems to determine the vesicular pools present within the terminal but also to reflect recent terminal history.

The very possibility of modulation of vesicular ACh content is hardly accomodable under the scope of the so-called "vesicular theory" where the average number of ACh molecules "packed" inside a synaptic vesicle is believed to correspond to the well defined number of ACh molecules that are released at the same time –the quantum of transmitter molecules. Therefore the vesicular theory implies that the vesicular transmitter content should not change significantly.

Conversely, if we assume that a quantum of ACh molecules is generated by transient opening of an ACh-conducting pore at the plasma membrane the hypothesis of a decrease in vesicular ACh upon stimulation gains considerable momentum. In order to keep steady the 7000-10000 molecules that compose a quantum in *Torpedo* nerve terminals (Dunant and Muller, 1986; Girod et al., 1993) ACh leakage from within the synaptic vesicle space could function as an "on demand" (by exchanging vesicular ACh for the Ca^{2+} entering vesicles) re-filing device of the cytoplasmic pool. This would prevent localised transmitter rundown of cytoplasmic ACh, near release sites, under intense stimuli at the same time that they capture large amounts of Ca^{2+} before returning them to the extracellular space by exocytosis. In a single run of exocytosis a vesicle would have prevented both ACh depletion and $[Ca^{2+}]$ build-up in the microdomain and contribute to maintaining the appropriate Ca^{2+} and ACh gradients across the plasma membrane to guarantee steady (quantal-like) fluxes upon stimulation.

Although the intimate relationship between synaptic vesicles and ACh secretion has been addressed in the past, in most cases the above-mentioned vesicular functions were mostly overlooked. In particular, the possibility that synaptic vesicles play a vital role in calcium homeostasis within a nerve terminal comes as striking when addressing systems that coordinate the release of ca. 10-20 ACh packets (subMEPPs) within less than 300 nm to compose a single quantum in response to a sudden $[Ca^{2+}]$ rise in 1/10 of a millisecond (Girod et al., 1993). Tampering with vesicular Ca^{2+} transport may compromise the amazing synchrony of mediatophores involved in the composition of a quantum or even compromise ACh release altogether by Ca^{2+}-induced desensitization.

In the context of this work it is interesting to notice that different types of metabolic inhibitors ranging from proton uncouplers like CCCP, creatine kinase inhibitors (FDNB), thiol oxidizing agents (diamide) and botulinum toxin (that decreases ATP content by

50%; creatine phosphate <20%, and prevents rapid ATP supply by blocking creatine kinase activity, in *Torpedo* tissue) implicate a decrease in ATP availability that evolves into blockade of evoked transmission, at the same time that an increase in the frequency of subMEPPs (that are now desynchronized) occurs, as well as an increase in the occurrence of the otherwise rare giant MEPP (Molgó and Pécot-Dechavassine, 1988; Dunant et al., 1988; Van Der Kloot et al., 2000). This could be an early result of ATP depletion within the terminal, with Ca^{2+} transport being compromised everywhere (vesicles included), and consequently desensitization of mediatophores and inactivation of VOCCs by subthreshold elevation of Ca^{2+}. All these processes will compromise evoked synchronized responses. At the same time individual mediatophores increase their open probability due to increased calcium leading into de-synchronisation. The same will probably happen to vesicular fusion but this time before having incorporated enough Ca^{2+} to deplete them of ACh. In that case, there will be a slow release of ACh from the vesicular matrix by exchange with extracellular Ca^{2+} and Na^{+} that could be on the basis of giant MEPPs, lasting tens of milliseconds.

3.2.4. Requirement of Synaptotagmin I for vesicular Ca^{2+}/H^{+} antiport activity

3.2.4.1. Test for a vesicular Ca^{2+}-transporting role for Synaptotagmin I

Action potentials elicit calcium entry through VOCCs, a process which lasts somewhere between 0.1 to 1 ms. The corresponding current has been estimated to be ~50 fA per channel with ~150 Ca^{2+} ions entering into an active zone during ~500 μs channel opening (Fenwick et al., 1982; Oheim et al., 2006). Active zones are believed to harbour clusters of Ca^{2+}-channels spaced at ~40 nm distance (Haydon et al., 1994) that contribute to improve the reliability of synchronous transmission (Shahrezaei et al., 2006; Stanley, 1997). Temporal fidelity is accomplished by close proximity of calcium sensors for transmitter release that are endowed with particularly low Ca^{2+}-affinity in a universe of 1000-1500 VOCCs μm^{-2} (Heuser et al., 1974; Pumplin et al., 1981; Roberts et al., 1990; Naoum and Hudspeth, 1994). Candidates for low affinity Ca^{2+} sensing are mediatophores at *Torpedo* synapses (at least 200 μm^{-2}; Israël et al., 1981; Muller et al., 1987; Brochier et al., 1992; Dunant and Israël, 2000; Morel et al., 2003; Dunant and Bloc, 2003; Dunant, 2006), and synaptotagmin I in synaptic vesicles (Chapman 2002;).

The proximity of calcium sensors to VOCCs guarantees their activation only few μs after calcium entry (Pumplin and Reese, 1978; Llinás et al., 1981b; Roberts, 1994) On the other hand, calcium rises steeply within 50 nm away from the membrane, forming a microdomain of elevated $[Ca^{2+}]_{int}$ within the same time course of transmitter activation and remains very high until it subsides immediately after channel closure (Roberts, 1994) that results in switching off transmitter release.

As we have seen above, the vesicular Ca^{2+}/H^{+}-antiport is able to shorten by at least ~2-fold the duration of transmitter release by rapidly sequestrating the divalent into nearby synaptic vesicles. Since the operational range of the antiport assessed in vitro ranged from ~100 μM up to near mM Ca^{2+} (being maximum around 500 μM Ca^{2+}; Gonçalves et al., 2000a), it is likely that the protein responsible for activating the Ca^{2+}/H^{+} exchange in the synaptic membrane has a rather low affinity for Ca^{2+} and operates only at high metal concentrations (i.e., after local $[Ca^{2+}]_{int}$ within the microdomain builds-up above 100 μM). It should also be rather abundant within synaptic vesicle membranes to cope with the demands for swift Ca^{2+} clearance from the microdomain.

Synaptotagmin I (Syt I) is one of the most abundant vesicular proteins (ca. 15 copies per SV; Takamori et al., 2006), with a short, intravesicular and glycosilated N-terminal, one transmembrane domain followed by a spacer domain, a membrane proximal C2A domain and finally by a distal C2B domain near the C-terminal (Reviewed by Marquèze et al., 2000). The intralumenal N-glycosilated domain is essential to address Syt I specifically to the vesicular membrane (Han et al., 2004). Syt I forms macrostructures through homo or hetero oligomerization with Syt I or with other synaptotagmins, respectively (Fukuda et al., 1999). Syt I (and II) forms stable SDS-resistant Ca^{2+}-independent oligomers via fatty acylated cysteine clusters between the transmembrane and the spacer (cytoplasmic) domain assembled near the amino terminal (Fukuda and Mikoshiba 2000; Fukuda et al., 2001).

The calcium-independent pre-assembly (probably at the endoplasmic reticulum) of Syt I into oligomers is a necessary step allowing the subsequent, much faster, Ca^{2+}-dependent oligomerization step (Fukuda and Mikoshiba 2000). This is thought to occur during transmission through C2B domain interactions (Chapman et al., 1995, 1998; Sugita et al., 1996), early after Ca^{2+}-entry and prior to Syt I interaction with syntaxin and other members of the SNARE complex (Davis et al., 1999). The process involves low affinity reactions with

$[Ca^{2+}]_{1/2}$ from ~140 up to 400 μM for the hetero-oligomerization of Syt I and II (Davis et al., 1999; Fukuda and Mikoshiba, 2000).

Both C2A and C2B can penetrate either the vesicular or the plasma membranes. In vitro kinetics of C2A Cis-membrane (vesicular) binding occurred within 500 μs while trans-membrane (plasma) interaction occurred far more slowly (>50 ms) (Bai et al., 2000), but could be much faster in vivo (Chapman, 2002). On the other hand the C2B domain is capable of driving Ca^{2+}-dependent oligomerization in the sub-millisecond range and before interacting with SNARE proteins (Davis et al., 1999). Moreover, it is sufficient for the Ca^{2+}-dependent binding of Syt to two membranes (Araç et al., 2006).

Ca^{2+} binding to isolated membrane bound C2B-C2A Syt I cytoplasmic domains form barrel-like structures constituted by seven bar-like C2B-C2A monomers that are linked into an 11 nm wide ring-like heptamer (Wu et al, 2003). The formation of C2B-driven oligomers is regulated by RNA and requires the interaction with anionic lipids (Earles et al., 2001; Bai et al., 2002; Fernandez et al., 2001; Wu et al, 2003). The fast, Ca^{2+}-dependent, assembly of Syt into ordered multimers constituting 11 x 11 nm heptameric barrels was proposed as a putative regulator of membrane embedded proteins, like fusion pores (Wang et al., 2001; Wu et al., 2003). In the frame of this work, we propose that it may participate in the regulation or constitute the functional protein that codes for the low affinity Ca^{2+}/H^{+}-antiport that drives vesicular calcium transport.

The functional role of synaptotagmin I has been chiefly investigated by using genetically modified animals and cell lines, as well as antibodies or other approaches. Different and sometime contradictory results were obtained. In synapses of synaptotagmin I-deficient mice or drosophilae, the rapid, phasic secretion of transmitter is impaired while asynchronous or late release may be either increased or not modified (DiAntonio et al., 1993; Littleton et al., 1993; Geppert et al., 1994; DiAntonio and Schwartz, 1994; Broadie et al., 1994; Mackler et al., 2002; Pang et al., 2006). This lead to the hypothesis that synaptotagmin I could be a specific calcium sensor involved in a rapid type of release, while asynchronous release would require another sensor, maybe another isoform of synaptotagmin (Sullivan, 2007; Xu et al., 2007). In other studies, it is mainly the parameters of the calcium dependency of release (apparent Km, co-operativity) which are altered in Syt I-modified systems (Marek and Davis, 2002). Conversely, in other systems, release, either phasic or

asynchronous, is surprisingly enhanced in synaptotagmin-deficient synapses or cells (Shoji-Kasai et al., 1992; Koh and Bellen, 2003; Tokuoka and Goda, 2003).

In this work we tested for a role of synaptotagmin I in vesicular calcium transport through a low affinity Ca^{2+}/H^{+}-antiport. The hypothesis arises from the above mentioned characteristics and may help to elucidate some discrepancies found in Syt literature. It is also readily testable by using PC 12 cells, which are particularly rich in electron lucent synaptic-like vesicles and large dense-core vesicles that generate robust A.O. fluorescence signals reflecting bafilomycin-dependent transvesicular H^{+}-gradients (Bloc et al., 1999; figure 14). The fluorophore acridine orange was used to monitor the gradient in post nuclear supernatant (PNS) fractions of PC-12 cell clones in order to compare Ca^{2+}-induced

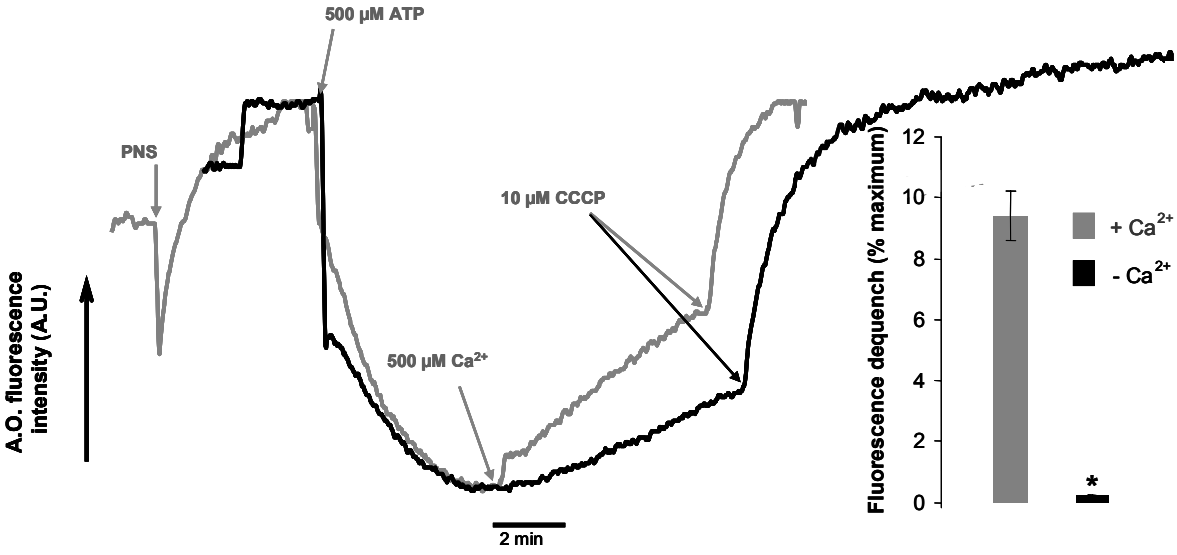

Figure 51. Ca^{2+}-induced dissipation of the proton gradient across acidic compartments of the synaptotagmin I containing G11 PC12 cell clone. Traces show fluorescence of acridine orange dye (3 µM). The probe is sensitive to the proton gradient across acidic compartments of the post nuclear supernatant (PNS) suspension (300 µg of protein/ml). After a period of stabilization, 0.5 mM ATP was added to allow the formation of H^{+} gradient within acidic organelles. Quenching of the probe's fluorescence occurs when the dye is exposed to acidic medium within acidic compartments, where it dimerises and accumulates. After complete gradient formation H^{+} gradient dissipation was assayed in the absence (black trace) or presence of 500 µM free [Ca^{2+}] (grey trace). Full dissipation of the proton gradient was induced by addition of the protonophore CCCP (10 µM). Traces are representative experiments of n= 4. **Inset**: Bars show proton gradient dissipation 30 s after calcium addition as compared to control (no addition). Values are average fluorescence increase ± SEM (n=4) in percentage of total gradient dissipation (with CCCP). Calcium induced a significant proton gradient dissipation from the acidic organelles of G11 PC-12 cells (Unpaired T-test: *p<0.01).

proton fluxes out of acidic compartments of synaptotagmin I-positive (G11) and synaptotagmin I-negative (F7) PC12 subclones, that had been selected by Shoji-Kasai et al. (1992). Figure 51 shows A.O. fluorescence assays with PNS from G11 subclones. Samples were introduced into a reaction saline medium which was fixed at pH 8.5. This ensures optimal assessment of the pH gradient established across acidic organelles. After equilibration, 0.5 mM Mg-ATP was added and the intensity of A.O. fluorescence rapidly decreased, revealing formation of the gradient. When the gradient was fully established, a reduction in A.O. fluorescence quench was elicited by adding 500 μM free [Ca^{2+}] to the reaction medium

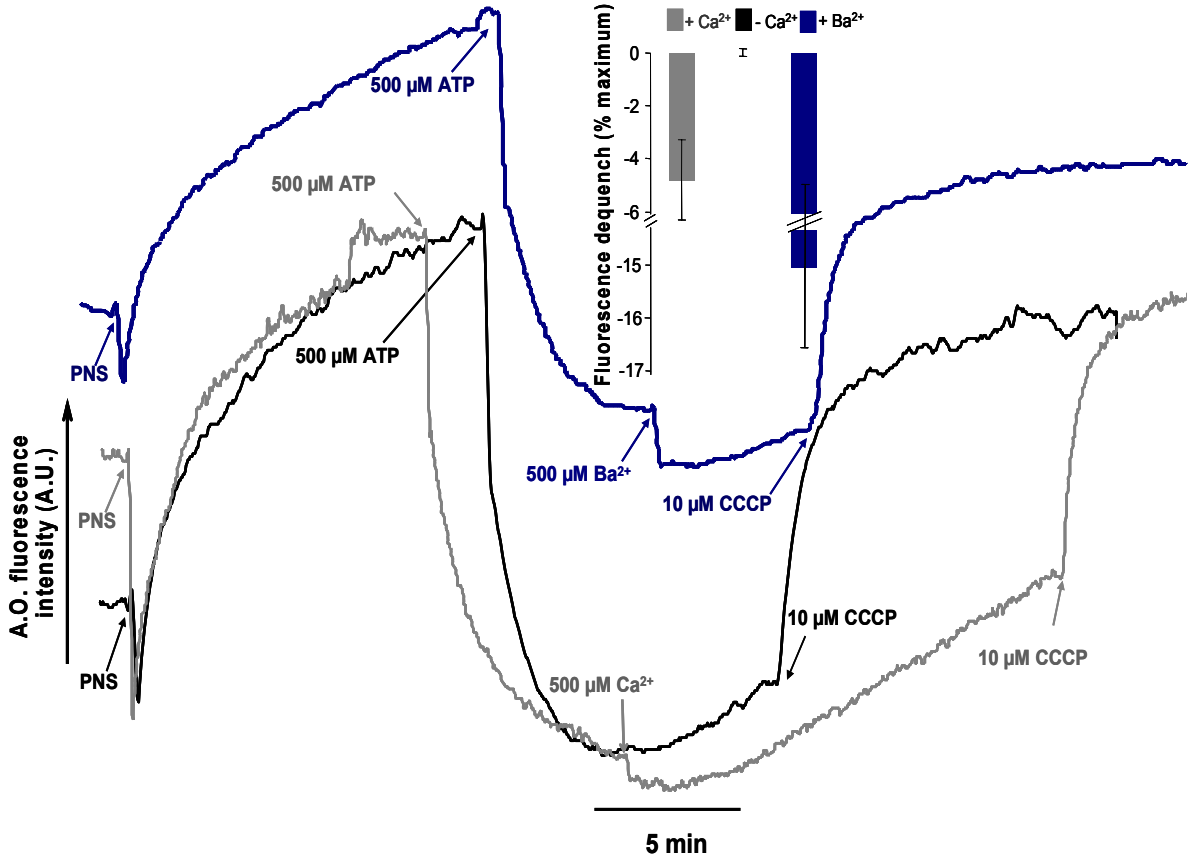

Figure 52. Ca^{2+}-effect on the proton gradient across acidic compartments of synaptotagmin I deficient F7 PC12 cell clone. Traces show fluorescence of acridine orange dye (3 µM) under the same experimental conditions as in figure 51. After complete H^+ gradient formation, dissipation was assayed in the absence (black trace) or presence of 500 μM free [Ca^{2+}] (grey trace). Blue trace shows a similar experience where 500 μM $BaCl_2$ was added instead of $CaCl_2$. Traces are representative experiments of n= 4. **Inset**: Bars show proton gradient dissipation 30 s after calcium addition as compared to control (no addition). Values are average fluorescence increase (or decrease in this case) ± SEM (n=4) in percentage of total gradient dissipation. Calcium and barium were unable to induce proton gradient dissipation from the acidic organelles of F7 PC-12 cells.

(grey trace and bar) which is suggestive of H^+-gradient dissipation presumably by a Ca^{2+}/H^+ antiport activity. Fluorecence dequench was compared to PNS samples not exposed to Ca^{2+} (black trace and bar).

In opposition to G11 subclones, synaptotagmin I-deficient cells (F7 -/-) assayed under similar conditions, failed to display a Ca^{2+}-dependent A.O. fluorescence dequench (figure 52). In fact, there was a slight increase in A.O. fluorescence quench when 500 μM $CaCl_2$ was added (grey trace and bar) that was similar to that displayed upon $BaCl_2$ addition instead of $CaCl_2$ (blue trace and bar) arguing in favour of an increase in the proton gradient rather than a dissipation induced by $CaCl_2$. $BaCl_2$ was used as a negative control since it was shown previously not to be able to dissipate the vesicular H^+ gradient (Gonçalves et al., 1999a). Addition of $BaCl_2$ under these conditions also provoked a slight A.O. quench (blue trace in figure 52) that could correspond to an increase in the pH gradient across acidic organelles, and could reflect a close dependence of ΔpH on Cl^- ions reported previously (Gonçalves et al., 1999b).

To confirm the results obtained with the subclones we proceeded with the transfection of the synaptotagmin negative subclone (F7 -/-) with the full synaptotagmin-I gene (Syt I) (figure 54). Moreover, we transfected the F7 -/- subclone with a transgenically encoded tagged synaptotagmin I (Syt_tagg) consisting of a 17-amino-acid tetracysteine motif engineered into the C-terminus of synaptotagmin-I that enables labelling with the membrane permeable fluorescein derivative, FlAsH (Syt_tagg) (Griffin et al., 1998; Gaietta et al., 2002; Marek and Davis, 2002). In this way we could test the effect of acute inactivation of synaptotagmin I transiently expressed in F7 (-/-) cells by FlAsH-FALI (Marek and Davis, 2002; figure 53).

Figure 53 shows that expression of FlAsH-bound synaptotagmin I (Syt_tagg) successfully recuperated Ca^{2+}-induced A.O. fluorescence dequench in F7 (-/-) cells (Panel A). Using F7 cells that are devoid of any endogenous synaptotagmin guarantees that all transfected synaptotagmin I molecules have a tetracysteine motif that binds FlAsH molecules with a dissociation constant of 10^{-11} (Gaietta et al., 2002). FlAsH labels nearly 100% of transfected Syt_tagg molecules allowing for complete synaptotagmin I photoinactivation within less than 2 minutes (Marek and Davis, 2002; Poskanzer et al., 2003; 2006). Complete synaptotagmin I photoinactivation was achieved by illuminating Syt_tagg PNS suspension during 1 minute with a 200W HBO U.V. lamp. Photoinactivated vesicles readily formed

transvesicular pH gradient upon Mg-ATP addition but Ca^{2+}-addition was no longer capable of inducing any A.O. fluorescence dequench (panel B in figure 53). This demonstrates that photoinactivation is specific for synaptotagmin I and does not affect nearby proteins (like the vesicular H^+-ATPase). In fact it has been suggested that it is mainly (if not only) the C2B domain of synaptotagmin I, that is adjacent to the FlAsH-binding epitope that is under the effects of photoinactivation (Marek and Davis 2002). The specificity of photoinactivation was also patented by the lack of inactivation after 1 minute irradiation of FlAsH-labelled G11 or Syt I cells that do not have the tetracysteine FlAsh-binding domain (not shown).

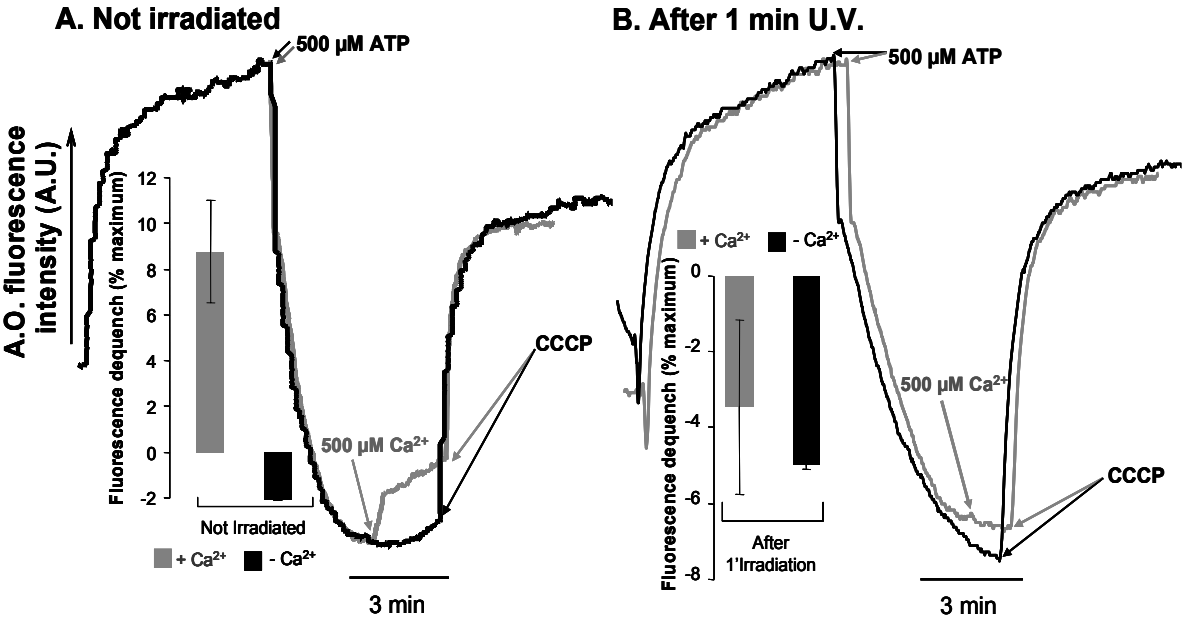

Figure 53. Ca^{2+}/H^+-antiport-dependent proton gradient dissipation associated with the presence of active synaptotagmin I in PC-12 cells acidic compartments. The F7 -/- clone was transfected with synaptotagmin I construct gene and labelled with FlAsH (Syt_tagg). The proton gradient within acidic compartments was monitored with acridine orange like in figure 51. Panel ***A***: Transfection of Syt_tagg into PC-12 cell clones results in gain of Ca^{2+}-induced proton gradient dissipation. After complete H^+ gradient formation, dissipation was assayed in the absence (black trace) or in presence of 500 µM free [Ca^{2+}] (grey trace). Full dissipation of the proton gradient was induced by addition (arrow) of the protonophore CCCP (10µM). Traces are representative experiments of n= 4. Panel **B**: Shows the same PNS preparation after being irradiated with a 200W HBO U.V. lamp for 1 min. Notice the lack of proton gradient dissipation upon calcium addition to irradiated Syt_tagg PNS. Traces are representative experiments (n=4-14). **Insets**: Bars show proton gradient dissipation 30 s after calcium addition as compared to control (no addition). Values are average fluorescence increase (or decrease) ± SEM (n=4-14) in percentage of total gradient dissipation. Calcium induced significant proton gradient dissipation from the acidic organelles of F7 PC-12 cells transfected with the Syt_tagg construct (Unpaired T-test: *p<0.01). However, 1 min irradiation with U.V. light was sufficient to eliminate the calcium dependent dissipation from the same preparation.

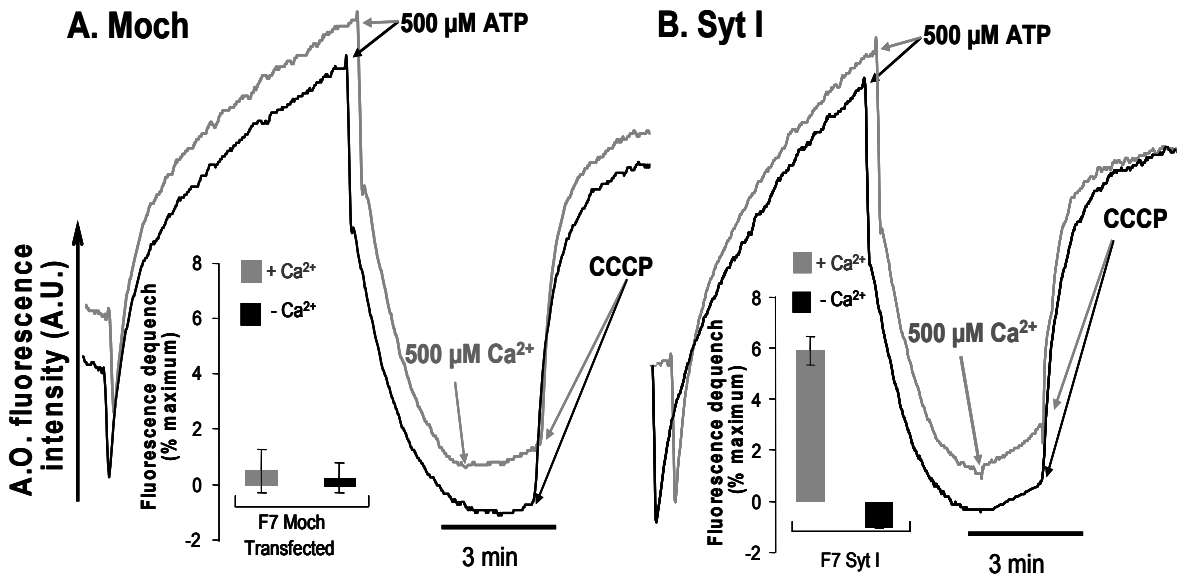

Figure 54. Synaptotagmin I is necessary for Ca^{2+}/H^{+}-antiport activity observed in PC-12 cell clones. Synaptotagmin I deficient F7 PC12 cell clones were transfected with either a non-encoding gene (moch transfected in panel **A**) or with synaptotagmin I gene (Syt I in panel **B**). Proton gradient across acidic compartments was monitored with the acridine orange dye as shown in figures 51-55. **Insets**: Bars show the proton gradient dissipation 30 s after calcium addition (grey traces) as compared to control (no addition; black traces). Values are the mean fluorescence increase ± SEM (n=4) in percentage of total gradient for each cellular preparation. Calcium induced significant proton gradient dissipation from the acidic organelles of F7 PC-12 cells transfected with the gene encoding synaptotagmin I (Unpaired T-test: *p<0.01).

Moreover, gain of function of F7 (-/-) clones did not occur with "moch" transfected (transfection of the insert without the synaptotagmin gene) cell PNS preparations (panel A in figure 54) but was evident in PNS prepared from F7 cells transfected with Syt I full gene (without the tetracysteine tag) (panel B in figure 54).

Briefly, a significant Ca^{2+}-induced A.O. fluorescence dequench was found only in the clones where an active synaptotagmin-I was expected to be present (figures 51-54). We can presume that the fluorescence dequench could have arisen from Ca^{2+}-induced H^{+}-gradient dissipation (presumably upon activation of Ca^{2+}/H^{+}-antiport activity). However, alternative explanations like the displacement of H^{+} upon Ca^{2+} binding to synaptotagmin I were not discarded.

A second way to asses Ca^{2+}-H^{+} antiport activity was to measure Ca^{2+} accumulation into organelles in the presence or absence of 0.6 µM bafilomycin A1 (figure 55). By selectively blocking the V-type H^{+}-ATPase, bafilomycin A1 prevents formation of the vesicular H^{+}

gradient. Thus, only the bafilomycin-sensitive fraction of Ca^{2+} accumulation is attributable to Ca^{2+}/H^{+} exchange. Samples of PNS were allowed to equilibrate for 6 min in pH 8.5 saline medium containing 10 μM orthovanadate (to inhibit Ca^{2+} accumulation through Ca^{2+}-ATPases). Then 0.5 mM Mg-ATP was added and a pH gradient was allowed to form during 2 min before application of $^{45}Ca^{2+}$ plus non radioactive $^{40}Ca^{2+}$ (final free concentration 550 μM; 0.5 mCi/mmol). Rapid filtration took place 2 min later.

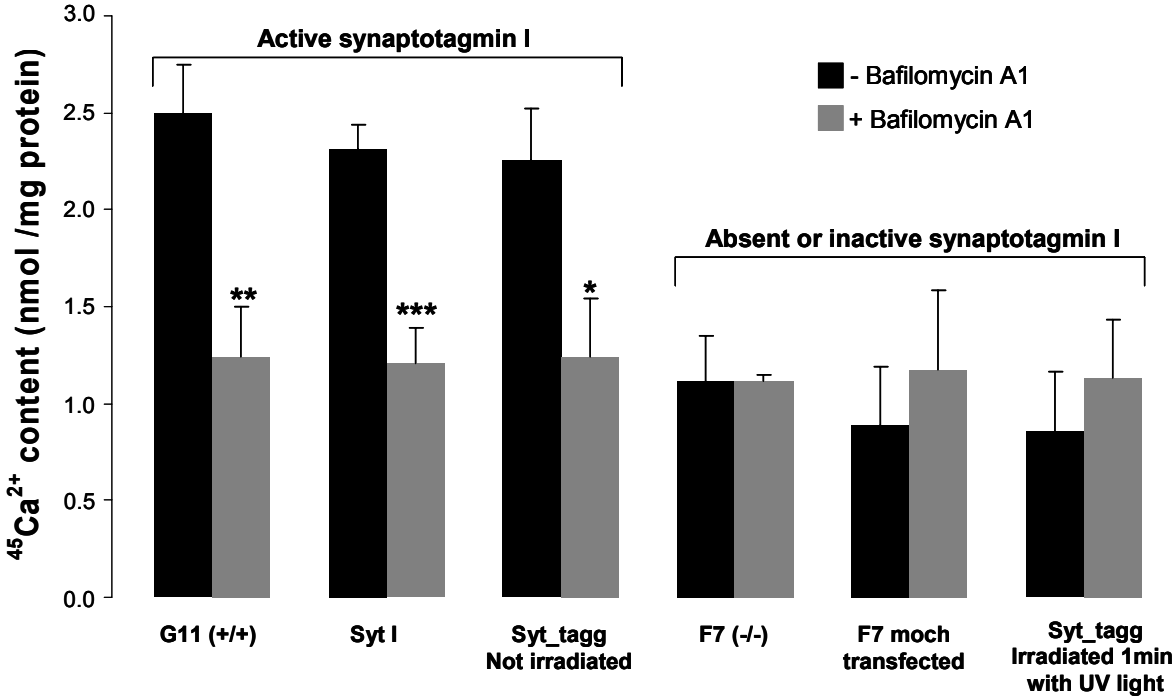

Figure 55. Synaptotagmin-dependent Ca^{2+} accumulation in bafilomycin sensitive organelles of PC-12 cells. PNS fractions were prepared from cells of either: synaptotagmin I containing G11 PC-12 cell clone; synaptotagmin I deficient F7 PC12 cell clone; in F7 cells transfected with either a non-encoding gene (moch transfected); the synaptotagmin I gene (Syt I) or with the Syt_tagg gene construct labelled with FlAsH (Syt_tagg). Where indicated, the Syt_tagg PNS preparation was irradiated with U.V. light during 1 min before the assay. $^{45}Ca^{2+}$-accumulation assays were carried out in presence (grey bars) or in the absence (black bars) of 0.6 μM bafilomycin A1. All PNS (0.3 mg protein/ml) were allowed to equilibrate for 6 minutes in reaction medium containing 10 μM Na-orthovanadate. Then, 1 mM ATP was added and a pH gradient was allowed to form for 2 minutes before $^{45}Ca^{2+}$ (550 μM free; 0.5 mCi/mmol calcium) addition. Rapid filtration took place 2 minutes after. Bars show the average ± SEM (n=3 to 11) $^{45}Ca^{2+}$ retained after rapid filtration. PNS from PC-12 cells carrying an active synaptotagmin I showed significant proton gradient-dependent $^{45}Ca^{2+}$ accumulation into their acidic organelles (Unpaired T-test: *<0.05; **p<0.01; ***p<0.001).

In PNS prepared from the clones containing an active synaptotagmin I (G 11 (+/+), Syt I, and non irradiated Syt_tagg), a substantial amount of Ca^{2+} was found to accumulate into

organelles (black bars in figure 55) over the value found in the correspondent bafilomycin A1 treated preparations (grey bars in figure 55). Such a H^+ gradient-dependent Ca^{2+} accumulation did not take place in PNS from clones where synaptotagmin I was either absent or inactivated by FALI (F7 (-/-), "moch", and UV irradiated Syt_tagg; black bars in figure 55).

A third approach consisted of adding PNS samples of PC12 cells (prepared as usual in a pH 7.4 medium) to the ATP-free pH 8.5 reaction saline already containing $^{45}Ca^{2+}$and $^{40}Ca^{2+}$ (concentration as before), as well as 10 μM orthovanadate. Under these conditions, taking advantage of the pH difference, Calcium can accumulate into organelles only if a Ca^{2+}/H^+ exchange antiport is present (+pH jump; grey bars in figure 56). Non specific accumulation was measured by pre-incubating PNS for 6 min in the ATP-free saline (pH 8.5) before adding Ca^{2+}. Such a pre-incubation annihilated the H^+ gradient and provided adequate controls (-pH jump; black bars in figure 56). Again, the G 11 (+/+), Syt I, and non irradiated Syt_tagg clones significantly accumulated Ca^{2+} over the non specific level (figure 56). Strikingly, the amounts of gradient-dependent Ca^{2+}-accumulation observed with these clones reached values similar to those observed with the previous approach using ATP-dependent H^+-gradient formation in presence or absence of bafilomycin A1 (figure 55). This seems to be indicative that pre-established H^+-gradients are sufficient for a vesicular Ca^{2+}/H^+-antiport activity under the present conditions. As for the F7 (-/-), the "moch", and the UV irradiated Syt_tagg clones, they did not show any Ca^{2+} accumulation attributable to Ca^{2+}/H^+ exchange (figure 56).

It should be noticed that the whole pH gradient observed in PC-12 cell PNS under the present conditions is attributable to the V-type H^+-ATPase activity (figure 14): It is fully dissipated by addition of 0.6 μM bafilomycin A1 (no further dissipation with CCCP).

An obvious control consisted of testing Ca^{2+} accumulation induced in a non specific manner by ionomycin, a Ca^{2+} ionophore (figure 57). PNS samples were added to an ATP-free medium containing 2 μM ionomycin, $^{45}Ca^{2+}$ (as before), and 10 μM othovanadate (grey bars; + ionomycin). Controls were like in figure 56 (black histograms). The level of non specific $^{45}Ca^{2+}$ binding was very similar to all cells. These basal $^{45}Ca^{2+}$ levels were also undistinguishable from the unspecific binding of $^{45}Ca^{2+}$ obtained in presence of ATP and bafilomycin (controls in figure 55). This indicates that the basal calcium levels are not significantly different among the (+/+) or (-/-) clones and are not sensitive to the addition of ATP when both the proton pump and Ca^{2+}-ATPases are inhibited (by bafilomycin and orthovanadate, respectively).

As for the amount of $^{45}Ca^{2+}$ retention in presence of ionomycin there was no statistical difference between the synaptotagmin containing (G11 and Syt I) versus synaptotagmin deficient (F7 and moch transfected) groups (figure 57). However, when we compare the G11 (+/+) subclone directly with F7 (-/-) there is a significantly lower Ca^{2+} retention capacity in synaptotagmin containing G11 cells ($p<0.01$). This could arise from having higher levels of free or bound calcium within the organelles of G11 (+/+) subclone when compared to F7 (-/-). Under such conditions radiolabelled calcium in the reaction medium would reach equilibrium with the free $^{40}Ca^{2+}$ ions already existent within the lumen of organelles and accumulate less $^{45}Ca^{2+}$.

Yet the amount of $^{45}Ca^{2+}$ accumulated within G11 clones energised with ATP in the absence of bafilomycin (figure 55) was significantly higher than the levels of $^{45}Ca^{2+}$ retained with ionomycin ($p<0.05$). This indicates that there must have been active transport capable of accumulating a surplus of $^{45}Ca^{2+}$ above the equilibrium level reached with ionomycin, since the amount of basal $^{45}Ca^{2+}$ retained in cells is similar. Furthermore, the existence of a pre established H^+-gradient seems to be sufficient to drive this active transport since pH-jump-dependent $^{45}Ca^{2+}$ retention with G11 preparation (figure 56) was similar to ATP-driven accumulation with the same subclone (figure 55). This is consistent with the operation of a secondary active transport system for Ca^{2+} provided by a vesicular Ca^{2+}/H^+-antiport.

The Ca^{2+}/H^+ antiport activity was not present in cells devoid of active synaptotagmin I (figures 55 and 56), which is also supported by the fact that they keep a considerable $^{45}Ca^{2+}$ retention capacity when permeabilized to Ca^{2+} by ionomycin (figure 57) for they are bound to be less Ca^{2+}-loaded in their acidic organelles at harvest time for PNS preparation. Such an increase in $^{45}Ca^{2+}$ retention capacity of F7 (-/-) subclones compared to G11 (+/+) is coincident with the data presented in previous chapters pointing out for a role of the Ca^{2+}/H^+-antiport in Ca^{2+} homeostasis if synaptotagmin I really is involved in such activity. Figure 57 shows also that F7 cells transfected with the Syt I gene accumulated significantly higher amounts of $^{45}Ca^{2+}$ than the G11 subclones ($p<0.001$). In this case the synaptotagmin deficient genetic background of F7 (-/-) cells probably overcomes the effects of transfecting Syt I genes into as much as 20% of cells (maximum transfection efficiency). Meaning that ~80% of the cells did not express functional antiport-driven Ca^{2+} transport at time of harvest (less basal calcium within organelles) against 20% of cells with a functional antiport (and higher basal calcium within organelles). Conversely, in figure 56 the results obtained with the same 20% of

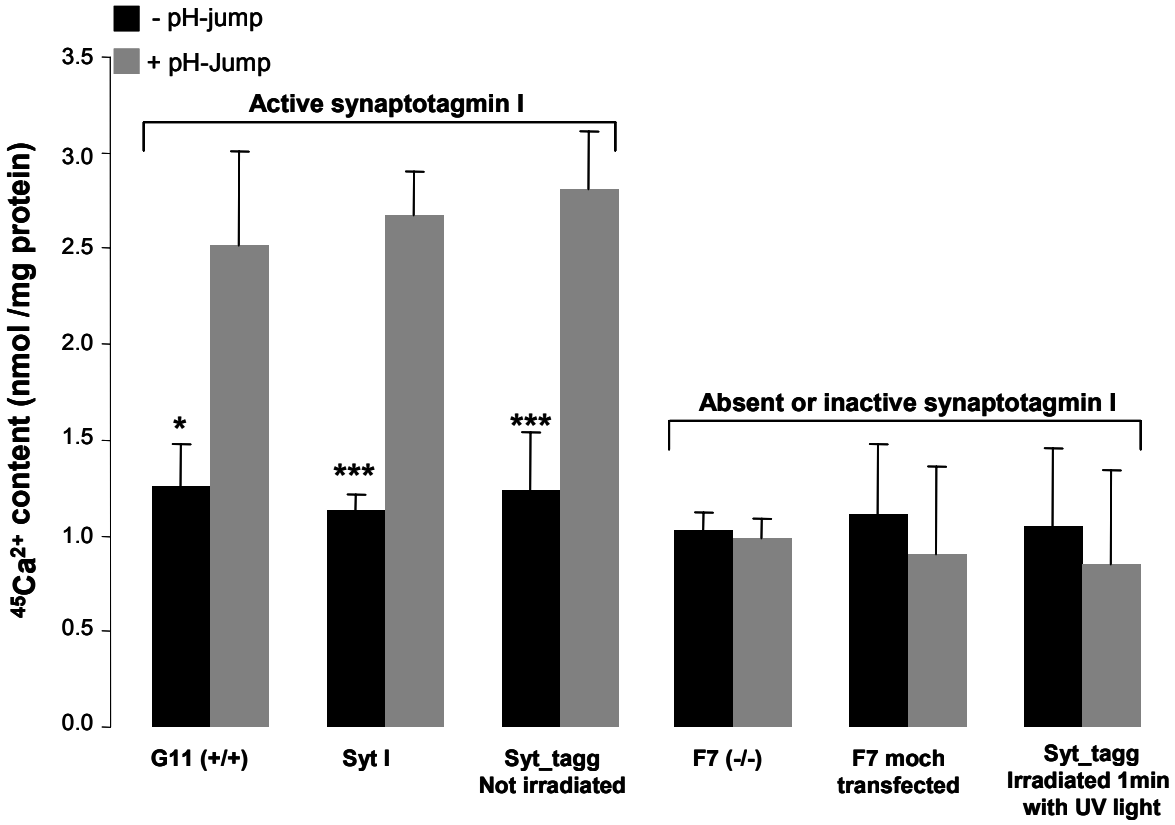

Figure 56. pH gradient-dependent Ca^{2+} accumulation associated with the presence of active synaptotagmin I in the acidic compartments of PC-12 cells. $^{45}Ca^{2+}$-transport was evaluated in PNS from the same PC12 clones as in figure 55. $^{45}Ca^{2+}$-accumulation assays were carried out by adding PNS (0.3 mg protein/ml prepared at pH 7.4) to ATP free saline medium (pH 8.6) already containing $^{45}Ca^{2+}$ (550 µM free; 0.5 mCi/mmol calcium) and 10 µM Na-orthovanadate (+pH-Jump in grey). Controls were carried out by allowing PNS to equilibrate for 6 min in ATP free saline medium (pH 8.6) before $^{45}Ca^{2+}$ (550 µM free; 0.5 mCi/mmol calcium) addition (-pH-Jump, in black). Rapid filtration took place 2 minutes after. Bars show the average ± SEM (n=3 to 10) of $^{45}Ca^{2+}$ retained after rapid filtration. PNS from PC-12 cells carrying active synaptotagmin I showed significant pH-jump dependent $^{45}Ca^{2+}$ accumulation into their acidic organelles (Unpaired T-test: *$p<0.05$; ***$p<0.001$).

Syt I transfected cells benefit from the Syt (-/-) background which is now essentially silent (null cells do not respond to ATP). In the context of this discussion it is equally interesting to notice that F7 (-/-) cells transfected with either synaptotagmin I constructs (Syt I or Syt_tagg) accumulated slightly less calcium than G11 cells. The difference is not significative but could result from having 20% instead of 100% of cells with active Syt I (figure 55).

The overall results presented above suggest the involvement of synaptotagmin I in H^+ gradient-dependent Ca^{2+} transport into acidic organelles in PC12 cells. Moreover, complete photoinactivation of Ca^{2+} transport (figures 53; 55 and 56) of Syt_tagg expressed in a

background with no endogenous synaptotagmin suggests that the C2B domain (near the FlAsH-binding motif) is essential for the putative Ca^{2+}/H^{+}-antiport activity observed since it has been suggested that only the domains nearer to the FlAsH binding tetracysteine domain will be affected by the destructive effects of FALI (Wang et al., 1996; Marek and Davis, 2002).

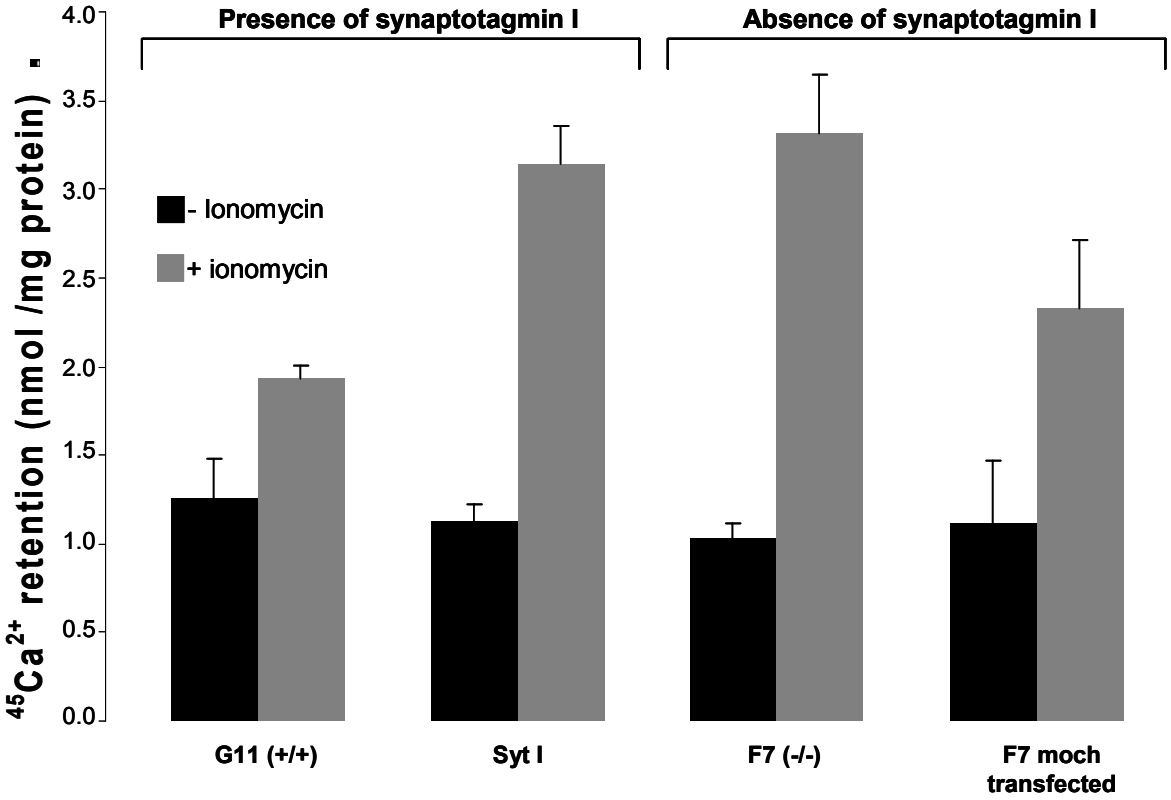

Figure 57. Ionomycin-induced Ca^{2+} retention in post nuclear supernatant (PNS) of PC-12 cells. $^{45}Ca^{2+}$-transport was evaluated in PNS of synaptotagmin I containing G11 PC-12 cell clones; synaptotagmin I deficient F7; F7 cells transfected with either a non-encoding gene (moch transfected) or with the synaptotagmin I gene (Syt I). $^{45}Ca^{2+}$-accumulation assays were carried out by adding PNS (0.3 mg protein/ml) to ATP free saline medium containing 2 µM ionomycin free acid; $^{45}Ca^{2+}$ (550 µM free; 0.5 mCi/mmol calcium) and 10 µM Na-orthovanadate (+ ionomycin). Controls (- ionomycin) were carried out by allowing PNS to equilibrate for 6 min in ATP free saline medium before $^{45}Ca^{2+}$ (550 µM free; 0.5 mCi/mmol calcium) addition. Rapid filtration took place 2 minutes after. Bars show the average ± SEM (n=3 to 9) of $^{45}Ca^{2+}$ retained after rapid filtration. Ionomycin induced calcium accumulation both in synaptotagmin I expressing or synaptotagmin I deficient subclones.

3.2.4.2. Ion permeable pore-forming oligomers

Here we report for the first time the involvement of synaptotagmin I in H^+-dependent vesicular calcium transport. The proximity of the C2B domain of synaptotagmin I to the FlAsH-binding motif of Syt_tagg points to the participation of C2B in this activity. Rapid high Ca^{2+}-dependent C2B-mediated oligomerization step (Chapman et al., 1996; Davis et al., 1999) could rapidly couple functional antiports to local high [Ca^{2+}] favouring rapid Ca^{2+} entry into vesicles at expense of a pre-established H^+-gradient.

Indeed, several proteins of the secretory apparatus that mediate rapid fluxes operate as oligomers. The synaptic tetra-spanning vesicle membrane protein synaptophysin is an hexameric homo-oligomer forming a large 150 pS channel (Thomas et al., 1988). The plasma membrane mediatophore is another homo-oligomer (~220 kDa) composed of 15 monomers of a 15 kDa protein that is homologous to the c sub-unit of the V0 sector of V-type H^+-ATPases (Israël et al., 1981; Muller et al., 1987; Brochier et al., 1992; Dunant and Israël, 2000).

There is also a striking resemblance between C2 domain-mediated synaptotagmin oligomerization and many hydrophilic pore-forming toxins forming amphipathic cyclical oligomers that are capable of penetrating into target membranes (Gouaux, 1997; Madeddu et al., 1985; Gilbert et al., 1999; Orlova et al., 2000).

Among those, one of the best studied proteins is a toxin extracted from black widow spider venom called α-latrotoxin. It is a hydrophilic ~130 kDa protein (determined under denaturating conditions; Dulubova et al., 1996) that spontaneously forms ~230-260 kDa asymmetric dimers. These dimers predominate in the absence of divalent cations (Ca^{2+}, Mg^{2+}) but acquire amphipaticity and ability to make membrane spanning pores upon divalent cation-regulated oligomerization into symmetrical cyclical tetramers of ~520 kDa (Orlova et al., 2000). Toxin action requires first the binding to one of the three receptor types (latrophilins, neurexins and receptor-like protein-tyrosin phosphatase σ; see Rohou et al., 2007; Ushkaryov et al., 2004, 2008) that facilitates membrane insertion of functional α-latrotoxin tetramers endowed with a 25 Å high conductance (220-400 pS) pore (Hurlbut WP et al., 1994; Hlubek et al., 2000; Van Renterghem et al., 2000; Hlubek et al., 2003). Pores cause large influx of Na^+, Ca^{2+} and water or the efflux of K^+, small transmitter molecules and ATP that are capable of eliciting Ca^{2+}-dependent or Ca^{2+}-independent transmitter release either directly or indirectly (McMahon et al., 1990; Krasilnikov and Sabirov, 1992; Adam-Vizi

et al., 1993; Deri et al., 1993; Hurlbut WP et al., 1994; Davletov et al., 1998; Ashton et al., 2000; Hlubek et al., 2003).

α-Latrotoxin and synaptotagmin I use oligomerization as an energy-efficient mechanism to hide the protomer hydrophilic domains within the oligomer, whilst exposing hydrophobic regions that are capable of insertion into membranes (Orlova et al., 2000; Chapman et al., 1996; Fukuda and Mikoshiba, 2000; Wu et al., 2003).

It is conceivable that the membrane insertion of the cytoplasmic domain of synaptotagmin I might be capable of creating a pore (similarly to α-latrotoxin) in the synaptic vesicle after the Ca^{2+}-dependent C2B-mediated rapid oligomerization step. The pore formed by synaptotagmin I oligomeric structure would then mediate rapid Ca^{2+}/H^{+}-antiport activity. This hypothesis is strengthened by the recently reported structure of the bacterial YiiP Zn^{2+}/H^{+}-antiport that forms homodimers that bind zinc through tetrahedral Zn^{2+}-binding sites located in a membrane spanning cavity (Lu and Fu, 2007).

3.2.4.3. Synaptotagmin I function(s) in transmitter release

The functional consequences of having a Ca^{2+}/H^{+} antiport activity participated by synaptotagmin I range from the control of secretion timing to the maintenance of calcium homeostasis (as presented in earlier chapters of this thesis). It could also help to conciliate apparently contradictory results obtained with Syt I null mutants or with acutely inhibited Syt I. On one hand loss-of-function mutations of synaptotagmin I cause severe secretion impairment in evoked transmitter release while increasing spontaneous uncoupled release in mouse hippocampal neurons (Geppert et al., 1994) and at Drosophila NMJ (DiAntonio et al., 1993; Littleton et al., 1993; DiAntonio and Schwartz, 1994; Broadie et al., 1994; Mackler et al., 2002; Pang et al., 2006). Evoked transmission seemed to be enhanced either by rather high basal activity (Marek and Davis, 2002) or increasing $[Ca^{2+}]_{out}$ (Yoshihara and Littleton, 2002). The later conditions would favour subthreshold intra-terminal Ca^{2+}-accumulation that could speed-up Ca^{2+}-inactivation processes like the desensitization of VOCCs, mediatophore, etc. This view is supported by an initially normal post-synaptic response followed by a time-dependent decrease in evoked transmission at squid giant synapses injected with either anti synaptotagmin I C2A (Mikoshiba et al., 1995) or anti C2B (Llinás et al., 2004) antibodies. The effects were attributed to decreased C2A-mediated exocytosis and C2B-mediated

endocytosis, respectively. This is to be expected if vesicular Ca^{2+}-transport is halted by either the lack of fusion of Ca-filled vesicles or compromised formation of Ca-empty vesicles by endocytosis and is consistent with ~2/3 reduction in the number of vesicles observed in synaptotagmin drosophila mutants (Reist et al., 1998). A time-dependent decrease in squid giant synapse transmission occurred also after compromising vesicle docking with a blocking peptide (Fukuda et al., 2000), evidencing the need for proximity to the Ca^{2+} source to activate the low Ca^{2+}-affinity vesicular Ca^{2+}/H^{+}-antiport activity. Furthermore, it was observed reduced transmission in flies without the C2A domain (Mackler et al., 2002) or with mutations in the C2B domain of synaptotagmin (Robinson et al., 2002). Therefore the C2B domain (rather than C2A) may be implicated in the process. More recently, three mice with mutations reported to affect Ca^{2+}-dependent self-oligomerization effectively reduced transmission also (Borden et al., 2005). This supports the idea that defective synaptotagmin C2B-mediated Ca^{2+}-dependent oligomerization may affect transmission by compromising vesicular Ca^{2+}/H^{+}-antiport Ca^{2+}-transport and activate Ca^{2+}-desensitising pathways in synapses working at rather high basal frequencies.

Conversely, in low frequency-stimulated systems like PC12 cells, secretion of dopamine and ATP was increased by ~70% and 600%, respectively in Syt -/- subclones (Shoji-Kasai et al., 1992) without affecting the time course of secretion (minutes). Secretion increase could have arisen from increased $[Ca^{2+}]_{int}$ transient due to the absence of rapid vesicular calcium transport. There was also an >6 fold increase in the ATP/dopamine release ratio in Syt I -/- subclones. Those transmitters are thought to be co-released from large dense-core vesicles and such ATP preservation in Syt I -/- could have arisen from the decrease in Ca^{2+}/ATP exchange from the vesicular matrix (Reigada et al., 2003) in the absence of a vesicular Ca^{2+}/H^{+}-antiport activity in those clones. With less Ca^{2+} entering the vesicle prior to fusion there would be less ATP displacement from the vesicular matrix and more ATP to be released by Syt -/- dense-core vesicles. An increase in the calcium transient in PC12 cells without Syt I is further supported by a significant increase in membrane accretion with the Syt I -/- as compared with Syt I +/+ PC12 subclones (Almers et al., 1994). Although rather slower fusion rates were obtained with freshly isolated chromaffin cells from Syt I null mice (Voets et al., 2001; Nagy et al., 2006) where Syt I and Syt II rescued a ready releasable pool while decreasing a slowly releasable pool (Nagy et al., 2006), therefore restoring synchronous transmission where the C2B domain is also involved (Nishiki and

Augustine, 2004). Again, if the Ca^{2+}-microdomain is sharpen in time and in space by a rapid vesicular Ca^{2+}/H^{+}-antiport one should expect the restoration of synchronous release (by activating only Ca^{2+}-sensors close to VOCCs) and reducing asynchronous release (high micromolar calcium is not expected to reach sensors away from the Ca^{2+}-source).

3.2.4.4. The C2A and C2B domains of synaptotagmin I

Work conducted at Graeme Davis's laboratory using a synaptotagmin I construct similar to the one used in this study implicated synaptotagmin I C2B domain acute disruption by FlAsH-FALI in the loss of calcium cooperativity of release (Marek and Davis, 2002) and loss of endocytosis capacity in *Drosophila* NMJ (Poskanzer et al., 2003) involving residues that are not involved in the C2B-mediated Syt I oligomerization (Poskanzer et al., 2006). In fact the C2B domain interacts also with Ca^{2+}-channels (Sheng et al., 1998); phospholipids (Schiavo et al., 1996; Fernandez et al., 2001) and the clathrin adaptor complex AP-2 (Zhang et al., 1994; Jorgensen et al., 1995; Chapman et al., 1998; Haucke and De Camilli, 1999). The interaction of synaptotagmin I with diverse molecular partners highlights the participation in multiple stages of the vesicular cycle. Tampering with Syt I binding to Ca^{2+}-channels might affect Ca^{2+}-cooperativity if the calcium sensors for transmitter release "drift away" from high $[Ca^{2+}]_{int}$ reached near the calcium source. Disrupting the poly-lysin motif within the C2B domain of Syt I affects phospholipids and AP-2 interaction (Zhang et al., 1994; Fukuda et al., 1995; Chapman et al., 1998; Haucke and De Camilli, 1999; Mackler and Reist, 2001) that control vesicular size while the endocytic rate is controlled by Ca^{2+}-coordinating aspartate residues within the C2B domain of Syt I (Poskanzer et al., 2006). Synaptotagmin I interacts also with phospholipids and syntaxin through its C2A domain (Kee and Scheller, 1996; Ubach et al., 1998; Fernandez et al., 2001) and has been recently implicated in the temporal control of phasic transmission in crayfish NMJ (Hua et al., 2007). Binding of Syt I to P/Q VOCCs (Charvin et al., 1997) and to SNARE proteins syntaxin and synaptobrevin (see above) might also contribute to some perturbations observed in Syt I-deficient systems. For instance, SNAP-25 has been shown to depress the voltage sensitivity of P/Q channels. This inhibitory effect is unblocked when the active SNARE complex is formed and Syt I is needed for this formation (Zhong et al., 1999). Therefore, by this effect as well, phasic calcium entry as well can be perturbed in the absence of an active Syt I.

3.2.4.5. High versus low basal release rates

An increase in rapid transmission similar to the one reported with nerve-electroplaque synapses of *Torpedo* prisms intoxicated with bafilomycin (section 3.2.1.1.) was possible to observe in systems working with low resting release probability where subthreshold Ca^{2+} rise is less likely to occur. Synaptotagmin I overexpression in both buccal ganglia and sensory-motor neurons of Aplysia resulted in a decrease in the amplitude of the EPP by 32% and 26%, respectively. Conversely, when a synaptotagmin antisense oligonuclotide was applied to sensory-motor neurons there was an increase in 50-75% in the amplitude (Martin et al., 1995). Concordantly, Hua et al. (2007) demonstrated a facilitatory effect of an antibody directed against C2A domain of Syt I in the phasic nerve terminal EPP from crayfish NMJ. The anti-Syt antibody increased the amplitude and reduced the rise time of the evoked synaptic response. The effect was more obvious in lower $[Ca^{2+}]_{out}$, where an increase in intra-terminal $[Ca^{2+}]$, due to compromised Syt I should be more effective than at high calcium, closer to maximum activation of secretion (see also discussion in section 3.2.1.1).

Interestingly, crayfish NMJ were shown to respond to increases in $[Ca^{2+}]_{out}$ with enhanced and enlarged EPPs. However, even if stimulated at low frequency, there was a gradual decrease of synaptic transmission that affected the estimation of the Hill coefficient for Ca^{2+} tested over time from low $[Ca^{2+}]_{out}$ to high $[Ca^{2+}]_{out}$ and was further reduced in fibbers submitted to the Syt I antibody (Hua et al., 2007).

A parallel can be established between the effects of bafilomycin in *Torpedo* synaptosomes (partially depolarized) and systems working at high basal rates of release since both have to cope with high Ca^{2+}-turnover rates to cope with persistent Ca^{2+}-entry. When rapid extrusion through the vesicular Ca^{2+}/H^{+}-antiport is compromised (for instance CCCP; bafilomycin or absence of functional Syt I) basal calcium levels will slowly rise; increase spontaneous MEPPs (Molgó and Pécot-Dechavassine, 1988; Van Der Kloot et al., 2000); decrease evoked release (Sanchez-Prieto et al., 1987); while increasing asynchronous release (as mentioned above with Syt I null mutants) or simply subside due to Ca^{2+}-desensitization (or fatigue) of calcium channels or of the release apparatus (Birman and Meunier, 1985; Israël et al., 1987; Forsythe et al., 1998; Lee et al., 1999; Findlay, 2004; Guo and Duff, 2006; Kreiner and Lee, 2006).

On the other hand, if the system works at low basal frequency, like with *Torpedo* prisms or PC12 cells, calcium entry will be accommodable by slower Ca^{2+}-extrusion systems that depend on metabolic energy, like Ca^{2+}-pumps. No desensitization will occur and an increase in the phasic calcium transient will be the prevailing effect of tampering with Syt I-mediated Ca^{2+}/H^{+}-antiport activity.

3.2.4.6. Role of local pH changes

It is tempting to propose complementary roles for the antiport like the modulation of vesicular fusion itself by inducing a local pH drop. Low-pH-mediated membrane fusion after the acidification of endosomes was established for virus (Wahlberg and Garoff, 1992; Klimjack et al., 1994; Bentz, 2000; Stegmann, 2000; Bentz and Mittal, 2003). Virus acquire coiled coil trimeric structures when exposed to low pH (Bentz, 2000; Stegmann, 2000; Gibbons et al., 2004; Modis et al., 2004). Similarly, mammalian v-SNARE-t-SNARE pairing lead to the formation of coiled-coil tetrameric structures (Sutton et al., 1998; Weber et al., 1998). On the other hand the targeting of cytosolic proteins that regulate intracellular trafficking events can itself be regulated by low pH (Zeuzem et al., 1992; Gu and Gruenberg, 2000; Maranda et al., 2001; Lee et al., 2005) either through transduction of intra-organelle pH status influencing cytosolic partners though pH-dependent conformational changes in transmembrane proteins (Gu and Gruenberg, 2000) or through H^{+}-leak pathways (Miedema et al., 1996; Wu et al., 2001) that could be produced by antiports (Akhter et al., 2002; Lee et al., 2005). Localized acidic microenvironments are emerging as important signalling events capable of influencing the recruitment of proteins relying on specific epitopes like the FYVE domain that interacts with phosphatidylinositol 3-phosphate [PtdIns(3)P]-enriched membranes that selectively address proteins to specific membrane localizations according to local acidic microenvironments (Lee et al., 2005). Conversely, H^{+} microenvironment inhibits the binding of phosphatidylinositol-4,5-phosphate (PtdIns-4,5-P2) to the cardiac Na^{+}/Ca^{2+} exchanger irrespective of hole PtdIns-4,5-P2 membrane concentration and down-modulates its Ca^{2+} affinity (Posada et al., 2007).

3.2.4.7. Synaptotagmin I interaction with phospholipids

Phosphatidylinositol phosphates are important signalling molecules that are targeted by synaptotagmin I. The C2B domain of synaptotagmin binds preferentially phosphatidylinositol-3,4,5-phosphate (PtdIns-3,4,5-P3) at resting Ca^{2+} but shifts to PtdIns-4,5-P2 in high calcium (Schiavo et al., 1996). Both lipids are more abundant at the plasma membrane but could also be found in the vesicular membrane (Holz et al., 2000; Manna et al, 2007). PtdIns-4,5-P2 was proposed to participate both in exo and endocytosis (Reviewed by Chapman, 2002 and Rohrbough and Broadie, 2005). By analogy to FYVE domain-bearing proteins and to the cardiac Na^+/Ca^{2+} exchanger, synaptotagmin could direct its preferential lipid (specially to PtdIns-4,5-P2 and Phosphatidylserine) binding to cis (vesicle) or trans (plasma) membranes at different stages of the secretory cycle through the influence of local H^+ environment created by its own Ca^{2+}/H^+-antiport activity. Even if rapid exocytotic burst is strictly Ca^{2+}-dependent the slower exocytotic phase determined in melanotrophs by membrane capacitance is inhibited at low pH (6.2) (Thomas et al., 1993, 1994; Almers et al., 1994). Synaptotagmin -/- subclones showed an increase in both the rapid Ca^{2+}-dependent exocytotic burst (probably due to increased high Ca^{2+}-transient) but also in the slower H^+-inhibited phase (Almers et al., 1994) where the putative H^+-sensitivity of PtdIns-4,5-P2-protein interactions could play an important role in exo-endocytic rates.

Even though the lipidic aspects of synaptotagmin I interactions were not addressed experimentally here they will be considered as hypothesis included in the sequence of events supported by the experimental work presented throughout this thesis.

4. Conclusions and perspectives

4.1. Conclusions

The results presented in this thesis as well as experimental evidences reported by others lead to the proposition of a model contemplating the effects of vesicular calcium transport by synaptic vesicles in neurotransmission.

We hypothesise the following sequence of events in a cholinergic synapse submitted to stimulation:

1) Synaptic vesicles begin as organelles that are actively, but slowly, filled with transmitter within the terminal (Schmidt et al., 1980; Kiene and Stadler, 1987; Stadler and Kiene 1987; Reviewed by Williams in 1997); ACh is synthesised in the cytoplasm and transported against protons into synaptic vesicles where it binds to a charged matrix (Reigada et al., 2003).

2) At rest, Ca^{2+} entering nerve terminals are pumped-up into synaptic vesicles by a Ca^{2+}-pump working in the low micromolar range (Israël et al., 1980; Michaelson et al., 1980; Rephaelis and Parsons, 1982; Gonçalves et al., 2000a) that contributes, along with reticulum and plasma membrane pumps, to long-term Ca^{2+} homeostasis (figure 58 C and section 3.2.2). As the vesicles move closer to the first row directly above the plasma membrane in an active zone they probably have already pumped a considerable amount of Ca^{2+}.

3) Ca^{2+}-ACh exchange promotes the dissociation of ACh from the internal vesicular matrix (Reigada et al., 2003). ACh leaks-out into the cytosol feeding the cytoplasmic pool in a stimulus-dependent manner (the more calcium enters the terminal, the more Ca^{2+}-ACh exchange will occur within vesicular matrices; see section 3.2.3). Ca^{2+} binding to the vesicular matrix under dehydrated conditions results in the shrinking of vesicular matrix by glycosaminoglycan cross-linking facilitated by ACh/ATP unbinding and is directly related to SV volume and density (Maler and Mathieson, 1985; Kiene and Stadler, 1987; Stadler and Kiene 1987; Reviewed by Williams in 1997);

4) Once in close proximity to the active zone, vesicles will participate in very rapid calcium sequestration by the Ca^{2+}/H^{+}-antiport (figure 58 A/B and section 3.2.1) whose effective range lies within ~100 to 800 μM (max at ~500 μM) Ca^{2+} concentration (Gonçalves et al., 2000a). Such Ca^{2+} concentrations develop very rapidly

(<50 μs) within nanodomains near Ca^{2+}-channel mouths (Roberts, 1994) and activate mediatophores and synaptotagmin I that are physically attached to VOCCs.

5) Both Ca^{2+}-sensors (Mediatophores in plasma and synaptotagmin I in the vesicular membranes) suffer rapid (μs) conformational changes resulting in the opening of the ACh-permeable mediatophore that releases ACh within <300 μs of Ca^{2+} entry (Girod et al., 1993);

6) At the same time synaptotagmin I accomplishes its Ca^{2+}-dependent oligomerization step providing for the active form of the vesicular Ca^{2+}/H^{+}-antiport (section 3.2.4) that uses the steep Ca^{2+} and H^{+} gradients across SV membranes to remove Ca^{2+} swiftly (μs up to ms range) from the active zone (figure 58 A and sections 3.2.1 and 3.2.4).

7) Very rapid calcium sequestration by the vesicular Ca^{2+}/H^{+}-antiport shortens the time-course of secretion by abruptly decreasing the number of Ca^{2+} ions within an active zone and helping to lower $[Ca^{2+}]$ to subthreshold values (otherwise ACh release is prolonged from <300 μs to over 1 ms (figure 58 B and section 3.2.1)). A brief calcium transient also prevents asynchronous ACh release from mediatophores located away from the active Ca^{2+}-channel by lowering the Ca^{2+} load within the terminal. When rapid Ca^{2+} sequestration is absent local $[Ca^{2+}]$-microenvironments away from the calcium sources may develop rather slowly (ms instead of μs) and contribute to asynchronous transmitter release.

8) Additionally, rapid vesicular Ca^{2+}-transport will add an extra amount (possibly final) of Ca^{2+} into the vesicle, filling it up, exchanging the last ACh molecules for Ca^{2+} ions and finishing loading the vesicle with Ca^{2+} before fusion occurs a millisecond up to few minutes later (see section 3.2.3).

9) Rapid vesicular Ca^{2+}-sequestration through the antiport contributes to maintain calcium homeostasis (figure 58 and sections 3.2.1 and 3.2.2) by preventing excessive Ca^{2+}-binding to large quantities of endogenous mobile buffers responsible to lower $[Ca^{2+}]$ through buffered diffusion. Vesicular sequestration prevents both the rundown of unbound Ca^{2+} buffers within an activated active zone; at the same time it prevents excessive Ca^{2+} binding to large quantities of mobile buffer that have the ability to bind Ca^{2+} and unbind it after diffusing away from the Ca^{2+}-source. This

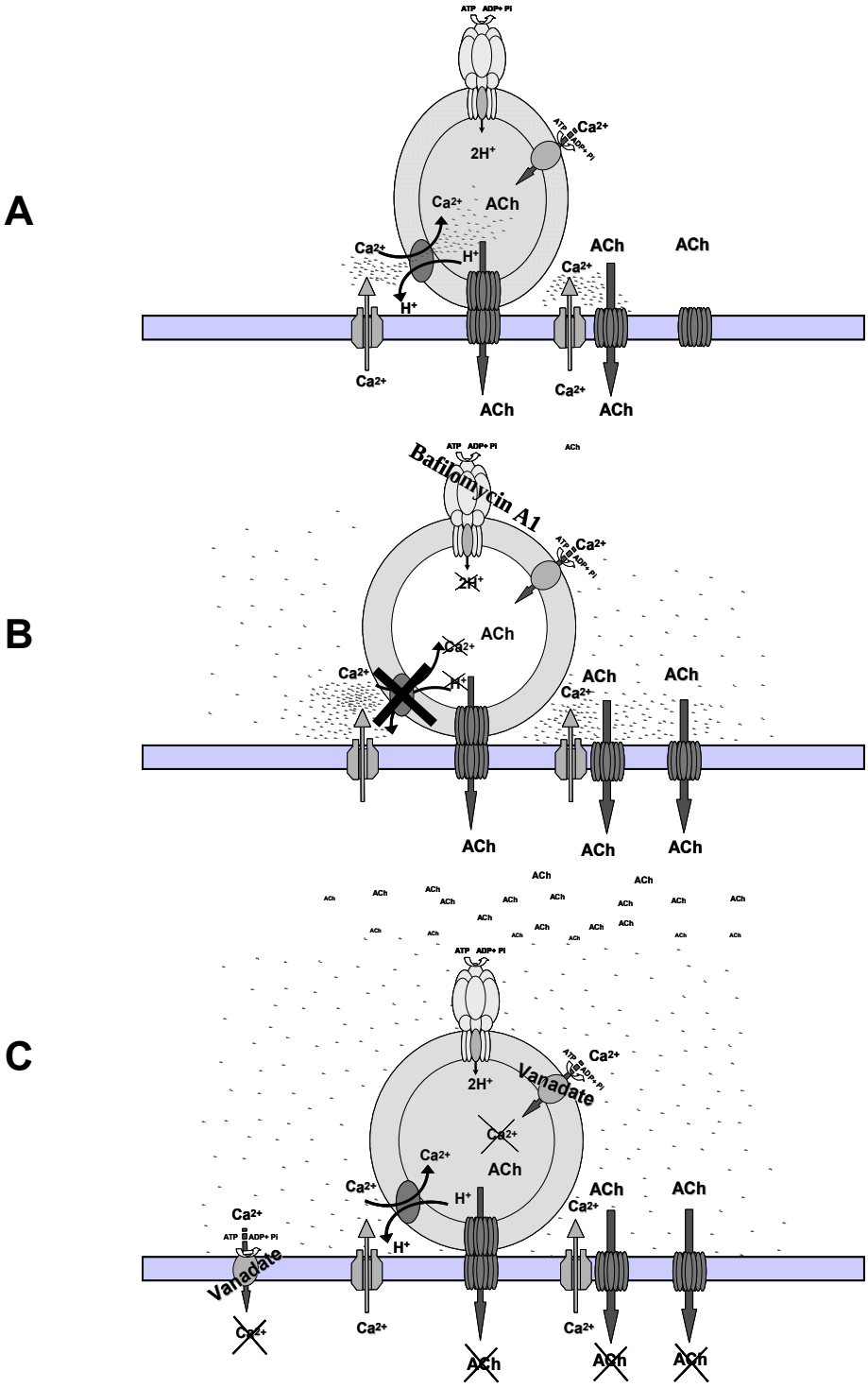

Figure 58. Vesicular calcium transport participation in Ca^{2+} dynamics in cholinergic nerve terminals. **Panel A** illustrates how vesicular calcium transport though the vesicular Ca^{2+}/H^{+} antiport may abbreviate the duration of ACh release. **Panel B** show how inactivation of the vesicular antiport with bafilomycin causes a rise in bulk cytosolic calcium and an extension of the Ca^{2+} microdomain, leading to increased ACh release. **Panel C** represents a nerve terminal desensitized by subthreshold [Ca^{2+}] rise after compromising Ca^{2+}-ATPases with orthovanadate.

simple mechanism may provide a mean to endure subthreshold Ca^{2+}-load (ca. 1 μM) and desensitize molecules like VOCCs and mediatophores.

Therefore there seems to be a joint participation of both the vesicular Ca^{2+}/H^{+} antiport along with Ca^{2+}-ATPases (including the vesicular Ca^{2+}-ATPase) in keeping resting calcium under the threshold of activation of Ca^{2+}-desensitization mechanisms.

10) Protons ejected from SVs by the Ca^{2+}/H^{+}-antiport activity will rapidly raise local cytosolic pH that may catalyze reactions involving PtdIns polyphosphates (like PtdIns-4,5-P2) with synaptotagmin and SNARE proteins adding a H^{+} switch to the Ca^{2+} signalling that is engaged after (>350 μs) normal secretion time for rapid secretion.

11) Calcium accumulated within a vesicle re-gains the extracellular space upon fusion by unbinding from the vesicular matrix now exposed to a largely neutral (pH~7) and Na^{+}-rich environment. Ca^{2+} exocytosis seems to be a cost-effective manner of disposing of the large amounts of Ca^{2+} accumulated within a nerve cell at the same time that provides a means to maintain the large fluxes of Ca^{2+}-ions occurring at high frequencies with minimal amounts of Ca^{2+}-ions accommodable in the tiny synaptic space.

12) The vesicle gets endocytosed back into the terminal along with the matrix that is mostly linked to transmembrane proteins (Kuhn et al., 1988; Reigada et al., 2003). After endocytosis vesicles will be refilled with transmitter back again through ACh active transport under internal SV acidic environment. This favours Na^{+}/ACh ion exchange from the vesicular matrix (Reigada et al., 2003) and the cycle may begin once more.

A final note concerning slower mechanisms of secretion depending on fusion to secrete active substances (rather than mediatophore-like plasma membrane proteins) should be added. At least some of them are also endowed with synaptotagmin I and a Ca^{2+}/H^{+}-antiport activity (as seen in PC12 cells) where most of the above described steps are likely to occur to control both calcium dynamics (see Shoji-Kasai et al., 1992) as well as homeostasis, even if no microsecond control of secretion will be conceivable or necessary.

4.2. Perspectives

In the course of this work it was possible to pin-point for the first time rapid and slow functions of vesicular Ca^{2+} transport in neurosecretion that had been missing since Ca^{2+} was described to be actively accumulated within vesicles almost 30 years ago. It was also possible to identify synaptotagmin I as an essential partner responsible for the vesicular Ca^{2+}/H^{+}-antiport activity enabling to relate information on vesicular Ca^{2+} transport with that of the secretory activity of other synaptic partners like SNAREs, mediatophores and membrane lipids.

As usual, the answers provided by this work raise new questions that may outnumber the answers provided. For instance:

1) Will other secretory systems (namely those working with slower kinetics) be equally sensitive to the inhibition of vesicular Ca^{2+}-transport systems?

2) What is the exact relationship between vesicular Ca^{2+}-transport and extracellular Ca^{2+} homeostasis?

3) What will be the effects of not having vesicular Ca^{2+}-transport in the quantic content of cholinergic and other transmitter synapses?

4) Is there really a dual Ca^{2+}/H^{+} code ruling the secretory orchestra?

5) What are the effects of the vesicular Ca^{2+}/H^{+} transport on other fast secretory systems using GABA or glutamate?

6) What will be the effects of the vesicular Ca^{2+}/H^{+} transport in the release of monoamines by the kiss-and-run mechanism?

7) What are the relative contributions to cellular calcium dynamics and homeostasis of the different sequestering (endogenous buffers) and extruding (pumps, exchangers and channels) in excitable and non-excitable cells?

While at the molecular level one could ask:

8) Can the antiport behave as a relatively large conductance pore?

9) What are the maximal Ca^{2+}-transport rates attainable by the Ca^{2+}-ATPase and the antiport?

10) What is the stoichiometry of Ca^{2+} transport against H^{+} efflux?

11) Is there an antiport activity in systems that do not express synaptotagmin I and II, like the mammalian inner hair cell synapse? If so, who codes for that activity?

12) Who codes for the Ca^{2+}-ATPase activity?

13) What is the molecular counterpart allowing for ACh leakage out of synaptic vesicles?

14) Are there similar counterparts for other fast transmitters like GABA, glutamate?

15) Is there any regulation of the vesicular transmitter content for slower secretory systems like monoamines and peptides?

At the level of complex systems this work allows to address at least a couple of questions more:

16) Is there an involvement (or the lack of it) of vesicular Ca^{2+}-transport systems in the aetiology of mental illness (including neurodegenerative disorders)?

17) Could we envisage the targeting of vesicular Ca^{2+}-transport systems to boost neural network performance (i.e., increase ACh release in Alzheimer's disease patients)?

It looks like we have pulled a thread from a long and interesting yarn.

Let there be funding.

5. Publications resultant from this work

5.1. Articles

Cordeiro JM, Bancila V, Bloc A, Gonçalves P and Dunant Y (2004). A calcium-proton antiport in presynaptic nerve terminals . In: Cholinergic mechanicsms: Function and dysfunction. Chapter 83: pp 527-529. Ed: Silman, I.; Soreq, H.; Anglisher, L.; Michaelson, D.; Fisher, A.. © Taylor and Francis 2004. (Proceedings book chapter).

Cordeiro JM, Dunant Y and Gonçalves PP (2006). Vesicular calcium transport shapes rapid acetylcholine secretion. Journal of Molecular Neuroscience 30, Issues 1-2: 41-44.

Bancila V, **Cordeiro JM**, Bloc A and Dunant Y. Nicotine induces glutamate release without change in the membrane potential or dissipation of the vesicular proton gradient. Journal of Neurochemistry 2008 (submitted).

Cordeiro JM, Gonçalves PP and Dunant Y. Synaptic vesicles regulate the time-course of secretion with a Ca^{2+}/H^{+} antiport. (under preparation).

Cordeiro JM, Gonçalves P.P. and Dunant Y. Desensitization of Acetylcholine release mechanism by subthreshold calcium. (under preparation).

Cordeiro JM, Boda B, Muller D, Gonçalves PP and Dunant Y. Requirement of synaptotagmin I for vesicular Ca^{2+}/H^{+} antiport activity. (under preparation).

Cordeiro JM, Dunant Y and Gonçalves PP. Modulation of vesicular acetylcholine content by calcium-acetylcholine exchange. (under preparation).

Cordeiro JM, Neves P, Dunant Y and Gonçalves PP. Drugs affecting V-type ATPase activity, also affect Ca^{2+}/H^{+} antiport modulation of Acetylcholine release. (under preparation).

5.2. Oral presentations

Gonçalves PP, Neves P, **Cordeiro JM**, Dunant Y. The Calcium/Proton Antiporter from Bacteria to Mammalian Central Nervous System. WCDA – World Conference on Dosing of Antiinfectives, September 9-11, 2004. Nurnberg, Germany.

Cordeiro JM, Dunant Y, Gonçalves PP. O transporte de cálcio pelas vesículas sinápticas regula a duração da neurotransmissão. I encontro nacional de pós-graduação em ciências biológicas & V simpósio de pós-graduação do Departamento de Biologia da Universidade de Aveiro. 2-4 maio de 2006. Aveiro, Portugal.

Cordeiro JM, Dunant Y and Gonçalves PP. Vesicular Ca^{2+}/H^{+} antiport regulates rapid ACh secretion timing. XVth National Congres of Biochemistry. Aveiro, Portugal. 8-10 December 2006.

5.3. Poster presentations

Da Silva **Cordeiro JM**, Bancila V, Bloc A and Dunant Y. A calcium-proton antiport in cholinergic and glutamatergic synaptic vesicles. XIth . International Symposium on Cholinergic Mechamnisms- Function and Disfunction and 2nd Misrahi Symposium on neurobiology. St Moritz, Switzerland, 5-9 May 2002.

Cordeiro JM, Dunant Y and Gonçalves PP. Role of vesicular Ca^{2+}/H^{+} antiport and Ca^{2+}-ATPase in rapid neurosecretion. 4th FENS meeting. Lisbon 10-14 July 2004.

Cordeiro JM, Gonçalves P.P. and Dunant Y. Vesicular Ca^{2+}/H^{+} antiport and Ca^{2+}-ATPase function in rapid neurosecretion. Second Meeting of the Lemanic Neuroscience Programs. Sept. 30th – Sat., Oct 1st, 2005. Diablerets, Switzerland.

Cordeiro JM; Dunant Y and Gonçalves PP. Vesicular calcium transport shapes rapid acetylcholine secretion. XIIth International Meeting on Cholinergic Mechanisms Alicante, Spain Oct 1-5, 2005.

Cordeiro JM, Dunant Y and Gonçalves PP. Tight temporal control of secretion by synaptic vesicle Ca^{2+}/H^{+} antiport. 35th Annual Meeting Society for Neuroscience. November 12 – 16, 2005, Washington, USA.

6. References

Abbott BC, Aubert X, and Fessard A (1958). La production de chaleur associée à la décharge du tissu électrique de la Torpille. J. Physiol. Paris; 50: 99-102.

Abdul-Ghani MA, Valiante TA, Pennefather PS (1996). Sr^{2+} and quantal events at excitatory synapses between mouse hippocampal neurons in culture. J. Physiol.; 495 (Pt 1): 113-125.

Accardi A and Miller C (2004). Secondary active transport mediated by a prokaryotic homologue of ClC Cl- channels. Nature.; 427(6977): 803-807.

Adams DJ, Takeda K, Umbach JA (1985). Inhibitors of calcium buffering depress evoked transmitter release at the squid giant synapse. J. Physiol.; 369: 145-159.

Adam-Vizi V, Deri Z, Bors P, Tretter L (1993). Lack of involvement of $[Ca^{2+}]_i$ in the external Ca(2+)-independent release of acetylcholine evoked by veratridine, ouabain and alpha-latrotoxin: possible role of $[Na^+]_i$. J. Physiol. Paris; 87(1): 43-50.

Adler EM, Augustine GJ, Duffy SN, Charlton MP (1991). Alien intracellular calcium chelators sttenuate neurotransmitter release at the squid giant synapse. J. Neurosci.; 11(6): 1496-507.

Ahdut-Hacohen R, Meiri H, Rahamimoff R (2006). ATP dependence of the non-specific ion channel in Torpedo synaptic vesicles. Neuroreport; 17(6): 653-656.

Akhter S, Kovbasnjuk O, Li X, Cavet M, Noel J, Arpin M, Hubbard AL, Donowitz M (2002). Na^+/H^+ exchanger 3 is in large complexes in the center of the apical surface of proximal tubule-derived OK cells. Am. J. Physiol. Cell. Physiol.; 283(3): C927-C940.

Alés E, Tabares L, Poyato JM, Valero V, Lindau M, Alvarez de Toledo G (1999). High calcium concentrations shift the mode of exocytosis to the kiss-and-run mechanism. Nat. Cell Biol.; 1(1): 40-44.

Almers W, Breckenridge LJ, Spruce AE (1989). The mechanism of exocytosis during secretion in mast cells. Soc. Gen. Physiol. Ser.; 44: 269-282.

Almers W, Lee A, Shoji-Kasai Y, Takahashi M, Thomas P, Tse F (1994). Final steps in Ca^{2+}-triggered exocytosis in neuroendocrine cells. pp: 97-107. In: Molecular and Cellular Mechanisms of Neurotransmitter Release. Edited by Stjärne, L; Greengard, P; Grillner, S; Hökfelt and Ottoson, D. Raven Press, Ltd, New York.

Alnaes E and Rahamimoff R (1975). On the role of mitochondria in transmitter release from motor nerve terminals. J. Physiol. (London) 248(2): 285-306.

Alvarez de Toledo G, Fernandez-Chacon R, Fernandez JM (1993). Release of secretory products during transient vesicle fusion. Nature.; 363(6429): 554-558.

Amaral DG and Witter MP (1989). The three-dimensional organization of the hippocampal formation: a review of anatomical data. Neuroscience; 31: 571-591.

Anderson CR and Stevens CF (1973). Voltage clamp analysis of acetylcholine produced end-plate current fluctuations at frog neuromuscular junction. J. Physiol.; 235(3): 655-691.

Araç D, Chen X, Khant HA, Ubach J, Ludtke SJ, Kikkawa M, Johnson AE, Chiu W, Südhof TC, Rizo J (2006). Close membrane-membrane proximity induced by Ca^{2+}-dependent multivalent binding of synaptotagmin-1 to phospholipids. Nat. Struct. Mol. Biol.; 13(3): 209-217.

Arai H, Berne M, Forgac M (1987). Inhibition of the coated vesicle proton pump and labeling of a 17,000-dalton polypeptide by N,N'-dicyclohexylcarbodiimide. J. Biol. Chem.; 262: 11006-11011.

Ashton AC, Rahman MA, Volynski KE, Manser C, Orlova EV, Matsushita H, Davletov BA, van Heel M, Grishin EV, Ushkaryov YA (2000). Tetramerisation of alpha-latrotoxin by divalent cations is responsible for toxin-induced non-vesicular release and contributes

to the Ca^{2+}-dependent vesicular exocytosis from synaptosomes. Biochimie; 82(5): 453-468.

Aubert X, Fessard A, and Keynes RD (1961). The thermal events during and after the discharge of the electric organ of Torpedo and Electrophorus, in Bioelectrogenesis (Chagas C. and Paes de Carvalho A., eds.), pp. 136-146. Elsevier, Amsterdam.

Augustine GJ, Santamaria F, Tanaka K (2003). Local calcium signalling in neurons. Neuron; 40: 331-346.

Avissar M, Furman AC, Saunders JC, Parsons TD (2007). Adaptation reduces spike-count reliability, but not spike-timing precision, of auditory nerve responses. J Neurosci.; 27(24): 6461-6472.

Babel-Guérin E (1974). Calcium metabolism and acetylcholine release in the electric organ of Torpedo marmorata. J.Neurochem.; 23: 525-532.

Bai J, Earles CA, Lewis JL, Chapman ER (2000). Membrane-embedded synaptotagmin penetrates cis or trans target membranes and clusters via a novel mechanism. J. Biol. Chem.; 275(33): 25427-25435.

Bai J, Wang P, Chapman ER(2002). C2A activates a cryptic Ca^{2+}-triggered membrane penetration activity within the C2B domain of synaptotagmin I. Proc. Natl. Acad. Sci. USA; 99(3): 1665-1670.

Bain AI and Quastel DM (1992).Quantal transmitter release mediated by strontium at the mouse motor nerve terminal. J. Physiol.; 450: 63-87.

Bajjalieh SM, Peterson K, Shinghal R, Scheller RH (1992). SV2, a brain synaptic vesicle protein homologous to bacterial transporters. Science. 257(5074):1271-3

Bajjalieh SM (2005). A new view of an old pore. Cell; 121(4): 496-497.

Baker PF, Hodgkin AL, Ridgway EB (1971). Depolarization and calcium entry in squid giant axons. J. Physiol. (London); 218(3): 709-755.

Bancila V, Bloc A, Dunant Y (2004). Nicotine induces glutamate release from hippocampal mossy fibre synaptosomes. In: Cholinergic mechanisms – function and dysfunction. Chapter 66. Silman I, Soreq H, Anglister L, Michaelson D, Fisher A. Taylor & Francis Ed. 459-461.

Bancila V, Cordeiro JM, Bloc A and Dunant Y (2008). Nicotine induces glutamate release without change in the membrane potential or dissipation of the vesicular proton gradient. Journal of Neurochemistry 2007 (submitted).

Bartol TM Jr, Land BR, Salpeter EE, Salpeter MM (1991). Monte Carlo simulation of miniature endplate current generation in the vertebrate neuromuscular junction. Biophys. J.; 59(6): 1290-1307.

Beck S, Sakurai T, Eustace BK, Beste G, Schier R, Rudert F, Jay DG (2002). Fluorophore-assisted light inactivation: a high-throughput tool for direct target validation of proteins. Proteomics; 2(3):247-255.

Bellingham MC and Walmsley B (1999). A novel presynaptic inhibitory mechanism underlies paired pulse depression at a fast central synapse. Neuron; 23: 159-170.

Bennett MVL, Wurzel M, and Grundfest M (1961). Properties of electroplaques of Torpedo nobiliana. J Gen Physiol 44, 757-804.

Bennett MR, Farnell L, Gibson WG, Dickens P (2007). Mechanisms of calcium sequestration during facilitation at active zones of an amphibian neuromuscular junction. J. Theor. Biol.; 247: 230-241.

Bentz J (2000). Membrane fusion mediated by coiled coils: a hypothesis. Biophys. J.; 78(2): 886-900.

Bentz J and Mittal A (2003). Architecture of the influenza hemagglutinin membrane fusion site. Biochim. Biophys. Acta; 1614(1): 24-35.

Beutner D, Voets T, Neher E, Moser T (2001). Calcium dependence of exocytosis and endocytosis at the cochlear inner hair cell afferent synapse. Neuron; 29(3): 681-690.

Beyenbach KW and Wieczorek H (2006). The V-type H^+ ATPase: molecular structure and function, physiological roles and regulation. J. Exp. Biol.; 209(Pt 4): 577-589.

Bezprozvanny I, Zhong P, Scheller RH, Tsien RW (2000). Molecular determinants of the functional interaction between syntaxin and N-type Ca^{2+} channel gating. Proc Natl Acad Sci USA; 97(25): 13943-13948.

Billups B and Forsythe ID (2002). Presynaptic mitochondrial calcium sequestration influences transmission at mammalian central synapses. J. Neurosci.; 22: 5840-5847.

Birman S and Meunier FM (1985). Inactivation of acetylcholine release from Torpedo synaptosomes in response to prolonged depolarizations. J. Physiol.; 368: 293-307.

Birman S, Israël M, Lesbat B, Morel N (1986). Solubilization and partial purification of a pre-synaptic membrane protein ensuring calcium-dependent acetylcholine release from proteoliposomes. J Neurochem.; 47: 433-444

Blaustein MP and Hodgkin AL (1969). The effects of cyanide on calcium efflux in squid axons. J. Physiol. (London); 198: 46-48.

Bloc A, Bugnard E, Dunant Y, Falk-Vairant J, Israël M, Loctin F, Roulet E (1999). Acetylcholine synthesis and quantal release reconstituted by transfection of mediatophore and choline acetyltranferase cDNAs. Eur J Neurosci. 11: 1523-1534.

Bollmann JH and Sakmann B (2005). Control of synaptic strength and timing by the release-site Ca^{2+} signal. Nat. Neurosci.; 8: 426-434.

Bonzelius F and Zimmermann H (1990). Recycled synaptic vesicles contain vesicle but not plasma membrane marker, newly synthesized acetylcholine, and a sample of extracellular medium. J. Neurochem.; 55(4): 1266-1273.

Borden CR, Stevens CF, Sullivan JM, Zhu Y (2005). Synaptotagmin mutants Y311N and K326/327A alter the calcium dependence of neurotransmission. Mol. Cell Neurosci; 29(3): 462-470.

Borges R, Travis ER, Hochstetler SE, Wightman RM (1997). Effects of external osmotic pressure on vesicular secretion from bovine adrenal medullary cells. J. Biol. Chem.; 272(13): 8325-8331.

Borst JG and Sakmann B (1999). Depletion of calcium in the synaptic cleft of a calyx-type synapse in the rat brainstem. J. Physiol.; 521 Pt 1: 123-133.

Boyd IA and Martin AR (1956). Spontaneous subthreshold activity at mammalian neural muscular junctions. J. Physiol.; 132: 61-73.

Bradford SE and Nadler JV (2004). Aspartate release from rat hippocampal synaptosomes. Neuroscience; 128(4): 751-765.

Brehm P, Steinbach JH, Kidokoro Y (1982). Channel open time of acetylcholine receptors on Xenopus muscle cells in dissociated cell culture. Dev Biol. 91(1): 93-102.

Broadie K, Bellen HJ, DiAntonio A, Littleton JT, Schwarz TL (1994). Absence of synaptotagmin disrupts excitation-secretion coupling during synaptic transmission. Proc. Natl. Acad. Sci. USA; 91(22): 10727-10731.

Brochier G, Gulik-Krzywicki T, Lesbats B, Dedieu JC, Israël M (1992). Calcium-induced acetylcholine release and intramembrane particle occurrence in proteoliposomes equipped with mediatophore. Biol Cell.; 74(2): 225-230.

Buchs PA and Muller D (1996). Induction of long-term potentiation is associated with major ultrastructural changes of activated synapses. PNAS; 93: 8040-8045.

Budd SL and Nicholls DG (1996). A reevaluation of the role of mitochondria in neuronal Ca^{2+} homeostasis. J. Neurochem.; 66: 403-411.

Burrone J, Neves G, Gomis A, Cooke A, Lagnado L (2002). Endogenous calcium buffers regulate fast exocytosis in the synaptic terminal of retinal bipolar cells. Neuron; 33(1): 101-12.

Castonguay A and Robitaille R (2001). Differential regulation of transmitter release by presynaptic and glial Ca^{2+} internal stores at the neuromuscular synapse. J Neurosci. 21: 1911-1922.

Catterall WA (2000). Structure and regulation of voltage-gated Ca^{2+} channels. Annu. Rev. Cell. Dev. Biol; 16: 521-555.

Cavalli A, Eder-Colli L, Dunant Y, Loctin F, Morel N (1991). Release of acetylcholine from Xenopus oocytes injected with mRNAs from cholinergic neurons. EMBO J.; 10: 1671-1675.

Ceccarelli B, Hurlbut WP, Mauro A (1973). Turnover of transmitter and synaptic vesicles at the frog neuromuscular junction. J. Cell Biol.; 57(2): 499-524.

Chapman ER (2002). Synaptotagmin: a Ca^{2+} sensor that triggers exocytosis? Nature Reviews; 3: 1-11.

Chapman ER, An S, Edwardson JM, Jahn R (1996). A novel function for the second C2 domain of synaptotagmin. Ca^{2+}-triggered dimerization. J. Biol. Chem.; 271(10): 5844-5849.

Chapman ER, Desai RC, Davis AF, Tornehl CK (1998). Delineation of the oligomerization, AP-2 binding, and synprint binding region of the C2B domain of synaptotagmin. J. Biol. Chem.; 273(49): 32966-32972.

Chapman ER, Hanson PI, An S, Jahn R (1995). Ca^{2+} regulates the interaction between synaptotagmin and syntaxin 1. J. Biol. Chem.; 270(40): 23667-13671.

Charlton MP, Smith SJ, Zucker RS (1982). Role of presynaptic calcium ions and channels in synaptic facilitation and depression at the squid giant synapse. J. Physiol.; 323:173-193.

Charvin N, L'evêque C, Walker D, Berton F, Raymond C, Kataoka M, Shoji-Kasai Y, Takahashi M, De Waard M, Seagar MJ (1997). Direct interaction of the calcium sensor protein synaptotagmin I with a cytoplasmic domain of the alpha1A subunit of the P/Q-type calcium channel. EMBO J; 16(15): 4591-4596.

Chmouliovsky-Moghissi M and Dunant Y (1979). Breakdown of creatine phosphate and ATP in nerve terminals and electroplaques of the Torpedo electric organ: comparison with the electrical energy dissipated. J. Neurochem.; 32: 1287-1294.

Christensen KA, Myers JT, Swanson JA(2002). pH-dependent regulation of lysosomal calcium in macrophages. J. Cell. Sci.; 115(Pt 3): 599-607.

Churchill GC, Okada Y, Thomas JM, Genazzani AA, Patel S, Galione A (2002). NAADP mobilizes Ca^{2+} from reserve granules, lysosome-related organelles, in sea urchin eggs. Cell; 111(5): 703-708.

Cohen MW, Jones OT, Angelides KJ (1991). Distribution of Ca^{2+} channels on frog motor nerve terminals revealed by fluorescent omega-conotoxin. J. Neurosci.; 11(4): 1032-1039.

Collin T, Chat M, Lucas MG, Moreno H, Racay P, Schwaller B, Marty A, Llano I (2005). Developmental changes in parvalbumin regulate presynaptic Ca^{2+} signaling. J. Neurosci. ; 25(1): 96-107.

Colquhoun D, Large WA, Rang HP (1977). An analysis of the action of a false transmitter at the neuromuscular junction. J. Physiol.; 266(2): 361-395.

Corthay J, Dunant Y, Loctin F (1982). Acetylcholine changes underlying transmission of a single nerve impulse in the presence of 4-aminopyridine in Torpedo. J. Physiol. Lond. ; 325: 461-479.

Cousin MA and Nicholls DG (1997). Synaptic vesicle recycling in cultured cerebellar granule cells: role of vesicular acidification and refilling. J. Neurochem.; 69(5): 1927-1935.

Couteaux R and Pécot-Dechavassine M (1973). Données ultrastructurales et cytochimiques sur le mécanisme de libération de l'acétylcholine dans la transmission synaptique. Arch. Ital. Biol.; 3: 231-262.

Couteaux R and Pécot-Dechavassine M (1970). Vesicules synaptiques et poches au niveau des « zones actives » de la jonction neuromusculaire. CR. Acad. Sci. (Paris) ; 271: 2346-2349.

Couteaux R and Pécot-Dechavassine M (1974). Les zone spécialisées des membane présynaptique. CR Acad Sci (Paris); 278: 291-293.

Creager R, Dunwiddie T, Lynch G (1980). Paired-pulse and frequency facilitation in the CA1 region of the in vitro rat hippocampus. J. Physiol.; 299: 409-424.

Cremona O and De Camilli P (2001). Phosphoinositides in membrane traffic at the synapse. J. Cell Sci. ; 114(Pt 6): 1041-1052.

Crider BP and Xie XS (2003). Characterization of the functional coupling of bovine brain vacuolar-type H^+-translocating ATPase. Effect of divalent cations, phospholipids, and subunit H (SFD). J. Biol. Chem.; 278(45): 44281-44288.

Curran MJ and Brodwick MS (1991). Ionic control of the size of the vesicle matrix of beige mouse mast cells. J. Gen. Physiol.; 98(4): 771-790.

David G and Barrett EF (2003). Mitochondrial Ca^{2+} uptake prevents desynchronization of quantal release and minimizes depletion during repetitive stimulation of mouse motor nerve terminals. J. Physiol.; 548: 425-438.

David G, Barrett JN, Barrett EF (1998). Evidence that mitochondria buffer physiological Ca^{2+} loads in lizard motor nerve terminals. J. Physiol.; 509: 59-65.

Davis FD, Bai J, Fasshauer D, Wolowick MJ, Lewis JL, Chapman, ER (1999). Kinetics of synaptotagmin responses to Ca^{2+} and assembly with the core SNARE complex onto membranes. Neuron; 24: 363-376.

Davletov BA, Meunier FA, Ashton AC, Matsushita H, Hirst WD, Lelianova VG, Wilkin GP, Dolly JO, Ushkaryov YA (1998). Vesicle exocytosis stimulated by alpha-latrotoxin is mediated by latrophilin and requires both external and stored Ca^{2+}. EMBO J.; 17(14): 3909-3920.

De Angeli A, Monachello D, Ephritikhine G, Frachisse JM, Thomine S, Gambale F, Barbier-Brygoo H (2006). The nitrate/proton antiporter AtCLCa mediates nitrate accumulation in plant vacuoles. Nature; 442: 939-942.

De Robertis E, Rodriguez De Lores Arnaiz G, Salganicoff L, Pellegrino de Iraldi A, and Zieher LM (1963). Isolation of synaptic vesicles and structural organization of the acetycholine system within brain nerve endings. J. Neurochem.; 10: 225-235

De Robertis EDP and Bennett HS (1955). Some features of the submicroscopic morphology of isolated cholinergic synaptic vesicles. Brain Res. 71:47-58.

De Robertis EDP, Pellegrino de Iraldi A, Rodriguez de Lorez Arnaiz G, Salganicoff L (1961). Electron microscopic observations on nerve endings isolated from rat brain. Anat. Rec.; 139: 220-221.

Deamer DW, Prince RC, Crofts AR (1972). The response of fluorescent amines to pH gradients across liposome membranes. Biochim. Biophys. Acta; 274(2): 323-335.

Del Castillo J and Katz B (1954). Quantal components of the end plate potential. J. Physiol. (London); 124: 560-573.

Del Castillo J and Stark L (1952). The effect of calcium ions on the motor end-plate potentials. J. Physiol. (London); 116: 507-515.

Delgado R, Maureira C, Oliva C, Kidokoro Y, Labarca P (2000). Size of vesicle pools, rates of mobilization, and recycling at neuromuscular synapses of a Drosophila mutant, shibire. Neuron.; 28(3): 941-953.

Deri Z, Bors P, Adam-Vizi V (1993). Effect of alpha-latrotoxin on acetylcholine release and intracellular Ca^{2+} concentration in synaptosomes: Na^{+}-dependent and Na^{+}-independent components. J. Neurochem.; 60(3): 1065-1072.

DiAntonio A, Parfitt KD, Schwarz TL (1993). Synaptic transmission persists in synaptotagmin mutants of Drosophila. Cell; 73(7): 1281-1290.

DiAntonio A and Schwarz TL (1994). The effect on synaptic physiology of synaptotagmin mutations in Drosophila. Neuron; 12(4): 909-920.

Diebler MF (1982). Acetylcholine release from isolated synaptic vesicles related to ionic permeability changes: continuous detection with a chemiluminescent method. J. Neurochem.; 39(5): 1405-1411.

Dipolo R, Requena J, Brinley FJ Jr, Mullins LJ, Scarpa A, Tiffert T (1976). Ionized calcium concentrations in squid axons. J Gen Physiol.; 67(4): 433-467.

Dobrunz LE and Stevens CF (1997). Heterogeneity of release probability, facilitation, and depletion at central synapses. Neuron. 18: 995-1008.

Dodge FA Jr, Miledi R, Rahamimoff R (1961). Strontium and quantal release of transmitter at the neuromuscular junction. J. Physiol.; 200(1): 267-283.

Dodge FA and Rahamimoff R (1967). Co-operative action of calcium ions in transmitter release at the neuromuscular junction. J. Physiol. (London); 193: 419-432.

Douglas WW and Rubin RP (1961). The role of calcium in the secretory response of the adrenal medulla to acetylcholine. J Physiol.; 159: 40-57.

Dröse S and Altendorf K (1997). Bafilomycins and concanamycins as inhibitors of V-ATPases and P-ATPases. J. Exp. Biol.; 200: 1-8.

Dudel J and Kuffler SW (1961). The quantal nature of transmission and spontaneous miniature potentials at the crayfish neuromuscular junction. J. Physiol.; 155: 514-529.

Dulubova IE, Krasnoperov VG, Khvotchev MV, Pluzhnikov KA, Volkova TM, Grishin EV, Vais H, Bell DR, Usherwood PN (1996). Cloning and structure of delta-latroinsectotoxin, a novel insect-specific member of the latrotoxin family: functional expression requires C-terminal truncation. J. Biol. Chem.; 271(13): 7535-7543.

Dumont RA, Lins U, Filoteo AG, Penniston JT, Kachar B and Gillespie (2001). Plasma membrane Ca^{2+}-ATPase isoform 2a is the PMCA of hair bundles. J.Neurosci.; 21: 5066-5078.

Dunant Y (1986). On the mechanism of acetylcholine release. Prog Neurobiol.; 26: 55-92.

Dunant Y (1994).Hormones and neurotransmitters release: four mechanisms of secretion. Cell Biol. Int.; 18(5): 327-336.

Dunant Y (2006). Acetylcholine release in rapid synapses: two fast partners -mediatophore and vesicular Ca^{2+}/H^{+} antiport. J. Mol. Neurosci.; 30(1-2): 209-214.

Dunant Y and Muller D (1986). Quantal release of acetylcholine evoked by focal depolarisation at the Torpedo nerve-electroplaque junction. J. Physiol. Lond.; 379: 461-478.

Dunant Y, Babel-Guein E, Droz B (1980b). Calcium metabolism and acetylcholine release at the nerve-electroplaque junction. J Physiol (Paris). Sep; 76(5): 471-478.

Dunant Y and Bloc A (2003). Low- and high-affinity reactions in rapid neurotransmission. Neurochem Res.; 28(3-4): 659-665.

Dunant Y, Gautron J, Israël M, Lesbats B, Manaranche R (1972). Acetylcholine compartments in stimulated electric organ of Torpedo marmorata. J. Neurochem.; 19: 1987-2002.

Dunant Y, Gautron J, Israël M, Lesbats B, Manaranche R (1974). Changes in acetylcholine level and electrophysiological response during continuous stimulation of the electric organ of Torpedo marmorata. J Neurochem.; 23: 635-643.

Dunant Y and Israël M (2000). Neurotransmitter release at rapid synapses. Biochimie; 82(4): 289-302.

Dunant Y and Israël M (1985). The release of acetylcholine. Scientific American 252: 58-66

Dunant Y and Israël M (1995). Mediatophore and other presynaptic proteins. A cybernetic linking at the active zone. J. Physiol. Paris; 89(3): 147-156.

Dunant Y, Loctin F, Marsal J, Muller D, Párducz A, Rabasseda X (1988). Energy metabolism and quantal acetylcholine release: effects of botulinum toxin, 1-fluoro-2,4-dinitrobenzene, and diamide in the Torpedo electric organ. J Neurochem.; 50: 431-439.

Dunant Y, Eder L, Servetiadis-Hirt L (1980a). Acetylcholine release evoked by a single or a few nerve impulse in the electric organ of Torpedo. J. Physiol. (London); 298: 185-203.

Dunant Y, Estade M, Magistris MR, Safran AB (1995). La toxine botulique. 1. Le pire des poisons. Med et Hyg.; 53 :1384-1389.

Dunant Y, Loctin F, Vallée JP, Párducz A, Lesbats B, Israël M (1996). Activation and desensitization of acetylcholine release by zinc at Torpedo nerve terminals. Pflugers Arch.; 432: 853-858.

Earles CA, Bai J, Wang P, Chapman ER (2001). The tandem C2 domains of synaptotagmin contain redundant Ca^{2+} binding sites that cooperate to engage t-SNAREs and trigger exocytosis. J. Cell Biol.; 154(6): 1117-1123.

Egelman DM and Montague PR (1999). Calcium dynamics in the extracellular space of mammalian neural tissue. Biophys. J.; 76(4): 1856-1867.

Evans RM and Zamponi GW (2006). Presynaptic Ca^{2+} channels- integration centers for neuronal signaling pathways.Trends Neurosci. 29(11): 617-24.

Fatt P and Katz B (1952). Spontaneous subthreshold activity at motor nerve endings.J Physiol. 117:109-128.

Fedchyshyn MJ and Wang LY (2007). Activity-dependent changes in temporal components of neurotransmission at the juvenile mouse calyx of Held synapse. J. Physiol.; 581(Pt 2): 581-602.

Fenwick EM, Marty A, Neher E (1982). Sodium and calcium channels in bovine chromaffin cells. J. Physiol. ; 331: 599-635.

Ferguson SM and Blakely RD (2004). The choline transporter resurfaces: new roles for synaptic vesicles? Mol. Interv. ; 4: 22–37.

Ferguson SM, Savchenko V, Apparsundaram S, Zwick M, Wright J, Heilman CJ, Yi H, Levey AI, Blakely RD (2003). Vesicular localization and activity-dependent trafficking of presynaptic choline transporters. J. Neurosci. ; 23(30): 9697-9709.

Fernandez I, Arac D, Ubach J, Gerber SH, Shin O, Gao Y, Anderson RG, Sudhof TC, Rizo J (2001). Three-dimensional structure of the synaptotagmin 1 C2B-domain: synaptotagmin 1 as a phospholipid binding machine. Neuron; 32(6): 1057-1069.

Fernandez JM, Villalon M, Verdugo P (1991). Reversible condensation of mast cell secretory products in vitro. Biophys. J. ; 59(5): 1022-1027.

Fessard A (1958). Les organes électriques, in Traité de Zoologie (Grassé P. P., ed.), pp. 1143-1238. Masson, Paris.

Findlay I (2004). Physiological modulation of inactivation in L-type Ca^{2+} channels: one switch. J. Physiol; 554(Pt 2): 275-283.

Forsythe ID, Tsujimoto T, Barnes-Davies M, Cuttle MF, Takahashi T (1998). Inactivation of presynaptic calcium current contributes to synaptic depression at a fast central synapse. Neuron; 20(4):797-807.

Fosse VM, Kolstad J and Fonnum F (1986). A bioluminescence method for the measurement of L-glutamate: applications to the study of changes in the release of L-glutamate from lateral geniculate nucleus and superior colliculus after visual cortex ablation in rats. J. Neurochem.; 47: 340-349.

Fossier P, Diebler MF, Mothet JP, Israël M, Tauc L, Baux G (1998). Control of the calcium concentration involved in acetylcholine release and its facilitation: an additional role for synaptic vesicles? Neuroscience; 85(1): 85-91.

Friel DD and Tsien RW (1994). An FCCP-sensitive Ca^{2+} store in bullfrog sympathetic neurons and its participation in stimulus-evoked changes in $[Ca^{2+}]_i$. J. Neurosci.; 14: 4007-4024.

Fukuda M, Kanno E, Mikoshiba K (1999). Conserved N-terminal cysteine motif is essential for homo- and heterodimer formation of synaptotagmins III, V, VI, and X. J. Biol. Chem.; 274(44): 31421-31427.

Fukuda M, Moreira JE, Lewis FM, Sugimori M, Niinobe M, Mikoshiba K, LLinás R (1995). Role of the C2B domain of synaptotagmin in vesicular release and recycling as determined by specific antibody injection into the squid giant synapse preterminal. Proc. Natl. Acad. Sci. USA; 92(23): 10708-10712.

Fukuda M, Moreira JE, Liu V, Sugimori M, Mikoshiba K, LLinás RR (2000). Role of the conserved WHXL motif in the C terminus of synaptotagmin in synaptic vesicle docking. Proc. Natl. Acad. Sci. USA; 97(26): 14715-14719.

Fukuda M, Kanno E, Ogata Y, Mikoshiba K (2001). Mechanism of sds-resistant synaptotagmin clustering mediated by the cysteine cluster at the interface between the transmembrane and spacer domains. J. Biol. Chem.; 276: 40319-40325.

Fukuda M, Kowalchyk JA, Zhang X, Martin TFJ, Mikoshiba K (2002). Synaptotagmin IX regulates Ca^{2+}-dependent secretion in PC12 cells. J. Biol. Chem..; 277:4601-4604.

Fukuda M and Mikoshiba K (2000). Distinct self-oligomerization activities of synaptotagmin family. J.Biol.Chem. 275: 28180- 28185.

Fulop T, Radabaugh S, Smith C (2005). Activity-dependent differential transmitter release in mouse adrenal chromaffin cells. J Neurosci.; 25(32): 7324-7332.

Gaietta G, Deerinck TJ, Adams SR, Bouwer J, Tour O, Laird DW, Sosinsky GE, Tsien RY, Ellisman MH (2002). Multicolor and electron microscopic imaging of connexin trafficking. Science; 296(5567): 503-507.

Galli T, McPherson PS, De Camilli P (1996). The V0 sector of the V-ATPase, synaptobrevin, and synaptophysin are associated on synaptic vesicles in a Triton X-100-resistant, freeze-thawing sensitive complex. J Biol Chem.; 271(4): 2193-2198.

Garcia AG, Garcia-de-Diego AM, Gandia L, Borges R, Garcia-Sancho J (2006). Calcium signaling and exocytosis in adrenal chromaffin cells. Physiol Rev. 86(4):1093-131.

Geppert M, Goda Y, Hammer RE, Li C, Rosahl TW, Stevens CF, Sudhof TC (1994). Synaptotagmin I: a major Ca^{2+} sensor for transmitter release at a central synapse. Cell; 79(4): 717-727.

Gerasimenko JV, Sherwood M, Tepikin AV, Petersen OH, Gerasimenko OV (2006). NAADP, cADPR and IP3 all release Ca^{2+} from the endoplasmic reticulum and an acidic store in the secretory granule area. J. Cell. Sci.; 119(Pt 2): 226-238.

Gibbons DL, Vaney MC, Roussel A, Vigouroux A, Reilly B, Lepault J, Kielian M, Rey FA (2004). Conformational change and protein-protein interactions of the fusion protein of Semliki Forest virus. Nature; 427(6972): 320-325.

Gilbert RJ, Jimenez JL, Chen S, Tickle IJ, Rossjohn J, Parker M, Andrew PW, Saibil HR (1999). Two structural transitions in membrane pore formation by pneumolysin, the pore-forming toxin of Streptococcus pneumoniae. Cell; 97(5): 647-655.

Girod R, Corrèges P, Jacquet J, Dunant Y (1993). Space and time characteristics of transmitter release at the nerve-electroplaque junction of *Torpedo*. J. Physiol.; 471: 129-157.

Girod R, Eder-Colli L, Medilanski J, Dunant Y, Tabti N, Poo MM (1992). Pulsatile release of acetylcholine by nerve terminals (synaptosomes) isolated from Torpedo electric organ. J. Physiol.; 450: 325-340.

Goda Y and Stevens CF (1994). Two components of transmitter release at a central synapse. Proc. Natl. Acad. Sci. USA; 91(26): 12942-12946.

Goffinet G (1978). Calcium-binding sites as determined by electron microscope X-ray microanalysis in the electrocytes of the electric organ of Torpedo marmorata. Histochemistry; 58(4): 307-317.

Gonçalves PP, Meireles SM, Gravato C, Vale MG (1998). Ca^{2+}-H^+ antiport activity in synaptic vesicles isolated from sheep brain cortex. Neurosci Lett.; 247(2-3): 87-90.

Gonçalves PP, Meireles SM, Neves P, Vale MG (1999a). Ionic selectivity of the Ca^{2+}/H^+ antiport in synaptic vesicles of sheep brain cortex. Brain Res. Mol. Brain Res.; 67(2): 283-291.

Gonçalves PP, Meireles SM, Neves P, Vale MG (1999b). Synaptic vesicle Ca^{2+}/H^+ antiport: dependence on the proton electrochemical gradient. Brain Res Mol Brain Res. 71(2): 178-84.

Gonçalves PP, Meireles SM, Neves P, Vale MG (2000b). Methods for analysis of Ca^{2+}/H^+ antiport activity in synaptic vesicles isolated from sheep brain cortex. Brain Res. Brain Res. Protoc.; 5(1): 102-108.

Gonçalves PP, Meireles SM, Neves P, Vale MG (2000a). Distinction between Ca^{2+} pump and Ca^{2+}/H^+ antiport activities in synaptic vesicles of sheep brain cortex. Neurochem Int. 37(4): 387-396.

Gornall AG, Bardawill ChJ, David MM (1949). Determination of serum proteins by means of the biuret reaction, J. Biol. Chem.; 177: 751–766.

Gouaux E (1997). Channel-forming toxins: tales of transformation. Curr. Opin. Struct. Biol.; 7(4): 566-573.

Graf E, Verma AK, Gorski JP, Lopaschuk G, Niggli V, Zurini M, Carafoli E, Penniston JT (1982). Molecular properties of calcium-pumping ATPase from human erythrocytes. Biochemistry; 21(18): 4511-4516.

Griffin BA, Adams SR, Tsien RY (1998). Specific covalent labeling of recombinant protein molecules inside live cells. Science; 281 (5374): 269 – 272.

Grohovaz F, Bossi M, Pezzati R, Meldolesi J, Tarelli FT (1996). High resolution ultrastructural mapping of total calcium: electron spectroscopic imaging/electron energy loss spectroscopy analysis of a physically/chemically processed nerve-muscle preparation. Proc. Natl. Acad. Sci. USA; 93(10): 4799-4803.

Grynkiewicz G, Poenie M, Tsien RY (1985). A new generation of Ca^{2+} indicators with greatly improved fluorescence properties. J. Biol. Chem.; 260(6): 3440-3450.

Gu F and Gruenberg J (2000). ARF1 regulates pH-dependent COP functions in the early endocytic pathway. J. Biol. Chem; 275(11): 8154-8160.

Guatimosim C, Romano-Silva MA, Gomez MV, Prado MA (1998). Recycling of synaptic vesicles at the frog neuromuscular junction in the presence of strontium. J. Neurochem.; 70(6): 2477-2483.

Guo J and Duff HJ (2006). Calmodulin kinase II accelerates L-type Ca^{2+} current recovery from inactivation and compensates for the direct inhibitory effect of $[Ca^{2+}]_i$ in rat ventricular myocytes. J. Physiol.; 574(Pt 2): 509-518.

Guo X, Macleod GT, Wellington A, Hu F, Panchumarthi S, Schoenfield M, Marin L, Charlton MP, Atwood HL, Zinsmaier KE (2005). The GTPase dMiro is required for axonal transport of mitochondria to Drosophila synapses. Neuron; 47: 379-393.

Han W, Rhee JS, Maximov A, Lao Y, Mashimo T, Rosenmund C, Sudhof TC (2004). N-glycosylation is essential for vesicular targeting of synaptotagmin 1. Neuron; 41(1): 85-99.

Harlow ML, Ress D, Stoschek A, Marshall RM, McMahan UJ (2001). The architecture of active zone material at the frog's neuromuscular junction. Nature; 409(6819): 479-484.

Harvey AM and MacIntosh FC (1940). Calcium and synaptic transmission in a sympathetic ganglion. J. Physiol. (London); 97:408-416.

Haucke V and De Camilli P (1999). AP-2 recruitment to synaptotagmin stimulated by tyrosine-based endocytic motifs. Science; 285(5431): 1268-1271.

Hausinger A, Volknandt W, Kretzschmar S, Kellner R, Zimmermann H (1996). Two synpatic vesicle proteins of 25 kDa: a comparison of the molecular properties and tissue distribution of svp25 and o-rab3. Neurochem. Int.; 28(3): 251-258.

Haydon PG, Henderson E, Stanley EF (1994). Localization of individual calcium channels at the release face of a presynaptic nerve terminal. Neuron; 13(6): 1275-80.

Haynes CL, Buhler LA, Wightman RM (2006). Vesicular Ca^{2+}-induced secretion promoted by intracellular pH-gradient disruption. Biophys. Chem.; 123: 20-24.

Heidelberger R, Heinemann C, Neher E, Matthews G (1994). Calcium dependence of the rate of exocytosis in a synaptic terminal. Nature; 371 (6497): 513-515.

Heinemann U, Lux HD, Gutnick MJ (1977). Extracellular free calcium and potassium during paroxsmal activity in the cerebral cortex of the cat. Exp. Brain Res.; 27(3-4): 237-243.

Hell JW, Maycox PR, Jahn R. (1990). Energy dependence and functional reconstitution of γ-aminobutyric acid carrier from synaptic vesicles. J. Biol. Chem.; 265: 2111–2117.

Hell JW, Maycox PR, Stadler H, Jahn R (1988). Uptake of GABA by rat brain synaptic vesicles isolated by a new procedure. EMBO J. 7: 3023-3029.

Helmchen F, Imoto K, Sakmann B (1996). Ca^{2+} buffering and action potential-evoked Ca^{2+} signaling in dendrites of pyramidal neurons. Biophys. J.; 70(2): 1069-1081.

Helme-Guizon A, Davis S, Israël M, Lesbats B, Mallet J, Laroche S, Hicks A (1998). Increase in syntaxin 1B and glutamate release in mossy fibre terminals following induction of LTP in the dentate gyrus: a candidate molecular mechanism underlying transsynaptic plasticity. Eur J Neurosci.; 10: 2231-2237.

Herrington J, Park YB, Babcock DF, Hille B (1996). Dominant role of mitochondria in clearance of large Ca^{2+} loads from rat adrenal chromaffin cells. Neuron; 16: 219-228.

Heuser JE, Reese TS, Landis DM (1974). Functional changes in frog neuromuscular junctions studied with freeze-fracture. J Neurocytol.; 3(1): 109-131.

Hiesinger PR, Fayyazuddin A, Mehta SQ, Rosenmund T Schulze KL, Zhai RG, Verstreken P, Cao Y, Zhou Y, Kunz J, Bellen HJ (2005). The v-ATPase V0 subunit a1 is required for a late step in synaptic vesicle exocytosis in Drosophila. Cell; 121(4): 607-620.

Hirayama BA, Loo DD, Wright EM (1994). Protons drive sugar transport through the Na^+/glucose cotransporter (SGLT1). J. Biol. Chem.; 269(34): 21407-21410.

Hlubek M, Tian D, Stuenkel E L(2003). Mechanism of alpha-latrotoxin action at nerve endings of neurohypophysis. Brain Res.; 992(1): 30-42.

Hlubek MD, Stuenkel EL, Krasnoperov VG, Petrenko AG, Holz RW (2000). Calcium-independent receptor for alpha-latrotoxin and neurexin 1alpha facilitate toxin-induced channel formation: evidence that channel formation results from tethering of toxin to membrane. Mol. Pharmacol.; 57(3): 519-528.

Hodgkin AL, Huxley AF, Katz B (1952). Measurement of current-voltage relations in the membrane of the giant axon of Loligo. J. Physiol. (London). 116:424-48.

Holz RW, Hlubek MD, Sorensen SD, Fisher SK, Balla T, Ozaki S, Prestwich GD, Stuenkel EL, Bittner MA (2000). A pleckstrin homology domain specific for phosphatidylinositol 4, 5-bisphosphate (PtdIns-4,5-P2) and fused to green fluorescent protein identifies plasma membrane PtdIns-4,5-P2 as being important in exocytosis. J. Biol. Chem.; 275(23): 17878-17885.

Hsu S, Augustine GJ, Jackson J (1996). Adaptation of Ca^{2+}-triggeres exocytosis in presynaptic terminals. Neuron; 17: 501-512.

Hua SY, Teylan MA, Cimenser A (2007). An antibody to synaptotagmin I facilitates synaptic transmission. Eur. J. Neurosci; 25(11): 3217-3225.

Hubbard JI (1961). The effect of calcium and magnesium on the spontaneous release of transmitter from mammalian motor nerve endings. J. Physiol.; 159: 507-517.

Hubbard JI, Jones SF, Landau EM (1968). On the mechanism by which calcium and magnesium affect the release of transmitter by nerve impulses. J. Physiol.; 196: 75-86.

Humeau Y, Doussau F, Grant NJ, Poulain B (2000). How botulinum and tetanus neurotoxins block neurotransmitter release. Biochimie; 82(5): 427-446.

Hurlbut WP, Chieregatti E, Valtorta F, Haimann C (1994). Alpha-latrotoxin channels in neuroblastoma cells. J. Membr. Biol.; 138(1): 91-102.

Iezzi M, Theander S, Janz R, Loze C, Wollheim CB (2005). SV2A and SV2C are not vesicular Ca^{2+} transporters but control glucose-evoked granule recruitment. J. Cell Sci. ; 118(Pt 23): 5647-5660.

Israël M (1972). Données actuelles sur la localisation de l'acétylcholine des jonctions myoneurales et nerf-électroplaque. Actualités Pharmacol. 25 :1-22.

Israël M and Dunant Y (2004). Acetylcholine- and glutamate-mediated transmission: one mediatophore with different specificities, or several mediatophores? In : Cholinergic mechanisms – function and dysfunction. Chap 66. Silman I., Soreq H., Anglister L., Michaelson D., Fisher A. Taylor & Francis Ed. 459-461.

Israël M, Gautron J, Lesbats B (1968). Isolement des vésicules synaptiques de l'organe électrique de la Torpille et localisation de l'acétiylcholine à leur niveau. C.R.Acad.Sc. Paris ; 266: 273-275.

Israël M and Lesbats B (1981a). Continuous determination by a chemiluminescent method of acetylcholine release and compartmentation in Torpedo electric organ synaptosomes. J. Neurochem.; 37: 1475-1483.

Israël M and Lesbats B (1981b). Chemiluminescent determination of acetylcholine, continuous detection of its release from *Torpedo* electric organ synapses and synapto*somes*. Neurochem. Int.; 3: 81-90.

Israël M, Lesbats B, and Bruner J (1993). Glutamate and acetylcholine release from cholinergic nerve terminals, a calcium control of the specificity of the release mechanism. Neurochem. Int.; 22: 53-58.

Israël M and Lesbats B (1982). Application to mammalian tissues of the chemiluminescent method for detecting acetylcholine. J.Neurochem.; 39: 248-250.

Israël M, Manaranche R, Marsal J, Meunier FM, Morel P, Frachon P, Lesbats B (1980). ATP-dependent calcium uptake by cholinergic synaptic vesicles isolated from *Torpedo* electric organ. J Membrane Biol. ; 54:115-26.

Israël M, Manaranche R, Mastour-Frachon P, Morel N (1976). Isolation of pure cholinergic nerve endings from the electric organ of Torpedo marmorata. Biochem. J. 160: 113-115.

Israël M, Manaranche R, Morel N, Dedieu JC, Gulik-Krzywicki T, Lesbats B (1981). Redistribution of intramembrane particles related to acetylcholine release by cholinergic synaptosomes. J. Ultrastruct. Res.; 75(2): 162-178.

Israël M, Meunier FM, Morel N, Lesbats B (1987). Calcium-induced desensitization of acetylcholine release from synaptosomes or proteoliposomes equipped with mediatophore, a presynaptic membrane protein. J. Neurochem.; 49: 975-982.

Israël M, Morel N, Lesbats B, Birman S, Manaranche R (1986). Purification of a presynaptic membrane protein that mediates a calcium-dependent translocation of acetylcholine. Proc. Natl. Acad. Sci. USA.; 83(23): 9226-9230.

Israël M, Whittaker VP (1965). The isolation of mossy fibre endings from the granular layer of the cerebellar cortex. Experientia; 21(6): 325-326.

Jena BP, Schneider SW, Geibel JP, Webster P, Oberleithner H, Sritharan KC (1997). Gi regulation of secretory vesicle swelling examined by atomic force microscopy. Proc. Natl. Acad. Sci. USA; 94(24): 13317-13322.

Jorgensen EM, Hartwieg E, Schuske K, Nonet ML, Jin Y, Horvitz HR (1995). Defective recycling of synaptic vesicles in synaptotagmin mutants of Caenorhabditis elegans. Nature; 378(6553): 196-199.

Juhaszova M, Church P, Blaustein MP, Stanley EF (2000). Location of calcium transporters at presynaptic terminals. Eur J Neurosci. 12: 839-846.

Kachoei BA, Knox RJ, Uthuza D, Levy S, Kaczmarek LK, Magoski NS (2006). A store-operated Ca^{2+} influx pathway in the bag cell neurons of Aplysia. J. Neurophysiol.; 96(5): 2688-2698.

Kamiya H and Zucker RS (1994). Residual Ca^{2+} and short-term synaptic plasticity. Nature; 371: 603-606.

Kane PM (2000). Regulation of V-ATPases by reversible disassembly. FEBS Letters; 469(2): 137-141.

Kass GE, Duddy SK, Moore GA, Orrenius S (1989). 2,5-Di-(tert-butyl)-1,4-benzohydroquinone rapidly elevates cytosolic Ca^{2+} concentration by mobilizing the inositol 1,4,5-trisphosphate-sensitive Ca^{2+} pool. J. Biol. Chem.; 264: 15192-15198.

Katz B and Miledi R (1968). The role of calcium in neuromuscular facilitation. J. Physiol.; 195: 481-492.

Katz B and Miledi R (1970). Further study of the role of calcium in synaptic transmission. J Physiol. 207: 789-801.

Katz B (1969). The release of neuronal transmitter substances. Liverpool University Press.

Katz B and Miledi R (1965). The effect of calcium on acetylcholine release from nerve terminals. Proc R Soc Lond B.; 161: 496-503.

Katz B and Miledi R (1967a). The timing of calcium action during neuromuscular transmission. J. Physiol. (London); 189: 535-544.

Katz B and Miledi R (1967b). A study of synaptic transmission in the absence of nerve impulse. J. Physiol. (London). 192: 407-436.

Katz B and Miledi R (1969). Tetrodotoxin-resistant electric activity in pre-synaptic terminals. J. Physiol. (London). 203: 459-487.

Katz B and Miledi R (1977). Transmitter leakage from motor nerve endings. Proc. R. Soc. Lond. B Biol. Sci.; 196(1122): 59-72.

Kee Y and Scheller RH (1999). Localization of synaptotagmin-binding domains on syntaxin. J. Neurosci.; 16(6): 1975-1981.

Keicher E, Bilbaut A, Maggio K, Hernandez-Nicaise ML, Nicaise G (1990). The Desheathed Periphery of Aplysia Giant Neuron. Fine structure and measurement of $[Ca^{2+}]_o$ fluctuations with calcium-selective microelectrodes. Eur. J. Neurosci.;3(1): 10-17.

Kidokoro Y and Rohrbough J (1990). Acetylcholine receptor channels in Xenopus myocyte culture; brief openings, brief closures and slow desensitization. J Physiol. 425:227-44.

Kiene ML and Stadler H (1987). Synaptic vesicles in electromotoneurones. I. Axonal transport, site of transmitter uptake and processing of a core proteoglycan during maturation. EMBO J.; 6(8): 2209-2215.

Kilic G, Angleson JK, Cochilla AJ, Nussinovitch I, Betz WJ (2001). Sustained stimulation of exocytosis triggers continuous membrane retrieval in rat pituitary somatotrophs. J. Physiol.; 532(Pt 3): 771-783.

Kim MH, Korogod N, Schneggenburger R, Ho WK, Lee SH (2005). Interplay between Na^+/Ca^{2+} exchangers and mitochondria in Ca^{2+} clearance at the calyx of Held. J Neurosci.; 25(26):6057-6065.

Kirichok Y, Krapivinsky G, Clapham DE (2004). The mitochondrial calcium uniporter is a highly selective ion channel. Nature; 427(6972): 360-364.

Kishimoto T, Liu TT, Ninomiya Y, Takagi H, Yoshioka T, Ellis-Davies GC, Miyashita Y, Kasai H (2001). Ion selectivities of the Ca^{2+} sensors for exocytosis in rat phaeochromocytoma cells. J. Physiol.; 533(Pt 3): 627-637.

Klimjack MR, Jeffrey S, Kielian M (1994). Membrane and protein interactions of a soluble form of the Semliki Forest virus fusion protein. J Virol; 68(11): 6940-6946.

Klingauf J and Neher E (1997). Modeling buffered Ca^{2+} diffusion near the membrane: implications for secretion in neuroendocrine cells. Biophys J.; 72(2 Pt 1): 674-690.

Koh TW and Bellen HJ (2003). Synaptotagmin I, a Ca^{2+} sensor for neurotransmitter release. Trends Neurosci.; 26(8): 413-22.

Kosaka T and Ikeda K (1983). Possible temperature-dependent blockage of synaptic vesicle recycling induced by a single gene mutation in Drosophila. J. Neurobiol.; 14(3): 207-225.

Krasilnikov OV and Sabirov RZ (1992). Comparative analysis of latrotoxin channels of different conductance in planar lipid bilayers. Evidence for cluster organization. Biochim. Biophys. Acta; 1112(1): 124-128.

Kreiner L and Lee A (2006). Endogenous and exogenous Ca^{2+} buffers differentially modulate Ca^{2+}-dependent inactivation of Ca(v)2.1 Ca^{2+} channels. J. Biol. Chem; 281(8): 4691-4698.

Kriebel ME and Gross CE (1974). Multimodal distribution of frog miniature endplate potentials in adult, denervated and tadpole leg muscle. J Gen Physiol; 64: 85-103.

Kuffler SW and Yoshikami D (1975). The number of transmitter molecules in a quantum: an estimate from iontophoretic application of acetylcholine at the neuromuscular synapse. J. Physiol. Lond.; 251: 465-482.

Kuhn DM, Volknandt W, Stadler H, Zimmermann H (1988). Cholinergic vesicle specific proteoglycan: stability in isolated vesicles and in synaptosomes during induced transmitter release. J. Neurochem.; 50(1): 11-16.

Laney DE, Garcia RA, Parsons SM, Hansma HG (1997). Changes in the elastic properties of cholinergic synaptic vesicles as measured by atomic force microscopy. Biophys. J.; 72(2 Pt 1): 806-813.

Lajas AI, Sierra V, Camello PJ, Salido GM, Pariente JA (2001). Vanadate inhibits the calcium extrusion in rat pancreatic acinar cells. Cell Signal; 13: 451-456.

Larrabee MG, Klingman JD, Leicht WS (1963). Effects of temperature, calcium and activity on phospholipid metabolism in a sympathetic ganglion. J. Neurochem.; 10: 549-570.

Lee A, Wong ST, Gallagher D, Li B, Storm DR, Scheuer T, Catterall WA (1999). Ca^{2+}/calmodulin binds to and modulates P/Q-type calcium channels. Nature; 399(6732): 155-159.

Lee CJ, Dayanithi G, Nordmann JJ, Lemos JR (1992). Possible role during exocytosis of a Ca^{2+}-activated channel in neurohypophysial granules. Neuron; 8(2): 335-342.

Lee SA, Eyeson R, Cheever ML, Geng J, Verkhusha VV, Burd C, Overduin M, Kutateladze TG (2005). Targeting of the FYVE domain to endosomal membranes is regulated by a histidine switch. Proc. Natl. Acad. Sci. USA; 102(37): 13052-13057.

Liley AW (1956). An investigation of spontaneous activity at the neuromuscular junction of the rat. J. Physiol.; 132: 650-666.

Lim DY, Park HG, Miwa S (2006). CCCP enhances catecholamine release from the perfused rat adrenal medulla. Auton Neurosci.; 128: 37-47.

Linial M, Levius O, Ilouz N, Parnas D (1995). The effect of calcium levels on synaptic proteins. A study on VAT-1 from Torpedo. J. Physiol. Paris; 89(2): 103-112.

Littleton JT, Stern M, Schulze K, Perin M, Bellen HJ (1993). Mutational analysis of Drosophila synaptotagmin demonstrates its essential role in Ca^{2+}-activated neurotransmitter release. Cell; 74(6): 1125-1134.

Llinás R, Steinberg IZ, Walton K (1981a). Presynaptic calcium currents in squid giant synapse. Biophys. J.; 33(3): 289-321.

Llinás R, Steinberg IZ, Walton K (1981b). Relationship between presynaptic calcium current and postsynaptic potential in squid giant synapse. Biophys J. 33(3):323-351.

Llinás R, Sugimori M, Silver RB (1992). Microdomains of high calcium concentration in a presynaptic terminal. Science; 256 (5057): 677-679.

Llinás RR, Sugimori M, Moran KA, Moreira JE, Fukuda M (2004). Vesicular reuptake inhibition by a synaptotagmin I C2B domain antibody at the squid giant synapse. Proc. Natl. Acad. Sci. USA; 101(51): 17855-17860.

Locke FS (1894). Notiz über des Einfluss physiologisher Kschslazlösung auf die electrische erregbarkeit von muskel und Nerv. Zentralbbl. Physiol.; 8: 166-167.

López JJ, Camello-Almaraz C, Pariente JA, Salido GM, Rosado JA (2005). Ca^{2+} accumulation into acidic organelles mediated by Ca^{2+}- and vacuolar H^{+}-ATPases in human platelets. Biochem. J.; 390(Pt 1):243-252.

López JJ, Redondo PC, Salido GM, Pariente JA, Rosado JA (2006). Two distinct Ca^{2+} compartments show differential sensitivity to thrombin, ADP and vasopressin in human platelets. Cell Signal. 18:373-381.

Lowry OH, Rosebrough NJ, Farral AL, Randall RJ (1951). Protein measurement with the folin phenol reagent. J. Biol. Chem.; 193(1): 265-275.

Lu M, Fu D (2007). Structure of the zinc transporter YiiP. Science; 317(5845): 1746-1748.

Lumpkin E and Hudspeth AJ (1998). Regulation of free Ca^{2+} concentration in hair-cell stereocilia. J.Neurosci.; 18: 6300-6318.

Lupa MT (1987). Calcium-insensitive miniature endplate potentials at the neuromuscular junction. Synapse. 1:281-292.

Mackler JM, Drummond JA, Loewen CA, Robinson IM, Reist NE (2002). The C(2)B Ca^{2+}-binding motif of synaptotagmin is required for synaptic transmission in vivo. Nature; 418(6895): 340-344.

Mackler JM and Reist NE (2001). Mutations in the second C2 domain of synaptotagmin disrupt synaptic transmission at Drosophila neuromuscular junctions. J. Comp. Neurol.; 436(1): 4-16.

Macleod GT, Marin L, Charlton MP, Atwood HL (2004). Synaptic vesicles: test for a role in presynaptic calcium regulation. J. Neurosci.; 24(10): 2496-2505.

Macleod GT, Chen L, Karunanithi S, Peloquin JB, Atwood HL, McRory JE, Zamponi GW, Charlton MP (2006). The Drosophila cacts2 mutation reduces presynaptic Ca^{2+} entry and defines an important element in Cav2.1 channel inactivation. Eur. J. Neurosci.; 23(12):3230-3244.

Madeddu L, Saito I, Hsiao TH, Meldolesi J (1985). Leptinotoxin-h action in synaptosomes and neurosecretory cells: stimulation of neurotransmitter release. J. Neurochem.; 45(6): 1719-1730.

Madhani HD and Fink GR (1998). The riddle of MAP kinase signaling specificity. Trends Genet.; 14: 151-155.

Mahapatra NR, Mahata M, Hazra PP, McDonough PM, O'Connor DT, Mahata SK (2004). A dynamic pool of calcium in catecholamine storage vesicles. Exploration in living cells by a novel vesicle-targeted chromogranin A-aequorin chimeric photoprotein. J. Biol. Chem.; 279(49): 51107-51121.

Maler L and Mathieson WB (1985).The effect of nerve activity on the distribution of synaptic vesicles. Cell Mol. Neurobiol.; 5(4): 373-387.

Manna D, Albanese A, Park WS, Cho W (2007). Mechanistic basis of differential cellular responses of phosphatidylinositol 3,4-bisphosphate- and phosphatidylinositol 3,4,5-trisphosphate-binding pleckstrin homology domains. J. Biol. Chem.; 282(44): 32093-32105.

Maranda B, Brown D, Bourgoin S, Casanova JE, Vinay P, Ausiello DA, Marshansky V (2001). Intra-endosomal pH-sensitive recruitment of the Arf-nucleotide exchange factor ARNO and Arf6 from cytoplasm to proximal tubule endosomes. J. Biol. Chem; 276(21): 18540-18550.

Marchbanks RM (1969). Biochemical organization of cholinergic nerve terminals. In: Cellular dynamics of the neuron pp: 115-135. Ed. Barrondes, S.H. Academic Press. New York and London.

Marchbanks RM and Israël M (1972). The heterogeneity of bound acetylcholine and synaptic vesicles. Biochem. J.; 129(5): 1049-1061.

Marchbanks RM and Wonnacott S (1979). Relationship of choline uptake to acetylcholine synthesis and release. Prog. Brain Res.; 49: 77-88.

Marek KW and Davis GW (2002). Transgenically encoded protein photoinactivation (FlAsH-FALI): acute inactivation of synaptotagmin I. Neuron. 36: 805-813.

Marquèze B, Berton F, Seagar M (2000). Synaptotagmins in membrane traffic: which vesicles do the tagmins tag? Biochimie; 82(5): 409-420.

Marsal J, Esquerda JE, Fiol C, Solsona C, Tomas J (1980). Calcium fluxes in isolated pure cholinergic nerve endings from the electric organ of Torpedo marmorata. J. Physiol. (Paris); 76(5): 443-457.

Marszalek P, Farrell B, Fernandez JM (1996). Ion-exchange gel regulates neurotransmitter release through the exocytotic fusion pore. Soc. Gen. Physiol. Ser.; 51: 211-222.

Marszalek PE, Farrell B, Verdugo P, Fernandez JM (1997). Kinetics of release of serotonin from isolated secretory granules. II. Ion exchange determines the diffusivity of serotonin. Biophys. J.; 73(3): 1169-1183.

Martin KC, Hu Y, Armitage BA, Siegelbaum SA, Kandel ER, Kaang BK (1995). Evidence for synaptotagmin as an inhibitory clamp on synaptic vesicle release in Aplysia neurons. Proc. Natl. Acad. Sci. USA; 92(24): 11307-11311.

Massimini M and Amzica F (2001). Extracellular calcium fluctuations and intracellular potentials in the cortex during the slow sleep oscillation. J. Neurophysiol.; 85(3): 1346-1350.

McGuinness L, Bardo SJ, Emptage NJ (2007). The lysosome or lysosome-related organelle may serve as a Ca^{2+} store in the boutons of hippocampal pyramidal cells. Neuropharmacology; 52(1): 126-135.

McMahon HT, Rosenthal L, Meldolesi J, Nicholls DG (1990). Alpha-latrotoxin releases both vesicular and cytoplasmic glutamate from isolated nerve terminals. J. Neurochem.; 55(6): 2039-2047.

McNaughton BL (1982). Long-term synaptic enhancement and short-term potentiation in rat fascia dentata act through different mechanisms. J. Physiol.; 324:249-262.

Meir A, Ginsburg S, Butkevich A, Kachalsky SG, Kaiserman I, Ahdut R, Demirgoren S, Rahamimoff R (1999). Ion channels in presynaptic nerve terminals and control of transmitter release. Physiol. Rev.; 79(3): 1019-1088.

Meir A and Rahamimoff R (1996). A voltage-dependent and calcium-permeable ion channel in fused presynaptic terminals of Torpedo. J. Neurophysiol.; 75(5): 1858-1870.

Mellow AM, Perry BD, Silinsky EM (1982). Effects of calcium and strontium in the process of acetylcholine release from motor nerve endings. J. Physiol.; 328: 547-562.

Mennerick S and Mathews G (1996). Ultrafast exocytosis elicited by calcium current in synaptic terminals of retina bipolar neurons. Neuron; 17: 1241-1249.

Meunier FM (1984). Relationship between presynaptic membrane potential and acetylcholine release in synaptosomes from Torpedo electric organ. J. Physiol.; 354: 121-137.

Michaelson DM, Avissar S, Ophir I, Pinchasi I, Angel I, Kloog Y, Sokolovsky M (1980). On the regulation of acetylcholine release: a study utilizing Torpedo synaptosomes and synaptic vesicles. J Physiol (Paris). 76(5): 505-514.

Michelangeli F, Ogunbayo OA, Wootton LL (2005). A plethora of interacting organellar Ca^{2+} stores. Curr. Opin. Cell Biol.; 17:135-140.

Miedema H, Staal M, Prins HB (1996). pH-induced proton permeability changes of plasma membrane vesicles. J. Membr. Biol; 152(2): 159-167.

Mikoshiba K, Fukuda M, Moreira JE, Lewis FM, Sugimori M, Niinobe M, LLinás R (1995). Role of the C2A domain of synaptotagmin in transmitter release as determined by specific antibody injection into the squid giant synapse preterminal. Proc. Natl. Acad. Sci. USA; 92(23): 10703-10707.

Miledi R (1973). Transmitter release induced by injection of calcium ions into nerve terminals. Proc R Soc Lond B Biol Sci. 183(73): 421-425.

Miledi R and Parker I (1981). Calcium transients recorded with arsenazo III in the presynaptic terminal of the squid giant synapse. Proc. R. Soc. Lond. B Biol. Sci.; 212: 197-211.

Miledi R and Slater CR (1966). The action of calcium on neuronal synapses in the squid. J. Physiol. (London). 184(2): 473-498.

Miledi R and Thies R (1971). Tetanic and post-tetanic rise in frequency of miniature end-plate potentials in low-calcium solutions. J Physiol. 212: 245-57.

Miledi R and Thies RE (1967). Post-tetanic increase in frequency of miniature end-plate potentials in calcium-free solutions. J. Physiol.; 192: 54P-55P.

Missler M, Zhang W, Rohlmann A, Kattenstroth G, Hammer RE, Gottmann K, Sudhof TC (2003). Alpha-neurexins couple Ca^{2+} channels to synaptic vesicle exocytosis. Nature; 423(6943): 939-948.

Mizuhira V, Hasegawa H (1997). Microwave fixation and localization of calcium in synaptic terminals using x-ray microanalysis and electron energy loss spectroscopy imaging. Brain Res. Bull.; 43(1): 53-58.

Modis Y, Ogata S, Clements D, Harrison SC (2004). Structure of the dengue virus envelope protein after membrane fusion. Nature; 427(6972): 313-319.

Molgó J, Pécot-Dechavassine M (1988). Effects of carbonyl cyanide m-chlorophenylhydrazone on quantal transmitter release and ultrastructure of frog motor nerve terminals. Neuroscience; 24(2): 695-708.

Montero M, Alonso MT, Carnicero E, Cuchillo-Ibáñez I, Albillos A, García AG, García-Sancho J, Alvarez J (2000). Chromaffin-cell stimulation triggers fast millimolar mitochondrial Ca^{2+} transients that modulate secretion. Nat. Cell Biol.; 2: 57-61.

Morel N, Dedieu JC, Philippe JM (2003). Specific sorting of the a1 isoform of the V-H^+ATPase a subunit to nerve terminals where it associates with both synaptic vesicles and the presynaptic plasma membrane. J. Cell Sci.; 116(Pt 23): 4751-4762.

Morel N, Israël M, Manaranche R (1978). Determination of ACh concentration in Torpedo synaptosomes. J. Neurochem.; 30(6): 1553-1557.

Morel N, Israël M, Manaranche R, Mastour-Frachon P (1977). Isolation of pure cholinergic nerve endings from Torpedo electric organ. Evaluation of their metabolic properties. J Cell Biol.; 75(1): 43-55.

Morel N, Manaranche R, Israël M, Gulik-Krzywicki T (1982). Isolation of a presynaptic plasma membrane fraction from Torpedo cholinergic synaptosomes: evidence for a specific protein. J Cell Biol.; 93(2): 349-356.

Morel N, Manaranche R, Gulik-krzywicki T, Isreal M (1980). Ultrastructural changes and transmitter release induced by depolarization of cholinergic synaptosomes. A freeze-fracture study of a synaptosomal fraction from torpedo electric organ. J Ultrastruct Res. 70(3):347-362.

Moser T, Neef A, Khimich D (2006). Mechanisms underlying the temporal precision of sound coding at the inner hair cell ribbon synapse. J. Physiol.; 576(Pt 1): 55-62.

Müller A, Kukley M, Uebachs M, Beck H, Dietrich D (2007). Nanodomains of single Ca^{2+} channels contribute to action potential repolarization in cortical neurons. J. Neurosci.; 27(3): 483-495.

Muller D and Dunant Y (1987). Spontaneous quantal and subquantal transmitter release at the Torpedo nerve-electroplaque junction. Neuroscience; 20: 911-921.

Muller D, Garcia-Segura LM, Párducz A, Dunant Y (1987). Brief occurrence of a population of presynaptic intramembrane particles coincides with transmission of a nerve impulse. Proc Natl Acad Sci USA; 84(2):590-594.

Muller D, Loctin F, and Dunant Y (1987). Inhibition of evoked acetylcholine release: two different mechanisms in the Torpedo electric organ. Eur J Pharmacol 133, 225-234.

Nägerl UV, Novo D, Mody I, Vergara JL (2000). Binding kinetics of calbindin-D(28k) determined by flash photolysis of caged Ca^{2+}. Biophys J.; 79(6): 3009-3018.

Nagy G, Kim JH, Pang ZP, Matti U, Rettig J, Südhof TC, Sørensen JB (2006). Different effects on fast exocytosis induced by synaptotagmin 1 and 2 isoforms and abundance but not by phosphorylation. J. Neurosci; 26(2): 632-643.

Nakata K, Okuda T, Misawa H (2004). Ultrastructural localization of high-affinity choline transporter in the rat neuromuscular junction: enrichment on synaptic vesicles. Synapse; 53(1):53-56.

Naoum PI, Hudspeth AJ (1994). Clustering of Ca^{2+} Channels and Ca^{2+}-Activated K^{+} Channels at Fluorescently Labeled Presynaptic Active Zones of Hair Cells PNAS USA. 91(16): 7578-82.

Neher E and Augustine GJ (1992). Calcium gradients and buffers in bovine chromaffin cells. J. Physiol.; 450: 273-301.

Neher E (1998). Vesicle pools and Ca^{2+}-microdomains: new tools for understanding their roles in neurotransmitter release. Neuron 20:389-399.

Neves G, Neef A, Lagnado L (2001). The actions of barium and strontium on exocytosis and endocytosis in the synaptic terminal of goldfish bipolar cells. J.Physiol.; 535 (3): 809–824.

Nishiki T, Augustine GJ (2004). Dual roles of the C2B domain of synaptotagmin I in synchronizing Ca2+-dependent neurotransmitter release. J. Neurosci; 24(39): 8542-8550.

Oheim M, Kirchhoff F, Stühmer W (2006). Calcium microdomains in regulated exocytosis. Cell Calcium. 40(5-6):423-439.

Ohsawa K, Dowe GHC, Morris SJ, Whittaker VP (1979). The lipid and protein content of cholinergic synaptic vesicles from the electric organ of Torpedo marmorata purified to constant composition: implication for vesicle structure. Brain Res.; 161: 447-457.

Ohsawa K, Dowe GHC, Morris SJ, Whittaker VP (1979). The lipid and protein content of cholinergic synaptic vesicles from the electric organ of Torpedo marmorata purified to constant composition : implication for vesicle structure. Brain Res.; 161: 447-457.

Orlova EV, Rahman MA, Gowen B, Volynski KE, Ashton AC, Manser C, van Heel M, Ushkaryov YA (2000). Structure of alpha-latrotoxin oligomers reveals that divalent cation-dependent tetramers form membrane pores. Nat. Struct. Biol.; 7(1): 48-53.

Osborne SL, Wallis TP, Jimenez JL, Gorman JJ, Meunier FA (2007). Identification of secretory granule phosphatidylinositol 4,5-bisphosphate-interacting proteins using an affinity pulldown strategy. Mol. Cell Proteomics; 6(7): 1158-1169.

Otsu Y, Shahrezaei V, Li B, Raymond LA, Delaney KR, Murphy TH (2004). Competition between Phasic and Asynchronous Release for Recovered Synaptic Vesicles at Developing Hippocampal Autaptic Synapses J. Neurosci. 24:420-433.

Pang ZP, Sun J, Rizo J, Maximov A, Sudhof TC (2006). Genetic analysis of synaptotagmin 2 in spontaneous and Ca^{2+}-triggered neurotransmitter release. EMBO J; 25(10): 2039-2050.

Párducz A and Dunant Y (1993). Transient increase of calcium in synaptic vesicles after stimulation. Neuroscience; 52(1): 27-33.

Párducz A, Loctin F, Babel-Guerin E, Dunant Y (1994). Exo-endocytotic activity during recovery from a brief tetanic stimulation: a role in calcium extrusion? Neuroscience. 62(1):93-103.

Párducz A, Toldi J, Joo F, Siklos L, Wolff JR (1987). Transient increase of calcium in pre- and postsynaptic organelles of rat superior cervical ganglion after tetanizing stimulation. Neuroscience; 23(3): 1057-1061.

Park YB, Herrington J, Babcock DF, Hille B (1996). Ca^{2+} clearance mechanisms in isolated rat adrenal chromaffin cells. J. Physiol.; 492:329-346.

Parpura V and Fernandez JM (1996). Atomic force microscopy study of the secretory granule lumen. Biophys. J.; 71(5): 2356-2366.

Parsegian VA (1977). Considerations in determining the mode of influence of calcium on vesicle-membrane interaction. Soc. Neurosci. Symp.; 2: 161-171.

Peters C, Bayer MJ, Buhler S, Andersen JS, Mann M, Mayer A (2001). Trans-complex formation by proteolipid channels in the terminal phase of membrane fusion. Nature; 409(6820): 581-588.

Pezzati R and Grohovaz F (1999). The frog neuromuscular junction revisited after quick-freezing-freeze-drying: ultrastructure, immunogold labelling and high resolution calcium mapping. Philos. Trans. R. Soc. Lond. B Biol. Sci.; 354(1381): 373-378.

Picollo A and Pusch M (2005). Chloride/proton antiporter activity of mammalian CLC proteins ClC-4 and ClC-5. Nature; 436: 420–423.

Plump AS, Erskine L, Sabatier C, Brose K, Epstein CJ, Goodman CS, Mason CA, Tessier-Lavigne M (2002). Slit1 and Slit2 cooperate to prevent premature midline crossing of retinal axons in the mouse visual system. Neuron; 33:219-232.

Posada V, Beauge L, Berberian G (2007). Maximal $Ca^{2+}{}_i$ stimulation of cardiac Na^+/Ca^{2+} exchange requires simultaneous alkalinization and binding of PtdIns-4,5-P2 to the exchanger. Biol. Chem.; 388(3): 281-288.

Poskanzer KE, Marek KW, Sweeney ST, Davis GW (2003). Synaptotagmin I is necessary for compensatory synaptic vesicle endocytosis in vivo. Nature; 426(6966): 559-563.

Poskanzer KE, Fetter RD, Davis GW (2006). Discrete residues in the c(2)b domain of synaptotagmin I independently specify endocytic rate and synaptic vesicle size. Neuron; 50(1): 49-62.

Prakriya M, Solare CR, Lingle CJ (1996). $[Ca^{2+}]$i elevations detected by BK channels during Ca^{2+} influx and muscarine-mediated release of Ca^{2+} from intracellular stores in rat chromaffin cells. J. Neurosci. 16(14):4344-59.

Pumplin DW and Reese TS (1978). Membrane ultrastructure of the giant synapse of the squid Loligo pealei. Neuroscience; 3(8): 685-696.

Pumplin DW, Reese TS, LLinás R (1981). Are the presynaptic membrane particles the calcium channels? Proc Natl Acad Sci USA; 78(11): 7210-7213.

Quesada I, Chin WC, Verdugo P (2003). ATP-independent luminal oscillations and release of Ca^{2+} and H^+ from mast cell secretory granules: implications for signal transduction. Biophys. J.; 85(2): 963-970.

Rabl K and Thoreson WB (2002). Calcium-dependent inactivation and depletion of synaptic cleft calcium ions combine to regulate rod calcium currents under physiological conditions. Eur. J. Neurosci.; 16(11): 2070-2077.

Rahamimoff R (1968). A dual effect of calcium ions on neuromuscular facilitation. J. Physiol.; 195: 471-480.

Rahamimoff R, DeRiemer SA, Sakmann B, Stadler H, Yakir N (1988). Ion channels in synaptic vesicles from Torpedo electric organ. Proc. Natl. Acad. Sci. USA; 85(14): 5310-5314.

Rahamimoff R and Fernandez JM (1997). Pre- and postfusion regulation of transmitter release. Neuron; 18(1): 17-27.

Rahamimoff R, Yaari Y. (1973) Delayed release of transmitter at the frog neuromuscular junction. J. Physiol.; 228: 241-257.

Reigada D, Diez-Perez I, Gorostiza P, Verdaguer A, Gomez de Aranda I, Pineda O, Vilarrasa J, Marsal J, Blasi J, Aleu J, Solsona C (2003). Control of neurotransmitter release by an internal gel matrix in synaptic vesicles. Proc. Natl. Acad. Sci. U S A; 100(6): 3485-3490.

Reist NE, Buchanan J, Li J, DiAntonio A, Buxton EM, Schwarz TL (1998). Morphologically docked synaptic vesicles are reduced in synaptotagmin mutants of Drosophila. J. Neurosci; 18(19): 7662-7673.

Rephaelis A and Parsons SM (1982). Calmodulin stimulation of $^{45}Ca^{2+}$ transport and protein phosphorylation in cholinergic synaptic vesicles. Proc. Natl. Acad. Sci. USA. 79(19): 5783-5787.

Ringer S (1882). Concerning the Influence exerted by each of the Constituents of the Blood on the Contraction of the Ventricle. J Physiol.; 3 (5-6):380-393.

Ringer S (1883). A further Contribution regarding the influence of the different Constituents of the Blood on the Contraction of the Heart. J Physiol.; 4(1):29-42.

Rizzuto R and Pozzan T (2006). Microdomains of intracellular Ca^{2+}: molecular determinants and functional consequences. Physiol Rev.; 86(1): 369-408.

Roberts WM (1993). Spatial calcium buffering in saccular hair cells. Nature; 363(6424):74-76.

Roberts WM (1994). Localization of calcium signals by a mobile calcium buffer in frog saccular hair cells. J Neurosci.; 14 (5 Pt 2): 3246-3262.

Roberts WM, Jacobs RA, Hudspeth AJ (1990). Colocalization of ion channels involved in frequency selectivity and synaptic transmission at presynaptic active zones of hair cells. J Neurosci.; 10(11): 3664-3684.

Robinson IM, Ranjan R, Schwarz TL (2002). Synaptotagmins I and IV promote transmitter release independently of Ca^{2+} binding in the C(2)A domain. Nature; 418(6895): 336-340.

Robitaille R, Adler EM, Charlton MP (1990). Strategic location of calcium channels at transmitter release sites of frog neuromuscular synapses. Neuron; 5(6): 773-779.

Robitaille R, Garcia ML, Kaczorowski GJ, Charlton MP (1993). Functional colocalization of calcium and calcium-gated potassium channels in control of transmitter release. Neuron; 11(4): 645-55.

Rohou A, Nield J, Ushkaryov YA (2007). Insecticidal toxins from black widow spider venom.Toxicon; 49(4): 531-549.

Rohrbough J and Broadie K (2005). Lipid regulation of the synaptic vesicle cycle. Nat. Rev. Neurosci.; 6(2): 139-150.

Rosenberry J (1975). Acetylcholine esterase. Advances in Enzymology and Related Areas of Molecular Biology; 43: 103-218.

Rothman JE (1994). Intracellular membrane fusion. Adv Second Messenger Phosphoprotein Res. 29: 81-96.

Roux I, Safieddine S, Nouvian R, Grati M, Simmler MC, Bahloul A, Perfettini I, Le Gall M, Rostaing P, Hamard G, Triller A, Avan P, Moser T, Petit C (2006). Otoferlin, defective in a human deafness form, is essential for exocytosis at the auditory ribbon synapse. Cell; 127(2): 277-89.

Rusakov DA and Fine A (2003). Extracellular Ca^{2+} depletion contributes to fast activity-dependent modulation of synaptic transmission in the brain. Neuron; 37(2): 287-297.

Sabatini BL and Regehr W (1996). Timing of neurotransmission at fast synapses in the mammalian brain. Nature; 384: 170-172.

Safieddine S and Wenthold RJ (1999). SNARE complex at the ribbon synapses of cochlear hair cells: analysis of synaptic vesicle- and synaptic membrane-associated proteins. Eur J Neurosci.; 11(3): 803-812.

Sakmann B, Methfessel C, Mishina M, Takahashi T, Takai T, Kurasaki M, Fukuda K, and Numa S (1985). Role of acetylcholine receptor subunits in gating of the channel. Nature; 318: 538-543.

Salpeter MM, Rogers AW, Kasprzak H, McHenry FA (1978). Acetylcholinesterase in the fast extraocular muscle of the mouse by light and electron microscope autoradiography. J. Cell Biol.; 78: 274-285.

Sanchez-Prieto J, Sihra TS, Nicholls DG (1987). Characterization of the exocytotic release of glutamate from guinea-pig cerebral cortical synaptosomes. J Neurochem.; 49(1): 58-64.

Sankaranarayanan S and Ryan TA (2001). Calcium accelerates endocytosis of vSNAREs at hippocampal synapses. Nat. Neurosci.; 4(2): 129-136.

Sasaki N, Dayanithi G, Shibuya I (2005). Ca^{2+} clearance mechanisms in neurohypophysial terminals of the rat. Cell Calcium; 37(1): 45-56.

Sbia M, Diebler MF, Morel N, Israël M (1992). Effect of N,N'-dicyclohexylcarbodiimide on acetylcholine release from Torpedo synaptosomes and proteoliposomes reconstituted with the proteolipid mediatophore. J. Neurochem.; 59: 1273-1279.

Scheel O, Zdebik AA, Lourdel S, Jentsch TJ (2005). Voltage-dependent electrogenic chloride/proton exchange by endosomal CLC proteins. Nature; 436(7049):424-427.

Schiavo G, Gu QM, Prestwich GD, Sollner TH, Rothman JE (1996). Calcium-dependent switching of the specificity of phosphoinositide binding to synaptotagmin. Proc. Natl. Acad. Sci. USA; 93(23): 13327-13332.

Schmidt H, Stiefel KM, Racay P, Schwaller B, Eilers J (2003). Mutational analysis of dendritic Ca^{2+} kinetics in rodent Purkinje cells; role of parvalbumin and calbindin D28k. J. Physiol.; 551(Pt 1):13-32.

Schmidt R, Zimmermann H, Whittaker VP (1980). Metal ion content of cholinergic synaptic vesicles isolated from the electric organ of Torpedo: effect of stimulation-induced transmitter release. Neuroscience; 5(3): 625-38.

Schmidt W, Winkler H, Plattner H (1982). Adrenal chromaffin granules: evidence for an ultrastructural equivalent of the proton-pumping ATPase. Eur. J. Cell Biol.; 27: 96-104.

Schneggenburger R and Forsythe ID (2006). The calyx of Held. Cell Tissue Res.; 326(2): 311-337.

Scranton TW, Iwata M, Carlson SS (1993). The SV2 protein of synaptic vesicles is a keratan sulfate proteoglycan. J. Neurochem.; 61(1): 29-44.

Shahrezaei V, Cao A, Delaney KR (2006). Ca^{2+} from one or two channels controls fusion of a single vesicle at the frog neuromuscular junction. J. Neurosci.; 26(51): 13240-13249.

Shahrezaei V and Delaney KR (2005). Brevity of the Ca^{2+} microdomain and active zone geometry prevent Ca^{2+}-sensor saturation for neurotransmitter release. J. Neurophysiol.; 94(3): 1912-1919.

Sheng ZH, Westenbroek RE, Catterall WA (1998). Physical link and functional coupling of presynaptic calcium channels and the synaptic vesicle docking/fusion machinery. J Bioenerg Biomembr.; 30(4): 335-45.

Shepherd GM (1991). Foundations of the neuron doctrine. New York. Oxford University Press.

Shiff G, Synguelakis M, Morel N (1996). Association of syntaxin with SNAP 25 and VAMP (synaptobrevin) in Torpedo synaptosomes. Neurochem Int.; 29(6): 659-667.

Shin OH, Rhee JS, Tang J, Sugita S, Rosenmund C, Sudhof TC (2003). Sr^{2+} binding to the Ca^{2+} binding site of the synaptotagmin 1 C2B domain triggers fast exocytosis without stimulating SNARE interactions. Neuron; 37(1): 99-108.

Shoji-Kasai Y, Yoshida A, Sato K, Hoshino T, Ogura A, Kondo S, Fujimoto Y, Kuwahara R, Kato R, Takahashi M (1992). Neurotransmitter release from synaptotagmin-deficient clonal variants of PC12 cells. Science; 256: 1821-3.

Siebert A, Lottspeich F, Nelson N, Betz H (1994). Purification of the synaptic vesicle-binding protein physophilin. Identification as 39-kDa subunit of the vacuolar H^+-ATPase. J. Biol. Chem.; 269(45): 28329-28334.

Simon SM and LLinás RR (1985). Compartmentalization of the submembrane calcium activity during calcium influx and its significance in transmitter release. Biophys J.; 48(3): 485-98.

Sollner T, Bennett MK, Whiteheart SW, Scheller RH, Rothman JE (1993). A protein assembly-disassembly pathway in vitro that may correspond to sequential steps of synaptic vesicle docking, activation, and fusion. Cell; 75(3): 409-418.

Sombers LA, Hanchar HJ, Colliver TL, Wittenberg N, Cans A, Arbault S, Amatore C, Ewing AG (2004). The effects of vesicular volume on secretion through the fusion pore in exocytotic release from PC12 cells. J. Neurosci.; 24(2): 303-309.

Song H, Ming G, Fon E, Bellocchio E, Edwards RH, Poo M (1997). Expression of a putative vesicular acetylcholine transporter facilitates quantal transmitter packaging. Neuron; 18(5): 815-826.

Stadler H and Kiene ML (1987). Synaptic vesicles in electromotoneurones. II. Heterogeneity of populations is expressed in uptake properties; exocytosis and insertion of a core proteoglycan into the extracellular matrix. EMBO J.; 6(8): 2217-2221.

Stadler H and Whittaker VP (1978). Identification of vesiculin as a glycosaminoglycan. Brain Res.; 22; 153(2): 408-413.

Stadler H and Tsukita S (1984). Synaptic vesicles contain an ATP-dependent proton pump and show "knob-like" protrusion on their surface. EMBO J.; 3(13): 3333-3337.

Stanley EF (1997). The calcium channel and the organization of the presynaptic transmitter release face. Trends Neurosci.; 20(9): 404-409.

Stanley EF (2000).Presynaptic calcium channels and the depletion of synaptic cleft calcium ions. J. Neurophysiol.; 83(1): 477-482.

Stegmann T (2000). Membrane fusion mechanisms: the influenza hemagglutinin paradigm and its implications for intracellular fusion. Traffic; 1(8): 598-604.

Strehler (1974). Methods in enzymatic analysis vol 4 Bergmeyer H.U., ed, pp: 2112-2115. Academic press, San Diego.

Südhof TC (2002). Synaptotagmins: why so many? J. Biol. Chem.; 277(10): 7629-7632.

Sugita S, Hata Y, Südhof TC (1996). Distinct Ca^{2+}-dependent properties of the first and second C2-domains of synaptotagmin I. J. Biol. Chem.; 271(3): 1262-1265.

Sulllivan JM (2007). Please Release Me. Neuron; 54: 493-494.

Sullivan WE and Konishi M (1984). Segregation of stimulus phase and intensity coding in the cochlear nucleus of the barn owl. J. Neurosci.; 4(7): 1787-1799.

Sun SZ, Xie XS, Stone DK (1987). Isolation and reconstitution of the dicyclohexylcarbodiimide-sensitive proton pore of the clathrin-coated vesicle proton translocating complex. J. Biol. Chem.; 262(30): 14790-14794.

Surrey T, Elowitz MB, Wolf PE, Yang F, Nedelec F, Shokat K, Leibler S (1998). Chromophore-assisted light inactivation and self-organization of microtubules and motors. Proc. Natl. Acad. Sci. USA; 95: 4293-4298.

Sutton R, Apps DK (1981). Isolation of a DCCD-binding protein from bovine chromaffin-granule membranes. FEBS Lett. 130: 103-106.

Sutton RB, Fasshauer D, Jahn R, Brunger AT (1998). Crystal structure of a SNARE complex involved in synaptic exocytosis at 2.4 A resolution. Nature; 395(6700): 347-353.

Swandulla D and Armstrong CM (1988). Fast-deactivating calcium channels in chick sensory neurons. J Gen. Physiol. 92: 197-218.

Takamori S, Holt M Stenius K, Lemke EA, Gronborg M, Riedel D, Urlaub H, Schenck S, Brugger B, Ringler P, Müller SA, Rammner B, Grater F, Hub JS, De Groot BL, Mieskes G,

Moriyama Y, Klingauf J, GrubMüller H, Heuser J, Wieland F, Jahn R (2006). Molecular anatomy of a trafficking organelle. Cell; 127(4): 831-846.

Tanaka R, Takeda M, Jaimovich M (1976). Characterization of ATPases of plain synaptic vesicle and coated vesicle fractions isolated from rat brains. J. Biochem. (Tokyo). 80(4): 831-837.

Tanaka T (1981). Gels. Sci. Am.; 244(1): 124-138.

Taussky, HH, Shorr, E (1953). A microcolorimetric method for the determination of the inorganic phosphorus. J. Biol. Chem.; 202: 675-685.

Thesleff S, Molgó J (1983). A new type of transmitter release at the neuromuscular junction. Neuroscience; 9: 1-8

Thomas L, Hartung K, Langosch D, Rehm H, Bamberg E, Franke WW, Betz H (1988). Identification of synaptophysin as a hexameric channel protein of the synaptic vesicle membrane. Science; 242(4881): 1050-1053.

Thomas L and Betz K (1990). Synaptophysin binds to physophilin, a putative synaptic plasma membrane protein. J. Cell Biol.; 111: 2041-2042.

Thomas P, Lee AK, Wong JG, Almers W (1994). A triggered mechanism retrieves membrane in seconds after Ca^{2+}-stimulated exocytosis in single pituitary cells. J. Cell Biol.; 124(5): 667-675.

Thomas P, Wong JG, Lee AK, Almers W (1993). A low affinity Ca^{2+} receptor controls the final steps in peptide secretion from pituitary melanotrophs. Neuron; 11(1): 93-104.

Tokuoka H and Goda Y (2003). Synaptotagmin in Ca^{2+}-dependent exocytosis: dynamic action in a flash. Neuron; 38(4): 521-4.

Troyer KP and Wightman RM (2002).Temporal separation of vesicle release from vesicle fusion during exocytosis. J. Biol. Chem.; 277(32): 29101-29107.

Tsien RY (1980). New calcium indicators and buffers with high selectivity against magnesium and protons: designs, synthesis, and proprieties of prototype structures. Bichemistry; 19: 2396-404.

Ubach J, Zhang X, Shao X, Südhof TC, Rizo J (1999). Ca^{2+} binding to synaptotagmin: how many Ca^{2+} ions bind to the tip of a C2-domain? EMBO J.; 17(14): 3921-30.

Umbach JA, Saitoe M, Kidokoro Y, Gundersen CB (1998). Attenuated influx of calcium ions at nerve endings of csp and shibire mutant Drosophila. J. Neurosci.; 18(9): 3233-3240.

Ushkaryov YA, Volynski KE, Ashton AC (2004). The multiple actions of black widow spider toxins and their selective use in neurosecretion studies. Toxicon 43: 527–542.

Ushkaryov YA, Rohou A, Sugita S (2008). a-Latrotoxin and Its Receptors. In: Handbook of Experimental Pharmacology 184; Pharmacology of Neurotransmitter Release. Südhof T.C., Starke K. (eds.). Springer-Verlag Berlin Heidelberg.

Uvnäs B and Åborg CH (1983). Cation exchange -a common mechanism in the storage and release of biogenic amines stored in granules (vesicles)? I. Comparative studies on the uptake of sodium and biogenic amines by the weak cation (carboxyl) exchangers Amberlite IRC-50 and Sephadex C-50 and by biogenic (granule-enriched) materials in vitro. Acta Physiol. Scand.; 119(3): 225-234.

Uvnäs B and Åborg CH (1987). Concomitant release by ion exchange of catecholamines (CA) and adenosine triphosphate (ATP) from bovine chromaffin granules superfused with isotonic sodium or potassium salt solutions. Acta Physiol. Scand.; 129(4): 585-586.

Uvnäs B and Åborg CH (1989). Role of Ion Exchange in Release of Biogenic Amines. News Physiol. Sci.; 4: 68-71.

Uvnäs B, Åborg CH, Bergendorff A (1970). Storage of histamine in mast cells. Evidence for an ionic binding of histamine to protein carboxyls in the granule heparin-protein complex. Acta Physiol. Scand.;78; Suppl. 336: 3-26.

Valtorta F, Meldolesi J, Fesce R (2001). Synaptic vesicles: is kissing a matter of competence? Trends Cell Biol.; 11(8): 324-328.

Van der Kloot W, Colasante C, Cameron R, Molgó J (2000). Recycling and refilling of transmitter quanta at the frog neuromuscular junction. J. Physiol.; 523 Pt 1: 247-258.

Van der Kloot W and Molgó J (1993). Facilitation and delayed release at about 0 degree C at the frog neuromuscular junction: effects of calcium chelators, calcium transport inhibitors, and okadaic acid. J. Neurophysiol; 69:717-729.

Van Renterghem C, Iborra C, Martin-Moutot N, Lelianova V, Ushkaryov Y, Seagar M (2000). alpha-latrotoxin forms calcium-permeable membrane pores via interactions with latrophilin or neurexin. Eur. J. Neurosci.; 12(11): 3953-3962.

Vautrin J and Kriebel ME (1991). Characteristics of slow-miniature endplate currents show a subunit composition. Neuroscience; 41: 71-88.

Verdugo P (1990). Goblet cells secretion and mucogenesis. Annu. Rev. Physiol.; 52: 157-176.

Verdugo P (1991). Mucin exocytosis. Am. Rev. Respir. Dis.; 144(3 Pt 2): S33-37.

Verstreken P, Ly CV, Venken KJ, Koh TW, Zhou Y, Bellen HJ (2005). Synaptic mitochondria are critical for mobilization of reserve pool vesicles at Drosophila neuromuscular junctions. Neuron; 47(3): 365-78.

Villalobos C, Nunez L, Montero M, Garcia AG, Alonso MT, Chamero P, Alvarez J, Garcia-Sancho J (2002). Redistribution of Ca^{2+} among cytosol and organella during stimulation of bovine chromaffin cells. FASEB J; 16(3): 343-353.

Voets T, Moser T, Lund PE, Chow RH, Geppert M, Südhof TC, Neher E (2001). Intracellular calcium dependence of large dense-core vesicle exocytosis in the absence of synaptotagmin I. Proc. Natl. Acad. Sci. USA; 98(20): 11680-11685.

Voets T, Neher E, Moser T (1999). Mechanisms underlying phasic and sustained secretion in chromaffin cells from mouse adrenal slices. Neuron; 23(3): 607-615.

Volknandt W, Schlafer M, Bonzelius F, Zimmermann H (1990). Svp25, a synaptic vesicle membrane glycoprotein from Torpedo electric organ that binds calcium and forms a homo-oligomeric complex. EMBO J.; 9(8): 2465-2470.

Von Grafenstein HR, Powis DA (1989). Calcium is released by exocytosis together with catecholamines from bovine adrenal medullary cells. J. Neurochem.; 53(2): 428-435.

Vyklicky L, Patneau DK, Mayer ML (1991). Modulation of excitatory synaptic transmission by drugs that reduce desensitization at AMPA/kainite receptors. Neuron; 7: 971-984.

Wadel K, Neher E, Sakaba T. (2007). The Coupling between Synaptic Vesicles and Ca^{2+} Channels Determines Fast Neurotransmitter Release. Neuron; 53(4): 563-575.

Wagner R. (1847). Ueber den feineren Bau des elektrischen Organs im Zitterrochen. Abh Ges Wiss Göttingen 3: 141-166.

Wahlberg JM and Garoff H (1992). Membrane fusion process of Semliki Forest virus. I: Low pH-induced rearrangement in spike protein quaternary structure precedes virus penetration into cells. J. Cell Biol; 116(2): 339-348.

Wang CT, Grishanin R, Earles CA, Chang PY, Martin TF, Chapman ER, Jackson MB (2001). Synaptotagmin modulation of fusion pore kinetics in regulated exocytosis of dense-core vesicles. Science; 294(5544): 1111-1115.

Wang CT, Lu JC, Bai J, Chang PY, Martin TF, Chapman ER, Jackson MB (2003).Different domains of synaptotagmin control the choice between kiss-and-run and full fusion. Nature; 424(6951): 943-947.

Wang FS, Wolenski JS, Cheney RE, Mooseker MS, Jay DG (1996). Function of myosin-V in filopodial extension of neuronal growth cones. Science; 273(5275): 660-663.

Wathey JC, Nass MM, Lester HA (1979). Numerical reconstruction of the quantal event at nicotinic synapses. Biophys. J.; 27:145-164.

Weber T, Zemelman BV, McNew JA, Westermann B, Gmachl M, Parlati F, Sollner TH, Rothman JE (1998). SNAREpins: minimal machinery for membrane fusion. Cell; 92(6): 759-772.

Whittaker VP, Michaelson IA, Kirkland RJ. (1964). The separation of synaptic vesicles from nerve-ending particles ('synaptosomes'). Biochem J.; 90: 293-303.

Whittaker VP (1959). The isolation and characterization of acetylcholine-containing particles from brain. Biochem J.; 72: 694-706.

Williams J (1997). How does a vesicle know it is full? Neuron; 18(5): 683-686.

Woodbury DJ (1995). Evaluation of the evidence for ion channels in synaptic vesicles. Mol. Membr. Biol.; 12(2): 165-171.

Wu MM, Grabe M, Adams S, Tsien RY, Moore HP, Machen TE (2001). Mechanisms of pH regulation in the regulated secretory pathway. J. Biol. Chem.; 276(35): 33027-33035.

Wu Y, He Y, Bai J, Ji S, Tucker W, Chapman E, Sui S (2003). Visualization of synaptotagmin I oligomers assembled onto lipid monolayers.PNAS; 100: 2082-2087.

Xu J, Mashimo T, Sudhof TC (2007). Synaptotagmin-1, -2, and -9: Ca^{2+} sensors for fast release that specify distinct presynaptic properties in subsets of neurons. Neuron; 54(4): 567-581.

Xu J and Wu L (2005). The decrease in the presynaptic calcim current is a major cause of short-term depression at a calyx-type synapse. Neuron; 46: 633-645.

Xu T and Bajjalieh SM (2001). SV2 modulates the size of the readily releasable pool of secretory vesicles. Nat. Cell Biol.; 3(8): 691-698.

Xu T, Naraghi M, Kang H, Neher E (1997). Kinetic studies of Ca^{2+} binding and Ca^{2+} clearance in the cytosol of adrenal chromaffin cells. Biophys. J.; 73:532-545.

Xu-Friedman MA and Regehr WG (2000). Probing fundamental aspects of synaptic transmission with strontium. J. Neurosci.; 20: 4414-4422.

Yamada KA and Tang CM (1993). Benzothiadiazides inhibit rapid glutamate receptor desensitization and enhace glutamatergic synaptic currents. J. Neurosci.; 13: 3904-3915.

Yamoah EN, Lumpkin EA, Dumont RA, Smith PJ, Hudspeth AJ and Gillespie PG (1998). Plasma membrane Ca^{2+}-ATPase extrudes Ca^{2+} from hair cell stereocilia. J. Neurosci.; 18: 610-624.

Yazejian B, Sun XP, Grinnell AD (2000). Tracking presynaptic Ca^{2+} dynamics during neurotransmitter release with Ca^{2+}-activated K^{+} channels. Nat. Neurosci.; 3(6): 566-571.

Yin Y, Dayanithi G, Lemos JR (2002). Ca(2+)-regulated, neurosecretory granule channel involved in release from neurohypophysial terminals. J. Physiol.; 539(Pt 2): 409-418.

Yoshihara M, Littleton JT (2002). Synaptotagmin I functions as a calcium sensor to synchronize neurotransmitter release. Neuron; 36(5): 897-908.

Young GPH, Young JDY, Deshpande AK, Goldstein M, Koide SS, Cohn ZA (1984). A Ca^{2+}-Activated Channel from Xenopus laevis Oocyte Membranes Reconstituted into Planar Bilayers. PNAS; 81: 5155-9.

Zenisek D and Matthews G (2000). The role of mitochondria in presynaptic calcium handling at a ribbon synapse. Neuron; 25: 229-237.

Zeuzem S, Feick P, Zimmermann P, Haase W, Kahn RA, Schulz I (1992). Intravesicular acidification correlates with binding of ADP-ribosylation factor to microsomal membranes. Proc. Natl. Acad. Sci. USA; 89(14): 6619-6623.

Zhai RG and Bellen HJ (2004). The architecture of the active zone in the presynaptic nerve terminal. Physiology (Bethesda); 19: 262-270.

Zhang JZ, Davletov BA, Sudhof TC, Anderson RG (1994). Synaptotagmin I is a high affinity receptor for clathrin AP-2: implications for membrane recycling. Cell; 78(5): 751-760.

Zhong H, Yokoyama CT, Scheuer T, Catterall WA (1999). Reciprocal regulation of P/Q-type Ca^{2+} channels by SNAP-25, syntaxin and synaptotagmin. Nat. Neurosci; 2(11): 939-941.

Zhou Q, Petersen CC, Nicoll RA (2000). Effects of reduced vesicular filling on synaptic transmission in rat hippocampal neurones. J. Physiol.; 525 Pt 1: 195-206.

Zoccarato F, Cavallini L, Alexandre A (1999). The pH-sensitive dye acridine orange as a tool to monitor exocytosis/endocytosis in synaptosomes. J. Neurochem.; 72: 625-633.

Zucker RS (1989). Short-term synaptic plasticity. Annu. Rev. Neurosci.; 12: 13-31.

Zucker RS and Lara-Estrella LO (1983), Post-tetanic decay of evoked and spontaneous transmitter release and a residual-calcium model of synaptic facilitation at crayfish neuromuscular junctions. J. Gen. Physiol.; 81: 355-372.